The Enhancement of a Multi-Terrain Mechatron for Autonomous Outdoor Applications

A thesis

submitted in partial fulfilment

of the requirements for the Degree

of

Master of Science in

Physics and Electronic Engineering

at the

University of Waikato

by

Christopher Luke Cawley

THE UNIVERSITY OF
WAIKATO
Te Whare Wānanga o Waikato

2006

ABSTRACT

Medium scale robotic vehicles which are easily portable by humans are achieving increased application as technology improves, particularly in certain outdoor environments. Conventional, manually operated equipment has difficulty traversing uneven terrain, such as in dangerous environments where the human operators may be at risk. Robots which are capable of autonomous operation can be used in place of traditional machinery to perform repetitive or difficult tasks thus reducing the risk to the human operators and increasing the overall productivity by operating for longer time periods. This thesis discusses the modification and enhancement of a multi-terrain robotic vehicle that will eventually be capable of autonomous operation.

The mechanical platform consists of a track-laying differential drive system supporting payloads in excess of 100 kg which was previously developed by the Mechatronics Group at the University of Waikato. The existing shell did not have any working systems onboard so a complete design and installation of the electronics has been completed and various sensory systems are evaluated and implemented. The required control and navigation software systems have been designed enabling robot control in an outdoor environment. The mechatron and the installed systems have been successfully tested in a variety of outdoor conditions.

ACKNOWLEDGEMENTS

The support and assistance throughout this project from the following people are greatly appreciated and thus require acknowledgement.

To Dr Dale Carnegie, my project supervisor and valued lecturer during undergraduate studies who made this project available for undertaking. The invitation to graduate level study and continued support and guidance throughout this project is greatly appreciated.

Assistance by the Physics Department technical staff during the project in all aspects of electronic and mechanical design was always willingly provided. Special thanks to Scott Forbes and Bruce Rhodes for their knowledge and humour throughout my time at Waikato.

My fellow graduate students deserve no less appreciation for their ability to discuss concepts and provide valued knowledge making the work environment interesting and supportive. Thanks in particular to Jason Edwards, Praneel Chand, and Chris Lee-Johnson.

Finally a special thank you to all of my family for your continued support and encouragement throughout my university studies, without which my success to date would not have been possible.

TABLE OF CONTENTS

ABSTRACT ..... **iii**
ACKNOWLEDGEMENTS ..... **v**
TABLE OF CONTENTS ..... **vii**
LIST OF FIGURES ..... **xiii**
LIST OF TABLES ..... **xix**

1. INTRODUCTION **1**
1.1 MOTIVATION FOR SYSTEM DEVELOPMENT 1
1.2 COMMERCIAL APPLICATIONS 2
1.3 PROJECT SPECIFICATIONS 3
1.4 PROJECT PLANNING 4
1.5 THESIS STRUCTURE 5

2. BACKGROUND **7**
2.1 PREVIOUS MECHATRONICS RESEARCH 7
2.2 RESEARCH OF CURRENT SYSTEMS 8
2.2.1 TALON™ 9
2.2.2 ACER 9
2.2.3 MATILDA Robotic Platform 10
2.2.4 PackBot 11
2.2.5 Urbie 11
2.2.5 Other robots 12
2.3 EXISTING PLATFORM 13
2.3.1 Drive Motors 14
2.3.2 Drive System Type 15
2.3.3 Advantages of Skid Steering 17
2.3.4 Disadvantages of Skid Steering 17
2.3.5 Existing Onboard Hardware 19
2.4 PROCESSOR ARCHITECTURE 20
2.4.1 Embedded Controller 21
2.4.2 FPGA 21
2.4.3 Handheld PC 21
2.4.4 Laptop Computer 21
2.4.5 Full Size PC 22
2.4.6 ShuttleX PC 22
2.4.7 Selected Architecture 22
2.5 ELECTRONICS POWER SUPPLY 23
2.6 BATTERY SELECTION 24
2.6.1 Required Specifications 24
2.6.2 Review of Battery Types 25
2.6.3 Battery Ratings 26
2.6.4 Selected Batteries 27
2.6.5 Charging Procedure 28
2.7 DATA ACQUISITION CARD 29
2.8 OTHER HARDWARE COMPONENTS 31

2.8.1 Wireless Network Adapters 31
2.8.2 Onboard Video Camera 32
2.8.3 Infrared Proximity Detectors 33
2.8.4 Electronic Compass 33
2.8.5 GPS Receiver 34
2.8.6 Inertial Sensor 35
2.8.7 Motor Drivers 35

3. MOTOR CONTROL 37
3.1 INTRODUCTION 37
3.1.1 DC Motor Theory 37
3.1.2 Possible Solutions 38
3.1.3 Differential Drive Motor Control 40
3.2 EXISTING MOTOR DRIVERS 41
3.2.1 Outdoor Mechatron 41
3.2.2 Co-operating Robots 42
3.2.3 Marvin 43
3.2.4 Underwater ROV 43
3.3 GENERIC MOTOR DRIVERS 43
3.3.1 Project Outline 44
3.3.2 Hardware Components 45
3.3.3 Software Interface 47
3.3.4 Testing and Evaluation 48
3.3.5 Modifications 50
Mounting Enclosure 50
PWM Frequency 51
Shielding 52
Smoothing Capacitors 52
Ferrite Beads 52
RFI Suppression Choke 53
3.3.6 Summary 54
3.4 REVIEW OF COMMERCIAL SYSTEMS 55
3.4.1 MAXI Motor Driver Kit 56
3.4.2 MD03 and MD22 57
3.4.3 Tecel D200 58
3.4.4 MDM5253 59
3.4.5 RoboteQ AX2550 60
3.5 SELECTED MODULES 61
3.5.1 Features 62
3.5.2 Interfacing 64
3.5.3 Handheld Controller 66
3.5.4 Programming 66
3.5.5 Status Codes 68
3.5.6 Robot Mounting 69
3.6 Initial Interface Design 70
3.7 Improved Motor Driver Interface 72
3.8 MICROCONTROLLER 75
3.8.1 Selected Controller 76
3.8.2 Power Supply 77
3.8.3 Memory Configuration 77

3.8.4 Programming....78
3.8.5 DAQ Card Interface....78
3.8.6 Motor Driver Interface....80
3.9 RADIO CONTROL....81

4. ELECTRONICS AND SENSORS....83
4.1 CENTRAL COMPUTER....83
4.1.1 Installation....83
4.1.2 Hard Drive Support....84
4.1.3 Communication Interfaces....85
4.2 POWER SYSTEM....85
4.2.1 Fuse Box....86
4.2.2 Wiring....86
4.2.3 Power Switch Panel....87
4.2.4 Power Distribution Board....88
4.3 SENSOR OPTIONS....89
4.3.1 Requirements....89
4.3.2 Positioning....90
4.3.2 Ranging....91
4.3.4 Other sensors....91
4.4 ELECTRONIC COMPASS....92
4.4.1 Previous Module....92
4.4.2 Review of Available Modules....93
KVH C100 Compass Engine....93
CMPS03....94
Handheld Units....95
Honeywell HMR3000....95
True North Revolution....96
TruePoint Compass Module....96
4.4.3 Selected Module....98
4.4.4 Interface Design....99
4.4.5 Mounting Enclosure....100
4.5 GPS....101
4.5.1 Background....101
4.5.2 Receiver....103
4.6 ACCELEROMETER....104
4.6.1 Advantages....105
4.6.2 Device Specifications....105
4.6.3 Theory of Operation....106
4.6.4 Sensitivity....107
4.6.5 Interface Design....108
4.6.6 Measuring Tilt....109
4.7 SHAFT ENCODERS....110
4.8 INFRARED SENSORS....111
4.8.1 Operation....111
4.8.2 Sensor Response....112
4.8.3 Range Calculation....113
4.8.4 Mounting....115
4.9 DAQ CARD CONNECTOR MODULE....118
4.10 ELECTRONICS ENCLOSURE....120

4.11 HARDWARE SUMMARY 121

5. SOFTWARE 123
5.1 APPLICATION REVIEW 123
5.1.1 LabVIEW 124
5.1.2 Visual C++ 125
5.1.3 Visual Basic 126
5.1.4 Java 127
5.1.5 MATLAB 128
5.1.6 Linux 128
5.1.7 Selected Software Platform 128
5.2 WIRELESS NETWORK 130
5.2.1 Login Procedure 130
5.2.1 Network Configuration 131
5.2.3 MATLAB Startup 131
5.3 DAQ CARD INTERFACE 132
5.3.1 DAQ Toolbox 132
5.3.2 NI-DAQmx Drivers 133
5.3.3 DLL Interface to NI-DAQmx 134
5.3.4 Channels and Tasks 136
5.3.5 Available Functions 137
5.3.6 MAX Studio 138
5.4 COMPASS INTERFACE 139
5.4.1 Demo Software 139
5.4.2 Connection 140
5.4.3 Data Collection 141
5.4.4 Configuration and Calibration 143
5.5 GPS INTERFACE 144
5.6 OTHER HARDWARE INTERFACES 146
5.6.1 Rangefinders 146
Mean 147
Weighted Mean 147
Median 148
Selected Method 148
5.6.2 Encoders 149
5.6.3 Accelerometer 150
5.6.4 Video Camera 151
5.7 SYSTEM CONFIGURATION 152
5.7.1 Timers/Callbacks 152
5.7.2 Persistent Variables 153
5.7.3 Low Level Control Loop 154
5.7.4 DAQ Safety Pulse 156
5.7.5 Navigation Control Loop 156
5.7.6 Data log Files 157
5.8 MECHATON CONTROL 158
5.8.1 Velocity Control 158
5.8.2 Heading Control 160
5.8.3 Obstacle Avoidance 161
5.8.4 Navigation 161
5.9 MICROCONTROLER CODE 162

5.10 USER INTERFACE 166
5.10.1 GUIDE 167
5.10.2 TabPanels 168

6. RESULTS & CONCLUSION 173
6.1 CURRENT CONSUMPTION 173
6.2 ACCELEROMETER 177
6.2.1 Stationary Readings 177
6.2.2 Collision Detection 178
6.2.3 Tilt Measurements 180
6.3 ELECTRONIC COMPASS 182
6.4 GPS EVALUATION 184
6.4.1 Positioning 184
6.4.2 Heading 185
6.4.3 Long Term GPS Response 186
6.4.4 Improving GPS Positioning 189
6.4.5 GPS Deficiencies 190
6.5 ROBOT MOTION 190
6.5.1 Motor Operation 191
6.5.2 Automatic Heading Control 192
6.5.3 Obstacle Avoidance 193
6.6 INITIAL FIELD TRIAL 193
6.7 TESTING OUTDOORS 195
6.8 FUTURE WORK 196
6.9 SUMMARY 197

GLOSSARY 199
REFERENCES 201
APPENDIX A: CIRCUIT DESIGN 203
A.1 MOTOR DRIVER INTERFACE BOARD 203
A.2 MICROCONTROLLER BOARD 204
A.3 ELECTRONIC COMPASS INTERFACE 205
A.4 GPS INTERFACE 206
A.5 ACCELEROMETER BOARD 207
APPENDIX B: CD CONTENTS 209

LIST OF FIGURES

Figure 1.1: Robots used in dangerous environments. ……1
Figure 2.1: Fleet of mobile robots within Mechatronics Group...……...……7
Figure 2.2: TALON military robot……...……9
Figure 2.3: ACER robot……..…10
Figure 2.4: MATILDA tracked robot……..……...……10
Figure 2.5: Packbot……...…..…11
Figure 2.6: Urban reconnaissance robot ……..…12
Figure 2.7: Collection of multi-terrain robots…… .....……...…12
Figure 2.8: Existing robot platform at project onset…… ……13
Figure 2.9: Drive motors from Dynamic Mobility……..…..…14
Figure 2.10: Typical motor performance characteristics……..…14
Figure 2.11: Underside of mechatron illustrating concept of differential drive…...16
Figure 2.12: Tracked vehicle negotiating difficult terrain…… ……...17
Figure 2.13: Skid steering on spot showing track movement and frictional forces. 18
Figure 2.14: Original microcontroller board and PC motherboard……..19
Figure 2.15: Original power supply consisting of UPS and ATX converter… …...19
Figure 2.16: Small form factor ShuttleX PC……22
Figure 2.17: Olympic OTC-1000A UPS and ACE-828C ATX supply…… …..….23
Figure 2.18: Hella Endurant battery…… ……..…27
Figure 2.19: National Instruments PCI-6229M DAQ Card…… ……..…30
Figure 2.20: Wireless network adapters …… …..….32
Figure 2.21: Logitech QuickCam Pro 4000 webcam…… ……..….32
Figure 2.22: Sharp GP2Y0A02YK infrared sensor ……...…...…33
Figure 2.23: Honeywell HMR3300 electronic compass module…… …..…34
Figure 2.24: Motorola M12+ Oncore GPS Receiver…… ……34
Figure 2.25: MMA7260Q 3-axis accelerometer …… .....….35
Figure 2.26: Rhino DS72K motor driver module……..…35
Figure 3.1: PWM signals and transmitted power…… …..……39
Figure 3.2: H-Bridge switching topography……..39
Figure 3.3: Differential drive configuration consists of two opposing motors… 40

Figure 3.4: Simplified single switch and relay drive circuit…… …….41
Figure 3.5: Itchy and Scratchy motor drivers……42
Figure 3.6: One of the H-Bridge power circuit boards previously designed… ……45
Figure 3.7: Previously designed microcontroller board…… ……46
Figure 3.8: Initial motor driver front end GUI…… ……..…47
Figure 3.9: Small 24 V motor driver test motor…… ……....48
Figure 3.10: Clean and noisy 5 V supply rail……...….49
Figure 3.11: Noise from PWM at 34.72 kHz and PWM signal…… ….....49
Figure 3.12: Mounting enclosure and cooling fans for motor driver…… ……50
Figure 3.13: Noise after PWM changed to 12 kHz…… ……....51
Figure 3.14: Inspection of single noise pulse (f ≈ 20 MHz)……..53
Figure 3.15: C215 RFI noise suppression choke and connection diagram……....53
Figure 3.16: Reduced noise density and amplitude after RFI choke added…… …..54
Figure 3.17: Assembled Modotronics MAXI motor driver kit…… …….56
Figure 3.18: MDO3 and MD22 motor drivers…… ……..57
Figure 3.19: Tecel Microcontrollers D200 DC Motor Driver Board…… ……58
Figure 3.20: MDM5253 motor driver board…… …….59
Figure 3.21: RoboteQ AX2550 controller module……...60
Figure 3.22: RHINO DS72K controller dimensions…… ……....62
Figure 3.23: Example scooter tiller head from Dynamic Controls Ltd…….64
Figure 3.24: RHINO suggested wiring diagram…… ……...65
Figure 3.25: Handheld motor driver controller…… …….66
Figure 3.26: Connection of handheld programmer to RHINO controller…….67
Figure 3.27: RHINO controllers mounted on plate at rear of mechatron……..69
Figure 3.28: Motor driver interface board utilizing PWM based DAC…… ……70
Figure 3.29: Simplified schematic of PWM interface board…….71
Figure 3.30: Simplified schematic of digital pot interface to motor drivers…… ….72
Figure 3.31: Schematic showing key switch control circuitry…… ……..73
Figure 3.32: Microcontroller header and optoisolated status signals……73
Figure 3.33: Completed RHINO motor driver interface board…….…74
Figure 3.34: Mounting enclosure for motor driver interface…….…74
Figure 3.35: Microcontroller board for motor control……...75
Figure 3.36: First microcontroller board and improved design…….…76
Figure 3.37: Microcontroller power supply……...…77

Figure 3.38: Radio Controller interface board……..…81
Figure 3.39: Radio control handheld transmitter……...…81
Figure 4.1: Computer installation – Original idea and revised option…… ……..…84
Figure 4.2: Protective hard drive cradle and mounting position…… ……...…84
Figure 4.3: USB to serial adapter…… ……...…85
Figure 4.4: Fuse enclosure……..…86
Figure 4.5: Subsection of wiring showing motor driver connection……..…87
Figure 4.6: Power switch and charging panel……...…88
Figure 4.7: Power distribution board……..…88
Figure 4.8: Earth's magnetic field……..…92
Figure 4.9: Initial Vector2X compass and interface board……...…93
Figure 4.10: KVH C100…… ……...…94
Figure 4.11: CMPS03 Low cost compass module…… ……...…94
Figure 4.12: MapStar fully integrated handheld compass module……...…95
Figure 4.13: HMR3000 compass module from Honeywell…… ……..……95
Figure 4.14: TrueNorth Revolution compass module……... …96
Figure 4.15: TruePoint compass module and protective housing……..…....…97
Figure 4.16: Axis of operation in a 3-axes compass module…… ……...…98
Figure 4.17: Compass module interface schematic……..…100
Figure 4.18: Compass module protective enclosure……...…100
Figure 4.19: Three GPS operation segments……..102
Figure 4.20: GPS antenna and receiver with interface board……..…103
Figure 4.21: GPS receiver and interface board in protective case……...…104
Figure 4.22: Capacitive sensing g-cells and ASIC……...…106
Figure 4.23: Beam and capacitor model of g-cells……..……107
Figure 4.24: Suggested g-levels for various applications……107
Figure 4.25: Accelerometer interface board and case…… ……108
Figure 4.26: Example of accelerometer tilt in Earth's gravity…….....…109
Figure 4.27: Newly manufactured encoder disks…..……..……110
Figure 4.28: Triangulation with infrared sensors…… ……....112
Figure 4.29: Infrared sensor response for different objects……....113
Figure 4.30: MATLAB curve fitting toolbox for infrared sensor data……...….114
Figure 4.31: Infrared sensor locations…….……116
Figure 4.32: Infrared sensor mounting brackets……..116

Figure 4.33: Lateral sensing distance for different object ranges…… …...117
Figure 4.34: Infrared based non-contact bumper…… ……117
Figure 4.35: Infrared sensor interface boards……..118
Figure 4.36: Labelled terminal blocks…….118
Figure 4.37: CB-68LPR terminal block and labelled connectors……....119
Figure 4.38: NI-PCI6229 DAQ card connector pinout…… ……...119
Figure 4.39: Electronics enclosure……...121
Figure 4.40: Block diagram overview of mechatron hardware…… ……..122
Figure 5.1: Example LabView G code……125
Figure 5.2: Typical Visual Basic development environment……..…126
Figure 5.3: Remote Desktop Connection…… ……....130
Figure 5.4: Network configuration……..……131
Figure 5.5: Position of NI-DAQmx driver software…… …..…….133
Figure 5.6: Load NI-DAQmx library into MATLAB…… …….....134
Figure 5.7: Unload NI-DAQmx library from MATLAB……..…..134
Figure 5.8: Excerpt from NI constants file……..…135
Figure 5.9: Function call example……..…135
Figure 5.10: Signal measurement and generation process……...……137
Figure 5.11: MAX Studio data acquisition interface…… ……..……139
Figure 5.12: DAQ card test panels and power-up states configuration panel…....139
Figure 5.13: HMR3300 demo software……..…….140
Figure 5.14: Excerpt from compass initialization code……..…….141
Figure 5.15: Excerpt from compass disconnection code……..……...141
Figure 5.16: Compass_GetReading code extract…… ……..…..…142
Figure 5.17: Initialize compass callback…… ……..……...…142
Figure 5.18: Determine current compass data output mode……...143
Figure 5.19: Example configuration function…… ….....…143
Figure 5.20: Storing GPS data into MATLAB structure……...……..145
Figure 5.21: mas to degree conversion……..……...…146
Figure 5.22: Infrared sensor circular buffer shift…… ……..……...…148
Figure 5.23: Encoder distance measurement……...…...…….149
Figure 5.24: Encoder velocity measurement……...…...…….150
Figure 5.25: Accelerometer data acquisition for tilt calculation…… …..….....…151
Figure 5.26: Excerpt from camera connection code……...……..…151

Figure 5.27: Extract from image acquisition code ……152
Figure 5.28: Extract from low level control loop variable initialization ……155
Figure 5.29: Customization of individual hardware access functions…….155
Figure 5.30: Excerpt from motor driver code showing safety pulse generation ….156
Figure 5.31: Unique data log file name creation…….157
Figure 5.32: Writing data to file using fprintf…….157
Figure 5.33: Use *get()* command to extract target velocity from sliders…….158
Figure 5.34: Heading error calculation for orientation control ……...160
Figure 5.35: SPI code to send data word to digital potentiometer ……..162
Figure 5.36: Radio control receiver calibration routine ……..163
Figure 5.37: Update digital potentiometer with RC data if RC signals are valid…164
Figure 5.38: Update digital potentiometer with DAQ card data valid ……165
Figure 5.39: Graphical User Interface (GUI) ……..166
Figure 5.40: GUIDE interface development environment ……..168
Figure 5.41: Initiate *tabpanel* configuration utility …….169
Figure 5.42: Sequence of tab panels……170
Figure 6.1: LEM current transducer……173
Figure 6.2: Current consumption for seven trials……175
Figure 6.3: Average current consumption for each test condition ……175
Figure 6.4: Operating time of starting vs deep cycle batteries……176
Figure 6.5: Comparison between front and rear impacts ……179
Figure 6.6: Compass and accelerometer pitch angle comparison ……...181
Figure 6.7: Compass and accelerometer roll angle comparison……..181
Figure 6.8: Effect of onboard IIR system filter on heading ……183
Figure 6.9: GPS Evaluation around 70 × 100 m path …….184
Figure 6.10: Heading comparison between GPS and compass ……186
Figure 6.11: GPS data logged over approximately 11 hours ……..188
Figure 6.12: Relative position over time in meters …….188
Figure 6.13: Dilution of Precision (DOP) vs Tracked satellites …….189
Figure 6.14: Improving GPS position based on DOP value……189
Figure 6.15: Mechatron velocity response forwards ……...191
Figure 6.16: Mechatron velocity response reverse……..191
Figure 6.17: Example responses for autonomous heading control …….192
Figure 6.18: Disengaged track and original pulleys with small flange……...194

Figure 6.19: New flange pulleys and positioning diagram ……..194
Figure 6.20: Images of successful robot operation in outdoor conditions ……..195
Figure 6.21: Robotic manipulator mounted on outdoor mechatron ……196
Figure 6.22: Completed mechatron in operation outdoors……..198

LIST OF TABLES

Table 2.1: Dynamic Controls WMT90112 motor specifications…… ……15
Table 2.2: Selected battery specifications……28
Table 3.1: RHINO programmer settings……..67
Table 3.2: RHINO fault code reference……...68
Table 3.3: Microcontroller to DAQ card connections……79
Table 4.1: Sensitivity selection……..107
Table 4.2: DAQ card connections summary……..120
Table 5.1: DAQ card function listing…… 137
Table 6.1: Mechatron power consumption test conditions……174
Table 6.2: Accelerometer stationary output voltage……..178

1. INTRODUCTION

Mobile robots capable of traversing difficult terrain are useful in a large number of circumstances where human labour is too expensive, dangerous or impractical. Such industries or environments would benefit from a robotic vehicle performing certain repetitive or specialized tasks such as those shown in Figure 1.1.

1.1 MOTIVATION FOR SYSTEM DEVELOPMENT

Research and development of multi-terrain robotic vehicles is often focused on specific applications and are therefore designed accordingly. The ability to be customized or reconfigured and function in an unstructured, outdoor environment is a desired feature of robotic platforms capable of autonomous operation.

An emerging trend is the use of automated technology in farming and other agriculture based industries. There is increasing potential for remote pasture analysis and animal management to be carried out by mobile robots. Valuable human labour can then be transferred to other tasks.

Figure 1.1 Robots used in dangerous environments LEFT: Volcano exploration[1] RIGHT: Robot entering tunnel for nuclear waste disposal[2]

[1] http://www.robovolc.dees.unict.it Robovolc is used to explore dangerous volcanic sites
[2] http://www.bechtel.com/Briefs/0305/Yucca.htm Testing of robots for tunnel construction and nuclear waste disposal

These devices have been restricted in the past due to technology limitations however, as sophisticated devices become available, the requirements of co-ordination, communication and precision control can be met by a robotic system.

Research and development of such a robotic system capable of replacing or complimenting human labour has been initiated by the construction of a multi-terrain mechatron (*Cordes,* 2002). This thesis uses the mechanical structure of this multi-terrain mechatron, equips it with sensors, motor drivers, intelligence and other electronics. High and low level software is developed and some mechanical modifications are implemented so that at the conclusion of this project the mechatron will have the capability to perform some autonomous tasks.

1.2 COMMERCIAL APPLICATIONS

The commercial applications for an autonomous mechatron capable of multi-terrain operation are wide ranging and not only limited to farming applications. Other potential applications include the following:

- **Forestry** – automatic tree grading and low level scrub clearing
- **Military** – tactical reconnaissance and explosive disposal missions
- **Security** – patrol of compound perimeter and intruder confrontation
- **Search and Rescue** – disaster relief and urban survivor location
- **Terrain Mapping** – digital profiling of open or underground terrain
- **Planetary Exploration** – environment evaluation and facility construction

Taking into account these possible applications the mechatron must be capable of carrying a large volume of application specific equipment. Therefore common robot components such as motor drivers and sensors must be efficiently designed to allow the addition of future components without overloading the mechatron.

1.3 PROJECT SPECIFICATIONS

The objective of this project is to research and implement the necessary hardware and software components required to eventually enable autonomous operation of a mobile mechatron. The mechanical shell of a track-laying multi-terrain robotic vehicle has previously been deigned and this project aims to equip it with the mechanisms for operation and evaluate the performance of the installed components.

An autonomous mechatron is one which can independently monitor its operating environment and make decisions that enable self control and execution of some desired tasks. The robot will eventually be capable of accepting and analyzing complex task descriptions for execution however, these high level functions are outside the scope of this project.

This project involves a number of different aspects to achieve the objectives including mechanical alterations, electronic circuit board design and software development in different computer languages. These concepts will be brought together to enable motion of the robot utilizing various sensors, electrical systems and control algorithms to eventually achieve autonomous operation.

Future research by the Mechatronics Group into mobile robotic platforms may utilize similar hardware and software elements to those used in this project, therefore an emphasis is on the appropriate selection of these systems. By providing a detailed review of commercially available sensors, motor driver units and computer peripherals useful for robot control, future designers can reduce development time by referring to this project.

This project considers the following attributes to produce a working mechatron:

- **Operating Environment –** Operation of the mechatron is primarily intended for outdoors where environmental conditions can greatly vary so onboard systems should be chosen for durability and measures taken to protect them from the elements.

- **Independent Operation** – All power supply systems and computational resources are to be mounted on the mechatron to facilitate self sufficient operation.

- **Manoeuvrability** – Design of motor control systems need to consider and take advantage of the differential drive configuration to enable high manoeuvrability over uneven terrain.

- **Software** – Interface software to the hardware components and control algorithms need to be designed to allow for future development and extension.

- **Future Work** – The design and implementation of each component must consider upgrades and additions during future development.

1.4 PROJECT PLANNING

To attain the project specifications the following objectives must be met and roughly adhere to the order of appearance:

- Examine initial mechanical platform and determine potential capabilities
- Determine and carry out mechanical modifications for operation and aesthetics
- Evaluate existing onboard electronics to establish operating conditions
- Select computer equipment for data processing and communications
- Identify and install a suitable power source and electronics supply
- Research and obtain sensors for robot localization and environment interpretation
- Design and construction of interface electronics for sensors and other peripherals
- Construct enclosure and mounting systems for sensors and electronics
- Development of hardware for motor control
- Installation of wiring and power distribution systems with overload protection
- Develop software interface to motors and sensors

- Calibration and testing of sensors
- Provide communication link with remote base station
- Test and evaluate mechatron performance outdoors

The final result of this thesis will be a multi-terrain robotic platform capable of autonomous operation outdoors. Supporting electronics and sensory systems will be installed and evaluated to provide navigation data and obstacle avoidance. An evaluation of available devices will facilitate future robotics research and a comprehensive graphical software interface will provide access to robot control and sensor data.

1.5 THESIS STRUCTURE

This thesis is divided into chapters and presented as follows:

Chapter 2 describes the background behind the project including the original mechanical platform and the motivation behind the system development.

Chapter 3 covers the theory and hardware associated with controlling the motors using both existing and newly constructed driver modules.

Chapter 4 outlines the electronics and sensory systems that have been evaluated and installed on the mechatron providing the means for future autonomous operation.

Chapter 5 details the software algorithms written to control the robot including hardware interfacing, sensor data acquisition and a user interface.

Chapter 6 presents the results of the various sensor evaluations and platform testing completed. The entire thesis is then summarized and a brief discussion on future work is outlined.

2. BACKGROUND

2.1 PREVIOUS MECHATRONICS RESEARCH

The Mechatronics Group at the University of Waikato has developed a number of medium to large scale robotic vehicles. The robots have been specifically designed for a number of different tasks and therefore exhibit a wide range of characteristics. Robots range from specially designed platforms for indoor operation up to large vehicles for underwater exploration and outdoor multi-terrain navigation. Each mechatron in the fleet of mobile platforms contains an onboard power supply and full PC computer for onboard intelligence and control.

Figure 2.1 LEFT: Marvin, CENTRE: ROV, Outdoor Mechatron, RIGHT: Itchy & Scratchy

Four of the Mechatronics Group projects are illustrated in Figure 2.1. The first robot in this collection is Marvin (Mobile Autonomous Robotic Vehicle for Indoor Navigation). Equipped with various range and security sensors, Marvin is intended to patrol indoor environments as a security device. Voice recognition and the ability to portray emotions enable effective human-machine interaction. Underwater exploration is the specialty of the Remote Operated Vehicle (ROV). Controlled from the surface, the ROV includes a number of sensors including an inertial navigation

system and a wide field of view imaging system. A pair of identical robots (Itchy and Scratchy) have been designed and built to investigate cooperative robotic interaction. The project aims the curb the trend of mechanical scaling to perform ever increasing tasks by utilizing multiple units working together in a controlled, outdoor environment.

The mechanical construction of a track-based, multi-terrain vehicle has also been carried out to investigate aspects of outdoor navigation. The outdoor robot directly complements the existing fleet of vehicles thus enabling robotics research to span a wide range of locomotion types and application environments. This platform will enable navigation and control system development suited to the dynamic and often difficult conditions found in an outdoor environment. The previous construction of this platform forms the base of this project and is discussed further in section 2.3.

2.2 RESEARCH OF CURRENT SYSTEMS

A number of robotic platforms exist which are suitable for navigation of multi-terrain environments. Research and development of such systems often focus on a very specific task and as a result are highly design specific, lacking the ability for reconfiguration. Other systems which are designed for research purposes, offering configuration options, are sparse and very expensive, exceeding budgetary limitations for this project.

Vehicles with a self-laying track locomotion system are usually designed for tele-operated tasks such as bomb disposal and traversing uneven terrain. In contrast, wheeled robots that use non-differential steering such as an Ackerman configuration are often useful for field operation and generally large, open spaces where speed is considered more important than manoeuvrability. Existing in the department was a self-laying, tracked mechatron capable of multi-terrain operation. To further explore the functionality and operation of an outdoor robot, a decision to either modify the current platform or investigate commercial systems was required. Some manufactured designs which relate to this project were researched and evaluated based on system configuration and onboard hardware pertaining to outdoor operation.

2.2.1 TALON™

The range of TALON™ robots (Figure 2.2) from Foster-Miller[3] provides a powerful and durable tracked robotic platform for use in the military. Used extensively by the U.S Army during missions in Iraq and Afghanistan, the rugged platform has proved successful in a number of scenarios including EOD and reconnaissance.

TALON specifications:

- Direct connection to large range of weaponry
- Power: Lithium Ion 36 VDC 750 Whr battery
- Velocity: 0 – 2.32 ms^{-1}
- Weight: 34 – 54 kg
- Dimensions: 0.86 × 0.57 × 0.28 m (excludes arm)

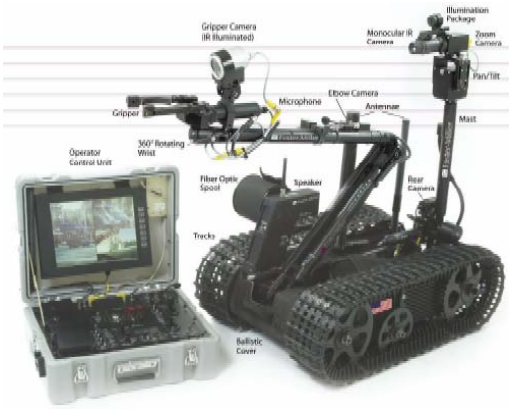

Figure 2.2 TALON military robot

- Controller: Remote controlled using OCU (Operator Control Unit)
- Sensors: fixed focus colour camera, LED lighting Options include: IR camera, colour zoom cameras, radiological/biological/chemical sensors, GPS compass.

The TALON supports a payload of 45 kg with the ability to drag a weight up to 91 kg and a range of manipulators can be attached capable of lifting 11 kg. Communication with the controller is through high-gain wireless up to 1200 m or Kevlar wrapped fibre optics cable.

2.2.2 ACER

An Armoured Combat Engineer Robot (ACER) is available from Mesa Robotics Inc[4] for use in heavy duty military based environments. The robot (Figure 2.3) is highly mobile and easily transportable while having the durability to operate in the full range of weather conditions including ice, snow, rain, sand and dust. The ACER robot includes Ballistic Steel amour plating and has been designed for very heavy duty use

[3] http://www.foster-miller.com
[4] http://www.mesa-robotics.com

in a hazardous environment. Attachments such as earthmoving buckets and blades enable terrain clearing and forced building entry. The large 1134 kg payload capacity enables transport of equipment including an 11339 kg towing capability.

ACER specifications:

- Power: Turbocharged 60 HP Diesel engine with hydraulic system for tracks and auxiliary tools
- Velocity: 0 – 2.8 ms^{-1}
- Weight: 1905 kg
- Dimensions: 2.1 × 1.58 × 1.42 m
- Controller: Line of sight operation with portable briefcase type controller

Figure 2.3 ACER robot

2.2.3 MATILDA Robotic Platform

A smaller scale robotic platform called MATILDA shown in Figure 2.4 is also available from Mesa Robotics Inc. The tracked platform is designed for remote controlled missions primarily military related although provisions are available for mounting of custom built manipulators and instrumentation. Robot control utilizes a combination of RF and fibre-optics with a manually operated briefcase control station.

MATILDA specifications:

- Power: 12 VDC NiMH (4- packs)
- Operating Time: 4 – 6 hours
- Velocity: 0 – 0.9 ms^{-1}
- Weight: 27.7 kg
- Dimensions: 0.76 × 0.53× 0.3 m
- Controller: 900 MHz portable control module with 2.4GHz video, joystick control of vehicle/camera/manipulator
- Sensors: pan/tilt colour camera, IR thermal imaging, optional CBRN sensor kit for chemical/biological and radiological detection

Figure 2.4 MATILDA tracked robot

A number of different track sets are available for traversing a range of operating surfaces including slick (marble) floors and snow/icy conditions. Equipped with imaging sensors and 220.5 kg or 441 kg tactical trailers, the MATILDA robot is best suited for tele-operated applications such as explosives disposal, logistics and equipment supply, surveillance and search and rescue.

2.2.4 PackBot

PackBot, shown in Figure 2.5, is a highly specialized, rugged robot designed to assist with Explosive Ordnance Disposal (EOD). PackBot is manufactured by IRobot Corporation[5].

PackBot Specifications:

- Power: 80 × 3000 mAh NiMH cells
- Velocity: 3.7 ms^{-1} (high speed mode)
- Weight: 18.1 kg
- Dimensions: 0.41 × 0.88 × 0.18 m (base)
- Controller: Pentium III core running Linux
- Sensors: encoders, GPS, Superbrite and IR LED array, compass and attitude sensors, vision system

Figure 2.5 Packbot

The lightweight, tread-based construction is suitable for numerous military and law enforcement tasks over difficult terrain including stairs and rubble. The OmniReach manipulator system can reach up to 2 meters in any direction to safely disrupt various incendiary devices.

2.2.5 Urbie

A portable, urban reconnaissance robot, shown in Figure 2.6, has been developed in a joint venture between NASA's Jet Propulsion Laboratory and the Carnegie Mellon University. This small scale tracked robot is based on a platform similar to the PackBot (section 2.2.4) and is designed to operate over difficult terrain in urban hostage situations or disaster relief.

[5] http://www.irobot.com

Urbie Specifications:

- Power: 100 W NICAD Pack
- Velocity: 0.8 ms^{-1}
- Weight: 22 kg
- Dimensions: < 650 mm long
- Controller: dedicated Pentium PC for both vision and navigation systems
- Sensors: 3-axis gyros, accelerometers, stereo cameras, sonar, laser rangefinder, DGPS

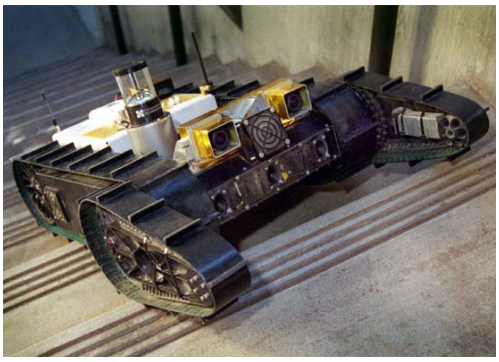

Figure 2.6 Urban reconnaissance robot

The robot exhibits a number of useful capabilities of a multi-terrain vehicle, utilizing the various sensors, the robot can accomplish stair climbing and stereo vision based obstacle avoidance.

2.2.5 Other robots

Other robotic vehicles exist which are capable of multi-terrain operation under different operating conditions and system configuration. Some of these are illustrated in Figure 2.7, however most are not suitable for our application for a range of reasons including cost and functionality. For example, the OmniTread robot (top left) can negotiate very irregular terrain but is not capable of carrying a useful payload or manipulator. The SPIKE robot (like ACER in 2.2.2) uses a diesel engine and exhibits a very large payload capacity however these robots are too heavy and expensive to run for our applications.

Figure 2.7 Collection of multi-terrain robots. Clockwise from top left: OmniTread, SPIKE, URBOT, Lemming Robot, Ranger Modular robot, MARV

2.3 EXISTING PLATFORM

Evaluation of commercially available platforms (section 2.2) reveals how unsuitable they are for fulfilling the research purposes of this project. A low cost, medium scaled track-based platform was required that could negotiate rough terrain and provide a base for further research into outdoor robotics. The limiting factor with most of the systems evaluated was the high cost and limited payload capacity. These factors formed the motivation behind the design and construction of a custom unit.

The existing mechanical platform (*Cordes, 2002*), is that of a track-laying mechatron incorporating differential skid-style steering (section 2.3.2) similar to a tank or bulldozer. This configuration provides a high level of stability and manoeuvrability particularly suited to uneven terrain. A solid steel chassis construction ensures the mechatron is sufficiently robust to cope with the irregularities of an outdoor environment and provide the strength for a substantial payload capacity.

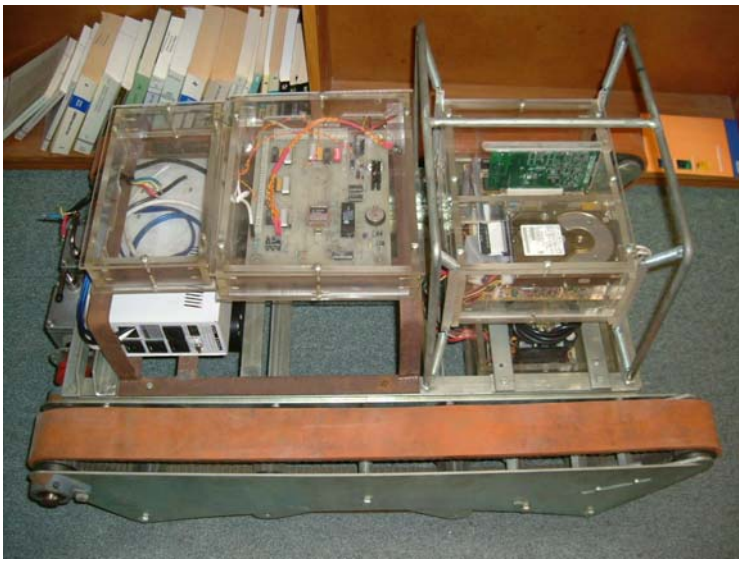

Figure 2.8 Existing robot platform at project onset

The track design incorporates dynamic tensioning and a bogie mechanism to allow the tracks to contour to the terrain. A payload capacity of over 100 kg enables the addition of a wide range of manipulators and instrumentation to be added depending on the application. A top mounted steel frame is used to attach a robotic arm or similar appendage depending on the required task. The robot in its original state at the onset of this project is shown in Figure 2.8.

2.3.1 Drive Motors

The drive system consists of a pair of permanent magnet, brush type DC motors. Developed locally by a New Zealand company, Dynamic Controls Ltd, the motors, shown in Figure 2.9 were designed for use in mobility devices for the elderly and disabled. As the motors are designed for wheelchair use, they exhibit a high power output of 230 W and thus are ideal for mobile robotic vehicles that need to powerfully negotiate uneven surfaces. An attached gear reduction unit consists of a worm and helical pair driving two pinion gears. The resulting reduction ratio between the motor shaft and track is 394.33:1 and approximately 12:1 between the drive pulley and track. The belt length is 2.3 m so the tracks travel a linear distance of 0.19 m for each revolution of the gearbox.

Figure 2.9 Drive motors from Dynamic Mobility

The typical performance characteristics including efficiency and power output of the motors are shown in Figure 2.10, the motor specifications are listed in Table 2.1.

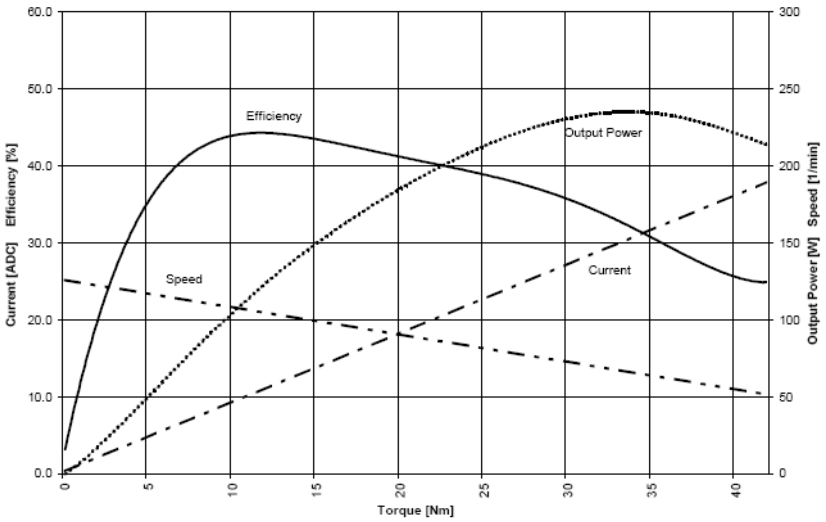

Figure 2.10 Typical motor performance characteristics

Some key points to note from the performance characteristics are the relationship between efficiency and current. Although the rated current of 8 – 10 Amps produces the highest efficiency of about 45%, actual operating current usually exceeds this value meaning the motors are operating relatively inefficiently. This disadvantage is however compensated by the large increase in output torque for a small decrease in efficiency thus providing the power to the drive system required for rugged terrain and slope negotiation. The maximum torque of 55 Nm is achieved at very low efficiency and high currents, increasing the risk of motor burn out.

Motor Type	Permanent magnet commutator 24 V DC
Power Output (max)	230 W at 65 RPM
No Load Current	3.3 A (max)
Continuous Current	8.0 A
Torque Constant	1.1 Nm/A
Max Torque	55 Nm (50 A controller)
Parking Brake Type	Electro-mechanical 24 V DC
Parking Brake Holding Torque	> 50 Nm at output shaft
No load speed at output shaft	120 RPM nominal
Weight	5.5 kg each
Typical Backlash	1.5°
Motor Resistance	250 mΩ

Table 2.1 Dynamic Controls WMT90112 motor specifications

2.3.2 Drive System Type

The pair of motors are attached to rigid sets of tracks constructed from truck supercharger belts mounted on either side of the robot chassis thus forming a differential drive system. This configuration (also termed skid steering) is often used in tracked vehicles designed for operation in unstable or loose surfaces due to the extra traction.

A turn is accomplished by driving the tracks on each side of the vehicle at different velocities. Symmetrical robots can rotate about the geometric centre by driving each

side at an equal but opposite velocity whereas straight line motion is achieved with identical velocities in the same direction.

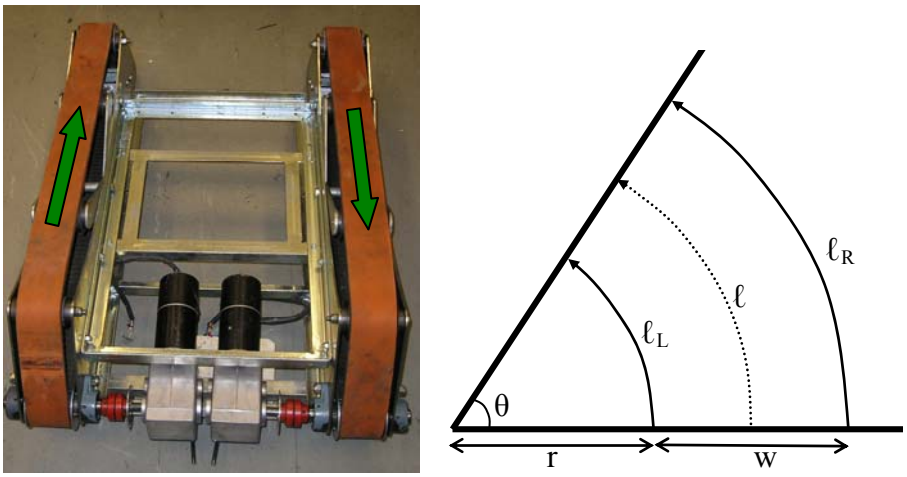

Figure 2.11 LEFT: Underside view of mechatron showing differential drive RIGHT: Correlation diagram between track motion and mechatron movement

These concepts are illustrated in Figure 2.11. An underside image of the mechatron shows the pair of tracks on either side with the two drive motors at the centre-rear of the mechatron. The green arrows represent the relative track directions of travel required to execute a clockwise rotation (as viewed from above).

The turning radius is dependent on the relative velocity and therefore the distance travelled by each track segment as in Equations 2.1 – 2.3. The distance travelled by the mechatron is given by Equation 2.4 and illustrated in Figure 2.11 however, these formulae must be treated as approximations, particularly for tracked vehicles and turning angles greater than 10 degrees[6] because small errors caused by track slippage can rapidly accumulate rendering calculation results unreliable.

$$\ell_L = r\theta \qquad \textbf{Equation 2.1}$$

$$\ell_R = (r + w)\theta \qquad \textbf{Equation 2.2}$$

$$\theta = \frac{\ell_R - \ell_L}{w} \qquad \textbf{Equation 2.3}$$

$$\ell = \frac{\ell_R + \ell_L}{2} \qquad \textbf{Equation 2.4}$$

[6] http://rossum.sourceforge.net/papers/DiffSteer/DiffSteer.html

2.3.3 Advantages of Skid Steering

The main advantage of a locomotion system utilizing differential drive or skid-style steering is the very high manoeuvrability of the vehicle. The ability to rotate on the spot and turn a corner of practically any radius is very useful particularly when avoiding obstacles.

Tracked vehicles have a larger footprint compared to wheeled and legged robots enabling increased traction and stability, particularly on loose or uneven terrain such as shown in Figure 2.12. The continuous positive drive enables tracked vehicles to effectively power through many terrains and climb over obstacles that wheeled locomotors of similar diameters cannot negotiate.

Figure 2.12 Tracked vehicle negotiating difficult terrain

Geometrically symmetrical tread-based robots also have the added advantage of equal manoeuvrability in either direction as compared to wheeled robots with Ackerman steering or a tricycle configuration. A preference is not given to forward or reverse motion enabling the mechatron to immediately reverse the direction of travel in a confined space because a turn is not required.

2.3.4 Disadvantages of Skid Steering

There are a number of disadvantages to skid-style steering. The most prominent is the high power requirements to implement a vehicle turn. Driving both tracks in different

directions and to a lesser extent different velocities is inherently inefficient and demanding on the power supply.

The worst case occurs when turning on the spot. As the vehicle rotates, the track contact points move in an increasingly horizontal direction towards the track end points as illustrated in Figure 2.13 (indicating a clockwise rotation). The high lateral forces due to friction produce excessive wear on the tracks, particularly on rough surfaces.

An indication of the frictional is shown in Figure 2.13. The magnitude of the friction in proportional to the distance from the centre and therefore it follows that the total force required depends on the total contact length and the weight of the vehicle. The required forces can be reduced by designing a short, wide vehicle, using large turning radii and placing most of the vehicle weight at the geometric centre.

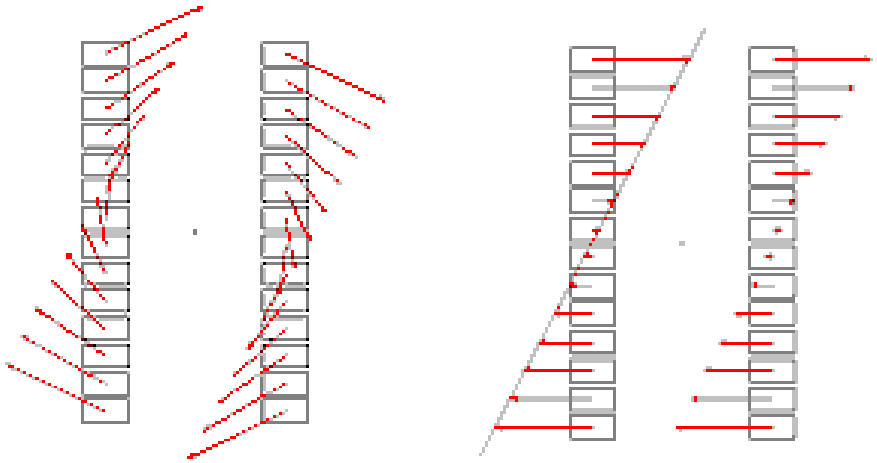

Figure 2.13 Skid steering turning on spot LEFT: Track segment movement direction RIGHT: Relative friction forces between track and ground to overcome

Another important factor for autonomous robotic systems is the loss of odometry information. Tracked differential drive vehicles inherently lose accuracy of position information due to the non-uniform movement of the treads when turning. Any slippage of the treads across the ground, even during relatively straight line motion results in rapid accumulation of odometry errors which cannot be eliminated without another method of positioning.

2.3.5 Existing Onboard Hardware

This section describes the existing hardware components present on the mechatron at the onset of this project. Although the mechatron could accomplish remote controlled movement at the completion of the initial mechanical design, this was not the case at the start of this project. The mechatron did not have any working electronic systems due to many of the components being relocated to other projects. This formed the motivation to undertake a complete overhaul and redesign of all electronic systems.

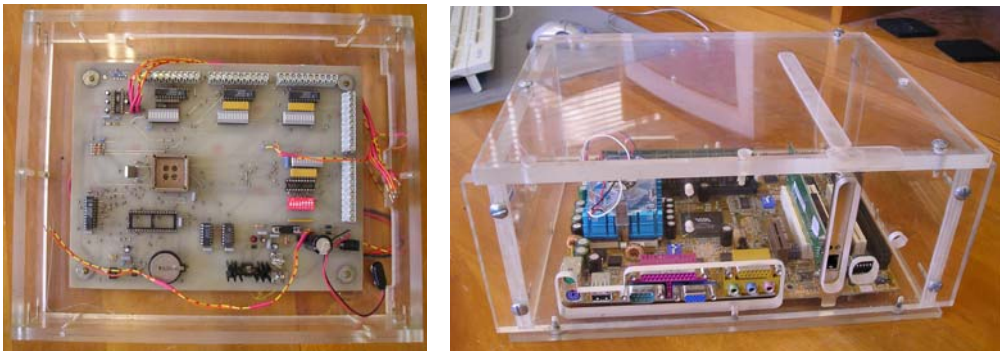

Figure 2.14 Original microcontroller board and PC motherboard

The original 8051 based microcontroller and PC motherboard is shown in Figure 2.14. The microcontroller provides adequate space for modifications and connection to peripherals however, the excessively large size of the board and plastic enclosure complicates mounting. The existing power supply system consisting of a UPS and ATX converter are shown in Figure 2.15. Plastic boxes secure the ATX converter and transformers making the entire power supply excessively bulky and heavy.

Figure 2.15 Original power supply consisting of UPS and ATX converter

2.4 PROCESSOR ARCHITECTURE

A number of different hardware architectures are available to perform the onboard processing algorithms required by this project. Data input/output, communications and hardware control and monitoring are some of the tasks required of the central controller.

Requirements of the architecture specific to this project are outlined below:

1) **High Processor Speed:** The CPU speed directly affects the number of computational tasks that can be executed each second. A higher CPU clock enables increasingly complex algorithms to be performed however at the expense of increased power consumption which is not desirable for battery based applications.
2) **Data Memory:** The data memory (RAM) is used for the temporary storage of variables and data for the current application. Fast access to memory with a large capacity is important for computationally intensive processes such as image processing and floating point math.
3) **Program Memory:** Program memory is used to store the operation instructions for robot control. To enable complex tasks such as motor control and navigation algorithms a large program memory is required because these tasks utilize a large number of instructions. In addition to storing the actual robot-control application, the program memory stores other applications such as the operating system and data analysis software therefore a storage capacity exceeding gigabytes is desirable. The program memory must also be easily reprogrammable allowing code modification.
4) **Interfacing:** It is expected a large number sensory devices and other electronic systems will require interfacing to the main CPU. The selected architecture must include provisions for a wide range of interfacing protocols such as serial communications and data acquisition.

Available systems were researched and evaluated on the basis of cost, size, processing capability and system integration. Some of the solutions considered are discussed in the following sections.

2.4.1 Embedded Controller

A wide range of embedded microcontrollers are available offering high processing capability and low power consumption depending on the model. Data input/output and many communication peripherals are often standard however functionality is limited by program memory size mainly measured in kilobytes.

2.4.2 FPGA

FPGA (Field Programmable Gate Array) technology allows hardware based designed to be implemented on a single IC. Although providing in-application reconfiguration, FPGA's are limited by gate number and development of external interfaces.

2.4.3 Handheld PC

Small computers such as a Palm PC offer reasonable processing power and very low power consumption however connection to other hardware is difficult. Development tools and driver support is not as widely available for handheld PC's as standard computers, increasing implementation complexity.

2.4.4 Laptop Computer

A laptop computer or notebook provides substantial processing power compared to other small systems and low power consumption however the cost is high and upgrades require entire system replacement. Data acquisition devices are often limited to low cost USB systems with limited functionality.

2.4.5 Full Size PC

A full scale desktop PC provides the highest processing capability for a relatively low cost however the size and power consumption limits the usefulness on a mobile robot.

2.4.6 ShuttleX PC

A Shuttle PC provides a good compromise between a laptop computer and full size desktop PC. Processing power is comparable to a standard PC while complex data I/O can be achieved using the onboard PCI slot and USB ports.

2.4.7 Selected Architecture

The ShuttleX PC is the selected primary control architecture for this project (Figure 2.16). The small form factor and lower power consumption compared to a full PC are ideal qualities for mobile robotic applications. The system provides ample processing power for hardware control and navigation algorithms and allows for future component upgrades if required.

Figure 2.16 Small form factor ShuttleX PC

The specifications of the computer system are:

- AMD Athlon® XP 2800+ CPU
- 512 MB RAM
- 80 GB Hard drive
- Dimensions: 290 × 203 × 180 mm (l × w × h)
- 1 × AGP 8x Graphics Adapter
- 1 × PCI Adapter
- Windows XP Professional Operating System

2.5 ELECTRONICS POWER SUPPLY

A suitable power supply unit is required to power the numerous onboard electronic systems. The Mechatronics group has previously used an uninterruptible power supply (UPS), shown in Figure 2.17 to convert the 24 V DC battery supply to the 230 V AC. The high voltage is regulated to supply the computer and electronics by a standard ATX PC power supply. Although this system worked and provided a cheap and simple solution, a number of disadvantages were apparent and problematic for mobile robots:

- Heavy 19 kg weight of UPS
- Large physical size of UPS takes up room on mechatron
- Conversion of 24 V DC to 230 V AC then back to DC is inefficient
- The UPS must be started by mains supply thus not appropriate for outdoor use

Figure 2.17 LEFT: Olympic OTC-1000A UPS RIGHT: ATX Switch mode power supply ACE-828C

Rather than design a custom DC – DC converter for each electronic subsystem a commercial switch mode power supply has been selected. Illustrated in Figure 2.17, the ACE-828C Industrial Power converter accepts 18 – 32 V input and outputs 3.3 V, ±5 V and ±12 V for the computer and peripherals.

A study of efficiency (*Payne*, 2004) shows an increase of 30 % to 77 % efficiency of the ATX converter over the UPS based system. This is important for a mobile robotic application where conservation of energy is crucial to an acceptable running time.

2.6 BATTERY SELECTION

A number of different technologies are available to provide power to the motors and other onboard electronic systems. Specialized devices such as fuel cells provide a high power density to weight ratio but are restrictedly expensive. Cheaper and self sufficient forms of energy such as solar panels provide endless energy but operation is restricted to outdoors during daylight. In addition, a large installation would be required to provide the high power required in this application. Due to the large size and weight of the vehicle, batteries have been selected as the primary energy source. Batteries are lower cost than the alternative systems researched and they can provide the high capacity and high currents required by the motors and other electronics.

2.6.1 Required Specifications

A number of prerequisites have been considered when selecting a suitable battery type. Physical dimensions of the robot platform inherently limit battery size and weight however, these factors must be considered against operating time because larger batteries generally mean a higher capacity. The battery technology itself is also considered important because although some advanced options do exist such as high capacity gel cells, the high price of these exceed the budget of this project and cannot be used at this stage.

An analysis of the actual power consumption is discussed further in section 6.1 however a summary of the battery requirements are shown here:

- Drive motors require 24 V DC
- Electronics ATX converter require 18 – 32 V DC
- Dimensions to fit chassis battery tray
- Weight not to significantly reduce payload capacity
- Approximately 20 – 25 Amps continuous current
- Approximately 35 – 40 Amps peak current
- Operation time exceeding 1.5 hours during development

2.6.2 Review of Battery Types

There are many varieties of battery available on the market, each specializing to a different application and energy requirement. There are five main categories of rechargeable batteries available for consideration:

- Sealed Lead Acid (SLA) or flooded lead acid (FLA)
- Nickel-Cadmium (NiCad)
- Rechargeable alkaline-manganese (RAM)
- Nickel – metal hydride (NiMh)
- Lithium-ion (Li-ion)

The energy capacity of a battery is usually a direct relation to the physical size of the battery and for this reason coupled with the low cost, only lead-acid batteries are considered. SLA batteries have the lowest energy density of all battery types but this is factored with the high durability and capacity. The highest energy density attainable is from Li-ion batteries, however they are very expensive and to get comparable energy storage to an SLA would require a very large battery installation. Ni-Cad and Ni-Mh batteries are good solutions for smaller scale robots, they do however suffer problems such as memory effect and high self discharge rates, and the high cost is also a limiting factor in this project.

The lead-acid battery is the most suitable type for this application and three main categories are available:

1) Automobile Starting Battery
2) Deep Cycle Battery
3) Marine Deep Cycle Battery (hybrid)

The automotive battery is designed with thin lead plates, constructed in a sponge-like fashion to provide very high currents in a short period of time. The thin plates allow good contact between the sulphuric acid and current generating active material. The depth of discharge is quite small, about 1 – 5% and is therefore easily recovered by the charging system. Conversely, deep cycle batteries are constructed with thick plates of solid lead and a higher density active material. This allows discharge with less plate deterioration but does limit the current output compared to a starting battery

of similar size. The marine deep cycle battery, often called a “hybrid” is essentially a combination of the previous two types. They can be used for engine starting in marine environments but are also suited to deep cycling for powering onboard electronic systems. Although cheaper than normal deep cycle batteries they cannot be discharged as frequently without damage resulting. The cost of deep cycle batteries is significantly higher than the automotive variety and a number of subcategories are available.

Flooded or “wet” batteries are the most common and cheapest form of sealed lead, deep cycle battery. These have a tendency to leak if tipped over or mounted in a non-horizontal position but do allow consumed water (by H_2 and O_2 gas production) to be topped up. Valve Regulated Batteries (VRLA) (also called SLA) maintain a positive pressure of 3 – 5 psi within the battery causing internal recombination of the oxygen and hydrogen gas. This allows the battery case to be sealed, preventing acid spillage and emission of corrosive gas even in difficult installations. The VRLA groups exhibit two different types of technology. The Gelled Electrolyte (Gel Cell) uses a “jelly” like electrolyte so that no spillage is possible. AGM batteries use a glass fibre material to retain the electrolyte and prevent movement.

The gel cells are generally better suited to cycling than the AGM but they are not as robust and resilient as the flooded. Another technology combines the low maintenance and sealed nature of the VRLA while retaining the resilience and integrity of the flooded type. The RVP (Recombinant Vent Plugs) battery comprises a palladium catalyst fitted to the vent plug where the hydrogen and oxygen is combined into water before returning to the battery cell itself. This option was not explored because batteries suitable for the mechatron could not be sourced locally in a reasonable time frame.

2.6.3 Battery Ratings

A number of different battery rating methods are in use, some more suited to certain types of battery. Standards set by SAE (Society of Automotive Engineers) have been adopted by New Zealand battery manufacturers to standardize battery features.

The *Reserve Capacity* (RC) rating gives the time, in minutes, that a fully charged battery can supply a constant 25 amps at 25 °C. The CCA rating is *Cold Cranking Amps* and is more applicable to automotive batteries than batteries designed for deep cycling. The CCA rating gives the discharge load in amperes that the fully charged battery can supply for 30 seconds at -18 °C and maintain a minimum 1.2 Volts per cell. The A/Hrs rating (Amp/hours) gives a rough indication of the current the battery can supply for different time periods. A battery rated 50 A/Hrs could supply roughly 50 A for 1 hour, 25 A for 2 hours or 12.5 A for 4 hours and so on. The RC and A/Hrs ratings are the most useful indicators for battery capacity for a mobile robot application.

2.6.4 Selected Batteries

For the final mechatron implementation, a system of Gelled Electrolyte batteries would be ideal however during development and testing marine deep cycle (hybrid) batteries have been selected. This reduces the overall cost of battery installation while still providing the high current and battery life required in a mobile robot.

Figure 2.18 Hella Endurant battery

Two 12 V Hella Endurant Cyclemaster flooded batteries, Figure 2.18 are connected in series to provide 24 V to the motors and electronics. The battery specifications are outlined in Table 2.2

Manufacturer	Hella
Model	MDC24/85 Endurant Cyclemaster
CCA	515 Amps
Capacity	85 A/Hrs
Dimensions	270 × 170 × 250 mm (l×w×h)
Weight	19 kg each

Table 2.2 Selected battery specification

These batteries provide approximately 85 A/hrs / 25 A = 3.4 hours of operation time when fully charged assuming a constant current of 25 A (refer section 6.1). To extend the life of the batteries the running time should be reduced to ensure a 50% or less discharge thus providing 1 – 1.5 hours of reliable operation and meeting the desired criteria during development.

2.6.5 Charging Procedure

The batteries are individually charged using a pair of high current laboratory power supplies. It is possible to charge both batteries in series using a single supply however this is not recommended long term as it reduces the effectiveness of the charge and could cause damage over time due to slight differences between the batteries.

Batteries designed for deepcyling require a slightly higher charging voltage than standard automotive batteries. A charging voltage of 14.0 – 14.7 V (2.33 – 2.45 V per cell) is applied across each battery ensuring the ground of the power supplies is isolated. After periods of deep cycling where a significant portion of battery charge is consumed a lower charging voltage is used for the early stages of charging. This ensures the initially high charging currents do not damage the batteries. The charging voltage should also be reduced once the charging process is complete to prevent deterioration of the battery internals; this is called a "float" charge. A float charge however can also cause corrosion of the positive plates so the ideal solution is to remove the charge source completely and monitor the battery state, this can be achieved using some high end chargers.

It is important to note the depth of discharge significantly affects the battery lifetime and ability to hold a charge. If a battery is repeatedly drained to low levels the life of the battery will be less than if only partially discharged. The manufacturer of the selected batteries recommends a 50 % or less discharge to ensure battery integrity over time. This is the opposite effect as observed with NiCad batteries where is essential to fully discharge the battery before recharging.

Sulphation is a condition that develops when the battery is left flat or partially charged. A build up of sulphur in the water restricts current during charging and in severe cases will render the battery useless. Another process that affects battery longevity is called Acid Stratification which in turn increases the incidence of Sulphation. During charge and discharge cycles the consistency of the electrolyte changes. Charging produces acid while discharging produces water which is lighter than acid and floats towards the surface. When the battery is charged to a near full charge this higher cell voltage causes hydrogen and oxygen bubbles to rise through the electrolyte effectively mixing the acid and reversing the acid stratification condition. It is therefore important to fully charge the batteries at each charge cycle before use and ensure they do not sit in an uncharged state for extended periods of time.

The action of charging lead-acid batteries generally causes a loss of water which must be replaced. This process is only possible in flooded lead acid batteries which have removable vent caps. The electrolyte levels should be regularly checked and only topped up with clean water to within about 13 mm above the cell separator; it is important to not overfill the cells as this causes corrosion and a reduction in battery life.

2.7 DATA ACQUISITION CARD

A suitable Data Acquisition (DAQ) card was required for this project to increase the input/output (IO) capabilities of the main CPU processor. A DAQ card provides the means for complex hardware interfacing beyond the standard “legacy” ports such as the serial and parallel ports.

There exists a large number of data acquisition devices available, each best suited to different operating environments and tasks. As a result, the cost and performance characteristics can vary substantially between models. Primary tasks of the DAQ card in this project include acquisition of sensor data, connection to and control of a motor driver system and the ability to adapt to future project requirements.

A number of criteria based on the project requirements were used when evaluating the different DAQ devices available, these include the following:

- Interface to PCI slot or USB on ShuttleX motherboard
- Include software drivers suitable for use in MATLAB
- Fast acquisition of signals
- Analogue input channels for sensor data acquisition
- Analogue output channels for control and future systems
- Digital IO channels for communications and control
- Timers and counters for periodic signal generation and acquisition

A National Instruments M-Series multi-function DAQ (Data Acquisition) card (Figure 2.19) has been selected to meet these specifications. Although a number of low-cost, light weight USB devices exist, the performance and features of these are generally very limited. The selected PCI-6229M model connects to the PCI slot and offers increased performance with the added benefit of fitting within the computer case so valuable mounting space on the mechatron is not wasted.

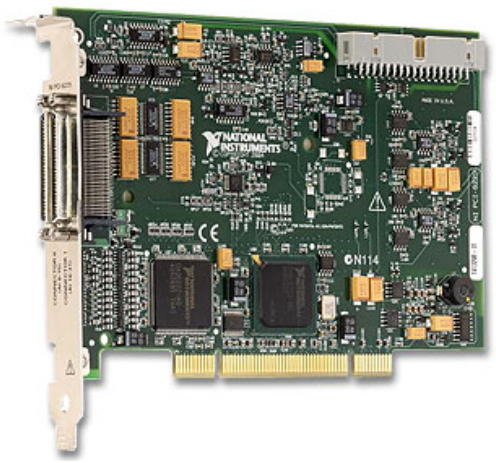

Figure 2.19 National Instruments PCI-6229M DAQ Card

These devices are low cost and provide optimised functionality for a wide range of applications in hardware control and sensor measurement.

Some key features of the card are:

- NI-STC2 and NI-PGIA Technology
- NI-DAQmx software drivers
- 32 16-bit Analogue Inputs 250 kS/s
- 4 16-bit Analogue Outputs 833 kS/s
- 48 TTL/CMOS Digital IO
- 32 DIO Hardware timed at 1 MHz
- 2 32-bit 80 MHz Timers/Counters
- 6 DMA Channels for fast data throughput

2.8 OTHER HARDWARE COMPONENTS

A number of other hardware components essential to this project have been selected and some of these are outlined in the following sections. A complete review and justification has been limited to a select number of important components however a brief description of most devices is included in this section for completeness.

2.8.1 Wireless Network Adapters

A pair of wireless network adapters has been selected to provide a communication channel between the mechatron and a remote base station. A laptop computer is currently used as the base station however depending on the future implementation of the device; a dedicated standalone base station may be utilized.

Figure 2.20 LEFT: DWL-120+ Wireless UBS Adapter RIGHT: DWL-650+ Wireless Cardbus Adapter

A PCMCIA card bus adapter is used for the laptop while a USB adapter is installed on the robot computer. Both devices are standard 2.4 GHz wireless adapters from D-Link, shown in Figure 2.20 using the 802.11b protocol. The devices are connected with an ad-hoc topology and transfer speeds are up to 11 Mbits/s with a strong signal. The connection procedure using Remote Desktop software is described in section 5.2.1.

2.8.2 Onboard Video Camera

An onboard colour video camera, Figure 2.21, provides the user with a real time view of the robot operating environment. This is used for robot monitoring or tele-operated control during configuration and testing.

Figure 2.21 Logitech QuickCam Pro 4000 webcam

The camera connects to the host PC through a USB 2.0 interface. Video resolution of 640x480 is achievable in addition to a 1.3 mega pixel still camera. The operation and connection to the webcam is described in section 5.6.4.

2.8.3 Infrared Proximity Detectors

A number of Sharp GP2Y0A02YK infrared (IR) detectors illustrated in Figure 2.22 provide a measure of distance to objects surrounding the mechatron. Each device produces an analogy DC voltage between 0.25 and 3 V giving a non-linear representation of measured distance, updated every 32 ms. The process of converting the voltage to a range measurement and the mounting of the sensors are described in section 4.8.

Figure 2.22 Sharp GP2Y0A02YK infrared sensor

The sensors use a signal triangulation method instead of reflected intensity; this gives greater immunity to signal variance for objects with different surface properties and orientation. A range of approximately 20 – 160 cm is achievable under low lighting conditions although this range is reduced in bright daylight due to sensor saturation.

2.8.4 Electronic Compass

An electronic compass (Honeywell HMR3300) shown in Figure 2.23 provides robot heading information for the navigation and guidance system. The compass module utilizes solid state magneto-resistive sensors to measure the Earth's magnetic field.

The compass measures orientation in 3-axes giving measures of heading, pitch and roll. Additionally, the heading is compensated for tilts of ±60° using the onboard 2-axis accelerometer. Communication is through an ASCII based serial interface. Compass modules are described in more detail in section 4.4.

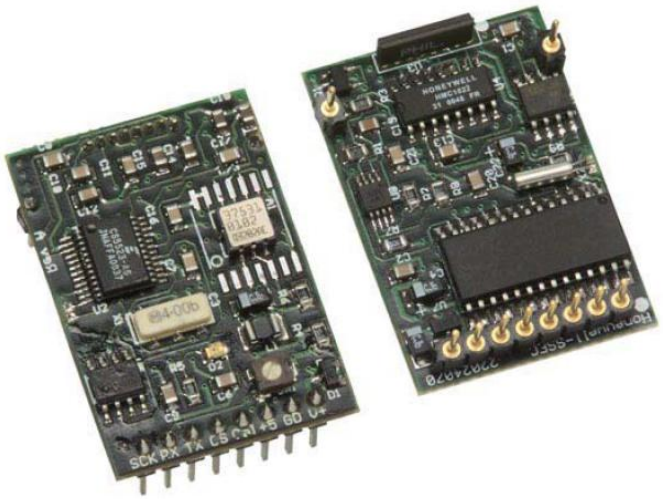

Figure 2.23 Honeywell HMR3300 electronic compass module

2.8.5 GPS Receiver

Absolute positioning of the mechatron is achieved using a GPS (Global Positioning System) antenna and receiver. The Motorola M12+ Oncore receiver, Figure 2.24, uses the NAVSTAR satellite GPS system to accurately determine 3-dimensional position, velocity and time worldwide.

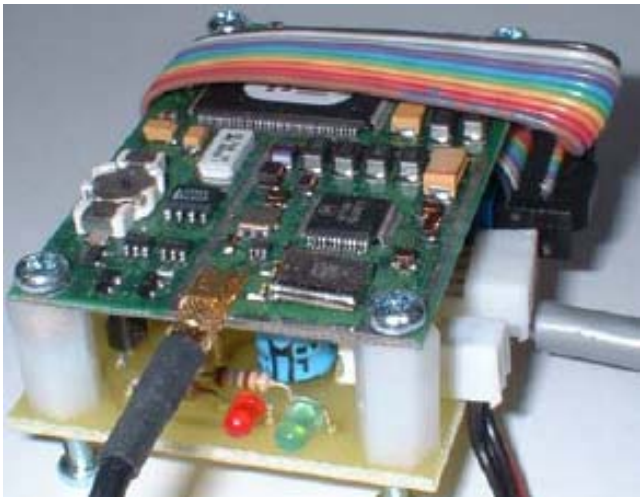

Figure 2.24 Motorola M12+ Oncore GPS Receiver

The GPS receiver communicates through a serial data interface and positioning information is reported once each second. The receiver includes a 12 channel design meaning 12 satellites can be tracked simultaneously. The GPS system and implementation is described in more detail in section 4.5.

2.8.6 Inertial Sensor

A 3-axis accelerometer shown in Figure 2.25 provides the means for an inertial navigation system to complement the GPS receiver. The MMA7260Q sensor from Freescale Semiconductor is a low cost, capacitive micro machined device including selection between four g sensitivities in the range ±1.5 g to ±6 g.

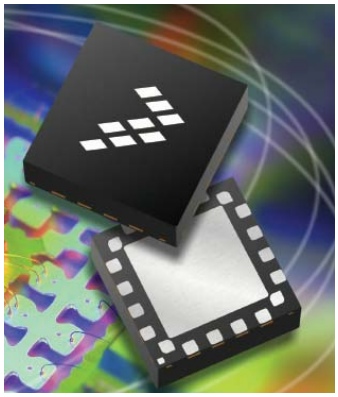

Figure 2.25 MMA7260Q 3-axis accelerometer

2.8.7 Motor Drivers

A pair of high power, reliable motor driver units (Figure 2.26) has been selected to effectively control the mechatron drive motors. The Rhino DS72K scooter controllers manufactured by Dynamic Controls provide a number of advantages over other systems researched including programmable drive characteristics and that they have been designed for the drive motors being used. Motor drivers and the implemented motor control hardware are discussed in more detail in Chapter 3.

Figure 2.26 Rhino DS72K motor driver module

3. MOTOR CONTROL

3.1 INTRODUCTION

The process of effective and reliable motor control forms the base of this chapter. A number of factors provide the motivation to create a single motor driver solution for robot control. As technology advances, changes in platform topology and component availability create problems when hardware peripherals such as DAQ cards and PC's become obsolete and are upgraded. A motor driver should be relatively immune to such events, still having the capacity to function and interface to future systems. Another crucial feature is a generic or modular design topology. Other robotic platforms could utilize the same motor drivers reducing robot design time and troubleshooting complexity.

As stated in section 2.3.1, the drive motors are of DC variety, therefore the motor drivers must be capable of transferring the high current 24 V supply from the batteries through to the motors. A number of methods are available to achieve this and are discussed in the following sections with an analysis of the various advantages and disadvantages of each.

3.1.1 DC Motor Theory

A number of different motor types exist which are suited to different applications. Since this project utilizes DC motors, a discussion on the principles of operation is limited to this type. Although a few varieties are available, the DC motor essentially consists of three main components. The *rotor* is the inner moving part that forms the motor shaft where a load can be attached. Surrounding the central shaft is the *stator*, this part remains stationary and usually consists of two or more permanent magnetic pole pieces. A continuous copper wire called the *armature winding* is wound around the rotor and produces a magnetic field when a current flows through it.

A mechanical commutator is connected to the rotor and winding assembly which reverses the current polarity as the shaft rotates, thus generating a changing magnetic field around the windings. The interaction between the changing magnetic dipoles of the rotor and the constant stator magnets produce a torque and force the rotor to continuously spin.

3.1.2 Possible Solutions

Two broad categories of motor control are possible, *analogue* and *digital*. Analogue motor controllers, while relatively cheap and easy to implement for small manually operated drive systems can be very troublesome for computer controlled applications. A common technique is to convert the digital control signal to an analogue voltage which then controls the motor voltage with a device such as a variable resistor. This method is very inefficient and would dissipate excess power as heat, producing significant stresses on the components. The complexity arises when a mechanical actuator is required to adjust the variable resistor thus further impeding accurate motor response.

Digital solutions that utilize relays are a good option when the frequency of switching is small and no form of velocity control is required. A mechanical relay will only allow simple on/off operation as a computer controlled mechanical switch. Direction control can be achieved by adding a second relay for polarity reversal; however the functionality is still too limited for this project and is not used. The high currents present in the motors would easily burn out most readily available relays, therefore expensive industrial grade devices would be required increasing project cost. Relays also have a limited lifetime due to contact wear so are not suitable for the frequent operation in a robotic vehicle.

A superior solution is to form a switching arrangement utilizing semiconductor switches and a digital controller such as an embedded processor. The controller has the facility to pulse the high power switches with a pulse width modulated (PWM) square wave, (Figure 3.1) which in turn determines the power delivered to the motors from the supply by the different levels of duty cycle.

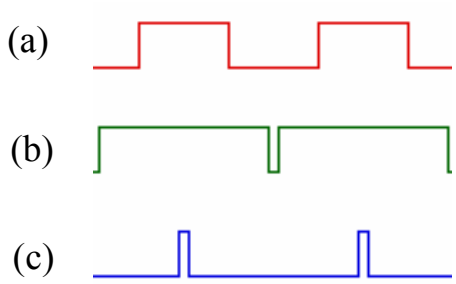

Figure 3.1 PWM signals and transmitted power (a) 50% (b) 90% (c) 10%

The integration of a digital controller in the motor driver has the added advantage of separating the timing critical motion control algorithms (PWM generation) from the higher level robot software. This is particularly important when a non-real-time operating system such as Microsoft Windows XP is used where process timing cannot be guaranteed constant.

PWM signals cannot directly control the motors therefore a power converter is required and the most common form of switching motor driver is the H-Bridge topology illustrated in Figure 3.2. Four switching devices are connected to provide four quadrants of DC motor operation, driving and breaking in both the forward and reverse directions.

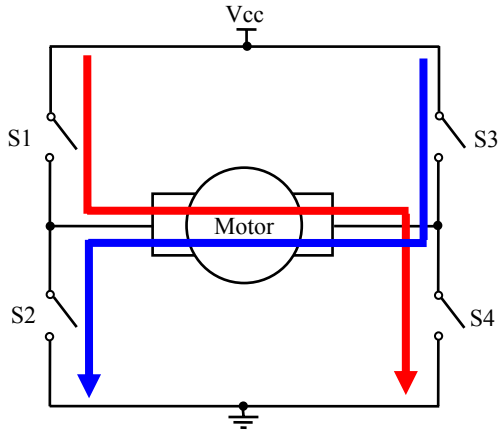

Figure 3.2 H-Bridge switching topography

The H-bridge works by directing the motor current in a certain path by manipulating the four switches S1 – S4. Forward motion is achieved by turning on switches 1 and 4 with 2 and 3 off. Likewise, when 2 and 3 are on and 1 and 4 are off, the motor rotates in the reverse direction. Braking can be achieved by opening the high side (S1 S3) switches and closing the low, thus creating a feedback loop through the motor and ground.

3.1.3 Differential Drive Motor Control

The implementation of a differential drive motor control system presents a different set of challenges compared to conventional speed or position only designs where control of only one motor is necessary. Two motors are used to individually drive each side of the robot, Figure 3.3, so the motor driver must have at least two channels and be capable of controlling both motors in tandem. The motor driver should also have provision for different control modes in order to adapt to different driving preferences or robot installations.

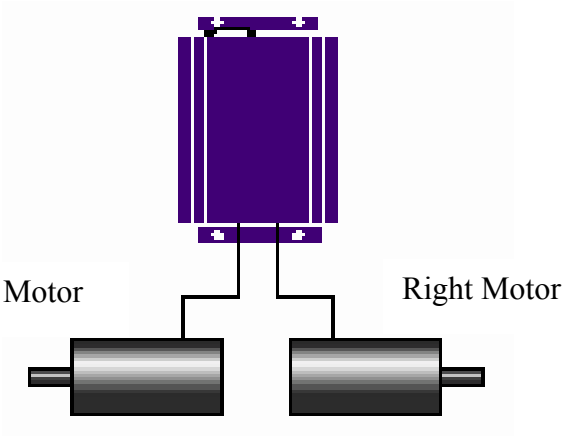

Figure 3.3 Differential drive configuration consists of two opposing motors

Independent speed commands are required to individually command each motor. This type of operation is best suited to generic motor control applications where the final drive configuration is unknown or changeable and is therefore compatible with other robotic vehicles under development.

Combined speed and steering commands are used to control the motors in combination. The forward/reverse velocity information is coupled with the left/right steering information to propel and rotate the vehicle accordingly. This method provides a cost effective and straightforward way of moving and steering differential drive systems such as tank-style robots.

3.2 EXISTING MOTOR DRIVERS

Previous motor controller circuits designed within the Mechatronics Group have been quite varied and focus on platform specific designs. The main parallel between most robotic platforms is that they run from a 24 V battery system. This section discusses some of the past attempts at motor control and their shortfalls with respect to this project.

3.2.1 Outdoor Mechatron

The original motor driver design for the outdoor mechatron was custom built and utilized both a DAQ card and microcontroller to supply control signals to the high power circuitry. A simplified power drive circuit for the motors is illustrated in Figure 3.4. The logic control signal drives a Darlington pair which is optoisolated from the high power circuit for protection of the microcontroller.

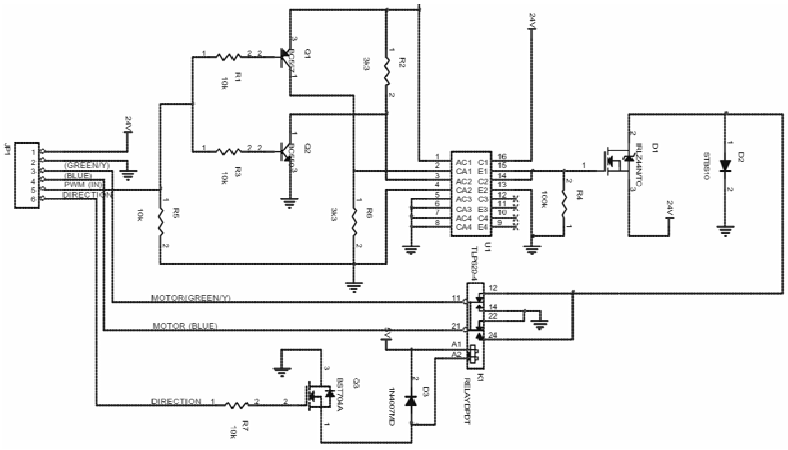

Figure 3.4 Simplified single switch and relay drive circuit

Relays were used to implement direction switching however it is desirable to replace such mechanical components with semiconductors to reduce risk of failure. Another major limitation of this design was the lack of protection circuitry. The high loads and back emf created by the motors produced excessive strain on the components often resulting in damage after short operating periods. Development of a new driver interface requires switch protection and snubber circuitry to dissipate the transient currents.

3.2.2 Co-operating Robots

The pair of co-operating robots (Itchy & Scratchy, section 2.1) use a different type of drive configuration to that of the outdoor mechatron's original circuit. A tricycle based design is used with one motor for drive and the other positioned at the rear for steering. Consequently the drive circuits are designed for a pair of motors with a lower power rating than the outdoor mechatron making them unsuitable.

The motor drivers, illustrated in Figure 3.5, use a parallel communication protocol with the microcontroller that is specific to the installed LabPC+ DAQ card. Although the DAQ card has been recently upgraded to the NI PCI-6025E, the requirement of this communication mode is still present which restricts implementation to robots with this type of DAQ card and thus restricting the use of newer devices.

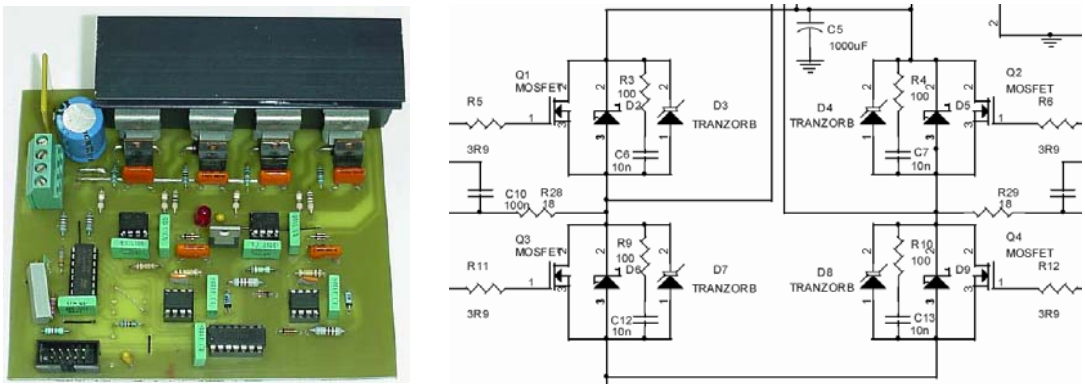

Figure 3.5 Itchy and Scratchy motor drivers LEFT: H-bridge circuit RIGHT: Simplified schematic showing H-bridge and snubber circuitry

The power circuit uses a PWM H-bridge switching 24 V and 15 A up to 31 kHz. Logic signals are 5 V and temperature and current sensing circuitry is installed. These motor driver circuits include protection measures to prevent damage to the MOSFETs including 1) free wheeling diodes, 2) R-C snubber and 3) transient suppression diodes. Although these have mostly worked successfully, a couple of incidents have occurred where the driver circuitry has failed. Due to the larger loading of the outdoor mechatron it was concluded these motor drivers could not be guaranteed to function under the high current conditions and so a different system was required.

3.2.3 Marvin

Documentation of the original motor drivers is sparse however it is known they were unreliable and later replaced by those originally implemented on the outdoor mechatron (3.2.1). Other circuits were designed and tested but none were successful in continuous operation. More recently Marvin (section 2.1) was fitted with the drivers specified in 3.2.2, however problems with reliability and the dependence on certain hardware means they are not suitable for future research on Marvin. This robot also utilizes a differential drive so development of drivers for the outdoor mechatron considered the additional design criteria ensuring driver compatibility.

3.2.4 Underwater ROV

Like other robots, the ROV (section 2.1) uses a combination of 8-bit micro and DAQ card to provide control. The original system (*King*, 2002) used a PWM controlled half bridge rectifier for each motor however, operational problems led to a redesign (*Jungwirth (et. al),* 2004) which also added a bootstrap circuit to correctly drive the MOSFETs.

The motors are universal 110 VAC AEG, and therefore require a different driving circuit to those previously mentioned which falls outside the scope of this project.

3.3 GENERIC MOTOR DRIVERS

The first attempt at creating a set of universal motor drivers was completed by a previous master's student (*Jensen,* 2004). The project aimed to reduce robot development time and simplify troubleshooting by creating a generic system for use on multiple robotic vehicles. Consisting of a low power microcontroller board and high current H-bridge driver the project potentially represented a significant step forward for the Mechatronics Group.

The set of generic motor drivers were initially designed for the control of robotic vehicles within the Mechatronics Group at the University of Waikato however future development could commercialize the circuitry. These units were intended to be installed on the outdoor mechatron, with this project aiming to ensure correct operation and a reliable method of control.

Evaluation and testing of the system however outlined significant shortcomings of the drivers thus they are not suitable for implementation on the outdoor mechatron.

This section describes the project and hardware developed including additional modifications to the original modules. Results of testing and the reasons for not installing the units on the mechatron are also discussed.

3.3.1 Project Outline

The proposed motor driver solution consists of a pair of high power H-bridge driver boards and a low voltage microcontroller board for control. The digital circuit replaces the DAQ card functions found in some other projects and provides the PWM signals to control the switches. The power circuit controls the 24 V source to the motors while providing circuit monitoring feedback such as current and temperature.

Low level control of the power driver circuit was separated from the main PC CPU to free up valuable resources for other program tasks such as navigation of the platform. As the controller must be adaptable to future hardware and software requirements the system was separated into the two main components based on function thus simplifying design and construction.

The following design criteria were also considered during the project:

1) Control of more than one motor
2) Easy transition from old designs incorporating digital communications
3) Bi-directional communication with circuit monitoring
4) Utilize component protection circuitry

3.3.2 Hardware Components

The high power components of the motor drivers consist of a pair of H-bridge driver boards (Figure 3.6). Each utilize a full bridge, MOSFET based design allowing speed and direction control in the four quadrants (section 3.1.2) of operation. An additional MOSFET switch enables control of the electro-mechanical brake systems present on Marvin and the outdoor mechatron.

A HIP4081A MOSFET driver IC from Intersil Corporation provides the necessary drive signals to control the switches while current sense resistors monitor power dissipation. The overall circuit design is a slight modification of the layout suggested by the Intersil datasheet with added logic to enable direction control.

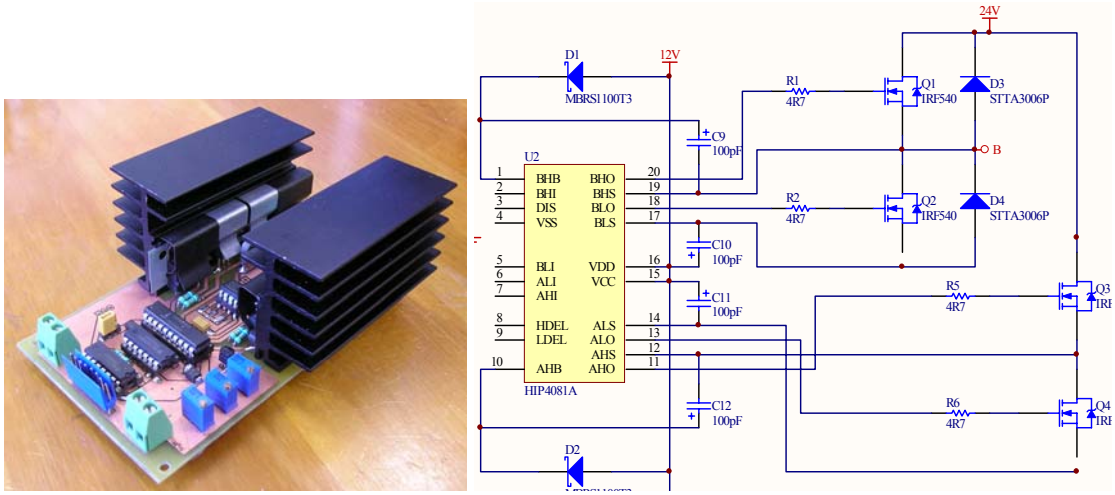

Figure 3.6 LEFT: One of the H-bridge power circuit boards RIGHT: Simplified schematic showing H-bridge and HIP4081A MOSFET driver circuitry

Adjustment of dead-time switching between high and low side MOSFETs (to ensure shoot though does not occur) is realized with two 500 kΩ variable resistors, another 10 kΩ resistor is available to trim the midpoint of the current sense circuitry to enable calibration and correct determination of current through the H-bridge.

Switch protection consists of a RCD (resistor-capacitor-diode) snubber circuit to dissipate excess voltage transients during switching. Provisions to attach zener diodes are available to achieve faster clamping however power dissipation is lower than the RCD snubber.

Control signals for the power boards are generated by a microcontroller board shown in Figure 3.7. The PCB has a number of connector systems for interfacing to the motor driver boards, power supply and computer controller.

The popular 8051 architecture was selected for the 8-bit embedded controller allowing straightforward development and reprogram ability. Five channels of PWM outputs are available providing the necessary resources to control two H-bridge boards.

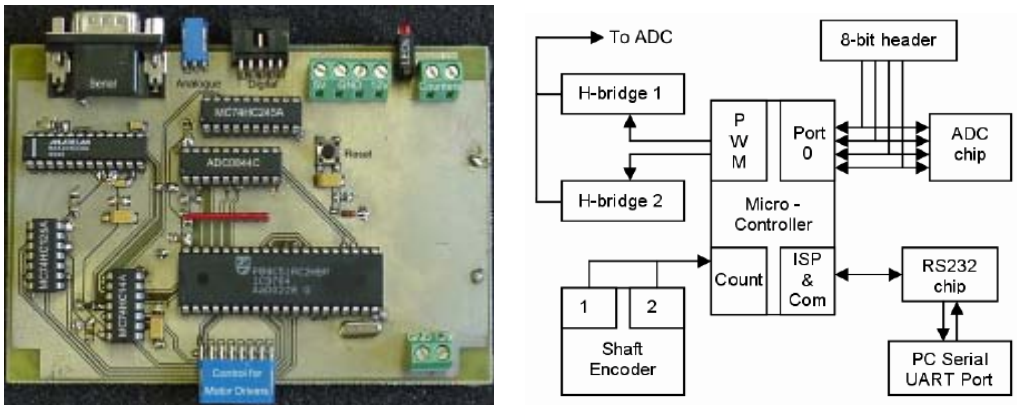

Figure 3.7 LEFT: Microcontroller board RIGHT: Microcontroller functionality

Communication and control channels for the design include a number of different protocols enabling compatibility with previously designed systems. An external ADC chip (ADC0844) provides four channels and outputs the data to an 8-bit parallel bus. This allows motor control from an external analogue control system if it was later required.

The same 8-bit data bus is also connected to an external header providing a digital interface compatible with parallel communication protocols such as those previously implemented with the LabPC+ DAQ card. Finally a serial RS-232 interface is available to connect to a standard PC legacy serial port allowing direct computer control. A summary of the microcontroller functionality is illustrated in the right hand diagram of Figure 3.7.

3.3.3 Software Interface

At the time the generic motor drivers were being developed, the majority of robot programming was done using the MATLAB language. It was envisaged this software package would become the standard development environment for future projects and as a result the motor driver software was based around it. Although MATLAB is used as a major development tool, the final implementation of the robotic control software may be based on C++ or some other real time language including a Linux based system. These would better utilize the hardware resources and reduce the latency associated with a Windows based applications therefore new motor control system development has to account for this.

Four main functions were created to communicate with the microcontroller using the serial port through MATLAB and the underlying Java Language platform. The functions **conect_micro.m** and **disconnect_micro.m** setup and initialized the serial port objects and deleted them at program termination. The **talk_micro.m** function acted as an interface to both the **read_micro.m** and **write_micro.m** functions for data transfer of motor commands and status feedback.

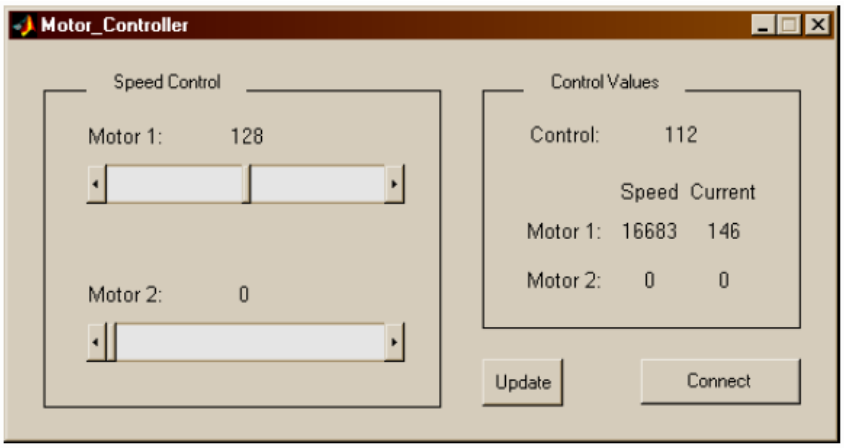

Figure 3.8 Initial motor driver front end GUI

A GUI (Graphical User Interface), shown in Figure 3.8, was created as the front end for the MATLAB drivers. The interface provided a useful tool when testing and troubleshooting the drivers and microcontroller code however functionality was limited and did not provide means for easy customization of driver parameters.

3.3.4 Testing and Evaluation

Before integrating the motor drivers into the mechatron control system and mounting on the robot, performance testing was carried out to determine their suitability. Due to the lack of documentation at the onset of testing and the incomplete assembly of some boards, initial testing was unsuccessful and full operation was not possible. Assistance from the developer enabled initial basic circuit operation and the removal of some software bugs present in the original design.

A small 24 V test motor was utilized during testing of the motor drivers to help ensure correct operation before implementation on high power motors. The test motor, shown in Figure 3.9, operates at the same voltage as the heavy duty motors on the mechatron but at a much lower current, thus reducing the electronic stresses on the drive circuitry.

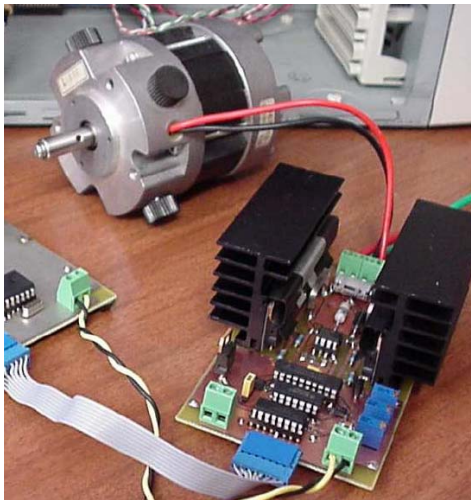

Figure 3.9 Small 24 V motor driver test motor

Although some of the problems later discovered with this initial motor driver design were related to the induced electrical stress from the high power motors, testing with the small motor was useful for investigating different switching techniques and software development. The portability of the test motor and driver circuitry enabled bench testing and diagnostics without needing to move the entire mechatron and associated drive components.

A significant problem discovered with the drivers was the detection of excessive switching noise on the power rails of the low power electronic subsystems. Graphs comparing the clean 5 V rail and the effect of the noise signal when the motor drivers are activated is shown in Figure 3.10.

Noise pickup through the oscilloscope leads was ruled out indicating the noise was permeating through the system, possibly due to a grounding problem.

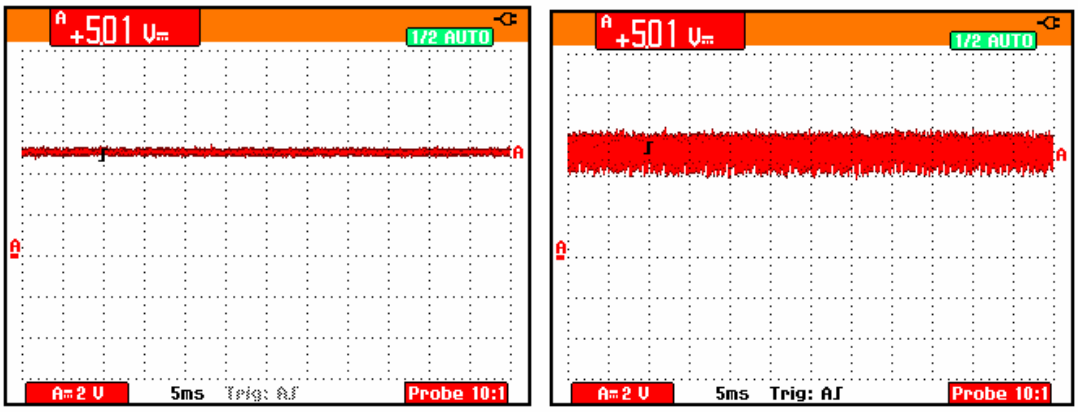

Figure 3.10 LEFT: Clean 5 V supply rail RIGHT: Noise on 5 V rail

A closer inspection of the noise signal (Figure 3.11) revealed it was the same frequency as the PWM driver signal of 34.72 kHz. This presented a useful starting point for determining a potential set of solutions aimed at removing the noise.

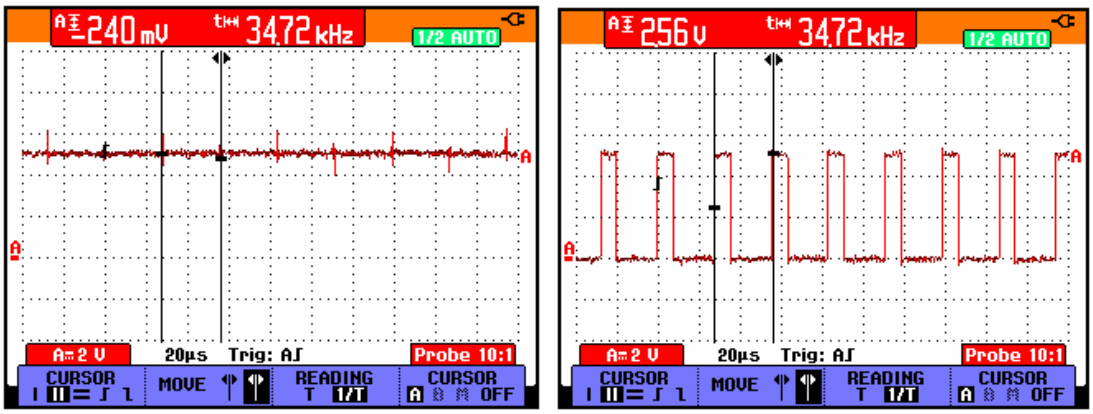

Figure 3.11 Noise from PWM at 34.72 kHz LEFT: Noise close up RIGHT: PWM signal

In addition to the unwanted noise superimposed on the power rails the motor drivers also suffered severe reliability problems during testing. On numerous occasions a

failure of the high power circuitry caused destruction of components and on one occasion a small fire on the PCB. Although the exact cause of the problem has not yet been resolved it is understood a shoot-through event is most likely. This has occurred due to a failure of either the MOSFET driver IC to correctly co-ordinate switching or the MOSFETs themselves becoming overstressed during operation.

Irregularities were located in the microprocessor code between the two driver channels, seemingly causing one unit to fail more often than the other. Modifications to the switching algorithms and dead-time adjustments were therefore completed in an effort to reduce component stress however the problem, persisted indicating other issues.

3.3.5 Modifications

A number of modifications were made to the original motor driver design, both for robot mounting and in an attempt to provide reliable and noise free operation. This section describes these additions and the results obtained.

Mounting Enclosure

A modification not directly related to the reduction of noise signals was the creation of a suitable enclosure for the driver units. Made of clear acrylic plastic the enclosures are designed to provide protection of the circuitry from environmental effects while allowing a stable mounting platform to the robot chassis.

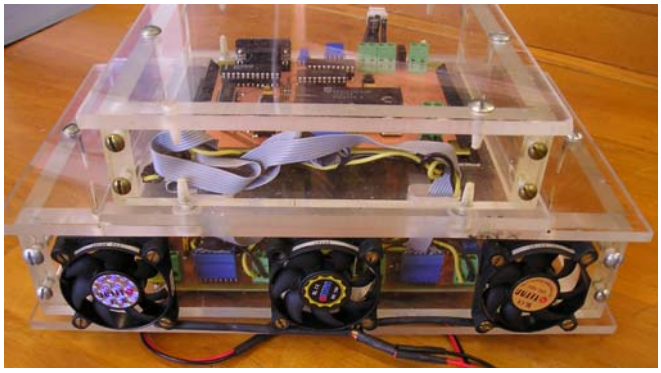

Figure 3.12 Mounting enclosure and cooling fans for motor driver

Two enclosures are attached together as shown in Figure 3.12 separately housing the high power boards from the microcontroller to reduce interference. Three cooling fans and opposite air inlets have been fitted to provide airflow along the heat sinks to dissipate excess heat from the MOSFETs and diodes.

PWM Frequency

The PWM frequency of the H-bridge drivers was changed in the microcontroller from 36 kHz down to 12 kHz. A lower PWM frequency results in a lower MOSFET switching frequency and therefore a reduced current draw on the battery supply should result in less switching noise.

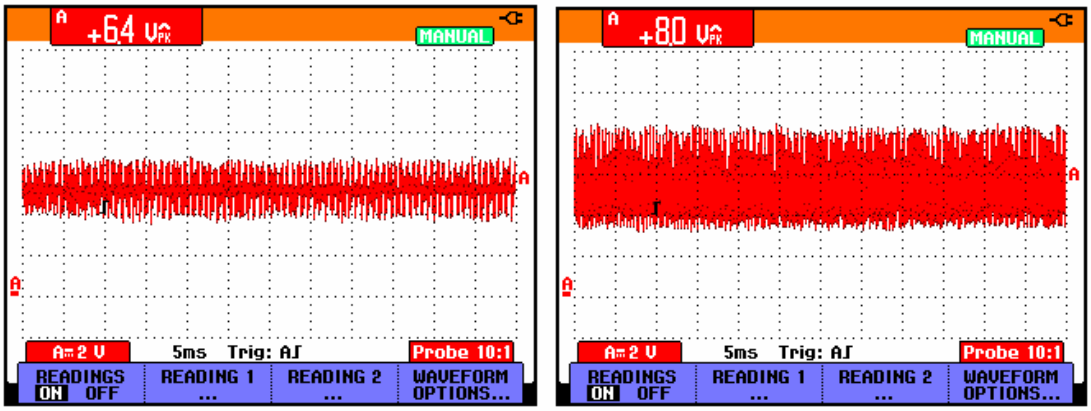

Figure 3.13 Noise after PWM changed to 12 kHz LEFT: Low duty cycle RIGHT: High duty cycle

Although this slightly reduced the noise, the problem was still present as indicated in Figure 3.13 showing the noisy 5 V power rail. The graphs also illustrate the significant increase in noise present as the duty cycle in increased. The graph on the left shows noise reaching a maximum of 6.4 V (5 V power with noise = 2.8 V peak-to-peak) for the lowest level of PWM available. When the duty cycle is increased enough to allow the motor to turn, overcoming the static inertia, the noise increases to a maximum of 8.0 V as shown on the right hand graph, potentially causing damage to any connected circuitry.

Shielding

The effect of electromagnetic interference (EMI) from the drive motors was investigated. A thick aluminium shielding plate was placed between the motors and driver units to act as a ground plane and direct the noise away from the low power circuits. The components were also physically separated by the largest distance possible as noise intensity reduces according to the inverse square of distance.

Neither method produced any noticeable difference to the noise magnitude indicating it was not radiating through space but rather conducting through the cables. Twisting the motor cables was also tested to cancel any differential mode noise present however again this did not completely remedy the underling problem.

Smoothing Capacitors

The fact the noise signal appears at the same frequency as the PWM switching frequency indicates a problem with the power supply not sourcing sufficient current. Sealed Lead Acid batteries cannot supply high currents at the required rate because they are relatively high impedance so as frequency increases the battery resistance dominates and restricts current flow.

A large variety of high capacity smoothing capacitors were added to the battery supply rails to act as fast responding charge reservoirs. Low pass filters were also added to the PWM lines to smooth out the high frequency components of the signal edges however these methods did not completely remove the noise.

Ferrite Beads

Instead of analyzing the frequency of occurrence of the noise signals (~36 kHz) the frequency of the actual noise pulse (~20 MHz) was inspected as shown in Figure 3.14. Ferrite beads can be used to attenuate these high frequency signals and were

investigated to remove the noise, particularly from conduction along the ground wires between circuits.

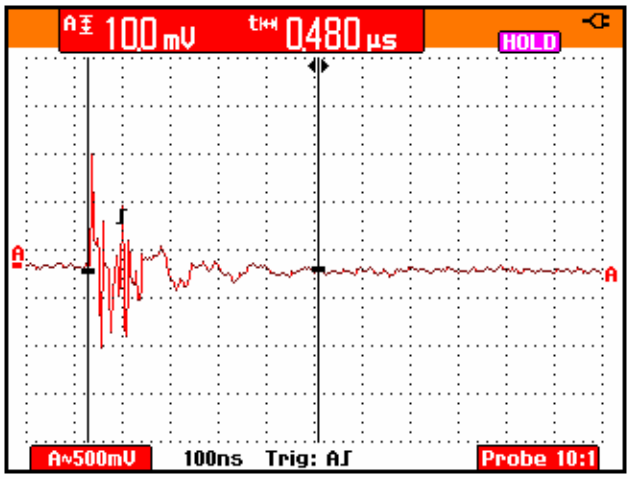

Figure 3.14 Inspection of single noise pulse (f ≈ 20MHz)

Ferrite beads can be modelled as a series combination of an inductor and resistor, as frequency increases the resistive component dominates and dissipates noise in the form of heat. By placing the beads in series between all low power supply rails, signal lines and ground planes on the microcontroller and H-bridge boards, the conduction of noise was reduced but still not eliminated sufficiently for normal operation.

RFI Suppression Choke

Common mode noise can be reduced by installing EMI suppression filters on all lines on which noise is conducted. The noise is often suppressed with two inductors connected in series within the signal lines in the form of a RFI suppression choke (Figure 3.15). The connection diagram for the selected ROXBURGH EMI C215 15A device from Farnell is illustrated in the right hand diagram of Figure 3.15.

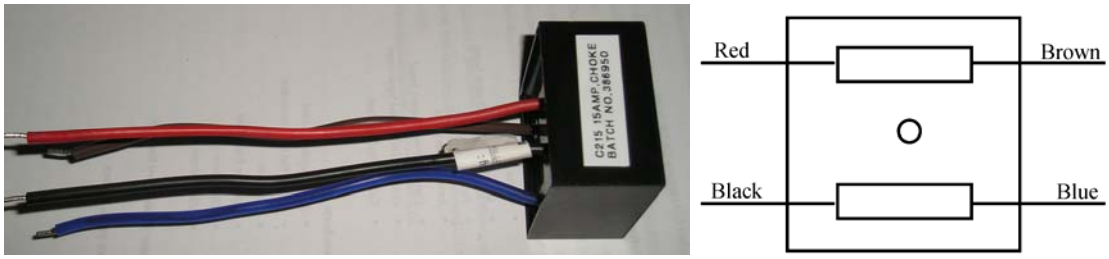

Figure 3.15 LEFT: C215 RFI noise suppression choke RIGHT: Connection diagram

These devices were connected in a number of different locations such as between the ATX power supply and batteries and between the driver boards and batteries. The most success was achieved when the units were attached between the drive motors and the motor driver boards as illustrated in Figure 3.16.

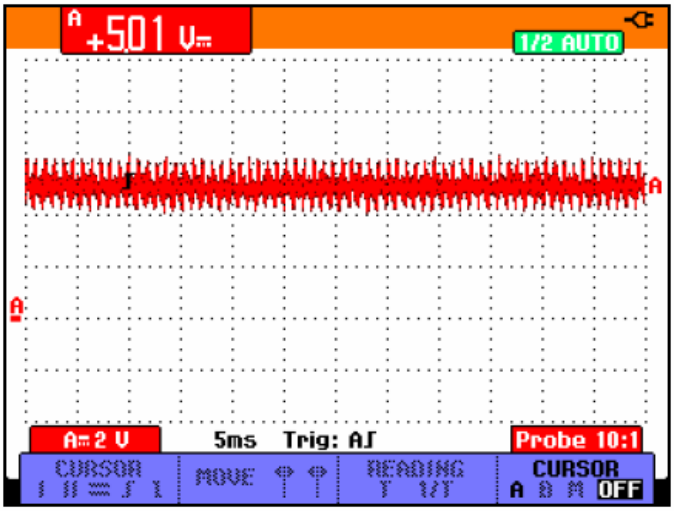

Figure 3.16 Reduced noise density and amplitude after RFI choke added

The density and amplitude of noise was greatly reduced compared to previous methods (Figure 3.13) indicating attenuation of high frequency noise by the inductors however a significant amount still remained. Future work would involve experimentation with chokes of different inductance than the specified 1 mH of these devices, possibly better targeting the noise components.

3.3.6 Summary

The preceding sections have presented an analysis and problem solving strategy to implementing the previously developed motor driver circuits. Although a vast number of modifications were made to the units in an effort to remove noise, each with varying degrees of success, a single underlying cause could not be found. It can be concluded that measures to protect circuits and enhance noise immunity should be designed into the project from initial stages as it is much more difficult to subsequently make modifications when a problem is realized.

Although further analysis of the initial microprocessor code and a continual pursuit of noise reduction would eventually resolve reliability issues it was decided not to continue this path. The cost of replacement parts was already exceeding the price of some commercially available systems and development time would be better spent on other areas of the project. The decision was therefore made to cease the ongoing maintenance and repair and rather investigate commercial motor drivers and the interface required to implement them.

3.4 REVIEW OF COMMERCIAL SYSTEMS

The motor drivers will be eventually installed on the other robotic vehicles under research so the system must adhere to a number of criteria. Most importantly the system must be robust and reliable; each of the large robots could cause serious damage to itself or the surrounding environment if the robot became uncontrollable due to motor driver failure.

Other desirable attributers include the following:

- **Portable to other robots:** It should be possible to design a system around the commercial device capable of controlling other robots with minor alterations.
- **Reasonable Cost:** The cost of the devices must be low enough not to exceed project budget requirements without a significant compromise on quality.
- **Uncomplicated Interface:** A reasonably straightforward interface requiring minimal adjustment is desirable to reduce development time and complications resulting from highly customized systems.
- **Product Support:** Commercial systems offering product support should be easily accessible for servicing in case of failure.
- **Physical Restrictions:** Certain limitations relating to driver dimensions and weight must be considered for positioning on the mechatron.
- **Features:** As many extra functions additional to motor driving as possible such as circuitry protection and intelligent software.

This section discusses some of the commercial motor driver boards considered for this project including the advantages and limitations of each.

3.4.1 MAXI Motor Driver Kit

A compact H-bridge motor driver kit shown in Figure 3.17 is available from the MONDO-TRONICS website[7]. They provide digital control of the power converter from a standard PC parallel port or serial port by adding the optional "Serial Motor Interface".

Some features are:

- Two motors per module
- 10 – 40 V range of motor voltages
- 10 A (max) continuous current with heat sinks attached
- Optoisolation between digital and analogue circuits
- Variable speed control via PWM inputs

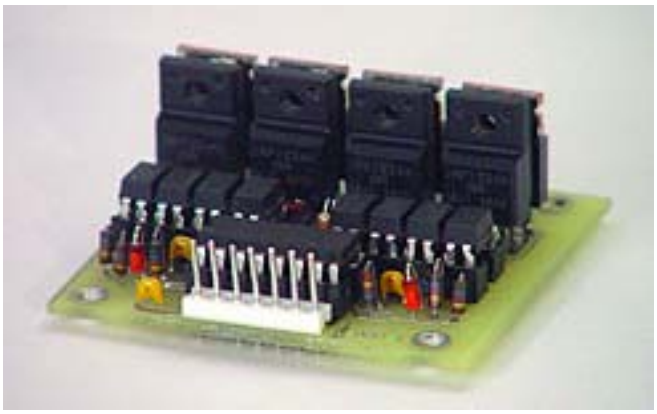

Figure 3.17 Assembled Mondotronics MAXI motor driver kit

The modules come in kit form meaning construction is required before they can function. Additionally these modules are simply the H-bridge component of the driver. A combined unit is preferred because suitable control hardware consisting of a microcontroller would still need to be developed.

The outdoor mechatron uses high powered motors that generate large amounts of electrical noise. The MAXI motor driver kits are too simplistic, lacking the necessary high current capability or protection circuitry such as a snubber or transient suppression device. They are therefore not suitable for this project.

[7] http://www.robotbuilder.co.uk

3.4.2 MD03 and MD22

A pair of similar H-bridge motor driver boards is available from Robot Electronics[8] in the UK. The MD03 and MD22, shown in Figure 3.18 provide robust medium power motor control with a vast array of features. A number of control methods are available such as an I^2C bus, analogue inputs and the ability to interface to a hobby style radio control receiver thereby offering versatility in implementation. The MD22 module, in addition to controlling two modules independently, incorporates a useful differential drive function. This enables one input to control forward/reverse velocity while the other is used for steering, a useful feature for the outdoor mechatron. The MD03 offers many of the same features as the MD22 however it can also accept PWM inputs from a microcontroller. Although it has only one channel, multiple MD03 units can be cascaded for any motor driver application providing a higher current capability than the MD22. Although both boards offer desirable features, (particularly the MD22 differential drive feature), the current requirements of this project (at least 25 A per channel) exceed those of both units and are therefore not suitable.

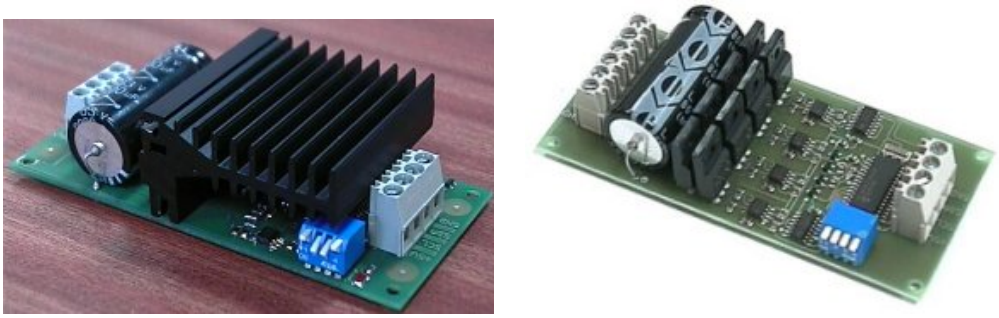

Figure 3.18 LEFT: MD03 RIGHT: MD22

Summary of MD03 and MD22 features:

	MD03	**MD22**
Number of motors:	1	2
Voltage:	5 – 50 V	5 – 50 V
Max Current:	20 A	27 A (13.5 A per chan)
Price (ea).	£45.00	£40.00
Control Modes:	I^2C Bus (up to 8 MD03 units) 0 – 2.5 – 5 V Analogue input 0 – 5 V Analogue input (sep. dir.) RC Receiver PWM at 20 kHz	I^2C Bus (up to 8 MD22 units) Dual 0 – 2.5–5 V Analogue input Dual 0 – 5 V Analogue input RC Receiver – individual control RC Receiver - with steering

[8] http://www.robot-electronics.co.uk

3.4.3 Tecel D200

A high power H-Bridge DC motor driver board, shown in Figure 3.19 is available from Tecel Microcontrollers[9]. The D200 is capable of driving many different motors of any voltage up to 55 V making it suitable for use on a number or robot platforms. The board contains a single switching bridge meaning two units are required for this project. Onboard protection diodes and provisions for snubber circuitry are advantages not found on some other boards researched.

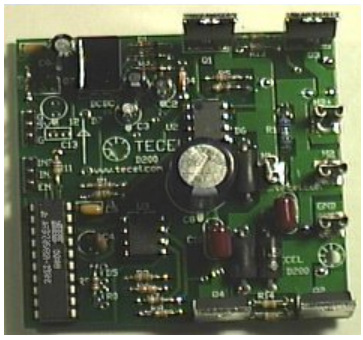

Figure 3.19 Tecel Microcontrollers D200 DC Motor Driver Board

D200 features:

- Power semiconductors: 4 110A MOSFETs
- Current: Max 15 A with heat sinks
- Voltage: 5 V for digital circuits, 0 – 55 V for motor
- Board size: 63.5 × 63.5 mm
- Circuit Protection: Filter capacitors, VTS diodes, snubber circuit ready
- Onboard DC-DC converter for MOSFET bias voltages
- Digital truth table and PWM inputs

Although the literature claims a board maximum of 60 A, the deceptive wording is actually indicating this is shared between the four MOSFETs. In other words the board cannot supply 30 A in one direction for extended periods of time and the continuous current rating is actually 15 A when heat sinks are installed. This means the board does not meet the current needs of this project and the additional hardware and software development needed for PWM generation is not desirable.

[9] http://www.tecel.com

3.4.4 MDM5253

The MDM5253[10] DC motor driver module shown in Figure 3.20 is a three channel H-bridge power amplifying module capable of controlling 3 DC motors simultaneously. Control is via logic level PWM inputs at a frequency up to 20 kHz, additionally the module provides feedback on motor current and position sensors such as potentiometers or rotary encoders.

Some specifications of the MDM5253 are:

- 3 independent motor channels
- Output drive of 5 – 28 V
- 5.0 Amp inductive DC load current capability
- PWM inputs
- Automatic PWM over-current limiting and short-circuit protection
- Analogue current feedback and connectors for position feedback signals

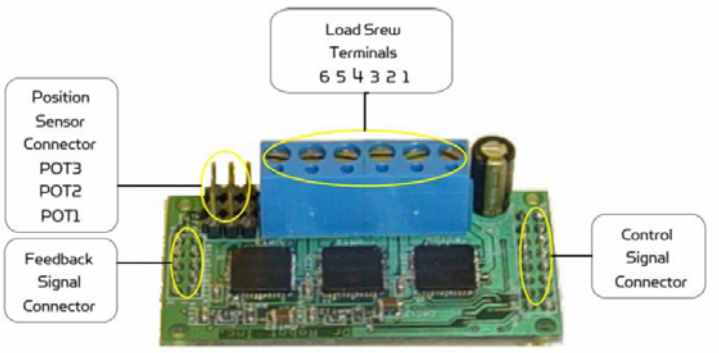

Figure 3.20 MDM5253 motor driver board

The MDM5232 module provides some useful features for DC motor control such as position and current feedback however the small size of the module makes it useful for only low power applications. Integrated motor control IC's have been used instead of the usual MOSFET H-bridge topology thus substantially reducing the current drive capabilities. Although some circuit protection features are available, the board is not designed to handle large inductive loads such as those present on the outdoor mechatron. This unit is best suited to smaller scale robotics projects such as robotic manipulators where multiple, small servo motors are required.

[10] http://www.drrobot.com

3.4.5 RoboteQ AX2550

The AX2550 module from RoboteQ[11] (Figure 3.21) is a high power, dual channel digital speed controller for computer guided robotic vehicles. The compact size and large drive capability make it suitable for a wide range of systems. A number of input types are possible including an R/C receiver, analogue joystick, wireless modem or embedded controller giving the unit versatility. Independent and mixed motor control schemes are available such as coordinating differential drive motion by setting vehicle speed and rotation. Closed and open loop control modes are possible enabling both velocity and position control with the addition of suitable sensors.

Figure 3.21 RoboteQ AX2550 controller module

Key Features:

- 2 channels capable of driving 120 A motor loads
- Microcontroller based design for accurate and reliable operation
- Interfaces to R/C receivers, serial lines, analogue signals, microcomputers
- Support for open and closed loop control of velocity and position
- Intelligent electronic protection and current limitation
- Data logging output to PC or PDA
- Durable weather shock resistant heat sinking enclosure
- Field upgradeable software and programmable configuration options

The combined features and versatility of this device make it ideal for the demanding motor control required in this project. The only limitation is the cost of US$495 however, it would be the preferred solution if the Rhino controllers (section 3.5) were not located.

[11] http://www.roboteq.com

3.5 SELECTED MODULES

As discussed, a number of commercial motor controllers have been researched and evaluated for installation on the outdoor mechatron. A common restriction amongst many of the devices available is the limited current capability. Many devices are available for small to medium power motor control applications and the few found for high power were too expensive and specialized for this project.

Another problem encountered was the difficulty of finding a complete solution integrating high power drive and computerized control. Many devices provide the high current H-bridge topography however they lack a control module to supply the real-time PWM signals. These systems would require additional control hardware to be developed to control the switching of the H-bridge units. Although the main CPU could perform these tasks through suitable hardware such as a DAQ card, a separate controller is preferred to decrease the software demands on the main CPU leaving it available for more complex, high level tasks.

The selected motor controllers for the outdoor mechatron are a pair of RHINO DS72K devices from Dynamic Controls Ltd[12]. Designed for mobility scooter control, each module can supply currents of 70 A and are designed for small to medium sized scooters and wheelchairs. The controllers are therefore sufficiently powerful to drive the mechatron even in the most demanding outdoor conditions.

The RHINO motor drivers provide reliable and smooth operation by utilizing an onboard microcontroller for control and circuit management. The microcontroller provides the feature benefits and safety attributes offered by a digital system while retaining the smoothness of an analogue controller. The units utilize high current output components to sustain a powerful drive with high load compensation. This allows excellent speed stability over various driving terrains.

[12] http://www.dynamicmobility.co.nz

The specifications of the RHINO DS72K controllers are:

Drive Motor Type:	Permanent magnet
Battery Voltage:	17.5 to 32 V (24 V nominal)
Operating Current:	Max: 70 A
	Continuous: 25 A @ 25°C
Quiescent Current:	Key Off: 1.5 mA
	Sleep: 2 mA
	Neutral: 50 mA
Parking Brake Output:	1.3 A (max) @ 24 V
Dimensions:	155 mm × 100 mm × 44 mm (Figure 3.22)
Weight:	650 grams each
Enclosure:	Die-cast aluminium with Nylon base plate
Mounting:	3 × M4 screws
Price:	NZ$276 per unit appx.

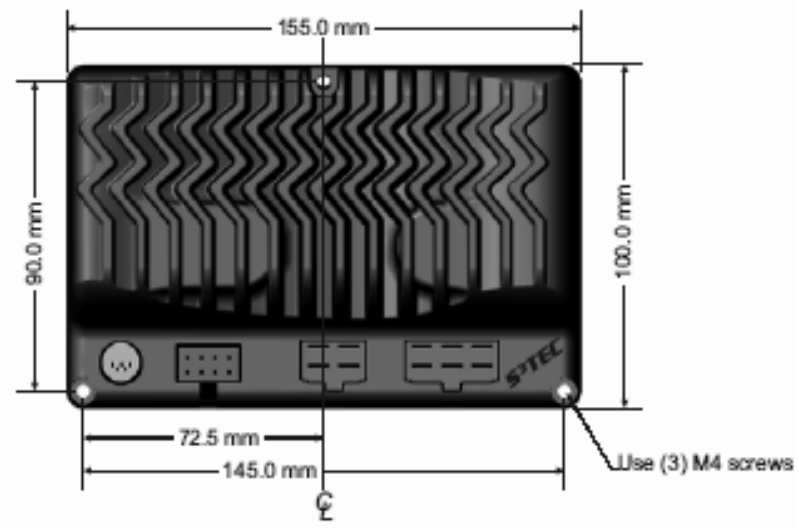

Figure 3.22 RHINO DS72K controller dimensions

3.5.1 Features

One of the main reasons for selecting the Rhino controllers is reliability. It is important for mobile robots, particularly large scale devices to have dependable motor drivers to reduce the risk of malfunction and consequent damage. The most

advantageous characteristic of the RHINO controllers is that they have been designed to control the same motors installed on the mechatron. This was the major consideration in selecting these drivers as this meant they were inherently designed to cope with the loads and stresses present. This could not be guaranteed with most other commercially available systems.

Safety features include automatic motor protection algorithms. These calculate when the units are pushed too hard and the controller needs to reduce speed, thus preventing motor burn out. Battery management software monitors current consumption and uses "battery saver" technology to prevent damage to the cells. The drivers are also capable of power regeneration, charge is returned to the batteries during braking and slope decent extending the run-time for each charge.

Other controller features include:

- **'S-curve' and 'S3-TEC'** algorithms provide smooth driving on many surfaces with well controlled acceleration and braking
- **Die-cast Aluminium** enclosures provide a solid, weather proof mounting platform and integrated heat sink for excess power dissipation
- **Soft stop** algorithms ensure the vehicle comes to a smooth shutdown in the event of error
- **Slope safety** limits roll back on hills to safe values
- **Automatic shutdown** enables sleep mode after long periods of inactivity to conserve power
- **Diagnostic indicators** provide useful feedback to the user regarding system status (section 3.5.5)
- **Flexible throttle control** options (wig-wag, engager or speed input) allow left hand, right hand or single ended operation
- **Data logging** for fault codes and operating time enable easy diagnostics
- **Fully programmable** operating characteristics enable system specific configuration (section 3.5.4)

3.5.2 Interfacing

The controllers have been designed to interface to a mobility scooter tiller head such as the one shown in Figure 3.23. The resultant interfacing system for the mechatron must therefore be compatible in order for the controllers to correctly function.

Figure 3.23 Example scooter tiller head from Dynamic Controls Ltd

The standard wiring diagram for the controllers is illustrated in Figure 3.24. Connection of the high power components such as battery supply and motor use AMP 250 series 6 and 4-way plug housing, the logic connectors use an 8-way AMP Mini Mate'N'Lok plug housing. Three each of battery +ve and battery –ve terminals are available on the driver modules, two of which provide the battery power using separate fused cable pairs while the other provides power to the tiller unit or interfacing module. An electromagnetic brake system is connected to the motor driver modules through the same connector as the drive motors.

The main interfacing considerations are the logic connections, particularly the throttle controller. The control input is designed to connect to a potentiometer so the challenge was to construct a computer controlled interface to replace the analogue reference voltage and wiper configuration. The throttle –ve pin is internally connected to battery negative through 500 Ω to prevent fault current and to allow the throttle resistance to be checked. Throttle +ve is connected to +5 V internally to provide an interface that is symmetrical around 2.5 V. The system requires (checked by the

onboard microcontroller) a resistance between 4.4 kΩ and 5.4 kΩ to be connected between the throttle +ve and throttle –ve pins.

A 0.5 – 4.5 V signal with respect to the negative battery voltage can be applied to the throttle wiper pin providing a 2 V range for each direction of motor control. However, voltage drops between the battery negative point of the driving interface and the RHINO controller's internal battery negative circuitry will affect the control signal. To minimize the effect of these common mode voltage drops the ideal solution is for the driving interface to generate a ± 2 V signal with respect to the average voltage between throttle +ve and throttle –ve.

When the throttle is in the neutral position the following voltages should be present with respect to battery negative:

Throttle –ve	**0.5 ± 0.1 V**
Throttle Wiper	**2.5 ± 0.1 V**
Throttle +ve	**4.5 ± 0.1 V**

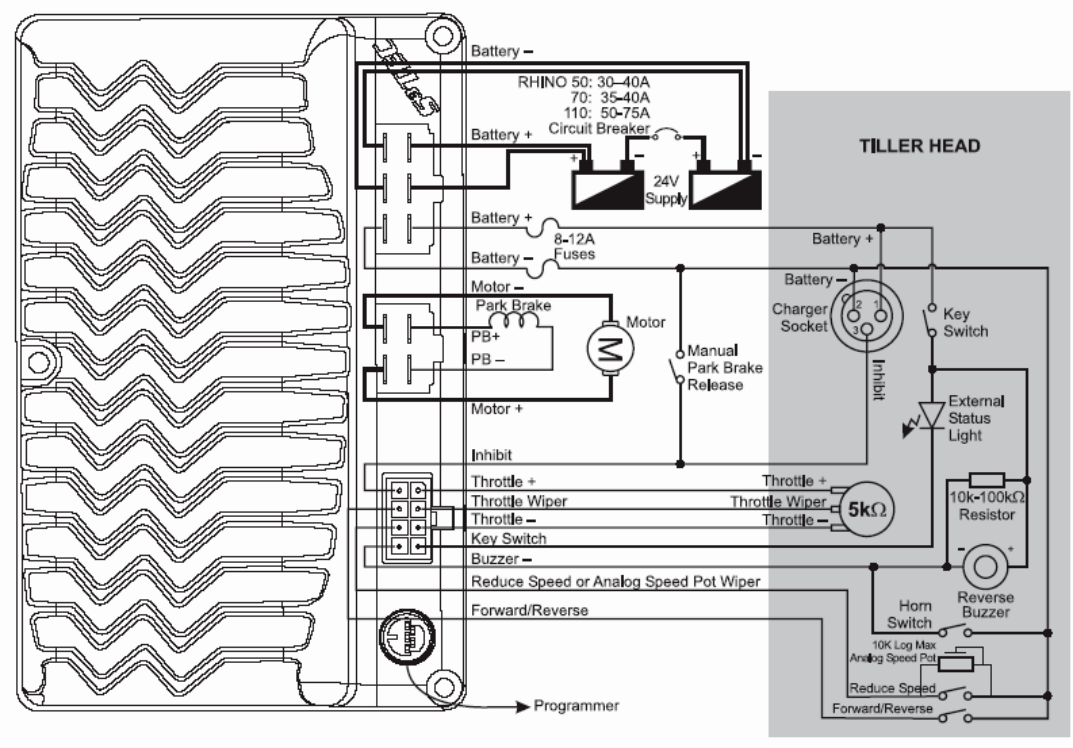

Figure 3.24 RHINO suggested wiring diagram

3.5.3 Handheld Controller

To perform initial testing and functionality verification of the motor drivers a manually operated hand held controller was developed. The device models the simple interfacing requirements detailed in section 3.5.2, consisting of two 10 kΩ potentiometers for velocity control. Switches for power control are connected to the "Key switch" pin via an LED through to 24 V and 10 kΩ resistors are connected in parallel with the pots to meet the 5 kΩ criteria as the exact devices were not available.

Each group of controls interfaces to one of the motor driver units providing independent differential control of the drive motors. A green LED indicates when power is activated and also acts as the status feedback to flash error codes if they are present. Motor control is achieved by rotating the potentiometer knobs from the centre point in the desired direction of rotation, clockwise for forwards drive and anti-clockwise for reverse.

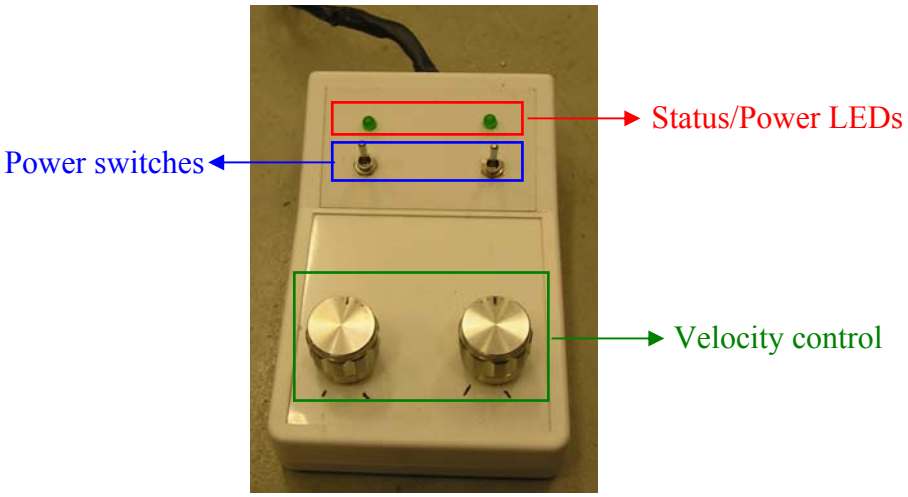

Figure 3.25 Handheld motor driver controller

3.5.4 Programming

The onboard microcontroller allows custom programming of the drive characteristics to improve performance and best suit the intended application. Two versions of the handheld programmer are available giving different levels of access to the settings. The “Dealer” version allows modification of simple drive parameters such as velocity and acceleration while the “Manufacturer” version also allows customization of

system settings such as motor resistance and throttle threshold levels. The programmer connects to the RHINO through an adapter cable to the programming port as shown in Figure 3.26. An additional power supply is not required as the programmer is powered by the controller, therefore the controller units must be switched on. Automatic safety features ensure the controllers cannot be operated while the programmer is connected. A software version of the programmer (Dynamic Wizard) is also available providing full PC access to all settings through a USB adapter.

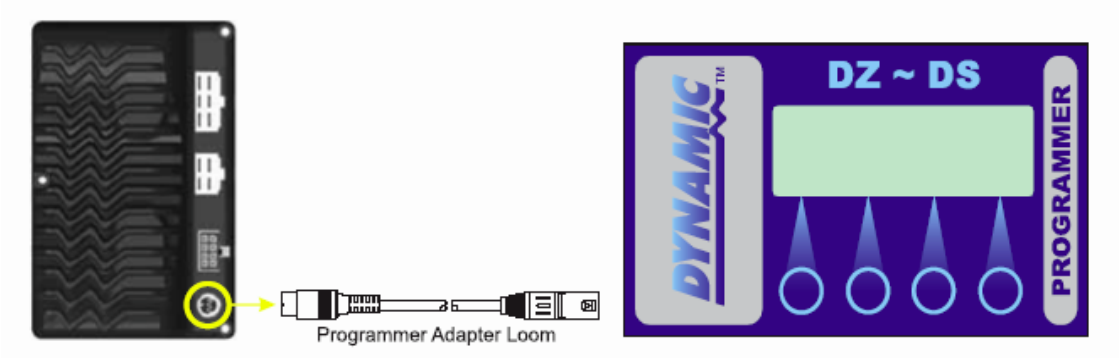

Figure 3.26 Connection of handheld programmer to RHINO controller

A large number of settings can be customized using the manufacturer programmer, a full list of these are listed in the RHINO documentation (Appendix B). All settings are factory set to suit most end users, only a couple of settings related to acceleration and maximum velocity required modification for use on the outdoor mechatron. Table 3.1 summarizes the settings used.

Acceleration (1 – 10):	4
Deceleration:	7
Max Speed (0 – 255):	255
Forward Speed (1 – 10):	10
Reverse Speed:	10
Reduce Speed:	5
Motor Resistance:	60 mΩ
Sleep time:	30 min
Max Current:	70 A
Soft Start Period:	50 (800 ms)
Park Brake Delay (1 – 30):	6
Pot Neutral:	128

Table 3.1 RHINO programmer settings

3.5.5 Status Codes

The RHINO controllers provide status and diagnostic information to assist the user in correcting faults with the scooter system. A fault with the controller or motor control system will cause the status LED to flash and a horn to sound (if later fitted). The sequence of light flashes and horn bursts represent a particular fault, referred to as the "flash code".

Depending on the severity of the error and its impact on equipment/user safety, the controllers will either display the code as a warning only or display the code and prevent all operation until repaired. Once the appropriate fault has been located and remedied, the controllers require a reset (power cycling) before operation can resume.

An explanation and probable cause of each error flash code can be obtained by plugging in the programming device (3.5.4) or referring to Table 3.2 below taken from the RHINO user manual.

Flash Code/Fault	Impact on Robot	Description
1 Battery needs recharging	Will drive	Battery charge is running low, recharge soon
2 Battery voltage low	Drive inhibited	Batteries are empty, recharge now
3 Battery voltage high	Drive inhibited	Batteries are overcharged, either due to charger or excessive travelling down slopes
4 Current limit timeout	Drive inhibited	Over current for too long, robot may be stalled or motor damaged. Turn off for a few minutes
5 Brake Fault	Will Drive Drive Inhibited	Park brake switch on during drive (not installed on robot) Park brake wiring may be faulty
6 Out of neutral at power up	Drive Inhibited	Throttle needs to be in neutral position during power up
7 Speed pot error	Drive Inhibited	Throttle wiring/resistance faulty
8 Motor volts error	Drive Inhibited	Motor or motor wiring is faulty
9 Internal error	Drive Inhibited	Other errors. (Contact service)
10 Push to fast fault	Drive Inhibited	Robot has been pushed faster than programmed limit (Not applicable)

Table 3.2 RHINO fault code reference

3.5.6 Robot Mounting

Mounting of the RHINO controllers to the robot platform is via a stainless steel mounting plate ensuring a strong and stable attachment. Measuring 330 mm × 230 mm, the plate was bent along the centre to produce an angled platform to which the controllers are bolted. Recommendations by the manufacturer for an inclination angle of 15 – 75° were followed to allow free draining of moisture and adequate ventilation for the cooling holes.

The units are positioned side by side at the rear of the mechatron directly above the drive motors as shown in Figure 3.27. This ensures the controllers are sufficiently distant from electronic systems to prevent EMI noise from disrupting circuitry. This is also achieved by keeping the cables between the motors, batteries and drive units as short as possible.

Both units are marked with an 'L' or 'R' indicating which side of the mechatron they are to be attached. The corresponding cables and connectors have easy access to the units easing maintenance and are also labelled to ensure correct connection and operation.

Figure 3.27 RHINO controllers mounted on plate at rear of mechatron

3.6 Initial Interface Design

The first design of the motor controller board, shown in Figure 3.28, was based on supplying a controlled analogue voltage to the throttle wiper pin. Since a mechanical potentiometer is not able to provide an analogue voltage using a digital controller, a suitable DAC (Digital to Analogue Converter) was investigated. Although a number of different methods were available including custom designed DAC IC's, an initial system employing PWM (Pulse Width Modulation) was developed.

PWM is a useful technique for controlling analogue circuits and can be achieved by using the digital outputs of a microprocessor. The analogue voltage is digitally encoded through the use of high resolution counters to modulate a square wave at varying duty cycles. The analogue signal is retrieved at the receiving end by using a suitable low pass RC (resistor-capacitor) filter to remove the modulating high frequency.

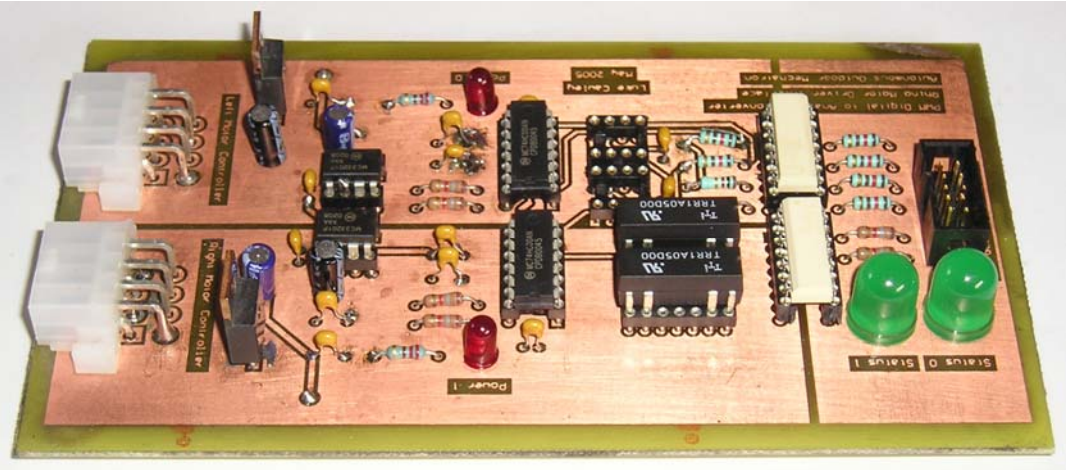

Figure 3.28 Motor driver interface board utilizing PWM based DAC

One of the main advantages of PWM is that the controlling signal remains digital from the microcontroller to the system, increasing noise immunity and increasing the length of the communication channel available. PWM generation is a common and easily accessible feature on most microcontrollers thus providing a simple, low cost implementation.

A simplified schematic of the PWM based interface board is shown in Figure 3.29. The input PWM signals from the microcontroller pass through a logic gate buffer, two stage low-pass filter network and op-amp based voltage follower before reaching the controllers. Two control lines are used to control the power through the key switch lines and solid-state relays (not shown). All signals from the microcontroller are opto-isolated from the motor driver to prevent potential damage using a TLP620-4 four element photo-coupler.

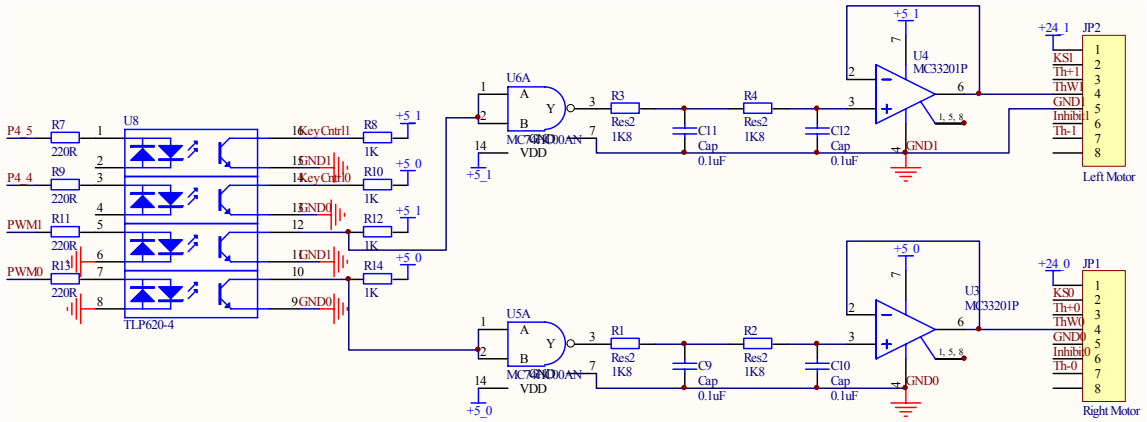

Figure 3.29 Simplified schematic of PWM interface board

A number of problems were present with this first design preventing it from operating correctly. The main issue was the analogue voltage reaching the throttle wiper was not correctly referenced. It was important to precisely keep the voltage between the Th +ve and Th –ve pins otherwise the controllers would detect a problem and flash an error code indicating the throttle wiring was faulty.

This was a particularly difficult task because minor fluctuations in PWM levels and circuit voltages easily caused the output to exceed threshold limits. This was further complicated by the unstable low-pass network, causing unpredictable voltage fluctuations. Modifications to the RC values helped improve the response however, it was at the expense of a dead zone where the output voltage was discontinuous for a changing PWM.

These problems could have been remedied by further tweaking of the filter components and the implementation of voltage limiting circuitry at the output stage. A different interfacing method was however, developed to enable higher precision control of the motors.

3.7 Improved Motor Driver Interface

The improved design for the motor driver interface board more closely matched the interfacing attributes of the tiller head units. The motor drivers are designed to accept a 5 kΩ mechanical potentiometer across the throttle pins. Therefore, the most effective method of controlling the wiper voltage with a computer was through a digital potentiometer.

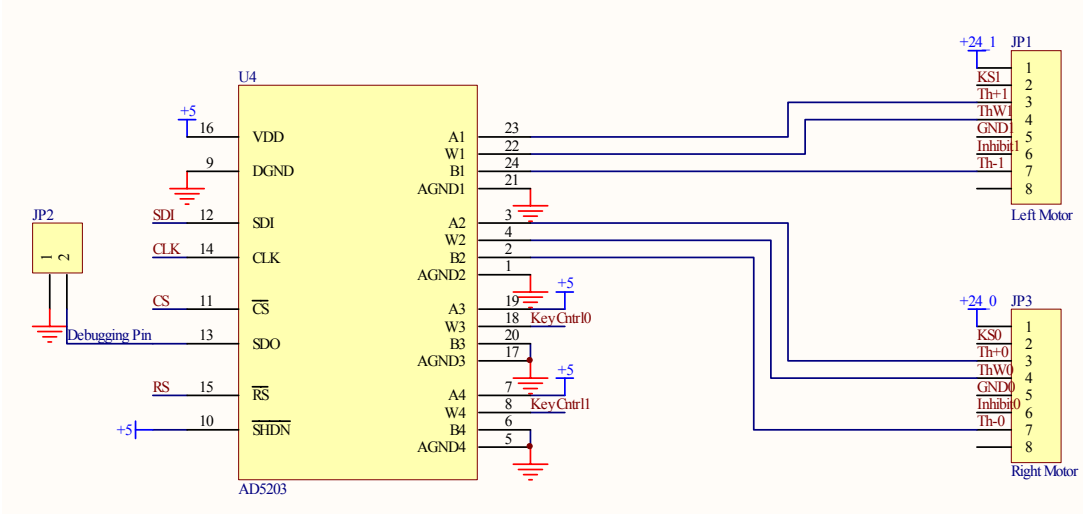

Figure 3.30 Simplified schematic of digital pot interface to motor drivers

The AD5203 digital potentiometer from Analogue Devices is connected to the motor driver modules as indicated by Figure 3.30. Four individually operated and isolated digital pots are available with two connected to the throttle connections while the other two are used in the key switch circuitry to provide power control. The digital pot reference points are directly connected to Thr +ve and Thr –ve on the motor drivers ensuring the wiper voltage can never become out of range as occurred with the PWM interface. The digital pots are 10 kΩ devices therefore additional 10 kΩ resistors are connected in parallel across the two reference points meeting the 5 kΩ criteria.

The key switch circuitry is shown in Figure 3.31. An analogue voltage from the digital potentiometers is converted to a digital control signal by the triggered op-amp circuit to operate DIP reed relays. The relays replace the mechanical switches installed on the handheld controller or tiller head assembly and pass current through the status/power LED to the RHINO controllers.

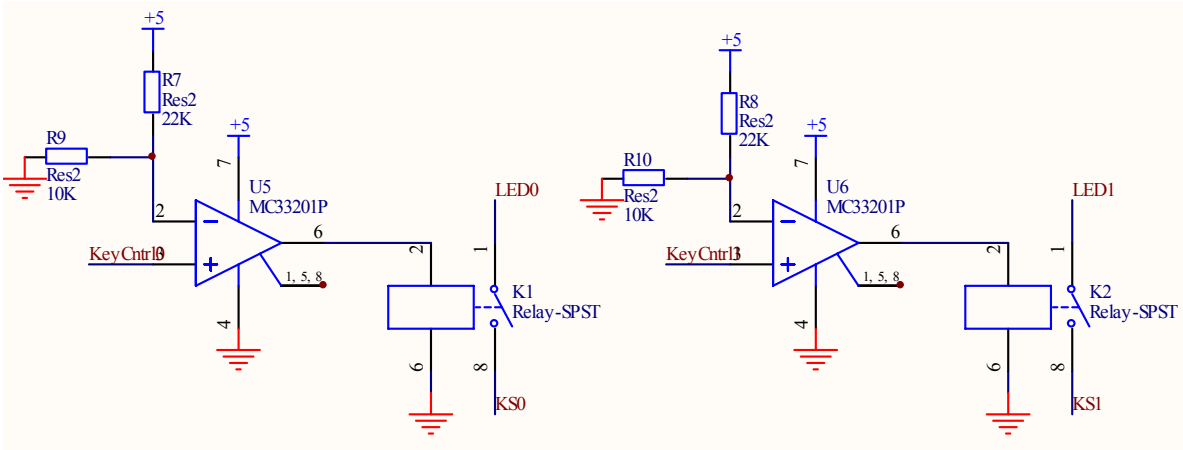

Figure 3.31 Schematic showing key switch control circuitry

The resolution is 64 positions providing a large number of individual power settings adequate for the outdoor mechatron. A drop-in replacement is available (AD8403) providing 256 positions if required by future applications; the only modification required is minor adjustment of the microprocessor code (section 5.9).

Interface and control of the digital potentiometer is through a microprocessor SPI (serial peripheral interface) bus. The microcontroller connector, Figure 3.32, provides access to the four SPI control lines *CLK, RS, SDI* and *CS* in addition to the two opto-isolated status feedback signals *STAT0* and *STAT1*.

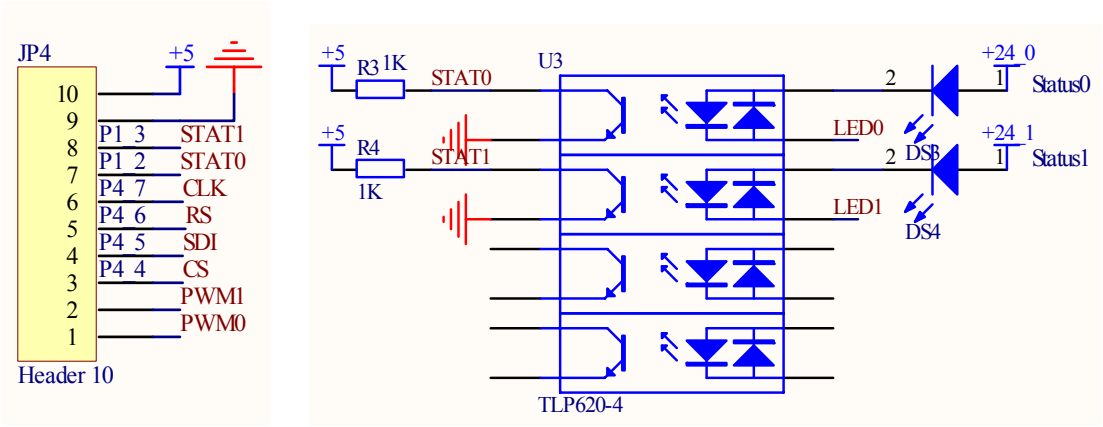

Figure 3.32 LEFT: microcontroller header RIGHT: optoisolated status signals

The completed hardware interface to the motor drivers is illustrated in Figure 3.33. Important components such as the motor driver connectors, and microcontroller interface are highlighted. The advantage of this microcontroller system in addition to

effectively controlling the outdoor mechatron is the straightforward portability to other robotic vehicles. A plastic enclosure, shown in Figure 3.34, is designed to protect the interface board and provide a strong mounting platform to the mechatron chassis.

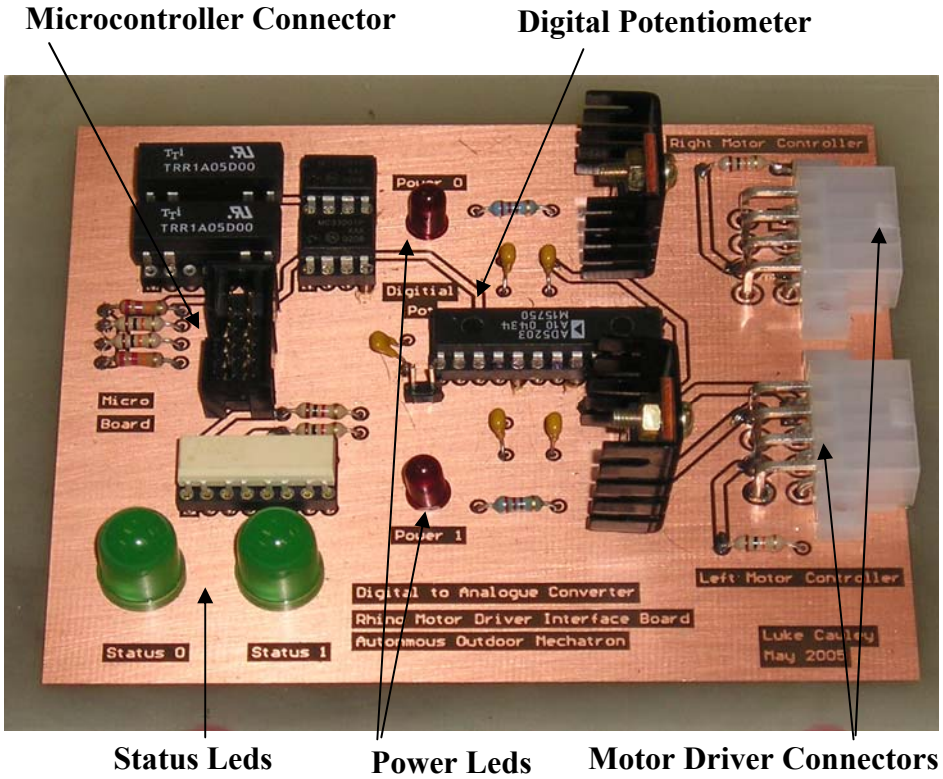

Figure 3.33 Completed RHINO motor driver interface board

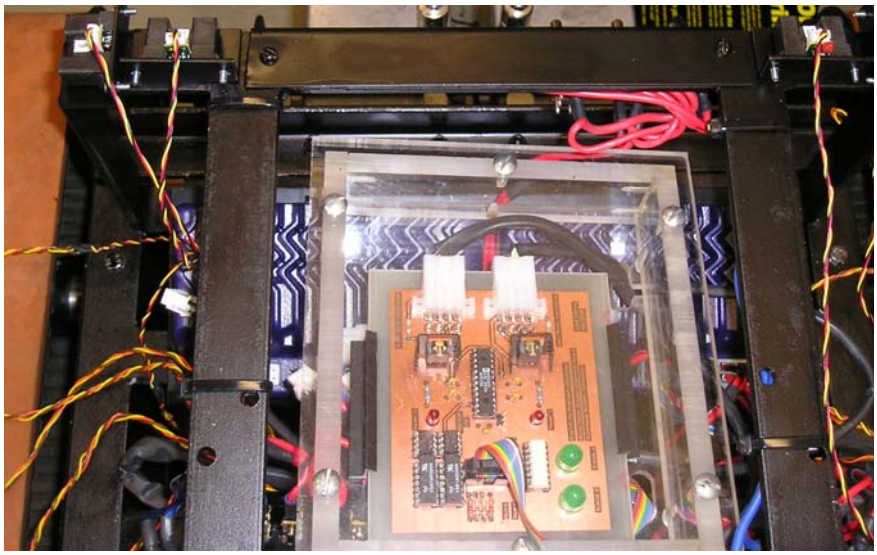

Figure 3.34 Mounting enclosure for motor driver interface

3.8 MICROCONTROLLER

Due to complications in timing when sending SPI control signals directly from the DAQ card (using the operating system's internal clock), an independent microcontroller system was developed. The microcontroller board, Figure 3.35, is connected to the motor driver interface board and provides control of the RHINO modules independent of the computer system.

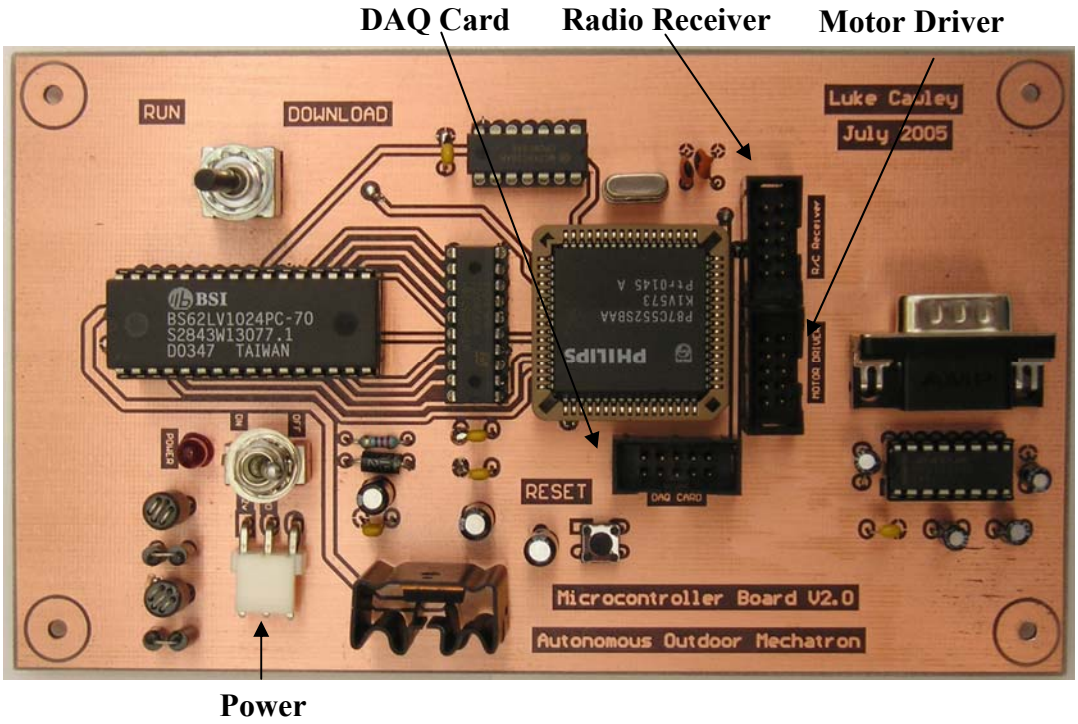

Figure 3.35 Microcontroller board for motor control

The primary task for the microcontroller is the interpretation of analogue and digital signals from the DAQ card in order to autonomously control the motors. The microcontroller is also interfaced to a radio control receiver enabling manual operation. The microcontroller provides automated mode switching between automatic (PC) and manual (RC) with failsafe protection. In the event of invalid or non-existent signals from the DAQ card or radio receiver, the motor controllers are deactivated until valid control is resumed.

3.8.1 Selected Controller

An 8051 based Philips microcontroller (P87C552) was selected for its familiarity within the Mechatronics Group and the range of on-chip peripherals suitable for this application. Listed below are the features associated with the 552:

- 80C51 CPU core
- 8 kB OTP EPROM
- 256 bytes internal RAM
- Two 16-bit timer/counters
- 8 channel 10-bit ADC
- Dual 8-bit PWM channels
- Five 8-bit IO ports
- Two External Interrupts
- Two hardware serial interfaces (I^2C bus and full duplex UART)
- Watchdog timer

An extensive development board was initially developed to allow future expansion however was consequently redesigned. Efficient mounting on a mobile robot requires a small, uncluttered design, particularly on Marvin where space is limited. Figure 3.36 compares the two designs, the radio-control interface is detached making it an optional addition and the full range of IO headers are replaced by design specific connectors to the DAQ card and motor drivers.

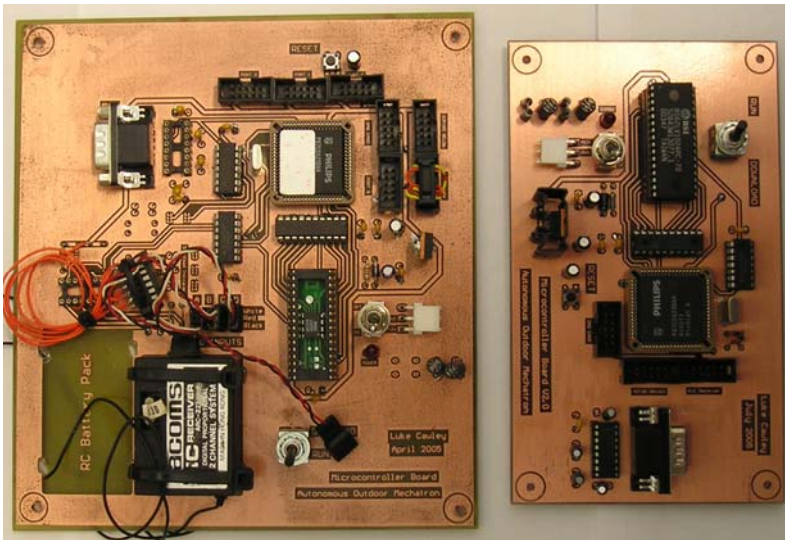

Figure 3.36 LEFT: First microcontroller board RIGHT: Improved design

3.8.2 Power Supply

The power distribution board (section 4.2.4) provides 12 V and ground rails to the microcontroller from the ATX PSU. Connection is through a polarized 2-pin header which also allows connection of a 9 V battery pack for manual operation (without PC turned on) or in case of power failure.

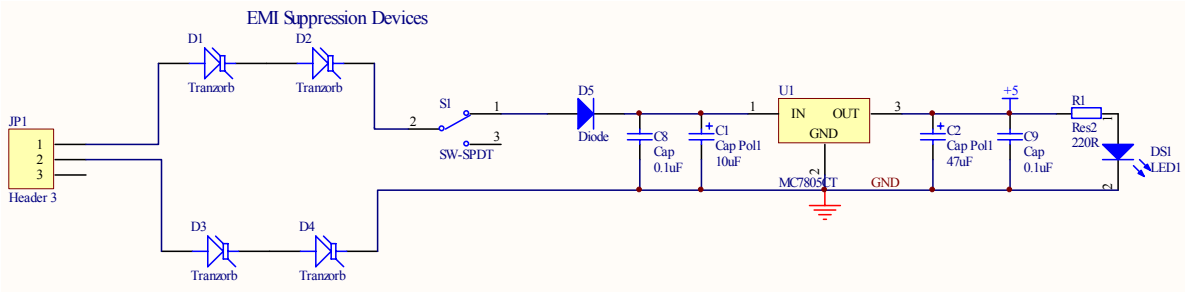

Figure 3.37 Microcontroller power supply

A MC7805CT voltage regulator is used to convert the 12 V into a constant 5 V supply to the microcontroller. Filtering capacitors are included on both the input and output stages of the regulator to remove high frequency noise and a diode (D5) provides protection against accidental polarity reversal. The full power supply circuit is shown in Figure 3.37.

Four inductive ferrite beads are included to suppress EMI present in the power supply. Connected in a series-parallel combination to reduce the noise on both rails, both pairs of beads are targeted at a different noise frequency to increase effectiveness.

3.8.3 Memory Configuration

The internal memory consists of an 8 kB OTP EPROM which means the memory locations reserved for programs can only be written to once. To enable in-system reprogramming with new application code, a non-volatile external memory device was incorporated into the design. The microcontroller is capable of addressing a total of 64 kB of external memory however this can be extended to 128 kB by taking advantage of the microcontroller's NPSEN (Not Program Strobe Enable) pin.

A low on NPSEN indicates the microcontroller is reading from program memory, therefore this line can be used to select the upper 64 kB (program) memory bank during operation. The lower 64 kB (data) memory bank can be accessed when PSEN is high thus giving data memory default access. This feature is used during download mode, using a boot loader program to write code to data memory (actually program memory), effectively "tricking" the microcontroller into updating the program code. This distinction between download mode and run mode is made with a toggle switch and logic circuitry as shown in the full schematic in Appendix A.2.

3.8.4 Programming

To enable downloading of new programs to external memory a boot loader client is programmed into the internal ROM of the microcontroller. The purpose is to receive new program code from the serial port and store it into external data memory so that it can be recalled as program memory during run mode.

The DOS *copy* command is used (via the *send to* command) on the PC to send the program HEX file through a serial cable and MAX232 transceiver. The boot code receives and manipulates it byte by byte for storage. A *RUN/PROGRAM* toggle switch is set to *PROGRAM* mode and the *reset* button pressed before code download can commence. Upon download completion the switch must be set to the *RUN* position and *reset* pressed to enable execution of the new code. This process must be repeated each time the program code is updated.

3.8.5 DAQ Card Interface

A suitable interface protocol was required between the DAQ card and microcontroller to transmit motor driver commands such as desired velocity and direction. As the velocity control algorithms (section 5.8) are implemented on the main PC (external to the micro), velocity feedback was not required however, suitable communication of motor driver status indicators was needed.

A summary of DAQ card to microcontroller connections is shown in Table 3.3. Two DAQ card analogue 0 – 5 V output channels are used to transmit the velocity control to the microcontroller ADC with 5 V representing maximum power and 0 V stopped.

Micro 10 Pin Header	**Micro Port**	**Function**	**DAQ Port**	**DAQ Connector**
1	P5.0	Speed 0	AO.0	22
2	P5.1	Speed 1	AO.1	21
3	P5.2	Direction 0	P0.0	52
4	P5.3	Direction 1	P0.1	17
5	P4.0	Power	P0.2	49
6	P4.1	Control Type	P0.3	47
7	P4.2	Status 0	P0.4	19
8	P4.3	Status 1	P0.5	51
9	GND	Ground	AOGND + DGND	
10	P3.2	Safety Pulse	P0.6	16

Table 3.3 Microcontroller to DAQ card connections

The digital IO lines on Port 0 of the DAQ card are used to transmit and receive the other control signals. The digital motor direction command (1=forward, 0=reverse) from the DAQ card are also received by the microcontroller onboard ADC. Although digital ports could have been used, this allows for future control expansion and the ability to control up to four motors. The four received analogue signals can be decoded into speed and direction by measuring the deviation in each direction from the 2.5 V midpoints.

A single power control line is used for both motor driver units to reduce the control lines necessary. Logic high on this line is converted to an SPI command for the digital potentiometer and turns on the key switch circuitry to activate the RHINO controllers. Two digital lines are used for feedback information on the motor driver status. These signals represent the same information transmitted by the large, green LED's on the interface board, signalling power activation and flashing error codes if any.

The *control type* line is used to signal the operation mode the microcontroller will operate in. A digital *high* or *low* represents one of two possible states:

1) PC Control Mode
2) Manual Control Mode

PC control mode is selected when the mechatron is to operate under computer control from the onboard software interface. Command signals are sent through the DAQ card to control the motor drivers. Conversely Manual control mode represents use of the radio control interface to manually operate the mechatron (detailed in section 3.9). The use of a control signal between these modes allows simple control switching within the onboard software interface to quickly disable or enable each mode as required. The *safety pulse* signal is used as a failsafe mechanism to trigger an external interrupt (discussed further in section 5.7.4) indicating a "still-alive" state of the control software during the PC control mode. In the event of software or computer hardware failure, the safety pulse will not be present and the microcontroller will automatically switch to manual control mode to activate the radio receiver. Further failsafe mechanisms (section 5.9) will bring the robot to a halt if the radio receiver signal is not present.

3.8.6 Motor Driver Interface

Interfacing between the microcontroller and motor driver control board is through a 10-way IDC plug and ribbon cable. Ports 1.3 and 1.2 are used for transmission of motor driver status to the microcontroller. Although the microcontroller PWM channels are no longer utilized in this design, they remain connected to pins 1 & 2 of the header allowing for future upgrades or addition of custom motor driver boards.

The connections to Port 4 are the control signals for the digital potentiometer. One way serial data communication is accomplished with the clock signal (*CLK*) and serial data input (*SDI*). The reset pin (*RS*) forces the wiper to each mid-scale position and chip select (*CS*) is used to select the current device, ultimately allowing more than one motor driver interface to be connected to the microcontroller.

3.9 RADIO CONTROL

Due to the large scale and weight of the Mechatron, a radio control (RC) receiver has been interfaced to the microcontroller to aid in robot transportation. The advantage is that the robot can be moved without requiring the main PC and software to be initialized, thus saving time and reducing power consumption.

The interface board, Figure 3.38 permits the operator to manoeuvre the mechatron around including loading onto a vehicle for transport without requiring at least two people to lift it. The handheld transmitter, Figure 3.39, is matched to the receiver with identical crystals. It is a two channel AM (Amplitude Modulation) device operating at 26.995 MHz.

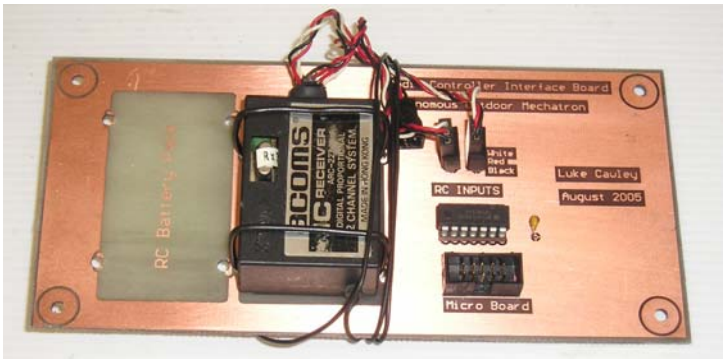

Figure 3.38 Radio Controller interface board

Figure 3.39 Radio control handheld transmitter

Logic gates are used to buffer the PWM radio signal before connection to the microcontroller through a 10-way IDC plug. The receiver is normally powered by a battery pack providing 4.8 – 6 VDC however this is not required by connecting directly to the microcontroller board regulated 5 V supply.

4. ELECTRONICS AND SENSORS

A number of electronic and sensory subsystems were developed to integrate with the central computer and robot hardware. These systems provide interface and control to the motor driver system, sensors and other peripheral devices required to achieve robot motion. Each component has been individually designed using a generic approach to interfacing. This modular design ensures straightforward troubleshooting and facilitates future upgrades and additions.

4.1 CENTRAL COMPUTER

At the heart of the robot electronics and control is the central processing computer. Chosen for its processing capability and small form factor, the ShuttleX PC (section 2.4) provides all the performance and upgradeability required in a mobile robotic platform.

4.1.1 Installation

Installation of the computer system on the mechatron requires consideration of component access and functionality. The recessed component tray at the front of the robot allows two mounting configurations of the ShuttleX illustrated in Figure 4.1. Although the initial idea took advantage of the recessed compartment to secure the PC case and lower the overall height, installation of other electronic components was difficult due to the limited space.

The revised design placed the computer above the compartment allowing space underneath for a custom electronics enclosure (section 4.10). Parallel steel bars are bolted to the mechatron frame to which the PC case can be attached ensuring it does not move. During development, cable ties secure the case to the steel beams to allow easy removal and access to the electronic components below. An extension to the

ATX power converter cables was required in order to mount the unit on top of the batteries and away from the CPU.

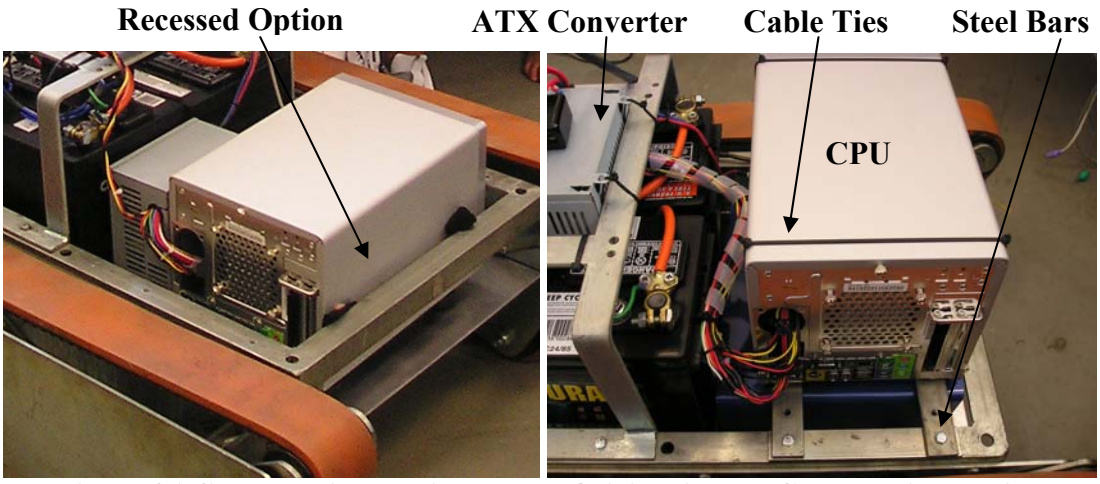

Figure 4.1 Computer installation LEFT: Original idea RIGHT: Revised option

4.1.2 Hard Drive Support

Excessive vibration and shock experienced by the mechatron when operating outdoors, particularly on uneven terrain, can damage the computer hard drive. Although future robot implementations would utilize a solid-state solution (such as a USB flash drive) for program and operating system storage, this was not possible during this project due to cost and the limited storage space of current devices.

A temporary solution to protect the hard-drive from mechanical damage was employed during development. The hard drive was removed from the original aluminium frame and repositioned in the upper (CD drive) section in a custom cradle. The cradle, made from rubber and foam padding is designed to absorb excessive vibration from robot motion thus protecting the hard drive from shock.

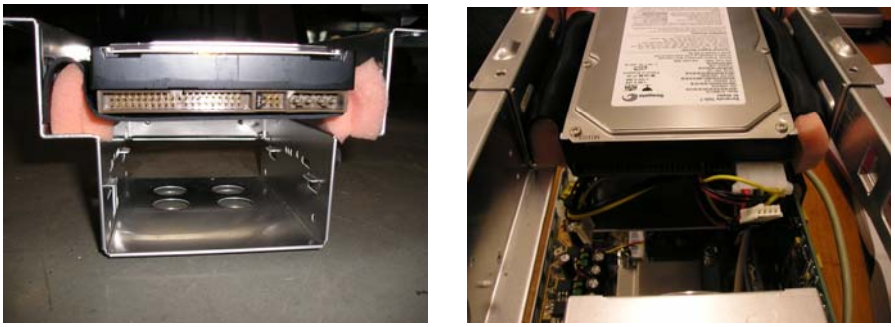

Figure 4.2 LEFT: Protective hard drive cradle RIGHT: Repositioned in ShuttleX case

4.1.3 Communication Interfaces

The ShuttleX computer contains one legacy serial (RS232) port and four Universal Serial Bus (USB) ports for connection to peripherals. The limited serial ports restrict the number of serial devices that can be connected which is a disadvantage as many devices such as sensors utilize this protocol.

Figure 4.3 USB to serial adapter

To allow connection to devices such as the compass and GPS modules, a modular connectivity system using a USB to serial converter is used (Figure 4.3). These devices allow standard RS-232 based designs to be connected to a PC through the USB ports, thus allowing a large number of devices to be connected (through a USB hub). The operating system sees the adapter as a standard COM port thus allowing configuration of port options such as COM number and data format through the control panel.

The onboard camera and wireless networking adapters are USB based to allow simple, future-proof connection. A single PCI slot is used for connection of the DAQ card and the AGP slot can be used to interface a graphics processing unit (GPU) for future computational applications such as 3D mapping.

4.2 POWER SYSTEM

The power system consisting of the batteries (section 2.6) and switch mode converter (section 2.5) provides energy to the motors and all electronic devices. A modular power distribution system has been designed to effectively power all peripherals ensuring compatibility with future additions and upgrades.

4.2.1 Fuse Box

A fuse box is installed between the battery terminals and electronic devices to ensure cut-out protection in case of a short circuit fault or excessive current draw. The unit, shown in Figure 4.4, is constructed of strong plastic and includes heavy duty contacts for durability and high current applications

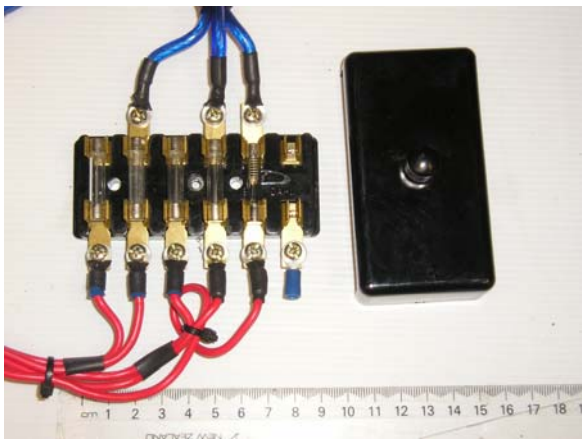

Figure 4.4 Fuse enclosure

Two separate circuits incorporating four 35 A fuses are used for the motor driver circuitry as recommended by the installation manual. A single 10 A fuse is used for the electronics supply connected to the switch mode converter leaving one fuse location free for future system configuration. High current cables (blue) connect to the positive battery terminal while 60 A rated cables (red) connect the fuse box to the peripherals.

4.2.2 Wiring

The wiring system was designed to ensure simple and reliable connectivity between components. Polarized connectors and colour coded wire looms help prevent incorrect connections and possible damage to expensive components.

Cables are kept as short as possible and twisted where appropriate to prevent problems with ground loops and unwanted conduction of noise signals. Cable ties and heat shrink tubing are used in abundance to keep cables tidy and grouped.

A subsection of the cable system is shown in Figure 4.5 indicating connection of the motor drivers, battery supply and fuse box. Other cables such as those used for charging connections and control signals are grouped and attached under the steel frame to reduce disorder.

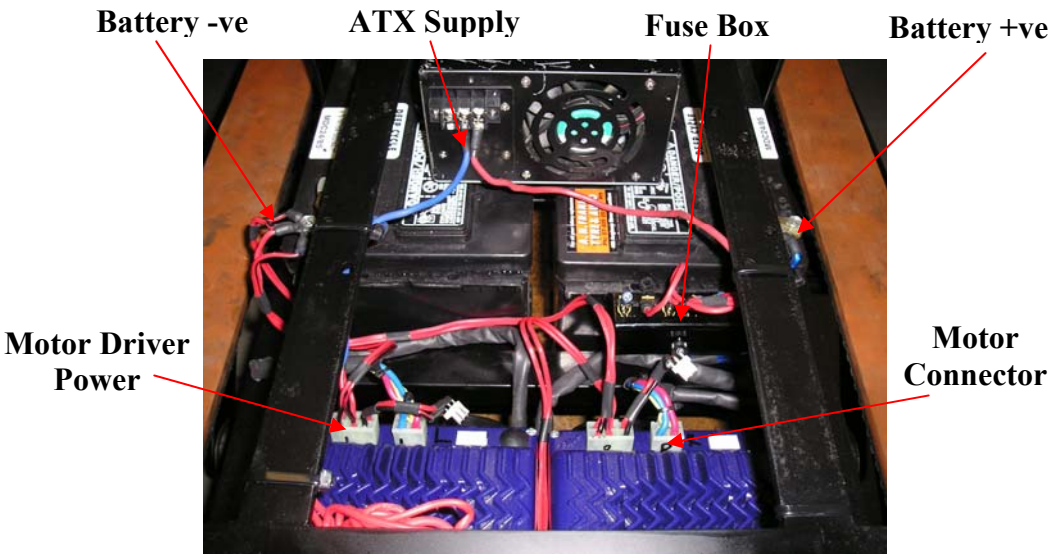

Figure 4.5 Subsection of wiring showing motor driver connection

4.2.3 Power Switch Panel

The switch mode ATX power supply, like most modern PC converters do not completely turn off when the computer is shutdown. They go into what is known as a "soft" shutdown mode which due to the supply's imperfect efficiency draws a small quiescent current. To prevent draining of the batteries over time, an external DPDT toggle switch is used to physically disconnect the power and ground rails from the supply.

This has been mounted on an easily accessible stainless steel plate, (Figure 4.6), at the rear of the mechatron chassis. Two additional switches are available for the motor driver units as it is often necessary to disable the motors while the electronic systems are running. The switches also provide a convenient "kill-switch" location to shut down the robot systems in case of emergency.

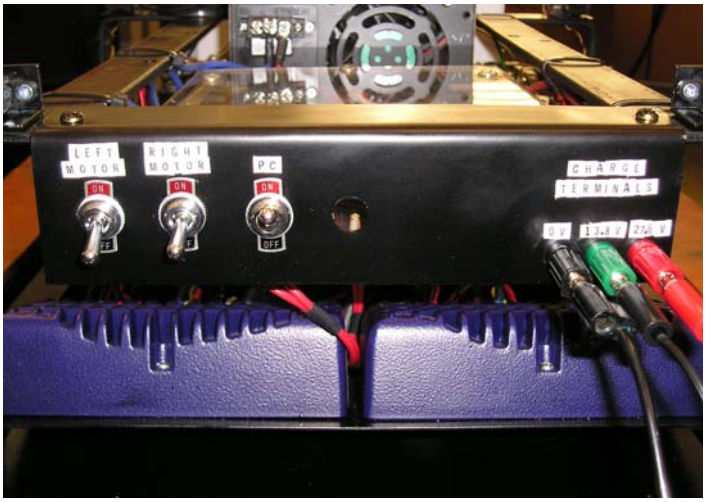

Figure 4.6 Power switch and charging panel

The three charging terminals are also located on the rear switch panel for accessibility reasons. An external power supply or battery charging system can be connected to charge the SLA batteries either individually or as a pair. It is not necessary to switch off the motor drivers while charging.

4.2.4 Power Distribution Board

A power distribution board illustrated in Figure 4.7 is designed to provide a central connection point for all electronic peripherals. Power is sourced from the ATX converter through the PCB mounted MOLEX connector providing +5 V, +12 V and two GND connections. Number coded for easy connection, the polarized connectors allow for 10 devices to be simultaneously connected.

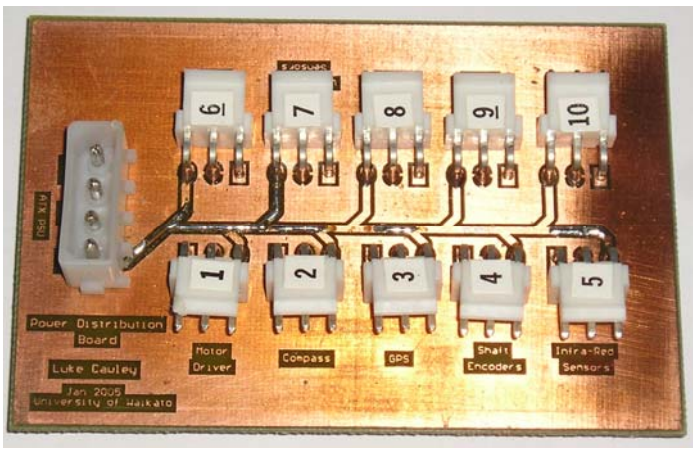

Figure 4.7 Power distribution board

4.3 SENSOR OPTIONS

In order for a mobile robot to operate autonomously it must be capable of detecting and analyzing the surrounding environment. To do this the mechatron must have the means to accurately gather environmental information and process it to enable intelligent decisions to be made on its operating process.

Although the detection and interpretation of surrounding objects is a natural process for humans and other animals, this is not as simply implemented on a robot. There currently does not exist a truly elegant or universal solution to mimic (for example) the human sense of sight in a robotic system. Humans seamlessly use sight to estimate range, analyze surrounding environment, detect potential hazards, acquire colour information and to recognize and clarify objects. Although much research is centred on developing this unified capability for a robotic system, the current methods rely on combining partial data from a range of sensing devices. Each sensor is designed to detect or measure a different type of environmental feature and relay this information to a computer controller for analysis.

4.3.1 Requirements

A number of sensors have been researched and evaluated for implementation on the outdoor mechatron. Although the primary operating environment is outdoors and over difficult terrain, the mechatron will also operate indoors during development. This is to facilitate algorithm testing such as obstacle avoidance and map building using walls and doorways as reference points and as a result the sensory systems must be selected to suit both environments.

Other key considerations in developing the sensor systems include the following:

- Obstacle detection
- Robot localization
- Attitude and orientation
- Terrain evaluation
- Course correction

- Object classification
- Ranging sensors
- Robot status and monitoring
- Application specific sensors

Some applications, such as localization require more than one type of sensor whereas certain sensory devices are capable of providing information suitable for a number of tasks. A short review of available sensor technology for integration into the robot follows in the next subsections.

4.3.2 Positioning

Information on robot positioning is crucial to the effective implementation of a navigation system. A robot cannot deduce its current location with respect to the entire operating environment or some goal point without some form of positioning sensors.

Positioning sensors can be grouped into two main categories based on the data acquisition techniques used. *Relative position* measurements acquire data referenced to a single point at the origin. All calculations are based on deviations from this point. Conversely, *absolute position* measurements use a universal reference such as a global co-ordinate system or a set of markers at known locations. This enables multiple robots operating in the same environment to use a common localization reference that does not require a common starting point.

An inherent problem with relative localization methods is the long term drift and instability of the results. All measurements have an associated error and therefore accumulate over time. Absolute positioning has the advantage of finite errors but do require extra infrastructure and expense to enable operation unless it already exists.

Sensors for robot positioning include:

- **Heading:** mechanical gyroscopes, fluxgate compass, Hall effect compass, magneto-resistive compass, optical/ring-laser gyroscopes, shaft encoders
- **Inclination:** accelerometers, reed-switches, mercury tilt switch

- **Locating Beacons:** ground based RF transmitters, GPS
- **Odometry/Velocity:** relative shaft encoders, absolute position sensors, ultrasonic ground speed sensor
- **Inertial Navigation:** accelerometers, gyroscopes

4.3.2 Ranging

Sensors used to measure distance are extremely useful on an autonomous mechatron. Range information is crucial to the safe avoidance of obstacles or classification of objects. Map building requires distance information to build up a picture of safe and unsafe territory.

Long range detection can be accomplished with laser range finders or ultrasonic transmitter/detector pairs. Infra red sensors are useful in mid to short range applications, particularly obstacle detection whereas extremely short range devices such as tactile or bump sensors are used as a last resort.

4.3.4 Other sensors

A wide range of other sensors can be integrated into the robotic system depending on the desired application. Robot monitoring sensors are used to ensure systems are operating efficiently and prevent malfunctions. Temperature sensors such as *thermistors* can monitor electronic circuits for over-heating while acceleration sensors can analyze the vibration signatures of moving parts such as motors indicating possible failure. Other environmental factors that can be monitored with sensors include chemical/gas detectors, pressure and humidity (*hygrometers*). Scene examination and object classification can be accomplished with a variety of imaging sensors such as cameras. Each of these can be installed on the outdoor mechatron but some are not required at this stage of the project.

4.4 ELECTRONIC COMPASS

An electronic compass provides robot heading information for the navigation and guidance system. Robot positioning by odometry alone rapidly accumulates errors particularly in tracked vehicles due the slippage of the drive components. The addition of a heading sensor to the control system can correct direction errors and increase the accuracy of the robot positioning software.

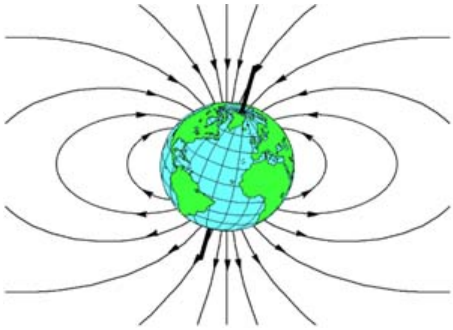

Figure 4.8 Earth's magnetic field

The Earth's magnetic field is approximately 0.6 gauss in an open-air environment[13] with the field lines directed from the magnetic South Pole to the magnetic North Pole. The magnetic field vector is horizontal near the equator but becomes increasingly vertical near the poles (inclination or dip angle), as shown by Figure 4.8. The field lines form the basis for magnetic compassing as units can be designed to measure the field strength in the plane (2-axis sensors) thus providing a measure of heading.

4.4.1 Previous Module

The electronic compass originally selected for this project (*Cordes*, 2002) was chosen for its significantly lower price than most other units available at the time and as a result functionality was limited. The Vector V2X, manufactured by PNI Corporation is a 2-axis magnetometer that measures magnetic field in a single plane. Accuracy when level is ±2° RMS however, this decreases rapidly when the unit is tilted.

[13] http://www.magneticsensors.com/landnav.html

A PCB interface board was designed (Figure 4.9) and DAQ card based interfacing software was written. The Vector2X produces serial binary coded decimal (BCD) or binary output format through the output pin representing the heading in degrees. However, communication problems with the device indicated it was faulty and could not be used.

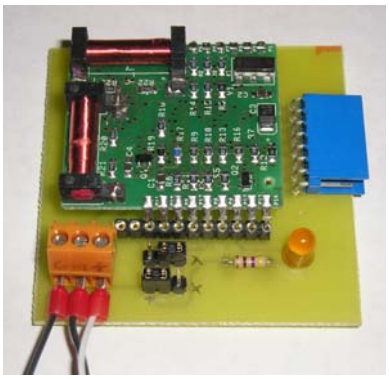

Figure 4.9 Initial Vector2X compass and interface board

The other major disadvantage with this module is the lack of accuracy when the unit is tilted. Modules with a 2-axis sensing element must remain horizontal or orthogonal to the Earth's gravitation component. This is not practical for a robotic vehicle designed for operation on rough and uneven terrain therefore selection of a 3-axis device or one which could be mechanically gimballed was required.

4.4.2 Review of Available Modules

A range of commercially available compassing solutions were evaluated for implementation of the outdoor mechatron. Some of these are discussed in the following sections outlining the benefits and shortfalls of each unit in relation to this project.

KVH C100 Compass Engine

The C1200 Compass Engine from KVH Industries[14], shown in Figure 4.10, is a standalone sensor designed for industrial applications. The module utilizes a detachable toroidal, fluxgate sensing element useful for remote mounting.

[14] http://www.kvh.com

Specifications include ±0.5° RMS accuracy when level, 100 – 0.04 Hz programmable response time and six analogue/digital interfacing methods including RS-232, NMEA-0183 and linear voltage.

Figure 4.10 KVH C100

Although the C100 has impressive features such as durability, and microprocessor controlled magnetic interference compensation, the high US$795 cost of the unit makes it unsuitable for this project.

CMPS03

The CMPS03 compass module (Figure 4.11) is available from Robot Electronics in the UK. At around NZ$66, the compass is very low cost and uses a pair of Philips KMZ51 magnetic field sensors mounted at right angles. This configuration means the module can only measure magnetic fields in a single plane and therefore the accuracy is poor compared to other units at 3 – 4°. Although the module is low cost and easily interfaced to a microcontroller through the I^2C interface, this module lacks the functionality for a mobile robot platform and is better suited to hobby use.

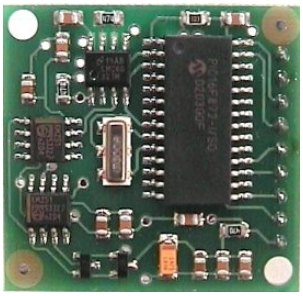

Figure 4.11 CMPS03 Low cost compass module

Handheld Units

A number of handheld compass modules such the MapStar in Figure 4.12 have been considered for installation on the outdoor mechatron. These devices are designed for outdoor use in surveying or construction and are therefore durable and highly accurate. Utilizing a range of sensing elements and user interface methods, handheld devices provide a ready to use solution however, difficulties with PC interfacing make them unsuitable for this project. Additionally, the cost far exceeds the OEM sensing modules due to the extra hardware for data display and configuration.

Figure 4.12 MapStar fully integrated handheld compass module

Honeywell HMR3000

A three axis electronic compass is available from Honeywell[15] providing a 20 Hz response time, 0.5° RMS accuracy and 0.1° resolution. The pitch and roll tilt ranges are ±40° and calibration routines are available for hard iron compensation of nearby ferrous objects.

Figure 4.13 HMR3000 compass module from Honeywell

[15] http://www.magneticsensors.com

Response times up to 20 Hz are possible due to the solid state sensing devices allowing a faster response compared to gimballed fluxgate sensors. The module, shown in Figure 4.13, comes with a protective plastic housing however functions per price (US$700) does not compare well to other devices investigated and is therefore not selected.

True North Revolution

The Revolution from True North Technologies[16] is a tilt compensated electronic compass with a heading accuracy of 0.5° and a ± 40° pitch and roll operating range. A key advantage of the Revolution, shown in Figure 4.14, is the quick connect external serial interface. This allows connection of the included PDA for testing and calibration during installation. A number of operating modes are available and the combination of 3-axis magnetometer and 2-axis electrolytic tilt sensors provide a 20 Hz response time. The Revolution has good features suitable for a robotic platform however, a completely solid state module was desired and the functionality-per-price (US$500) did not compare well to other modules. The handheld PDA unit was considered an unnecessary expense for a PC interfaced sensor system.

Figure 4.14 TrueNorth Revolution compass module

TruePoint Compass Module

The TruePoint compass module from Point Research Corporation (now available from Honeywell) is shown in Figure 4.15. The unit is designed for high performance

[16] http://www.tntc.com

military use with 1° RMS accuracy on each axis and a 50 Hz update rate. The unit is supplied with a durable aluminium housing and comprehensive test software. Data from three silicon magnetometers and three MEMS accelerometers are combined to provide highly accurate heading, pitch and roll data. The World Magnetic Model is also incorporated enabling the module to automatically provide global heading referenced to north and detection of magnetic anomalies. Although the high specifications and range of features make these modules the preferred solution, the high US$795 cost of the unit exceeds the project budget and therefore cannot be used.

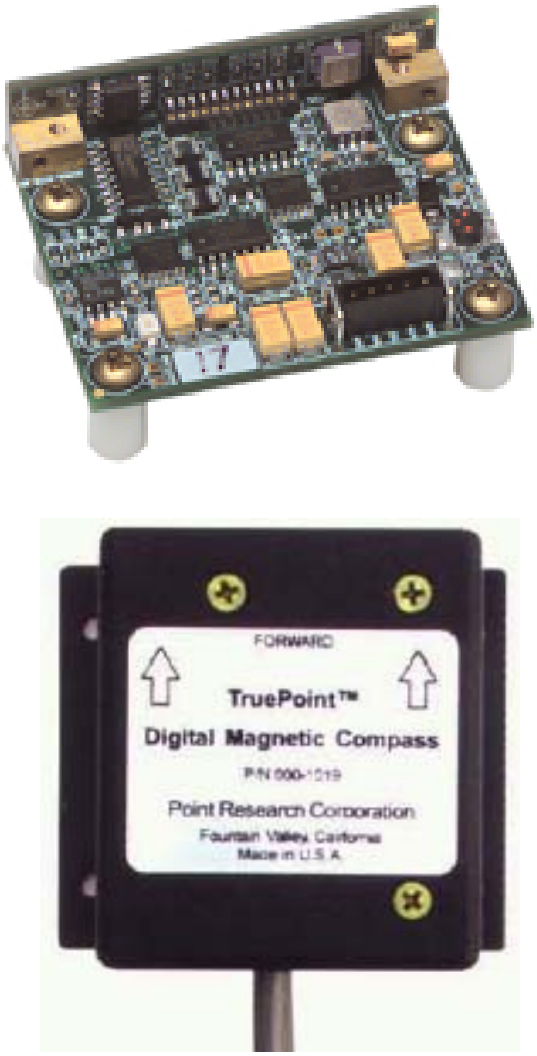

Figure 4.15 TruePoint compass module and protective housing

4.4.3 Selected Module

An HMR3300 electronic compass module from Honeywell was selected to satisfy the compassing requirements of the multi-terrain mechatron and other outdoor robotic vehicles under development by the Mechatronics Group. This unit, although costing more than some commercial systems evaluated, provided the best features per price available. The price of the HMR3300 compass module is NZ$729 or approximately US$385.

The compass measures orientation in 3-axes giving heading, pitch and roll data as illustrated in Figure 4.16. Additionally, the heading is compensated for tilts of ±60° using the onboard 2-axis accelerometer. Both SPI and UART interfacing methods are available to connect to a variety of systems.

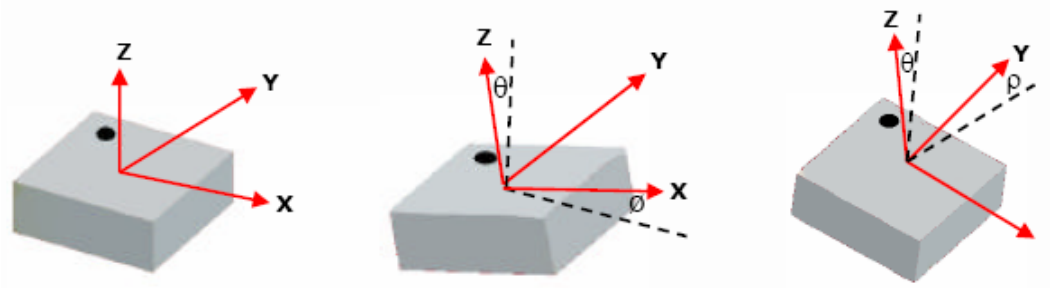

Figure 4.16 LEFT: No pitch or roll, heading in y-direction CENTRE: Roll is x-axis angle relative to ground RIGHT: Pitch is y-axis angle relative to ground

Solid state magneto-resistive sensors (Honeywell HMC1021 and HMC1022) are used to convert the Earth's magnetic field into a differential output voltage. This is fed to a multiplexed ADC converter and microcontroller system to apply offset corrections and heading calculations. An additional pair of inputs received from a 2-axis accelerometer is used to calculate pitch and roll angles and correct heading.

An advantage is the ability to compensate for hard iron distortions from nearby ferrous objects using the onboard calibration routine. This must be done when the module is fitted to the mechatron to ensure the robot's steel frame is included otherwise erroneous data may occur.

The specifications of the module are listed below:

- **Heading Accuracy:** 1 – 4° RMS depending on tilt
- **Resolution:** 0.1°
- **Pitch and Roll Range:** ± 60°
- **Pitch and Roll Accuracy:** 0.4 – 1.2°
- **Magnetic Field Range:** ± 2 gauss
- **Update Rate:** 8 Hz
- **Interface:** UART or SPI
- **Dimensions:** 25.4 × 36.8 × 11 mm
- **Weight:** 7.5 grams

Consideration must be given when the mechatron is in close proximity to power lines or steel structures as they can distort the magnetic field, however this problem may be remedied by fusing data from other sensors.

The HMR3300 was purchased with the demonstration kit to facilitate module testing and evaluation. The kit contains additional hardware and Windows software to form a complete development kit for electronic compassing. Included is the HMR3300 compass module, RS-232 adaptor motherboard, serial port cable with attached power supply, interface CD and operation manual. The software shows heading, pitch and roll through graphical ActiveX displays and allows calibration and zeroing of tilt angles.

4.4.4 Interface Design

The interfacing protocol selected is serial UART (as opposed to SPI) to allow connection to the PC through a USB to RS-232 converter. A PCB interface board was designed incorporating a MAX232 serial transceiver IC to convert the logic level serial data to high voltage for transmission over the serial line.

The schematic, shown in Figure 4.17 includes an onboard MC7805CT based power supply and indicator LED. A polarized connector supplies +12 V power from the power distribution board.

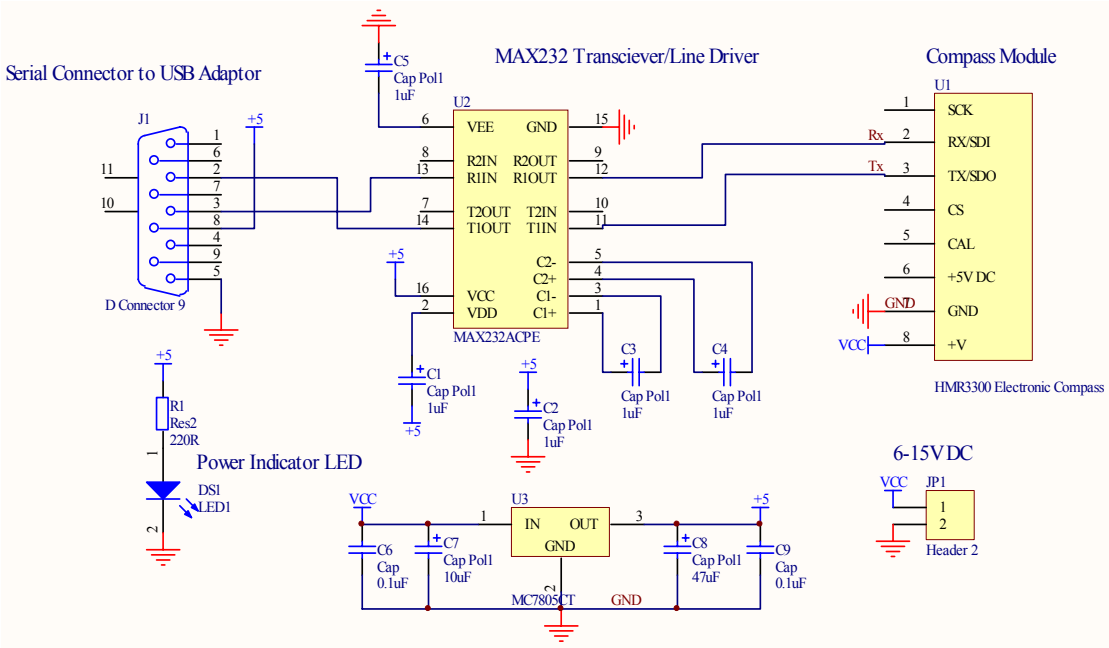

Figure 4.17 Compass module interface schematic

4.4.5 Mounting Enclosure

The compass module, interface PCB and USB to serial converter is mounted inside a blue plastic enclosure shown in Figure 2.18. The case protects the electronics from moisture and shock damage while providing a convenient mounting platform to the mechatron. Positioning on the robot is above the ShuttleX PC case (Y-axis facing forwards) keeping the module as far as possible from the motors and other high current wires to reduce magnetic interference impeding compass operation.

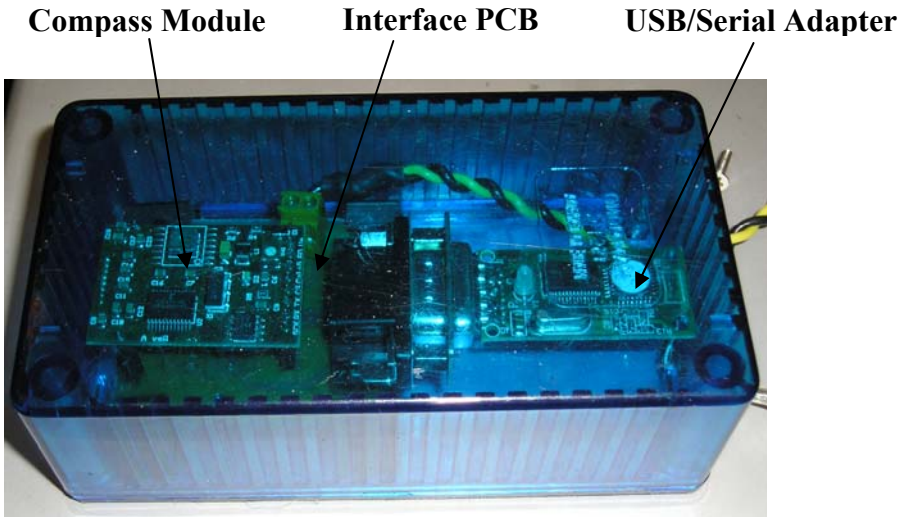

Figure 4.18 Compass module protective enclosure

4.5 GPS

Accurate positioning is crucial to the operation of an autonomous outdoor robot. The mechatron must have knowledge of its position relative to the goal location or positioning of known obstacles in order for it to carry out tasks. One form of sensor available to achieve reliable, absolute positioning is the Global Positioning System (GPS). GPS is a popular localization tool for navigation of mobile robots due to the constellation of orbiting satellites providing world-wide coverage. Relative positioning using odometry alone produces poor results accurate to only 5 – 10 m for straight line motion. The errors accumulate due to track slippage and uneven terrain requiring the implementation of an absolute positioning system such as GPS.

4.5.1 Background

GPS is an outdoor positioning system designed, financed and operated by the U.S. Department of Defence (DoD). The system was developed to provide continuous, worldwide 3D positioning to the full range of military platforms at sea, land and air.

Civilian use of GPS currently far exceeds military use despite the project origins however, as it is still operated by the DoD they have the ability to restrict performance at any time. Despite this limitation there is substantial innovation in civilian GPS technology and applications some of which are aimed at overcoming some of the current constraints applied by the operators.

GPS positioning works on the mathematical principle of 3-dimensional trilateration. This method uses the distance between the receiver and satellites to create an imaginary system of spheres around the satellites. The intersection points of the spheres represent the receiver location therefore at least 3-sattelites are required for a 3D fix. The receiver determines the locations of the satellites and distance to them by analyzing high frequency, low power radio signals sent by the satellites. A long digital pattern called a pseudo-random code is transmitted by the satellite which is compared to an identical signal generated by the receiver. The phase shift represents the signal travel time and therefore the distance (by multiplying by the speed of light).

In order to make this measurement both the satellite and receiver require a precise system of time keeping down to the nano-second. Atomic clocks using rubidium (and later caesium) are installed in each satellite to achieve accuracy and long term stability of a few parts in 10^{14} per day (about 1 sec in 3,000,00 years) . Costing between US$50 000 and $100 000 each and weighing more than 20 kg, atomic clocks are not suitable for the receiver equipment so quartz crystal clocks are used. They offer excellent short term stability therefore the receiver uses the timing signals from at least 4 satellites to update the onboard clock, effectively getting atomic clock accuracy for a fraction of the cost.

The GPS system consists of three segments as illustrated is Figure 4.19. The space segment consists of a constellation of 24 (27 including 3 backups) orbiting satellites and the signals they broadcast. They orbit on six equally spaced planes at an altitude of about 20200 km and period 11 hours 58 minutes guaranteeing at least four satellites are visible at anytime from any location.

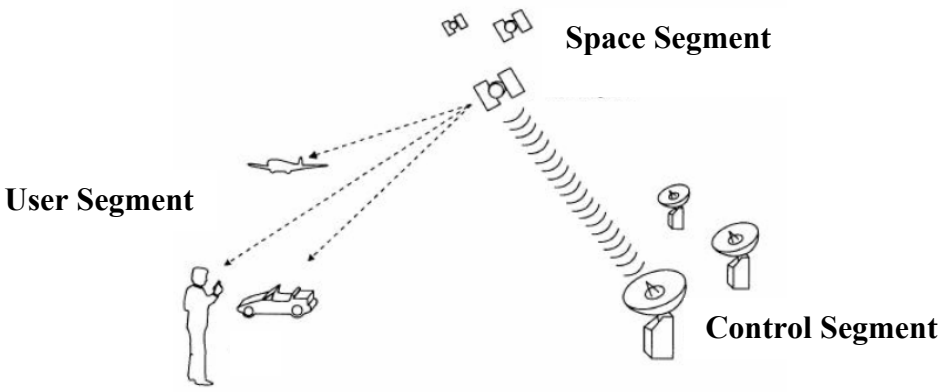

Figure 4.19 Three GPS operation segments

The control segment consists of five ground stations, including the master control at Schriever Air Force Base in Colorado Springs. These facilities provide satellite health monitoring, data up-linking, telemetry, satellite command and control, and the calculations of satellite orbit and clock offset. By tracking each satellite and calculating the ephemeris (satellite position) updated clock and repositioning data can be sent to the satellites to compensate for errors caused by gravitation forces and solar radiation pressure.

4.5.2 Receiver

The GPS receiver selected for this project is the M12+ Oncore from Motorola. It is a cost effective solution designed for automotive use and is therefore a physically small unit with low power consumption. Initialization times are small with a Time To First Fix (TTFF) of 15 – 60 s and an internal reacquisition time < 1s.

To enable the receiver to pick up signals from satellites, a suitable antenna must be connected. The module, shown in Figure 4.20 includes a micro-strip antenna, ceramic radio frequency (RF) filter and a signal preamplifier. The receiver and antenna pair is designed to receive L1 band (one of the two GPS carrier waves where L2 is for military use) signals at 1575.42 MHz. Modulated onto this signal at 1.023 MHz is the C/A (Course Acquisition) code which is a Pseudo Random Noise (PRN) sequence defined for each satellite. Tracking of 12 satellites simultaneously is possible as the receiver architecture consists of 12 channels. This allows selection and rejection of data from satellites with poor data or technical problems.

A range of features are available on the M12+ including data filtering and the input/output of almanac and ephemeris data. In addition to longitude and latitude, the M12+ also provides output data on 2D and 3D velocity, altitude, heading, time, and satellite status and signal quality. The module can also be configured for differential GPS which improves the positioning capabilities by using a base station to transmit correction data. The additional cost of the infrastructure and limited operating area however restricts the use of differential GPS for this project.

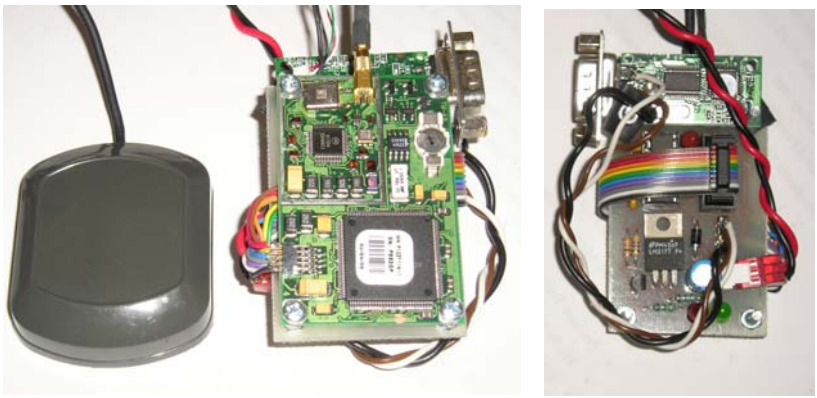

Figure 4.20 LEFT: GPS antenna and receiver RIGHT: Interface board

The GPS module was purchased as a standalone OEM unit meaning a suitable power supply and communication interface was not included. The requirements are a 2.75 – 3.2 V DC supply and as only a 3.3 V rail is available from the ATX converter, a custom 3 V circuit incorporating an LM317 voltage regulator was constructed. The serial communication interface uses a 0 – 3V signal at 9600 baud, 8 data bits, no parity and 1 stop bit. A MAX232 transceiver is used to convert to RS-232 voltage levels which are fed directly to the serial to USB converter for connection to the PC. The dimensions of the interface PCB are 60 × 40 mm and include LED's for power (green) and pulse–per-second (PPS) to indicate the module is operational (red).

Figure 4.21 LEFT: GPS receiver and interface board in protective case

Mounting of the GPS receiver is by a protective plastic enclosure similar to the compass module as shown in Figure 4.21. As the GPS receiver does not need to be in line of sight of the satellites, it is installed inside the metal electronics enclosure (section 4.10) for safety and aesthetics. Although the antenna will operate within some types of protective casing, it is positioned at the highest point possible at the centre of the mechatron. This decreases possible signal degradation and multi-path effects caused by reflections off other components.

4.6 ACCELEROMETER

The addition of a MMA7260Q inertial sensor from Freescale Semiconductor provides a means of measuring acceleration of the mechatron. Accelerometers can be used in a number of applications including robot positioning, impact detection and velocity detection.

4.6.1 Advantages

Certain operating environments can cause restriction or loss of the GPS signal such as canyons, large buildings or foliage such as under trees. The accelerometer can be used in sensor fusion applications as a backup or complement to standard GPS. Robot acceleration, and thus displacement by double integration, is measured to provide a reliable and accurate representation of robot position over the short term, thus allowing continued navigation without the GPS.

Additionally, the accelerometer can be used to "smooth-out" the noisy GPS data using Kalman filtering. Deficiencies in the GPS system (discussed in section 6.4.5) cause large position jumps even for stationary operation, these can be reduced by taking advantage of the complementary error attributes of the accelerometer and GPS listed below.

1) Accelerometer error is relative and increases without bounds
2) GPS error is absolute so is always limited to a certain degree

The fast response time and short term accuracy of the accelerometer can fill-in the gaps between GPS data and detect anomalies. If a large position change is reported by the GPS in a short time, (due to an error), the accelerometer data are used to confirm this or discount the data as physically impossible, thus improving localization accuracy.

4.6.2 Device Specifications

The MMA7260Q is a low cost, capacitive micro machined accelerometer (MMA) which features on board signal conditioning and temperature compensation. The small 6 × 6 × 1.45 mm 16-lead QFN package and low power consumption make it ideal for battery applications and integration on a mobile robot.

Also included within the module are switched capacitor based 1-pole low pass filters, this means external passive components are not required to set the cut-off frequency.

Other features and specifications of the module include:

- Selectable g-levels (1.5g/2g/4g/6g)
- Low current consumption 500 μA (3 μA sleep mode)
- Low voltage operation 2.2 – 3.6 V
- High sensitivity (800 mV/g @ 1.5 g)
- Fast turn on time
- Maximum survivable acceleration ±2000 g
- Zero g offset output voltage 1.65 V nominal

4.6.3 Theory of Operation

The acceleration sensing capability is derived from micro-electromechanical (MEMS) technology configured as surface micro-machined capacitive structures. These structures known as the sensing cells (g-cell) are combined with a signal conditioning ASIC (Figure 4.22) to form a single integrated circuit package.

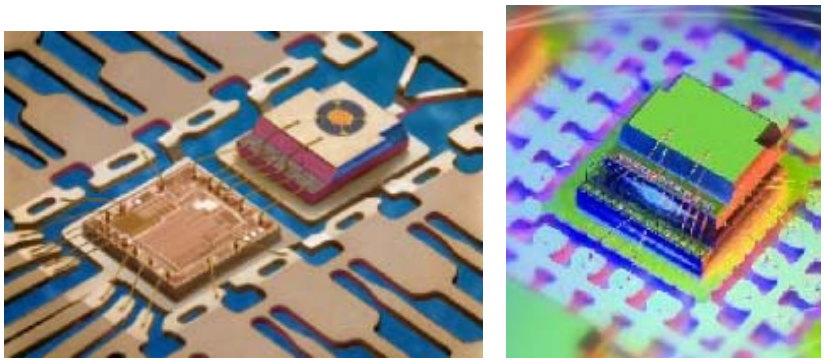

Figure 4.22 Capacitive sensing g-cells and ASIC LEFT: side by side RIGHT: stacked die

The g-cells are a mechanical semi-conductor structure made from polysilicon and can be modelled by a set of beams connected to a mass. The beams form two back-to-back capacitors as shown in Figure 4.23 which are deflected when subjected to acceleration. The changing capacitance between the beams according to Equation 4.1 is measured by a switched capacitor network and produces a ratiometric output voltage proportional to acceleration.

$$C = A\varepsilon / D \qquad \textbf{Equation 4.1}$$

C = capacitance, A = beam area, ε = dielectric constant, D = distance

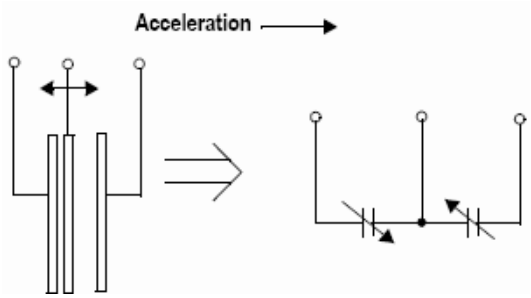

Figure 4.23 Beam and capacitor model of g-cells

4.6.4 Sensitivity

An advantage of the MMA7260Q is the g-select feature which enables selection between four different sensitivities. Depending on the logic levels at pins 1 and 2, g-levels of 1.5g, 2g, 4g and 6g are available as indicated by Table 4.1. Different g-levels are best suited different applications, for example 1.5 g is used for inertial navigation and free fall detection, while vibration analysis requires a much higher sensitivity as illustrated in Figure 4.24.

g-Select2	g-Select1	Range	Sensitivity
0	0	1.5g	800mV/g
0	1	2g	600mV/g
1	0	4g	300mV/g
1	1	6g	200mV/g

Table 4.1 Sensitivity selection

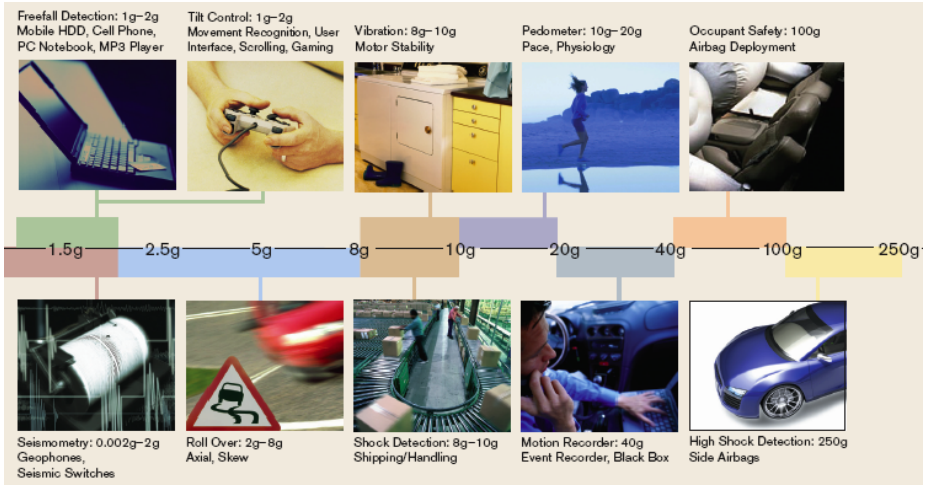

Figure 4.24 Suggested g-levels for various applications (www.freescale.com)

4.6.5 Interface Design

The accelerometer has three analogue output channels corresponding to the 3-axes of g-cell orientation. Acceleration in any of the directions X, Y, Z will produce a corresponding voltage on the output pins X_{out}, Y_{out} and Z_{out} determined by the current sensitivity setting.

An interface board (Figure 4.25) has been designed and fabricated to mount the accelerometer and provide a means of interfacing the output signals to a DAQ card for computer analysis. Low pass RC filters consisting of 10 kΩ resistors and 0.1 μF capacitors are connected between the outputs and DAQ card to minimize switching noise from the switched capacitor circuit.

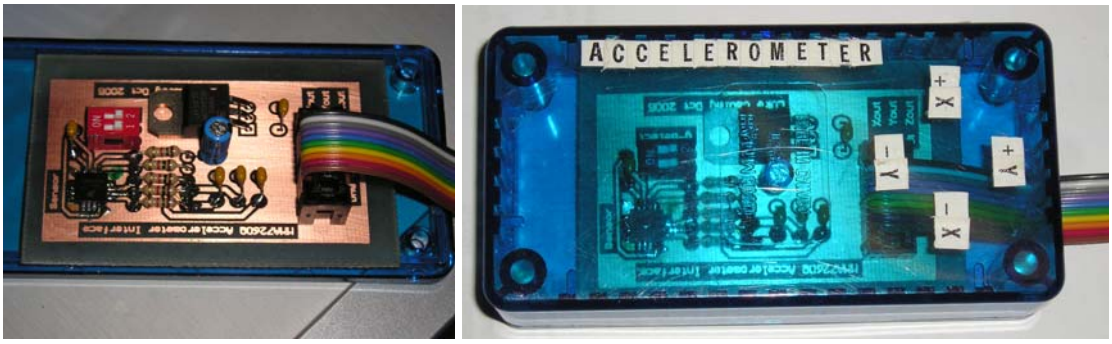

Figure 4.25 Accelerometer interface board and case

A 2-way DIP switch provides user configuration of the sensitivity by altering the logic levels on the g-select pins as per section 4.6.4. The 5 V input supply from the DAQ card is converted to 3.3 V by an onboard voltage regulator and decoupling capacitor circuit. The complete schematic is available in Appendix A.3.

A plastic mounting enclosure provides durability and weather protection to the accelerometer and circuitry. Indicator arrows on the case represent the module orientation and acceleration directions for each channel. Mechatron acceleration forwards is indicated by the + Y direction therefore the accelerometer should be mounted with the + Y arrow pointing ahead.

4.6.6 Measuring Tilt

Accelerometers are capable of measuring both dynamic and static forms of acceleration. Tilt is a type of static measurement where the Earth's gravity is the acceleration experienced by the module. Although tilt data are already available from the 3-axis compass module of section 4.4.3, the accelerometer can act as a backup device which has the added benefit of not being affected by stray magnetic fields or ferrous objects.

A level mounted accelerometer with the –Z axis pointing upwards will experience downwards acceleration in the +Z direction of 1 g (9.8 m/s) and 0 g in the X and Y directions. As the device is rotated the detected acceleration in the Z direction will decrease and it increases in the X and Y directions (depending on axis of rotation) thus experiencing acceleration in the range -1 g to +1 g as it rotates -90° to +90°.

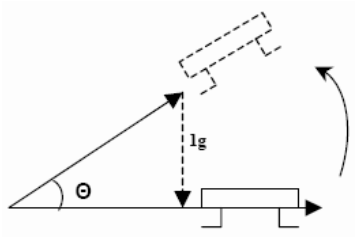

Figure 4.26 Example of accelerometer tilt in Earth's gravity

$$V_{out} = V_{offset} + \left(\frac{\Delta V}{\Delta g} \times 1.0g \times \mathbf{sin}\,\theta \right) \qquad \textbf{Equation 4.1}$$

where: V_{out} = Accelerometer output (volts)
V_{offset} = Accelerometer 0g offset
$\Delta V/\Delta g$ = Sensitivity
1.0g = Earth's gravity
θ = Angle of tilt

An example of accelerometer tilt is shown in Figure 4.26 with Equation 4.1 giving the corresponding output voltage for a given tilt angle. By rearranging the equation, the tilt angle can be calculated for each channel given the output voltage. The offset voltage represents the zero-g output and is 1.65 V for a 3.3 V supply. Positive acceleration will tend towards +2.45 V while negative towards 0.85 V.

Results of accelerometer tilt experiments and comparisons with the electronic compass output are discussed in section 6.2.3. Preliminary tests on using the accelerometer for collision detection are also explored in section 6.2.2.

4.7 SHAFT ENCODERS

Relative positioning of the mechatron is achieved using odometry to measure wheel/track rotation with encoders. Odometry has the advantage of being self-contained and always able to provide position estimation. The downside however, is that position error grows without limits unless an independent reference is periodically used.

An incremental shaft encoder (Honeywell HOA2001) is used to measure shaft rotation velocity and from this can infer relative position. The system works by mechanically blocking the light beam from the encoder sensor using an encoder disk attached to the drive shaft. The encoder disk consists of a series of evenly spaced holes around the perimeter. The time between the resulting square wave pulses is measured to calculate velocity because a certain fixed number of pulses represent a complete revolution and a known linear distance.

There are inherent inaccuracies in a track driven platform using dead-reckoning caused by deviations in the terrain or slippage/loss of traction in the tracks. For these reasons the encoders are primarily used for velocity control and distance measurement over short/straight trajectories instead of robot localization.

Figure 4.27 Newly manufactured encoder disks

A new set of encoder disks have been manufactured (Figure 4.27) due to damage of the previous units and an insufficient number of holes. Made of aluminium plate and bolted to the drive shaft couplings, the new disks have 24 evenly spaced holes; double that of the previous units. Although the original disks had a satisfactory resolution of approximately 19 mm per pulse, the problem arose during low velocity movement due to the slow update rate.

The control software had difficulty distinguishing between low velocity and zero velocity thus producing intermittent bursts of speed data. Although this problem will always exist for this type of low resolution encoder, it is not necessary to install a high resolution device (500 count/rev) due to the large scale of the operating environment. A software workaround has been developed to compensate which is described in section 5.8.

The gear ratio from the gearbox to the tracks is 12:1 meaning the drive shaft (and thus the encoder disk) must rotate 12 times for each revolution of the belt. With a belt length of 2.3 m this gives a linear travelling distance of 0.19 m per encoder revolution. Therefore, twenty-four, 15 degree spaced, incremental steps will produce a linear travelling distance of 7.9 mm per encoder pulse, which is more than adequate for the terrain and drive system type.

4.8 INFRARED SENSORS

Prior to the installation of a more sophisticated 3-dimensional, laser range finding device (*Carnegie (et. al),* 2005) infra red (IR) sensors are used as the primary mechanism for obstacle detection. Infra red sensors operate by transmitting a modulated electromagnetic signal in the infrared spectrum ($\lambda = 850$ nm $\pm$ 70 nm) and measuring the reflected signal.

4.8.1 Operation

A range to the object can be calculated using triangulation using a small linear CCD array. This approach gives the sensor increased immunity to ambient lighting

conditions and a longer detection range compared to other methods such as reflected intensity. The transmitted light reflects off a nearby object and creates a triangle between the emitter, point of reflection and detectors as indicated by Figure 4.28.

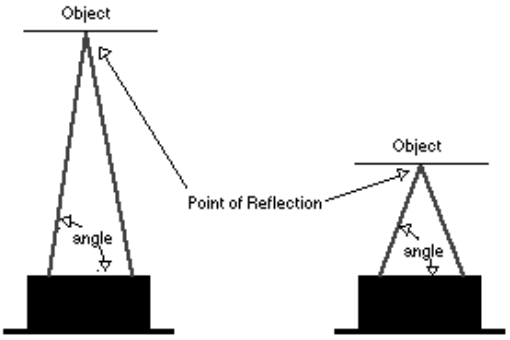

Figure 4.28 Triangulation with infrared sensors

Using a precision lens to direct the incident signal to the CCD array, the position along the detector and thus the incident angle can be calculated providing a measure of distance to the object.

4.8.2 Sensor Response

The output of the detectors (Sharp GP2Y0A02YK) is an analogue voltage corresponding to the measured distance which is updated every 32 ms. Due to the trigonometry in the triangle formed between the sensors and detected object, the output voltage does not change linearly with distance. This is shown in Figure 4.29 which illustrates an experimentally derived output voltage vs. range graph for a number of different objects.

The results show a number of interesting features about the operation of the sensors. Firstly, the response is relatively unaffected by the colour or reflectivity of the obstacles as the white cardboard, grey plastic and wooden particle board all exhibit similar responses. The exception lies with highly reflective objects such as shiny aluminium. Small changes in object orientation relative to the sensor cause the signal to be reflected causing spikes in the data.

Secondly, the maximum operating range of the devices can be determined by examining the point at which the data becomes very noisy or inaccurate. A maximum range of approximately 160 cm can be achieved with the particle board indoors while this drops to 100 cm outdoors due to ambient lighting.

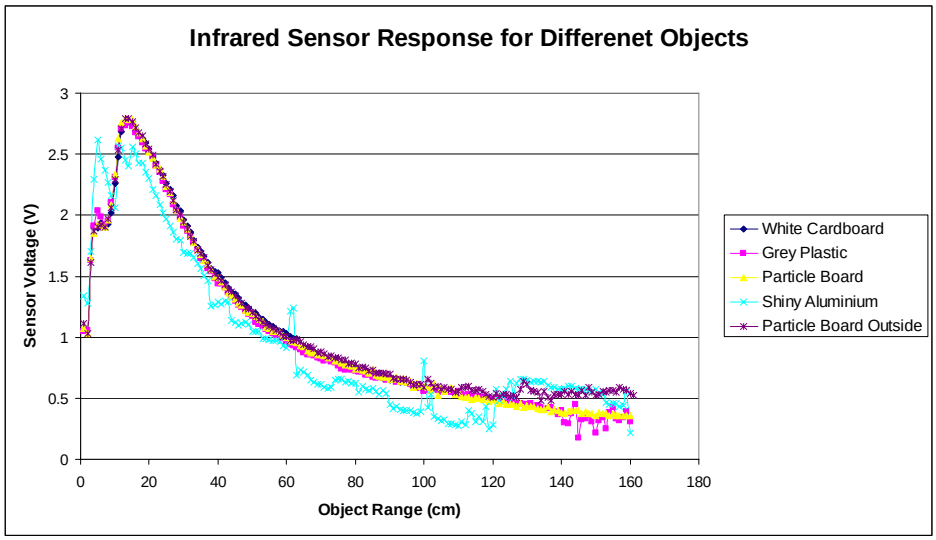

Figure 4.29 Infrared sensor responses for different objects

Thirdly (and finally) there is a sudden decrease in output voltage when the range falls below a certain value. This is an important consideration for obstacle detection on a mobile robot because it means an initial "dead-zone" of about 20 cm exists between the sensor and valid detection ranges. Additionally, this portion of the graph is not one-to-one which means more than one range is available for a particular output voltage. This can be disastrous if a robot misinterprets an object in close range as being further away. These problems are overcome by mounting the detectors within the robot frame ensuring valid ranging values always lie outside the robot perimeter.

4.8.3 Range Calculation

The experimentally determined sensor output versus distance data is plotted in MATLAB to generate a response data set. A smooth curve is fitted to the data using the Curve Fitting Toolbox (Figure 4.30) ensuring low range data points are excluded and thus preventing the equation curving back on itself. The theoretical response taken from the device datasheet is also shown and indicates a good correlation with experimentally derived results. The curve exhibits the same non-linear properties and

also curves back at low distances providing a non-unique relationship between distance and output voltage.

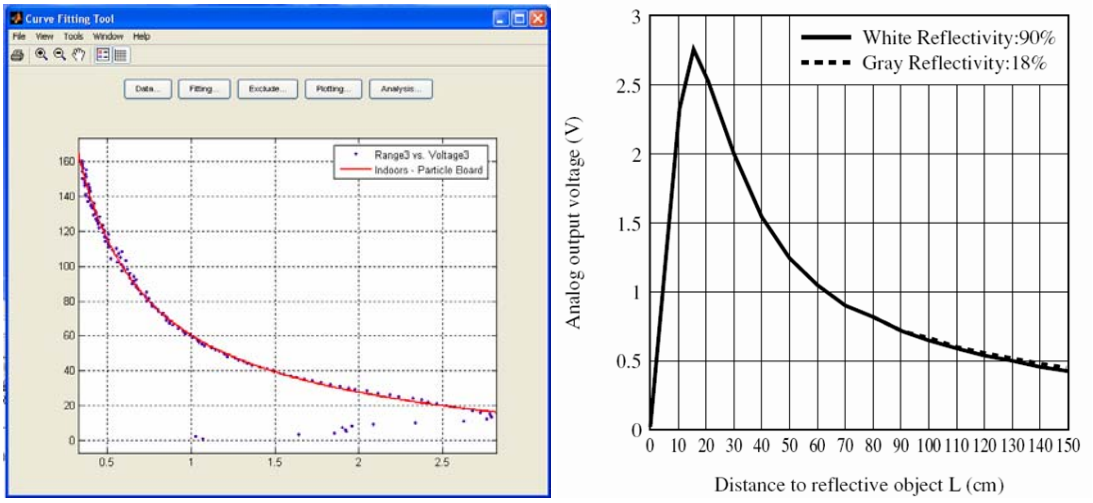

Figure 4.30 LEFT: MATLAB Curve Fitting toolbox for infrared data RIGHT: Theoretical infrared sensor response

The resulting equation giving object range indoors in terms of output voltage is a rational polynomial given by Equation 4.2. Utilizing a quadratic function on the numerator and linear function on the denominator the curve fits the experimental data very well. Additionally the equation for outdoor operation has been determined and accounts for the lower range detection ability due to ambient lighting conditions. The outdoors range equation is given by Equation 4.3.

$$IndoorRange(cm) = \frac{\left(p_1 V^2 + p_2 V + p_3\right)}{\left(V + q_1\right)} \qquad \textbf{Equation 4.2}$$

$$p_1 = -2.809$$
$$p_2 = 0.2903$$
$$p_3 = 68$$
$$q_1 = 0.08129$$

$$OutdoorRange(cm) = \frac{\left(p_1 V^2 + p_2 V + p_3\right)}{\left(V + q_1\right)} \qquad \textbf{Equation 4.3}$$

$$p_1 = 7.168$$
$$p_2 = -49.73$$
$$p_3 = 144.9$$
$$q_1 = 17.339$$

Software is used to ignore range values below 20 cm as these represent the sensor dead-zone while voltages below 0.36 V represent an object at 160 cm. Although it is possible no object is present in this case, it must be assumed an obstacle lies at maximum detector range (160 cm) to prepare the control system for object evasion thus ensuring effective route planning and obstacle avoidance in unknown areas.

4.8.4 Mounting

Twelve sensors have been installed around the periphery of the robot giving a wide field of view and reducing the risk of not detecting an obstacle. The interfacing electronics are designed to connect up to 16 sensors thus allowing for future expansion.

Particular attention is given to front-mounted sensors as these provide the most important information during normal operation. Front facing sensors can detect oncoming obstacles whereas the side mounted sensors can be used to "track" or monitor the obstacle as is passes by the mechatron. These additional sensors are also useful when reversing or making a turn (particularly stationary) to ensure objects are not within the turning radius.

The approximate mounting positions relative to the robot chassis is illustrated in Figure 4.31. Each infrared sensor is positioned 20 cm within the robot extremities thus compensating for the initial dead-zone.

Custom mounting brackets were fabricated from aluminium box tubing to attach the infra red sensors to the mechatron. The brackets form an L-shape to which M4 screws secure the sensors via the two mounting holes. Each bracket is attached to the mechatron with a single, centre mounted screw to enable sensor alignment as shown in Figure 4.32. The sensors may be rotated to face any direction thus altering the obstacle detection ability of the sensors in different areas of the mechatron.

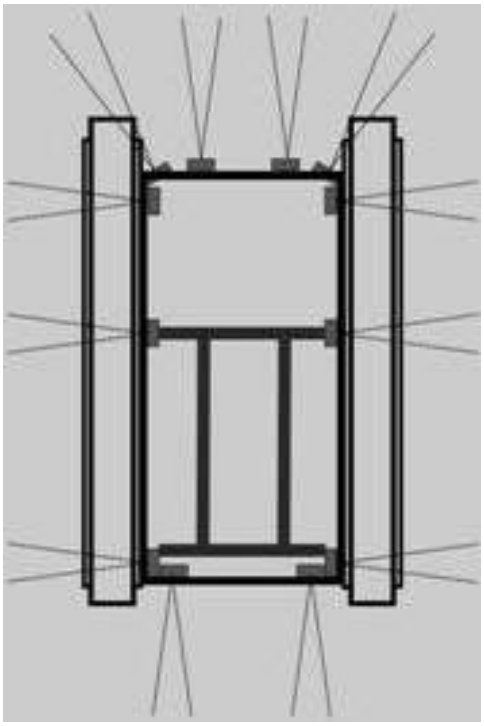

Figure 4.31 Infrared sensor locations

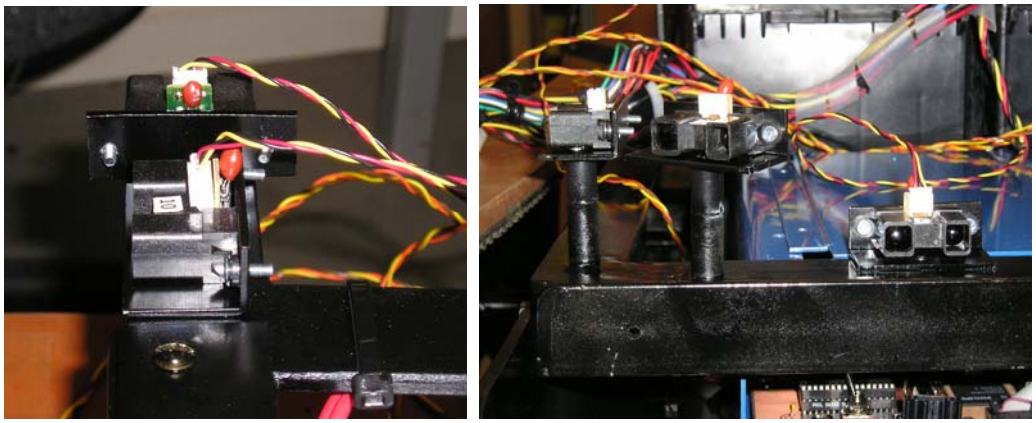

Figure 4.32 Infrared sensor mounting brackets

The side facing and angled sensors at the front of the mechatron have been mounted on plastic spacers to bring the sensing beam above the height of the tracks.

The infrared sensors have a very narrow filed of view compared to other ranging sensors such as ultrasound as indicated by Figure 4.33. Small obstacles can easily evade detection if they pass between the sensing beams of two adjacent sensors. To avoid this situation a continuous line of sensors could be installed around the entire robot increasing the sensing capability however this is expensive. A better solution is to rotate the sensors to create an effective bumper at the front of the robot as

illustrated in Figure 4.34. The two beams cross over each other creating the widest detection beam possible and cover a large area.

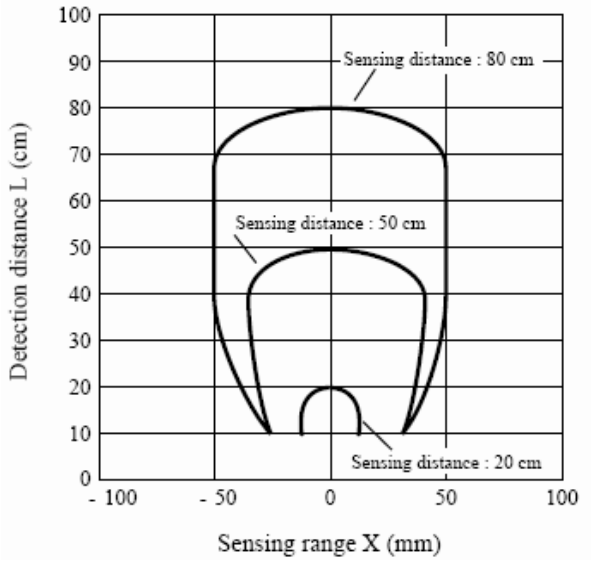

Figure 4.33 Lateral sensing distance for different object ranges

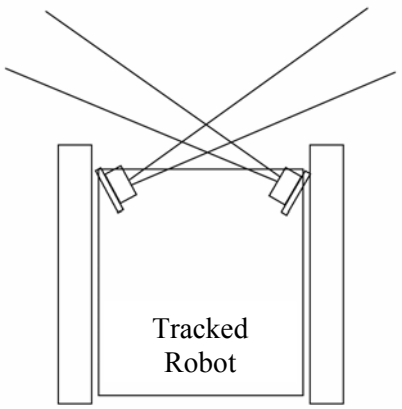

Figure 4.34 infrared based non-contact bumper

Each infra red sensor has a 0.1μF decoupling capacitor connected across the power rails directly on the package to ensure a stable supply. Connection to the DAQ card is accomplished with infrared sensor interface boards as shown in Figure 4.35. Labelled, polarized connectors are used for the sensor modules to supply power and receive the output signal. IDC 10-pin headers connect the interface modules to the DAQ card ADC for signal analysis and range extraction.

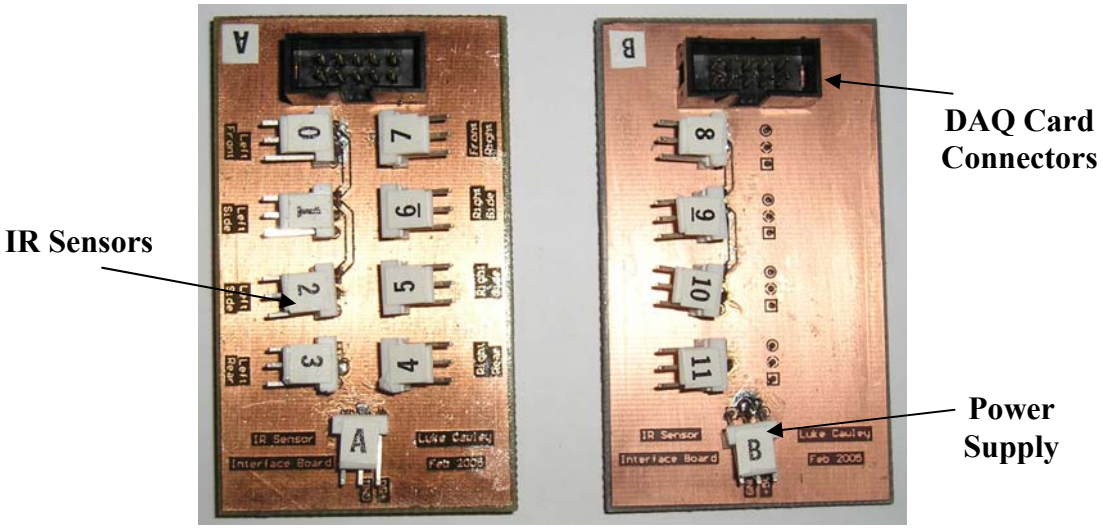

Figure 4.35 Infrared sensor interface boards

4.9 DAQ CARD CONNECTOR MODULE

Peripherals are connected to the DAQ using a pair of CB-68LPR terminal block connector modules from National Instruments (Figure 4.37). The M series DAQ card has two 68 pin connectors thus two NI SCH68-68 extended performance, shielded connector cables are used to interface to the terminal blocks. The cables use individually shielded and twisted wires keeping the analogue and digital sections separate thus reducing cross talk in high speed applications.

The connectors are termed "CON0" and "CON1" (Figure 4.36) with the cables and terminal blocks labelled accordingly. The functionality of each connector and its associated pins is described in Figure 4.38. DAQ features are essentially split evenly between the two connectors enabling many of the peripherals to be interfaced to one connector board.

Figure 4.36 Labelled terminal blocks CON0 above, CON1 below

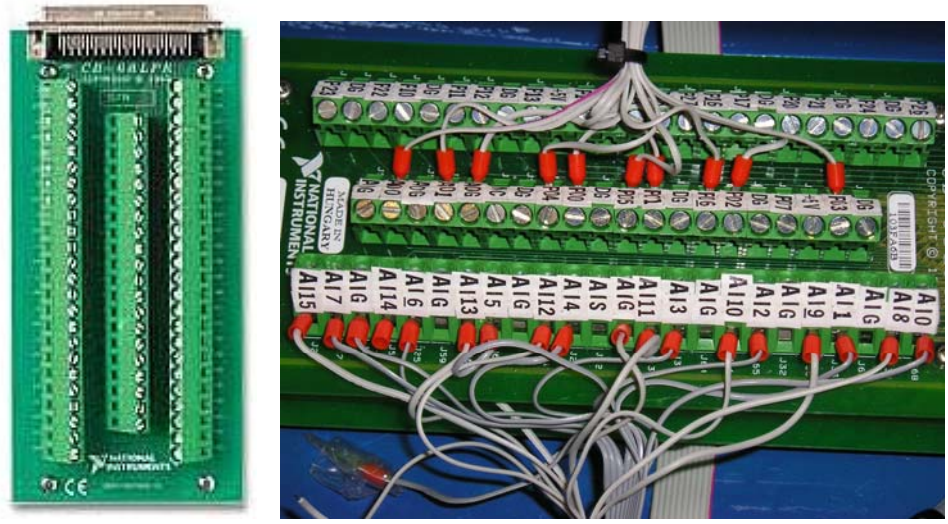

Figure 4.37 LEFT: CB-68LPR terminal block RIGHT: labelled connectors

All of the 16 infrared sensor outputs are connected to the analogue input (AI) pins AI 0 to AI 15 on the first terminal block while the accelerometer signals are connected to AI 16 to AI 18 on the second board. A complete list of DAQ card connections is shown in Table 4.2.

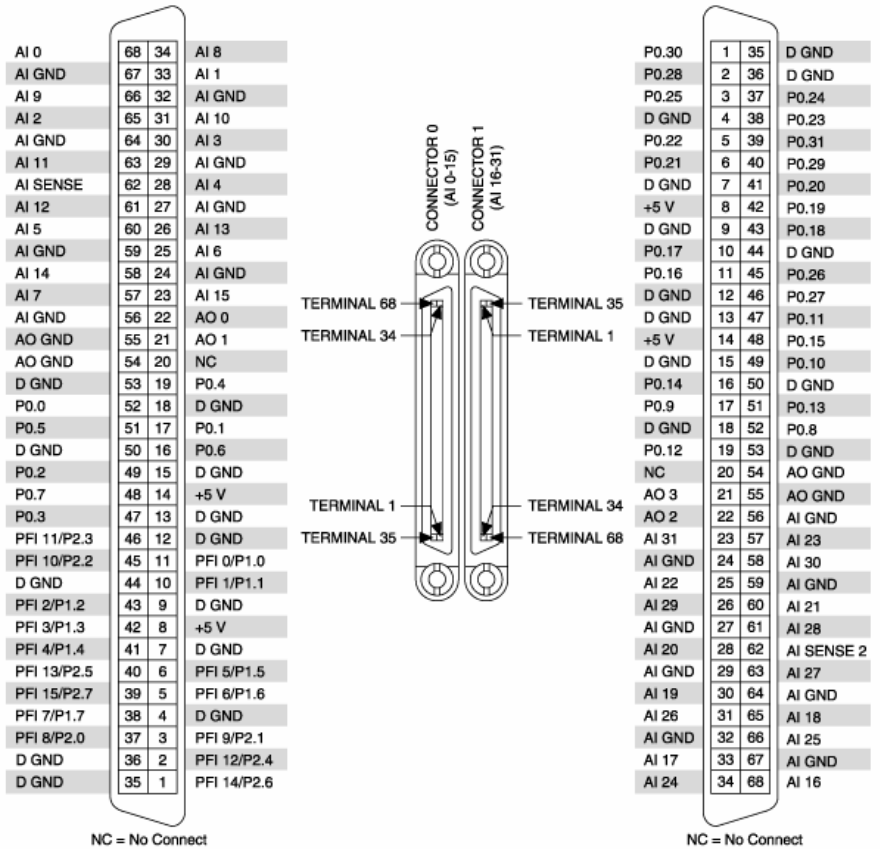
AI 0 68 34 AI 8
AI GND 67 33 AI 1
AI 9 66 32 AI GND
AI 2 65 31 AI 10
AI GND 64 30 AI 3
AI 11 63 29 AI GND
AI SENSE 62 28 AI 4
AI 12 61 27 AI GND
AI 5 60 26 AI 13
AI GND 59 25 AI 6
AI 14 58 24 AI GND
AI 7 57 23 AI 15
AI GND 56 22 AO 0
AO GND 55 21 AO 1
AO GND 54 20 NC
D GND 53 19 P0.4
P0.0 52 18 D GND
P0.5 51 17 P0.1
D GND 50 16 P0.6
P0.2 49 15 D GND
P0.7 48 14 +5 V
P0.3 47 13 D GND
PFI 11/P2.3 46 12 D GND
PFI 10/P2.2 45 11 PFI 0/P1.0
D GND 44 10 PFI 1/P1.1
PFI 2/P1.2 43 9 D GND
PFI 3/P1.3 42 8 +5 V
PFI 4/P1.4 41 7 D GND
PFI 13/P2.5 40 6 PFI 5/P1.5
PFI 15/P2.7 39 5 PFI 6/P1.6
PFI 7/P1.7 38 4 D GND
PFI 8/P2.0 37 3 PFI 9/P2.1
D GND 36 2 PFI 12/P2.4
D GND 35 1 PFI 14/P2.6
NC = No Connect
CONNECTOR 0 (AI 0-15)
CONNECTOR 1 (AI 16-31)
TERMINAL 68
TERMINAL 34
TERMINAL 1
TERMINAL 35
TERMINAL 35
TERMINAL 1
TERMINAL 34
TERMINAL 68
P0.30 1 35 D GND
P0.28 2 36 D GND
P0.25 3 37 P0.24
D GND 4 38 P0.23
P0.22 5 39 P0.31
P0.21 6 40 P0.29
D GND 7 41 P0.20
+5 V 8 42 P0.19
D GND 9 43 P0.18
P0.17 10 44 D GND
P0.16 11 45 P0.26
D GND 12 46 P0.27
D GND 13 47 P0.11
+5 V 14 48 P0.15
D GND 15 49 P0.10
P0.14 16 50 D GND
P0.9 17 51 P0.13
D GND 18 52 P0.8
P0.12 19 53 D GND
NC 20 54 AO GND
AO 3 21 55 AO GND
AO 2 22 56 AI GND
AI 31 23 57 AI 23
AI GND 24 58 AI 30
AI 22 25 59 AI GND
AI 29 26 60 AI 21
AI GND 27 61 AI 28
AI 20 28 62 AI SENSE 2
AI GND 29 63 AI 27
AI 19 30 64 AI GND
AI 26 31 65 AI 18
AI GND 32 66 AI 25
AI 17 33 67 AI GND
AI 24 34 68 AI 16
NC = No Connect

Figure 4.38 NI-PCI6229 DAQ card connector pinout

Signal Labels	DAQ Card Connector	Pin Number	Port Function	Description
Infrared sensor interface boards				
0 – 15	CON 0	68,33,65,30,28,60, 25,57,34,66,31,63, 61,26,58,29	AI.0 to AI.15	Analogue input channels Board A: 0 – 7 Board B: 8 – 15
G	CON 0	24,59	AI GND	Ground
Motor driver system microcontroller				
1 - 2	CON0	22,21	AO.0 to AO.1	Analogue output velocity control
3 – 8 & 10	CON 0	52,17,49,47,19,51, 16	P00 – PO6	Digital I/O control (Table 3.3)
9 (G)		54	AO GND	Ground
Accelerometer				
X, Y, Z	CON1	68,33,65	AI.16 – AI.18	Analogue input channels
5	CON1	14	+5V	+5 V Power supply
G	CON1	67	AI GND	Ground

Table 4.2 DAQ card connections summary

4.10 ELECTRONICS ENCLOSURE

An aluminium enclosure is installed on the mechatron to safely house the electronic systems. The box is secured to the robot frame and custom made aluminium plate by two bolts thus providing a secure mounting location for components. Included are two steel end plates and cover which when screwed together form a durable, weather proof enclosure.

The microcontroller board, radio-control interface board and DAQ card connectors are screwed to the base of the enclosure as shown in Figure 4.39. The underside of the enclosure lid is used to secure the power distribution board, infrared sensor interface boards and the GPS receiver thus best utilizing the space within the enclosure.

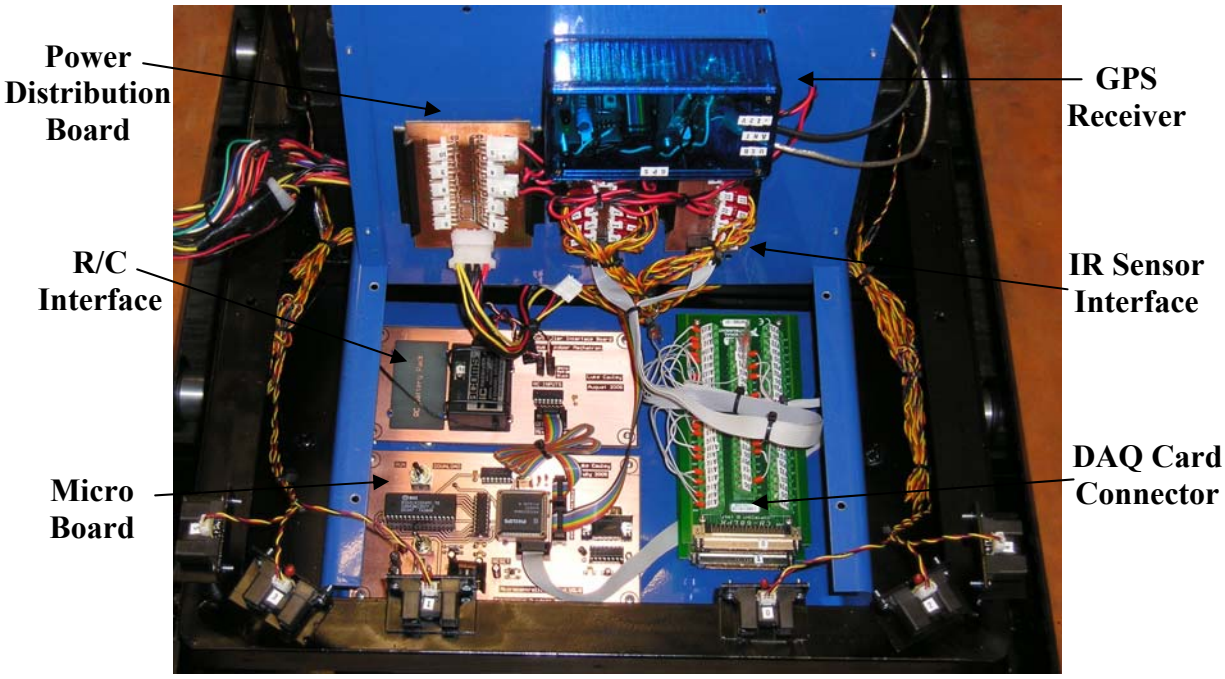

Figure 4.39 Electronics enclosure

4.11 HARDWARE SUMMARY

The mechanical shell of the mechatron did not have any working electronic systems installed at the onset of this project. The various electrical systems designed and implemented on the outdoor mechatron have been described. A block diagram overview of the hardware and associated connectivity is outlined in Figure 4.40.

A generic design approach has been used to ensure compatibility with future upgrades and portability to other robotic vehicles. A central computer is installed with the necessary communication interfaces and hardware protection for outdoor robot control. Power distribution to each electronic system is accomplished with a range of cabling and switches including fused protection and uniform modular connectors to each device.

A range of sensing options have been researched and the implementation of GPS, electronic compass, accelerometer and infrared range sensors provide the means for autonomous operation outdoors. Additional hardware including a DAQ card connection system and electronics enclosure provides convenient connection to and protection of the various electronic components.

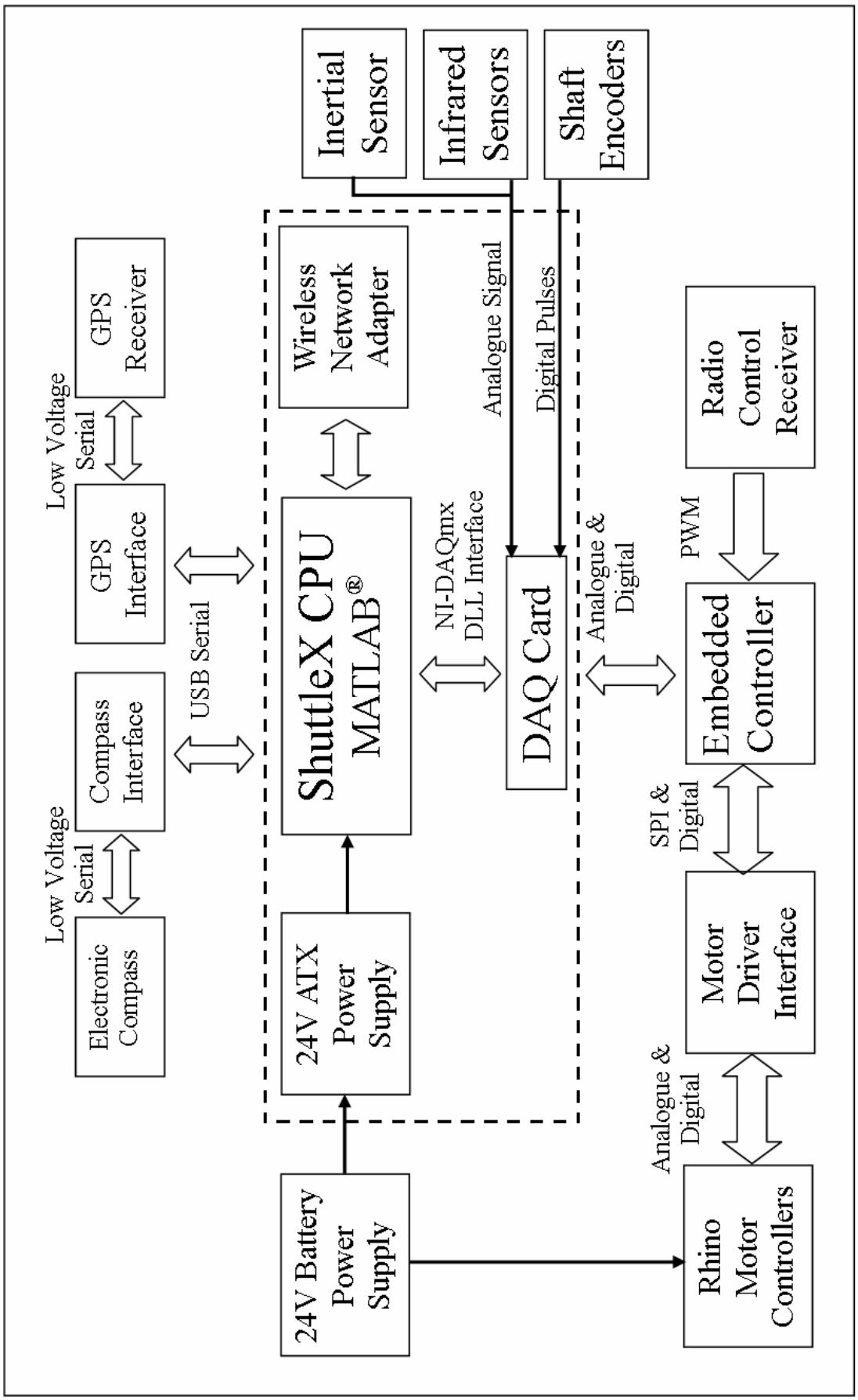

Figure 4.40 Block diagram overview of mechatron hardware

5. SOFTWARE

In order to control and monitor the outdoor mechatron a number of software systems were developed. These are required to provide control commands to the motor driver system, interface to sensors and other hardware for information extraction and to provide a suitable human-machine interface to the user. This chapter discusses the various software development platforms used and the algorithms developed to achieve autonomous operation on the multi-terrain, outdoor mechatron.

5.1 APPLICATION REVIEW

A number of different software platforms are available for algorithm development on the outdoor mechatron, each having advantages and disadvantages for certain applications. Selection of the most suitable platform was crucial to effective hardware-to-software communication for interfacing, control and interaction with the user.

Some of the requirements considered for choosing a software package are:

- **Architecture Compatibility:** Software must be compatible with the selected computer system architecture to allow installation and operation. Some operating systems and software packages are designed for non *i386* based architectures and therefore cannot be used.
- **Development Time:** Short development of algorithms is necessary for rapid prototyping and customization. Utilization of built in/prewritten functions for many tasks is preferred over complete development from the ground up.
- **Code Customization:** Rapid customization and alteration of algorithms is important during development. The process of updating and compiling code for testing must be accessible and reasonably straightforward.
- **Learning Complexity:** A low level of complexity is preferred to reduce the learning curve associated with a new system. Project objectives are more focused on producing robot operation than advanced programming.

- **Versatility:** The selected development environment must be versatile with respect to its interfacing and algorithm capabilities. Different types of hardware connection and function access will be experienced during development and the programming system must be capable of accessing these. Examples include DAQ card accessibility, serial port, and support for USB connected devices.
- **High Level Intelligence:** Future development will require the implementation of high level control systems and artificial intelligence so the selected platform must be capable of these. Examples of advanced algorithms include neural-networks and genetic algorithms which allow the mechatron to learn and adapt to its environment.

The following sub-sections describe some of the software development platforms available and their suitability for this project with consideration given to the above criteria.

5.1.1 LabVIEW

The application development environment LabVIEW from National Instruments is specifically designed for data acquisition and instrument control. The primary applications include test, measurement and data logging of data for display. Therefore LabVIEW is a good development platform for systems utilizing data acquisition DAQ hardware.

LabVIEW uses a graphical programming language developed by National Instruments called 'G' (Figure 5.1). Programs are generated by using wires to link together graphical block diagrams as opposed to lines of text in other languages. Each block diagram contains a combination of data objects and function statements to execute the desired operation. Programs containing blocks or groups of functions are called virtual instruments (VI's), and can be used to mimic the functionality and appearance of complete hardware instruments such as filters or analyzers.

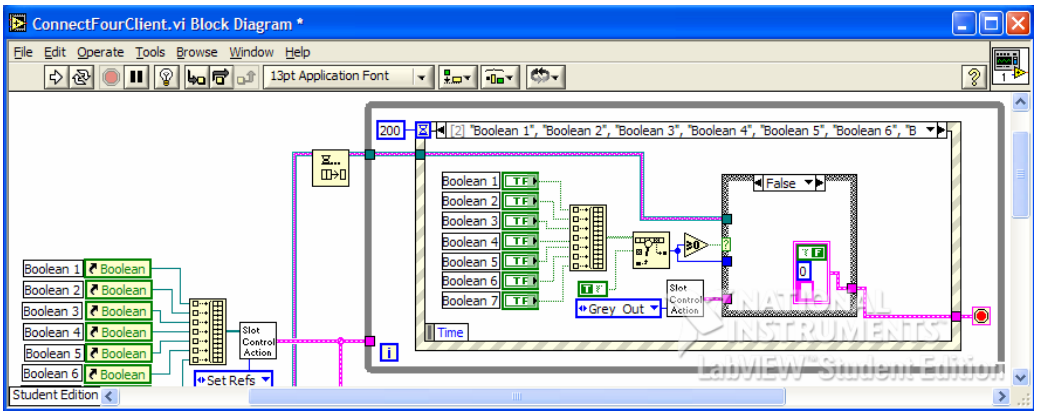

Figure 5.1 Example LabVIEW G code

Graphical programming can help programmers with little prior experience to visualize and construct simple programs however this can be restrictive to developers used to a text based language. Generally it takes longer to implement a function in G than it would using a text based language due to the extra requirement of generating and linking the VIs. In addition, G code can be more complex to understand due to the non-sequential nature of the block diagram. Many block diagrams consist of multiple layers which cannot always be viewed simultaneously thus decreasing readability.

5.1.2 Visual C++

Visual C++ is an object orientated programming language created by Microsoft for DOS and Windows based applications. The original C programming language (based on B and BCPL) was created in 1972 and became very popular due to its close association with the Unix operating system and ability for general purpose use[17] (later versions were commonly implemented in embedded controllers).

C++ is an enhanced version of C designed to support object orientated programming in which programs are designed in reusable modules to reduce development time and simplify code maintenance. Visual C++ further enhances the C++ platform to enable the creation of a graphical user interface (GUI).

[17] http://www.auridian.com/glossary/HTML/C.htm

Programming in Visual C++ is accomplished using the latest version of the Microsoft development application, Visual Studio 2005. Although all the necessary hardware and software interfaces can be achieved with Visual C++, the complexity and learning curve can exceed other available platforms. Future work may convert currently developed algorithms to Visual C++ however, it was not suitable at this stage of the project because rapid development of initial algorithms was required.

5.1.3 Visual Basic

Visual Basic (VB) is another programming language created by Microsoft for generation of GUI based applications. Based on the original BASIC (Beginners All-purpose Symbolic Instruction Code), VB is an event driven language most commonly used in business and database programming.

VB is designed to be accessible for both novice and experienced programmers due its straightforward code generation. Many functions are built into VB therefore creation of a GUI usually requires drag and drop placement of components and attribute configuration by writing additional lines of code (Figure 5.2).

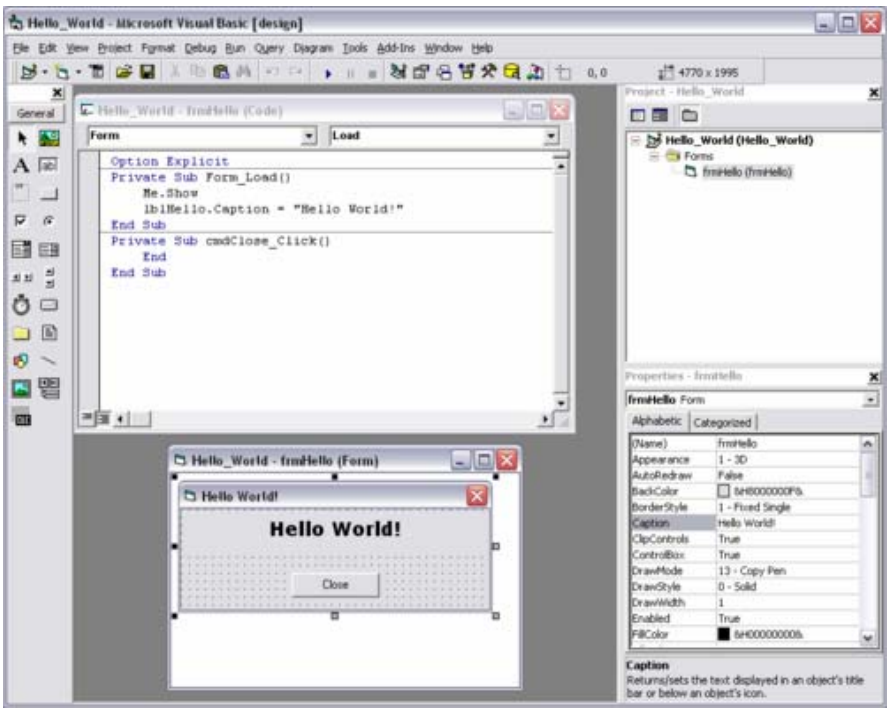

Figure 5.2 Typical Visual Basic development environment

As VB was designed as a simple language for rapid application development, some degree of controversy exists regarding its level of quality and usefulness compared to other high-level languages such as C++, particularly with respect to its avocation of poor programming practice[18].

Although much quicker to learn than Visual C++, VB was still a relatively unfamiliar language and additional development time would be better spent implementing a Visual C++ application. VB is better suited for GUI creation as a front end to databases rather than robot control and is therefore not selected.

5.1.4 Java

The Java programming environment is an object-orientated language developed by Sun Microsystems in the 1990's. It was designed to be platform independent so that it would operate on hardware differing in its storage facilities, memory capacity, network connections and processing capabilities.

Java in the past had widespread use in browser based internet applications such as games and interactive animations but has since been almost completely replaced by applications such as Macromedia Flash and Shockwave. In contrast it is used extensively in web page creation (JavaServer Pages) and is also used by MATLAB (5.1.5) to render the user interface and access the serial ports.

Although Java would be suitable for certain components of the robot control software such as the user interface, other areas such as hardware interfacing would be more difficult. Of particular concern is the connection to the DAQ card as Java is not listed as a supported platform by NI thus requiring extensive driver development beyond the scope of this project.

[18] Some critics of VB claim fundamental programming techniques are not learned with VB because much functionality is contained within the components and not visible to the programmer

5.1.5 MATLAB

MATLAB (Matrix Laboratory) is a numerical computing environment designed for technical computing both in industry and academic institutions. The basic data element in MATLAB is an array of dynamic floating point numbers making matrix manipulation a fundamental feature and specialty of MATLAB.

Other features enable rapid data manipulation for plotting and analysis, creation of graphical user interfaces and the ability to integrate other programming languages into a MATLAB application. MATLAB also provides a large selection of toolboxes for specialized tasks such as image processing, control system design and artificial intelligence. The built-in support for such high level algorithms (including neural networks and genetic algorithms) make MATLAB an ideal platform to base future, advanced software.

5.1.6 Linux

A highly preferred software platform among many hardware developers (such as robotics research) is the Linux operating system. Linux is part of the GNU project which aims to create a Unix-like operating system comprising completely free software.

Advantages of Linux based systems include the increased reliability and support for real-time control compared to Windows based applications which do not utilize the hardware as efficiently. The low cost and widespread support for Linux applications and drivers is beneficial however, the lack of prior experience with the platform within the Mechatronics Group would hinder development and increase project complexity. Consideration of a conversion to Linux is possible in the future when more information can be gained.

5.1.7 Selected Software Platform

Although the standard operating environment is not ideal for timing critical control applications such as robot management, MATLAB has been selected for this project.

Future modifications are possible that utilize specialized toolboxes such as the Real-Time Windows Target[19] to generate a precise control application.

Despite the lack of generic support for real-time applications, MATLAB does provide a useful platform for algorithm development during this stage of the project. Many useful functions are built-in such as serial port drivers and array manipulation, greatly reducing development time.

Asynchronous behaviour is possible for certain specialized functions such as timers and serial communications in the form of *callbacks*. These features have been utilized as often as possible to reduce the software overheads associated with polling. Caution must be exercised however when multiple execution scenarios are present simultaneously. A callback may be triggered before a previously queued execution of the callback has completed thus forcing the event to be added to the MATLAB execution queue. MATLAB can be configured to either 'drop' the new callback function or add it to the execution queue and due to the single-threaded nature of MATLAB these circumstances cause irregularities in the program timing.

MATLAB groups functions and program segments into separate *m-files* having the *.m extension. This enables intuitive segmentation of large programs and also facilitates debugging and customization of certain components. An entire library does not require editing and recompiling to make minor alterations to algorithms thus significantly reducing development time.

Another advantage of MATLAB is the compatibility with previously designed navigation and control system software. Although the outdoor mechatron software will be mostly custom developed, some parts of the existing code could easily be ported if necessary as it was originally written in MATLAB.

[19] The Real-Time Windows Target is a PC solution for prototyping and testing real-time systems. It uses a small real-time kernel to block operating access and give hardware priority to the application.

5.2 WIRELESS NETWORK

A portable laptop computer is used to communicate with the control PC on the outdoor mechatron. The Windows Remote Desktop software is utilized by the remote PC over a wireless network to log on to the mobile robot, effectively acting as the host PC's keyboard, mouse and screen eliminating the need for a wired connection.

5.2.1 Login Procedure

The Remote Desktop software is located within the accessories subfolder of the start menu on the laptop computer. When the robot computer has booted up, the login procedure can begin by typing the IP address of the mechatron followed by the user name and password (Figure 5.3).

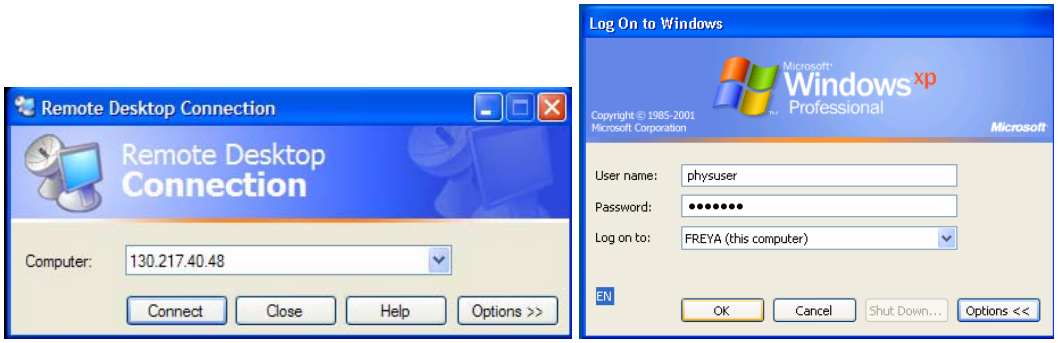

Figure 5.3 Remote Desktop Connection LEFT: IP address RIGHT: user details

The current setup allows both wired and wireless network configurations suitable for development within the lab and outdoors field testing. The wired configuration utilizes the University of Waikato LAN which assigns the robot an IP address such as *130.217.40.48*. Conversely, when using the wireless adapters; the IP address is *192.168.0.2*. The login details for both circumstances are:

User name: physuser
Password: thetank
Log on to: Freya (this computer)

Remote desktop software was selected over VNC terminal services due to problems with screen resolution and displaying graphics such as the GUI.

5.2.1 Network Configuration

The D-Link AirPlus software is used on both platforms to configure wireless networking properties (Figure 5.4). The SSID (service set identifier) defines the network name to *"Laptop2Tank"* and must be set on both computers. The connection mode is *ad-hoc* between two adapters, meaning the topology is self configuring and does not require an access point. The disadvantage is the occasional disconnection however this can be remedied by installing an access point in the future.

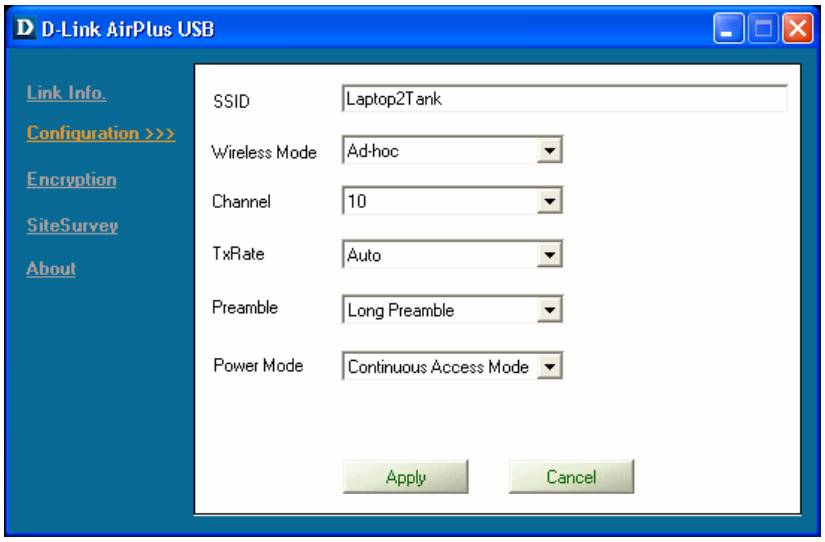

Figure 5.4 Network configuration

5.2.3 MATLAB Startup

The MATLAB installation is configured as a standalone license. This differs from conventional distributions connected to a local network to access license information because a permanent connection to a license server is not realistic for a mobile outdoor robot.

This presents a problem when using a terminal access program such as Remote Desktop because MATLAB does not allow control from a remote terminal under a

standalone license. The only practical problem this causes is that the user cannot start a MATLAB session through Remote Desktop software.

A workaround has been used which places MATLAB in the Windows Start Up directory, thus initializing the program at boot-up. Upon logging onto the system from the remote computer, MATLAB is available for immediate use. The major problem still remaining is a restart of MATLAB in the case of a program crash. If MATLAB stops responding and needs to close, the only way to reopen it from the laptop is to perform a restart. This is sometimes not necessary during in-house development as connection of external mouse, keyboards and monitors are possible to locally restart MATLAB.

5.3 DAQ CARD INTERFACE

A suitable interface between the NI-PCI6229 DAQ card and the MATLAB control environment is required to acquire sensor data for processing and for control of the motor driver system.

5.3.1 DAQ Toolbox

The only direct support for DAQ cards within MATLAB is through the Data Acquisition Toolbox. The DAQ toolbox is a collection of m-file functions and MEX-file dynamic link libraries (DLLs) that allow communication with some common DAQ hardware vendors including National Instruments.

The DAQ toolbox provides a useful framework for collecting measurement data for manipulation in the MATLAB environment. Functions include analogue input (AI), analogue output (AO) and digital input/output (DIO) however, more complex functions such as timers and counters are not supported. These functions are important for robot software such as measuring encoder pulses therefore the DAQ toolbox cannot be used.

5.3.2 NI-DAQmx Drivers

Supplied with the DAQ card hardware is a set of NI-DAQmx device drivers, currently at version 7.4. NI-DAQmx is the software required to communicate with and control the NI acquisition device. The *mx* denotes the drivers are designed for M series devices (such as the 6229) and are therefore required to operate them. NI-DAQmx drivers can be used to control non-M Series devices however the Traditional NI-DAQ *(legacy)* drivers cannot communicate with an M series device.

Driver software is essential for accessing the hardware capabilities and functions and acts as the interface between the hardware and application software as shown in Figure 5.5. As a result, compilation and execution of the mechatron control software is limited to machines with NI-DAQmx installed.

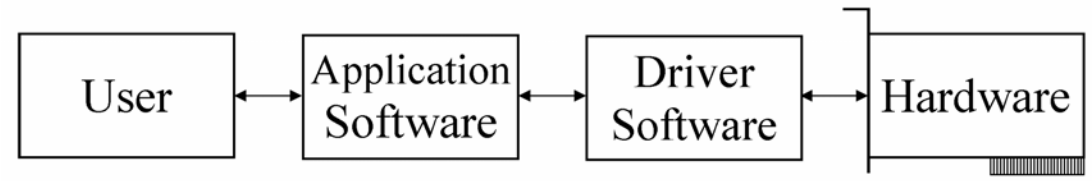

Figure 5.5 Position of NI-DAQmx driver software

The main functions of the drivers include the following:

- Manage data input and output from the DAQ device
- Control the data acquisition rate
- Configure onboard hardware peripherals and pin-to-function associations
- Integrate DAQ hardware with PC resources (processor interrupts, DMA, memory)
- Combine DAQ hardware with signal conditioning hardware

Supplied as part of the NI-DAQmx distribution are the various header files and libraries required for program development in ANSI C, Visual C++, Visual C# and Visual Basic .NET[20] however native support for MATLAB is not available.

[20] .NET is a software development framework designed by Microsoft for the Windows operating system

5.3.3 DLL Interface to NI-DAQmx

The NI-DAQmx drivers are interfaced to MATLAB using external DLL libraries included in the NI-DAQmx distribution. They are similar to the files included in a C or C++ project however a dynamic linked library (DLL) file in used instead of a standard library (.LIB) file.

MATLAB has built-in support for accessing external libraries through the *loadlibrary* function. The **DAQ_LoadLibrary.m** function (Figure 5.6) initializes the DAQ card interface by loading the NI-DAQmx drivers into memory. The calling syntax requires the name of the DLL file, header file and an optional alias name. The location of these files must be in the MATLAB path but by default are installed to:

nicaiu.dll C:\WINDOWS\system32

nidaqmx.h C:\Program Files\National Instruments\NI-DAQ\DAQmx ANSI C Dev\include

```
if ~libisloaded('DAQmxLib')
    loadlibrary('nicaiu.dll','nidaqmx.h','alias','DAQmxLib');
end
```

Figure 5.6 Load NI-DAQmx library into MATLAB

```
if libisloaded('DAQmxLib')
    unloadlibrary('DAQmxLib');
end
```

Figure 5.7 Unload NI-DAQmx library from MATLAB

A similar function, **DAQ_UnLoadLibrary.m** (Figure 5.7) is used to remove the drivers from MATLAB memory at the end of the program session. The file **DAQ_LoadNIConstants.m** contains the various constants and configuration attributes required for setting up the NI-DAQmx drivers to perform tasks. For example, the values required to set the active edge parameter of the sample clock to 'Rising' or 'Falling' are 10280 and 10171 respectively as shown in Figure 5.8.

```
%*** Value set for the ActiveEdge parameter DAQmxCfgSampClkTiming ***
DAQmx_Val_Rising = 10280; % Rising
DAQmx_Val_Falling = 10171; % Falling
```

Figure 5.8 Excerpt from NI constants file

The MATLAB functions *libfunctions* and *libfunctionsview* are used within **DAQ_ViewFunctions.**m to view the NI-DAQmx functions available and the required calling syntax. DLL functions are called in MATLAB using the *calllib* function which requires the library alias, name of function and the arguments to be passed to it. Driver functions are written in C therefore a corresponding MATLAB data type is required for each C data type when calling the driver functions.

This conversion is mostly done automatically as many data types match however, some do not such as pointers as shown in the function in Figure 5.9. This function retrieves the total number of samples acquired by the channel associated with **TaskHandle** and the information that is to be written to the variable **Data**. The argument required is a unit32 pointer which must be created with the MATLAB function *libpointer*. A suitable function calling file has been created for each NI-DAQmx function in use to provide the suitable interface and variable conversion. This enables MATLAB structured functions to be used to easily access external library functions without all the extra code being retyped each time.

```
function [status Data] = DAQ_GetReadTotalSampsPerChanAcquired(TaskHandle)

DataPtr = libpointer('uint32Ptr',0);

[status Data] =
calllib('DAQmxLib','DAQmxGetReadTotalSampPerChanAcquired',TaskHandle,DataPtr);
```

Figure 5.9 Function call example

One of the problems encountered was an incorrect data type in the nidaqmx.h header file. This file contains the function prototypes and thus the calling syntax for each NI-DAQmx function. The **DAQ_GetReadTotalSampsPerChanAcquired.m** function above requires a **uint64** type for the returned data however, this was not supported in

MATLAB. The solution was to vary the function prototype to a **uint32** data type to prevent the program crashing. This still allows very large numbers so will not affect normal operation. Support from MathWorks suggests the problem will be fixed in a future MATLAB release however the same methodology can be applied to other functions as they are encountered as a temporary solution.

5.3.4 Channels and Tasks

Important to the operation of DAQ card software is the concept of channels and tasks and how they relate to physical connections and timing configurations. Two types of channel are available, *physical* and *virtual*. A physical channel is a terminal or pin on the DAQ card at which an analogue voltage or digital signal can be generated or measured. Physical channels can include more than one terminal such as a differential voltage channel or a digital port of 8 bits.

Virtual channels are created in software with the purpose of combining physical channel information with other channel specific data such as terminal configuration, voltage range and data formatting. A number of virtual channel types are available depending on signal type and direction as listed below:

- Analogue input channels
- Analogue output channels
- Digital input/output channels
- Counter input/output channels

Virtual channels are created for different types of measurement activities using the various NI-DAQmx functions (5.3.5). Physical channels are passed to the create channel function as a string conforming to a channel naming convention. The syntax can use a combination of channel names, channel ranges and channel lists as shown in the examples below.

ai0 *analogue input channel 0* **port0** *all the digital lines on port 0*
Dev0/port0:1 *range of ports* **Dev0/ai0, Dev1/ai0:3** *list and range of channels*

A task combines one or more virtual channels with timing and triggering properties (Figure 5.10) required to make a measurement. Tasks represent the measurement or generation process that needs to be performed, and each task can contain only one type of channel such as an analogue input. Tasks are created and deleted using the NI-DAQmx functions outlined in section 5.3.5. Each task has an associated **TaskHandle** identifier which is used for future references to it, including adding channels and starting and stopping the task. It is important to stop and clear the task using the **TaskHandle** at session end otherwise errors will occur when the task is recreated and if the **TaskHandle** has been lost a computer restart is necessary.

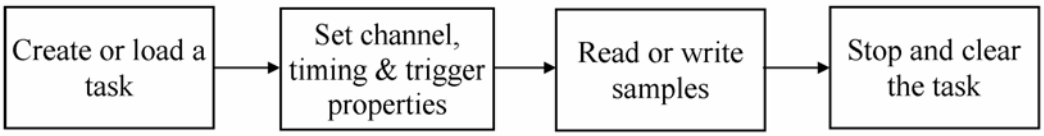

Figure 5.10 Signal measurement and generation process

5.3.5 Available Functions

Table 5.1 lists the MATLAB functions created to access the NI-DAQmx DAQ card drivers. Functions include task creation and deletion, measurement channel set up and timing configurations for data acquisition. Full code is available on the enclosed CD.

DAQ_LoadLibrary.m	DAQ_CreateAOVoltageChan.m
DAQ_UnLoadLibrary.m	DAQ_CreateDOChan.m
DAQ_ViewFunctions.m	DAQ_CfgInputBuffer.m
DAQ_ResetDevice.m	DAQ_CfgSampClkTiming.m
DAQ_Error.m	DAQ_CfgImplicitTiming.m
DAQ_GetExtendedErrorInfo.m	DAQ_GetReadAvailSampsPerChan.m
DAQ_CreateTask.m	DAQ_GetSampTimingType.m
DAQ_LoadTask.m	DAQ_GetReadTotalSampsPerChanAcquired.m
DAQ_StartTask.m	DAQ_SetReadOffset.m
DAQ_StopTask.m	DAQ_SetReadRelativeTo.m
DAQ_ClearTask.m	DAQ_WriteAnalogueF64.m
DAQ_CreateAIVoltageChan.m	DAQ_WriteDigitalLines
DAQ_CreateAOVoltageChan.m	DAQ_ReadAnalogueF64
DAQ_CreateCICountEdgesChan.m	DAQ_ReadCounterScalarU32.m
DAQ_CreateCIPulseWidthChan.m	DAQ_ReadCounterScalarF64.m
DAQ_CreateDIChan.m	DAQ_ReadDigitalLines.m
DAQ_CreateAIVoltageChan.m	

Table 5.1 DAQ card function listing

5.3.6 MAX Studio

Prior to developing the MATLAB interface code for control of the DAQ card the various sensor signals were tested using the Measurement and Automation Explorer (MAX). This utility provided by National Instruments allows direct communication with the DAQ hardware for channel configuration and data acquisition.

A screenshot of the MAX interface indicating a typical data acquisition session is shown in Figure 5.11. Configuration of NI-DAQmx tasks and channels including acquisition frequency, number of samples to acquire and the physical channels to use is accomplished on the various settings panels. Real-time display of acquired data during task operation is through graph, chart and table windows.

VILogger is a utility based within the MAX studio that allows creation of tasks to collect and log data to a file. During task execution the real-time data is viewed in the display window then exported to a Microsoft Excel spreadsheet file at task completion. Simple graphing of the acquired data can be done within Excel or imported into MATLAB for further analysis.

The MAX interface provides a number of test panels to investigate the functionality of the onboard hardware as shown in Figure 5.12. Direction communication with the digital IO ports, analogue inputs, analogue outputs and counter functions enables quick analysis of operation.

An important feature of the DAQ card is the customization of DIO channel states at computer start-up. This is accomplished with the Power Up States tab of the Device Properties configuration panel. Each port pin can be individually set as logic low, logic high or tristate depending on the application. The motor driver interface is connected to Port 0 of the DAQ card so to prevent motor operation at power up the control signals P0.0 – P0.3 have been changed from the default “tristate” to logic low. This ensures that the microcontroller turns off the drivers and defaults to manual or radio control mode (section 3.8.5) to allow robot transportation.

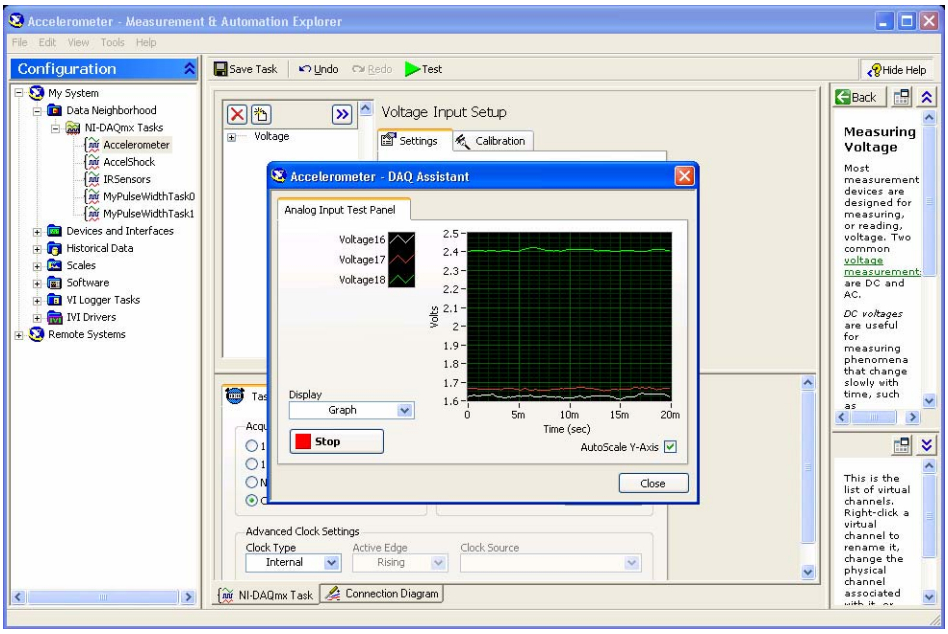

Figure 5.11 MAX Studio data acquisition interface

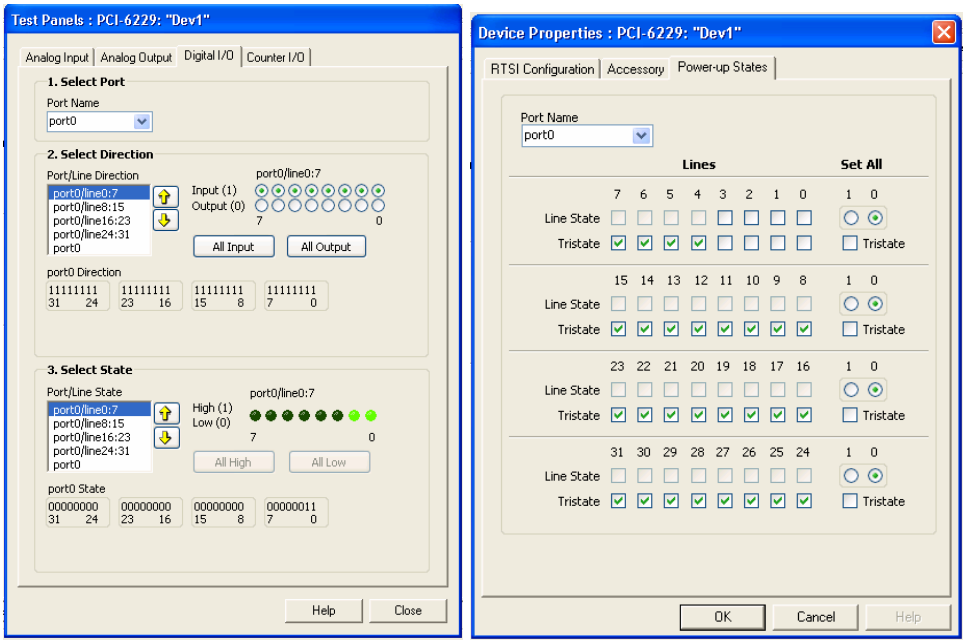

Figure 5.12 LEFT: DAQ Card test panels RIGHT: Power-up states configuration panel

5.4 COMPASS INTERFACE

5.4.1 Demo Software

Demonstration software is supplied with the HMR3300 compass development kit for evaluation and testing of the module. The program (Figure 5.13) provides a simple

interface to extract the heading, pitch and roll data from the compass. Data are displayed as both a text display and a graphical representation using aircraft instrument style ActiveX controls.

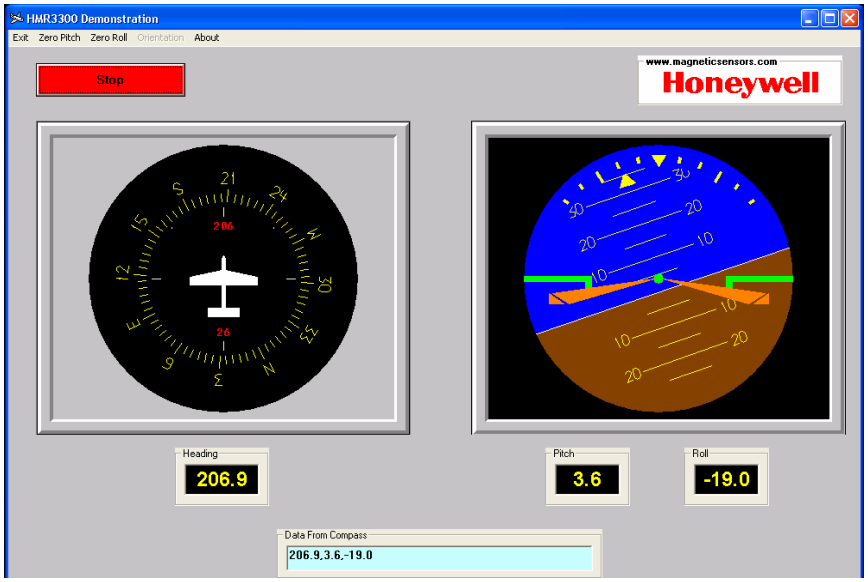

Figure 5.13 HMR3300 Demo software

This software provided a useful means to test operation of the modules when purchased but could not be used in the final software implementation. Heading and tilt data could be written to a data log file but not extracted directly for use in MATLAB; therefore custom interfacing software was required.

5.4.2 Connection

The compass module requires a serial port to send and receive data, thus USB connectivity is accomplished using the serial to USB converter from section 4.1.3. MATLAB provides generic support for serial communications so many of the systems level functions are performed behind the scenes.

A serial port object is created in **Compass_Connect.m** using the *serial* function with the required communication settings such as COM port number, baud rate and buffer size, shown in Figure 5.14. The port is opened using *fopen* and **Compass_Reset()** is

used to initialize the module. The function **Compass_Disconnect.m** is used to close and clear the serial port object at the end of the session as shown in Figure 5.15.

```
function Compass_Connect

global s_compass;

s_compass = serial('COM4','BaudRate',19200,... % Create Serial Port Object
        'DataBits',8,...
        'FlowControl','None',...
        'Parity','none',...
        'InputBufferSize',512,...
        'StopBits',1,...
        'ByteOrder', 'littleEndian',...
        'ReadAsyncMode', 'continuous',...
        'BytesAvailableFcnMode','terminator',...
        'Terminator','CR/LF');

 fopen(s_compass);                                % Connect to the device
```

Figure 5.14 Excerpt from compass initialization code

```
function Compass_Disconnect

global s_compass;

fclose(s_compass)              % Disconnect and clean up serial port object
delete(s_compass)
clear s_compass
```

Figure 5.15 Excerpt from compass disconnection code

5.4.3 Data Collection

Communication with the compass module uses ASCII based commands to set preferences and acquire data. Two modes of operation are available either "query" where the compass sends heading data after receiving a request command, or "auto mode" where the compass continuously sends data with a short delay between sets.

A single query is initiated using **Compass_GetReading.m** (Figure 5.16) which sends the ASCII code **Q* using *fprintf.* Two query modes are possible, either direct query (**Q)* or averaged query (**A)* where the compass automatically averages the last 20 samples before output. The data are then read from the serial port buffer with *fscanf* as a comma separated text string of heading, pitch and roll in degrees

```
function [A, count,msg] = Compass_GetReading(DataMode)

global s_compass;

switch DataMode
   case 'Q'
      fprintf(s_compass,'*Q','async');              % direct query

   case 'A'
      fprintf(s_compass,'*A','async');              % averaged over 20 samples

end

[A,count,msg] = fscanf(s_compass);
```

Figure 5.16 Compass_GetReading code extract

The alternative 'automatic' data output mode is used during normal compass operation to reduce the processor overhead associated with the query command and waiting for a response. The MATLAB serial port can be configured to generate a type of interrupt (called a callback) when the terminator character is received indicating data are available in the serial port buffer. This is achieved using the *BytesAvailableFcn* property of the serial port object to specify **CompassGetDataCallback** as the callback function. The callback reads the heading data from the buffer and outputs to the user interface for display and if specified, write to a data log file. The function **Compass_DataStopStart()** sends the ASCII command *S to toggle data output mode to 'auto' (refer Figure 5.17).

```
s_compass.BytesAvailableFcn = {@CompassGetDataCallback,handles};
Compass_DataStopStart('start');
```

Figure 5.17 Initialize compass callback

The *BytesAvailable* property is used within the **Compass_DataStopStart.m** function to determine the current mode as shown in Figure 5.18. It is then determined whether the current mode matches the desired mode and if the *S command to toggle the state needs to be sent. The *BytesAvailable* property indicates the number of bytes available to read in the input buffer and will therefore increase over time if 'auto' mode is set.

```
a = s_compass.BytesAvailable;
pause(0.2);
b = s_compass.BytesAvailable;

  if b>a
     CurrentMode = 'start';
  elseif a == b
     CurrentMode = 'stop';
  end
```

Figure 5.18 Determine current compass data output mode

It is important to flush the input buffer using **Compass_InputBufferFlush.m** after the 'stop' mode has been selected to ensure no full or partial data strings still remain in the serial buffer. This is to prevent future instances of the function calls misinterpreting the current mode or reading partial data strings.

5.4.4 Configuration and Calibration

The compass module provides commands to set and read various configuration options to customize operation. Separate functions have been written to automatically set or read the settings depending on the input string to the function as shown in the 'Variation Angle' example of Figure 5.19. A read request consists of the setting string ("#VAR" for variation angle) and a question mark while a write request will add an equals sign followed by the parameter to be written.

```
function A = Compass_VariationInput(angle)

global s_compass;

if length(angle)== 0                    % read operation requested
   fprintf(s_compass,'#Var?','sync');
   terminator = fscanf(s_compass);      % compass  returns terminator before  data
   [A,count,msg] = fscanf(s_compass);
else                                     % write operation requested
   fprintf(s_compass,['#Var=',angle],'sync');
   A = 'Done.';
end
```

Figure 5.19 Example configuration function

Other functions include the ability to change the baud rate, module orientation, system filter, magnetic filter, magnetic offset and declination angle. Additionally the output data type can be changed between heading/pitch data to raw magnetometer readings

using **Compass_OutputDataType.m** to send an *H or an *M respectively. The full listing of configuration functions and compass interfacing code is available on the included CD specified in Appendix B.

An important configuration function is the compass calibration routine, **Compass_SendCommand('*C')**. Once in calibration mode, the device sends magnetometer data appended by a "C" character to indicate calibration mode operation. During the calibration procedure, the compass and the platform it is mounted on is rotated through 360 degrees including as many pitch and roll combinations as possible. This process calibrates the compass to stray magnetic fields caused by nearby ferrous objects such as the robot chassis. Calibration mode is stopped by issuing another *C command.

5.5 GPS INTERFACE

Connection to the GPS module follows a similar process as the compass module except the serial port is COM5 instead of COM4 for the compass. The Motorola M12+ module is initialized by sending the Motorola Binary formatted instruction:

@@HarC<CR><LF> where: @@Ha = ASCII command
r = Output rate
C = Data checksum
<CR><LF> = string terminator

This command instructs the GPS to output a continuous data message every r seconds. The checksum is generated by calculating and exclusive OR on each byte of the message excluding the terminator using **GPS_Checksum.m**.

The serial callback function **GPSGetDataCallback.m** is called each time the GPS data are ready to be read from the serial port buffer. The returned message is 154 bytes in length and the *BytesAvailable* property is used to ignore data not of this length. In the event of a communication error and less than 154 bytes arte transmitted the serial port object will enter a non-responsive state unless the error checking is in place.

The position, time, satellite status and receiver status data are extracted from the returned data set and stored in a MATLAB structure using **GPS_ExtractMessage.m**. An example of date and time extraction is shown in Figure 5.20 where the returned data from the GPS is stored in array A and byte referenced using the brackets. The structure is created upon GPS connection using **GPS_MakeDataStructure.m**.

```
% Date
GPSPositionStatusData.Date.Month = A(5);
GPSPositionStatusData.Date.Day = A(6);
GPSPositionStatusData.Date.Year = (A(7)*256 + A(8));

% Time
GPSPositionStatusData.Time.Hours = A(9);
GPSPositionStatusData.Time.Minutes = A(10);
GPSPositionStatusData.Time.Seconds = A(11);
```

Figure 5.20 Storing GPS data in MATLAB structure

Position data is returned from the compass as four bytes, giving position is milli-arc-seconds (mas) ranging from -648000000 to 648000000. The function **GPS_mas2Deg** shown in Figure 5.21 is used to convert the mas into the more conventional degrees, minutes, and seconds representation.

Each byte is multiplied appropriately and added to give a 32 bit value where negative numbers are accounted for using the two's complement presentation. The resulting four byte value is divided by 3600000 to perform the mas to degree conversion and multiplied by 60 accordingly to give minutes and seconds.

In addition to providing an absolute position referenced to the WGS84 (World Geodetic System 1984) global co-ordinate system, GPS data can provide positioning relative to the robot origin. This is accomplished by converting an array of latitude, longitude co-ordinates to incremental changes in distance.

```
function data = GPS_mas2Deg(Byte1,Byte2,Byte3,Byte4)

num = Byte1*16777216 + Byte2*65536 + Byte3*256 + Byte4;

% convert from two's complement form if MSB is high (number is negative)
if(Byte1>127)
   data = bitcmp(num-1,32)/3600000;
   sign = -1;
else
   data = num/3600000;
   sign = 1;
end

deg = sign*floor(data);
min = sign*floor(mod(data,1)*60);
sec = sign*mod((mod(data,1)*60),1)*60;

data = [deg min sec];
```

Figure 5.21 mas to degree conversion

The function **GPS_Deg2m.m** performs this function utilizing Equation 5.1. This equation uses the fact the distances between latitudes remain constant over the planet but the distance between lines of longitude change with latitude and converge near the poles. The functions f(θ) and g(θ) are compensating factors for the Earth's geometry in terms of the relative latitude θ.

Equation 5.1

$$\Delta y = \Delta Lat\left[111132.09 - f(\theta)\right]$$
$$\Delta x = \Delta Lon\left[111415.13\cos(\theta) - g(\theta)\right]$$

5.6 OTHER HARDWARE INTERFACES

The following sections describe the software interfaces to the various other hardware components. Although these are not described in detail here, a full listing of source code is available on the accompanying CD-ROM.

5.6.1 Rangefinders

The DAQ card function **DAQ_ReadAnalogF64.m** is used to read 10 analogue voltage samples from each of the 12 infrared sensors connected and return a 120 element data array. Before the voltages are converted to a range using Equation 4.2 or

4.3, a suitable filter is applied to reduce noise generated from electrical interference and ADC inaccuracies. This is important because a small change in voltage represents a large change in measured range, particularly at long ranges. Therefore it is necessary to filter out noise before the voltage-to-range calculation is applied. A number of different filtering techniques were considered including:

- Mean
- Weighted mean
- Sliding median

Mean

The mean or average of a group of samples is the most effective way of filtering small amounts of noise. The function is easily implemented with the MATLAB function **mean** and provides a fast response to change. The downside is extreme values in the data set can significantly affect the result over the short term.

$$\overline{E} = \frac{\sum_{i=1}^{n} E_i}{n}$$ **Equation 5.2**

E_i: i^{th} sample
$\bar{E}$: mean of samples
n: number of data samples

Weighted Mean

The weighted mean provides an extension to the standard averaging function by allowing a different weighting factor to be applied to each data point. The sum of all the weighting factors must equal 1 and a number of different methods can be used to assign the weighting factors such as weights based on sample age or proximity to the median. Although MATLAB does not have any weighted mean functions built the algorithms can be generated very simply using basic arithmetic.

$$\overline{E} = \frac{\sum_{i=1}^{n} w_i E_i}{n}$$ **Equation 5.3**

w_i: i^{th} weighting factor

Median

The **median** function in MATLAB sorts the data set according to number magnitude and then selects the centre point as the median value. The median filter is less sensitive to transients than the mean or weighted mean however it is slower to respond to valid changes such as obstacles.

$$E_{med} = E_{n/2}, E_1 \le E_2 \le ... \le E_{n-1} \le E_n$$ **Equation 5.4**

Selected Method

To effectively remove the transients from the infrared readings a combination of the mean and median filters have been used to utilize the advantages of each. The 10 samples acquired for each channel are averaged using the **mean** function before being entered into a cyclic buffer. The buffer contains the last 10 averaged samples representing the last 10 control loop cycles using a First In First Out (FIFO) update strategy. The buffer array is shifted each cycle using the **circshift** function and shown in Figure 5.22 thus allowing the new data to be written over the oldest data.

```
IRSensorData.IRValues = circshift(IRSensorData.IRValues,1);
```

Figure 5.22 Infrared sensor circular buffer shift

The **median** is calculated for the 10 samples on each channel and this value represents the current filtered voltage which is then converted to a range. This method was chosen as any brief transients do not affect the sliding mean value however the response time is reduced so the number of samples is limited to 10. Depending on the future implementation, a weighted mean could also be effective if a suitable means of allocating weighting factors can be determined.

5.6.2 Encoders

The encoder pulses can be measured in two different ways using the DAQ card. Firstly a timer task can measure the elapsed time between pulses thus giving the pulse width and rotation velocity. Secondly a counter can be used to count the number of encoder pulses thus representing a total distance travelled. Both velocity and distance could be calculated from the other given the third variable, time, however as the DAQ card can directly provide this information it is the desirable method.

Unfortunately two different types of measurement (counter & timer) cannot be performed simultaneously on the same physical channels due to the way timing signals are routed within the DAQ card. A work around was discovered that utilizes the *DAQmxGetReadTotalSampPerChanAcquired* property. This property is read using the **DAQ_GetReadTotalSampsPerChanAcquired.m** function as shown in Figure 5.23. The distance travelled by each track is calculated from the previous distance value and an encoder constant of approximately 7.8 mm per encoder count (assuming straight line travel). It is clear distance measurements are only valid for straight line motion when the initial count values are known.

```
%% FIND TOTAL DISTANCE TRAVELLED
[status TotalDistanceCounts(1)] =
DAQ_GetReadTotalSampsPerChanAcquired(EncoderTime1TaskHandle);

[status TotalDistanceCounts(2)] =
DAQ_GetReadTotalSampsPerChanAcquired(EncoderTime0TaskHandle);

TotalRawDistance = double(TotalDistanceCounts);

%% FIND INCREMENTAL DISTANCE CHANGE
DistanceChange = TotalDistanceCounts-PreviousDistanceCounts;
PreviousDistanceCounts = TotalDistanceCounts;
```

Figure 5.23 Encoder distance measurement

The velocity measurement uses the DAQ card timers and thus the critical timing tasks are executed by the DAQ card hardware and not the MATLAB program. This ensures faults and timing inaccuracies due to the Windows Operating system and MATLAB environment do not occur. The DAQ card always holds the latest velocity information

within a buffer so a read request by the control software always receives the most up-to-date information regardless of the timing with respect to previous queries.

The 64-bit floating point pulse width measurement is acquired from the encoder tasks using **DAQ_ReadCounterScalarF64.m** as shown in Figure 5.24. The returned data represents the pulse width in seconds so a conversion to velocity is accomplished by dividing the linear distance travelled during one pulse by the time of the pulse.

```
[status Data] = DAQ_ReadCounterScalarF64(EncoderTime0TaskHandle);

% Keep track of previous encoder time
EncTime1 = [Data EncTime1(1)];

% Example velocity calculation (not exactly how it is in code)
Velocity = 0.0079/EncTime1;
```

Figure 5.24 Encoder velocity measurement

5.6.3 Accelerometer

Acquisition of accelerometer data is performed in a similar manner the infrared range finders in section 5.6.1. Each of the three output channels provides an analogue voltage between 0 and 3.3 V representing acceleration which is read by the function **DAQ_ReadAnalogF64.m** as shown in Figure 5.25. The DAQ card task is configured to read 10 samples on each channel at 4000 Hz thus producing a 30-element array and a 2.5 ms acquisition time for each cycle of the control loop.

The 10 samples from each channel are averaged to reduce noise and the X,Y signals are converted to a tilt angle representing pitch and roll. Equation 4.1 is rearranged to make the angle, θ the subject as shown by Equation 5.5. A multiplication by -1 ensures the data output matches the co-ordinate system of the compass module allowing sensor fusion and comparison between the results.

$$\theta = \sin^{-1}\left(\frac{V_{out} - V_{off}}{\Delta V / \Delta g}\right) \qquad \textbf{Equation 5.5}$$

```
%% Read Accelerometer Data
[status Data] = DAQ_ReadAnalogF64(AccelSensorReadTaskHandle,
10,3,10,0);

%% Calculate tilt angles
Angle = round((real(asind((mean(Data) - 1.65)./0.8))*10))/10;
Roll = -1*Angle(1);
Pitch = -1*Angle(2);

%% Update GUI Display
set(handles.AccelRollDisp,'String',num2str(Roll));
set(handles.AccelPitchDisp,'String',num2str(Pitch));

%% Log Data to file
if get(handles.AccelDataLogCheckbox,'Value') == 1
      fprintf(AccelDataLog,'%6.4f %5.1f %5.1f %5.1f\n',[time
Pitch Roll Angle(3)]);
end
```

Figure 5.25 Accelerometer data acquisition for tilt calculation

The accelerometer tilt angles are written to the user interface (section 5.10) for inspection and also to a data log file for future analysis.

5.6.4 Video Camera

Installed on the outdoor mechatron is the Image Acquisition Toolbox version 1.7 for MATLAB. This allows connection to, and image capture from digital cameras such as the installed Logitech Webcam. Connection to the video source in MATLAB is accomplished by creating a video input object and setting the required configuration parameters as shown in Figure 5.26.

```
% Delete previous image objects
delete(imaqfind);

% Create and configure video object
vidCamera =
videoinput('winvideo',1,get(handles.VideoFormat,'String'));
set(vidCamera,'FrameGrabInterval',str2num(get(handles.FrameInterv
al,'String')));
set(vidCamera,'FramesPerTrigger',Inf);
triggerconfig(vidCamera,'immediate');
imaqmem(100000000);

% Begin image acquisition session
start(vidCamera);
```

Figure 5.26 Excerpt from camera connection code

The video format is specified at object creation by **handles.VideoFormat**, which is customized within the user interface (section 5.10). The *FramesPerTrigger* is set to infinite which means the camera will continuously acquire data and store to RAM after the session is initialized with the **start** command.

The acquisition of image data is accomplished using the **getsnapshot** function as shown in Figure 5.27. This function returns the latest image acquired by the camera which is then displayed to the user through the GUI object, **handles.CameraImage**. Since the camera is continuously writing data to memory, a large buffer is allocated using **imaqmem**. Consequently it is necessary to periodically clear the buffer using **flushdata** to prevent memory overflow.

```
% Check if video object is valid
if isvalid(vidCamera)

     % Get latest camera image and send to GUI dispplay
     set(handles.CameraImage,'Cdata',getsnapshot(vidCamera));

     % Clear image memory buffer
     flushdata(vidCamera);
end
```

Figure 5.27 Extract from image acquisition code

5.7 SYSTEM CONFIGURATION

5.7.1 Timers/Callbacks

MATLAB is a single threaded programming language which means provisions for multiple tasks operating simultaneously are not available. This restriction limits the complexity of a robot control application because a large number of processes are required to perform all the necessary functions including hardware interfacing, motor control, navigation algorithms and high level task planning software.

Although the mechanisms for multi-threading and interrupts are not generically supported in MATLAB, asynchronous behaviour is available in the form of callback functions. A callback works in a similar manner to an interrupt except multiple

callbacks cannot be serviced simultaneously. The CPU cannot execute a callback function until a currently executing callback has completely finished, therefore problems with software bottle-necks due to callback queues can occur.

Callbacks consist of a specified function (usually within a m-file) which is run when a predetermined event occurs. Examples of callbacks include hardware based events such as serial port data availability (sections 5.4.3 and 5.5) or software triggered events such as error functions and timers.

Timer callbacks work by executing the specified function at periodic intervals. By including hardware interfacing and motor control software within the function, a "Control Loop" is generated that can continuously access robot control functions. Timers are created and configured using the **timer** function in MATLAB. The *BusyMode* property of a timer object specifies the action taken when multiple callback functions are encountered simultaneously. The available options are:

- *Error* – Generate an error
- *Drop* – Do not execute the latest callback function
- *Queue* – Execute the function at the next opportunity

The advantage with the implemented '*Queue'* option is that the callback is always executed however, delays occur when waiting for the previous function to finish which means a constant period control cycle cannot be achieved. Although important in some applications, the slight variation in control cycle time will not cause adverse behaviour in the outdoor mechatron due to the slow system dynamics.

5.7.2 Persistent Variables

Persistent variables are defined as variables local to the function in which they are declared. The advantage is that their values are retained in memory between calls to the function thus making them useful for use in callback functions that are called multiple times.

Persistent variables are similar to global variables in that MATLAB creates permanent space for them both however, other functions, including the command line can never have access to persistent variables. If the persistent variable does not exist the first time the persistent statement is issued, it is initialized to the empty matrix thus allowing the code to determine whether it has previously been executed. This is used to set up and initialize persistent variables only on the first call to the function.

5.7.3 Low Level Control Loop

A timer based callback function, **LowLevelControlLoopCallback.m** forms the base of robot control and component interfacing. The function is initiated using **StartRobotControl.m** to set up and start the timer with a period of 50 – 100 ms and a *fixedSpacing* execution mode.

This control loop provides the hardware interfacing to all components except the compass and GPS module as these have independent serial port callback functions (sections 5.4 and 5.5).

Tasks associated with this function include the following however the full code listing is reserved for the included CD (outlined in Appendix B) due to space restrictions:

- Motor driver system interface
- Velocity control
- Infrared sensor data acquisition
- Accelerometer data acquisition
- Video camera image capture
- Obstacle avoidance algorithms

Persistent variables are used to store information that must be preserved between calls to the function such as encoder counts and infrared sensor ranges. The DAQ card task handles are also stored as persistent as these are required each time a read or write communication is initiated. Each task handle is stored on the user interface at creation then read into the low level control loop during the first cycle. This reduces the software overhead that would be required if the handles are read each cycle. Persistent

variables are initiated to the empty matrix as mentioned in section 5.7.2 which allows the **isempty** function to check the status of the persistent variable *controlFlag.* If true, it is the first call to the function, all the variables are setup and task handles are read from the GUI as shown in Figure 5.28.

```
% if first call to this function persistent variables are empty
if(isempty(controlFlag))

    % no longer empty so initialization will not repeat
    controlFlag = 1;

   % Get Task Handles from GUI (not all shown here)
    AOSpeedWriteTaskHandle =
      str2double(get(handles.DAQTask1Handle,'String'));
    LeftDirectionTaskHandle =
      str2double(get(handles.DAQTask3Handle,'String'));
    RightDirectionTaskHandle =
      str2double(get(handles.DAQTask4Handle,'String'));

    % Perform other variable initializations

end
```

Figure 5.28 Extract from low level control loop variable initialization

Each task within the low level control loop can be individually enabled or disabled by the user during development for customization and debugging purposes. An, *if* statement at the start of each section determines from the GUI (section 5.10) whether interface and control of that component is to be executed or not as illustrated in Figure 5.29. The accelerometer interface code (not all shown here) will only run if the *ControlSelectAccelSensor* checkbox has a value of 1. The same process is applied to each function and full code is available on the accompanying CD (Appendix B).

```
% Accelerometer Sensor control Selected
if get(handles.ControlSelectAccelSensor,'Value') == 1

      % Read Accelerometer sensor data
      % Update interface display
      % Log data to file
end
```

Figure 5.29 Customization of individual hardware access functions

5.7.4 DAQ Safety Pulse

An important feature of the motor driver to DAQ card interface is the safety pulse. This signal indicates to the microcontroller the PC based software is operational and valid instructions are being sent. A digital signal is generated at the start and completion of the motor driver interface software within the low level control loop. At the start, logic high is generated while at the end it is logic low as shown in Figure 5.30.

```
%% Start of DAQ Pulse to Microcontroller

      % set pulse high
      [status] = DAQ_WriteDigitalLines(DAQPulseTaskHandle,1,1);

%% Execute other motor control algorithms

%% End of DAQ Pulse to Microcontroller

      % set pulse low
      [status] = DAQ_WriteDigitalLines(DAQPulseTaskHandle,1,0);
```

Figure 5.30 Excerpt from motor driver code showing safety pulse generation

This continuous digital signal sent from the DAQ card is used by the microcontroller to indicate the control loop is operational. In the event of a PC crash or MATLAB program fault the control loop would cease to work and without the safety pulse, the microcontroller could continue issuing the previous speed control commands to the motor drivers. This causes undesirable mechatron movement and possibly damage so the safety pulse is necessary to indicate to the microcontroller when to shut down the drivers and prevent operation.

5.7.5 Navigation Control Loop

A second timer controller callback function is the navigation control loop given in the file **NavigationControlLoopCallback.m**. This function executes at a slower rate than the low level control loop because changes to navigation commands do not need to have such a fast update rate. Currently this function is configured to run every 1 s however, this is easily modified to allow future additions and path planning algorithms to be implemented.

The primary function of this loop is the conversion of desired location data to the required heading and velocity commands for waypoint navigation. Execution of the callback function is continuously occurring however operation of the included functions can only occur if the control mode is set to autonomous (section 3.8.5) by use of a conditional statement.

5.7.6 Data log Files

A large amount of data is available from the various sensors and control algorithms to determine the robot state and operating conditions such as heading, velocity and control parameters. In addition to displaying this data on the user interface via text and graphic indicators, a system of data logging has also been implemented for debugging purposes.

Unique file names are generated upon creation using the **datestr** MATLAB function as shown in Figure 5.31. For example, the resulting data log file format for the compass data acquisition session is *Compass-20050121T150758.txt* which shows the name, year, date and time within the file name. Data are written to a text file using the MATLAB function **fprintf** as a table of values separated by tab characters as shown in Figure 5.32. Each robot control function has a corresponding checkbox on the user interface which allows customization of which data sets are to be logged to file.

```
CompassDataLog = fopen(strcat('Compass-
',strcat(datestr(clock,30)),'.txt'),'a');
```

Figure 5.31 Unique data log file name creation

```
if get(handles.CompassDataLogCheckbox,'Value') == 1
    fprintf(CompassDataLog,'%6.4f %5.1f %5.1f %5.1f %5.1f\n',
    [time TargetHeading Comp_Data(1) Comp_Data(2) Comp_Data(3)]);
end
```

Figure 5.32 Writing data to file using fprintf

5.8 MECHATON CONTROL

A number of low level control algorithms are required to implement robot motion before the higher level functions are fully developed. Velocity and heading control systems maintain a desired target determined by the navigation system while reactive obstacle avoidance manoeuvres the robot away from obstructions. Although outside the scope of this project, foundation work on the higher level navigation functions has been completed particularly for waypoint navigation.

5.8.1 Velocity Control

The target velocities (magnitude and direction) are acquired from the GUI based sliders (Figure 5.33) which are adjusted either from manual user control or by the navigation system. The latest encoder pulse width time for each track is read from the DAQ card using the function **DAQ_ReadCounterScalarF64.m.** If this function is called before the first encoder pulse is measured an error (-200277) will be generated by DAQ card. The work around is to check the function status value against the error and if a match occurs, the encoder time is set to a very high value indicating to the velocity control that the robot is stationary.

```
%% Get Desired Speed Values from Sliders
TargetVelocity(1) = get(handles.MotorDriverLeftSlider,'Value');
TargetVelocity(2) = get(handles.MotorDriverRightSlider,'Value');
```

Figure 5.33 Use *get()* command to extract target velocity from sliders

During each control cycle the encoder pulse time is converted to a velocity using the known encoder constant (7.9 mm per count). Due to the dynamics of the track drive system and irregularities in the terrain, the high resolution of the DAQ card timers ensure consecutive velocity values are not identical. This property is utilized to determine if the robot has stopped by checking the equality of the current and previous values. A counter variable is used to count the occurrences of equal time before the velocity is set to zero to eliminate false assumptions from statistical anomalies.

The counters help determine the zero velocity condition however, a problem arises when selecting the appropriate threshold number. This number corresponds to the number of control loop cycles executed before the actual velocity is assumed zero so consideration is given to the loop period and the resulting control response. Low values give a faster response to change whereas high values reduce the oscillatory behaviour at low velocities. This is because a number of control loops may execute between encoder counts thus causing the zero velocity condition and spurious bursts of velocity data at the pulses. This is remedied by specifying different counter thresholds based on the previous operating velocity. High velocities have a low threshold to rapidly detect a halt while low velocities have a higher threshold to ensure a stable readout for slow track movement.

The current motor velocities are entered into a matrix of the last 10 values and averaged to reduce the effects of noise and drive system irregularities (friction, terrain). An error value between the target and actual velocities is generated to enable feedback control however, it is set to zero if the magnitude is less than 5 cm/s. This error margin helps increase the control system stability without affecting the overall robot response due to the nature of its operation in an outdoors environment.

The control effort is calculated using a pseudo PI (Proportional Integral) algorithm given by Equation 5.6. This method is preferred over conventional PID (PI Derivative) control due to delays and inaccuracies inherent to the system. Derivative components would amplify these errors and produce undesirable control system oscillation and instability. Full PID control should be reinvestigated once a complete system model of the mechatron is generated. Saturation conditions are applied to the control effort to ensure it does not exceed the analogue voltage limitations of the DAQ card and microcontroller hardware. Special conditions such as starting from rest and a zero target velocity are accounted for by rapidly increasing or decreasing the control effort as required before writing to the analogue output channels.

$$u(k) = u(k-1) + Ke(k) \qquad \textbf{Equation 5.6}$$

where: $u(k)$ = current control effort $u(k-1)$ = previous control effort

K = controller gain $e(k)$ = current error value

5.8.2 Heading Control

Heading control consists of two main components, rotating on the spot and maintaining a desired trajectory during motion. By rotating on the spot the robot best utilizes its differential drive capability to achieve the desired orientation in a minimal area. The actual and target heading values are acquired from the compass module and user interface respectively to create a heading error (Figure 5.34). The algorithm uses the magnitude and sign of the heading error to automatically determine the most efficient rotation direction relative to the 360° (North) point.

The track velocities are then set accordingly, one forwards and the other reverse to achieve the desired rotation. The error magnitude is monitored during the rotation to dynamically adjust the track velocities based on threshold values. High velocities for long rotations and low velocities for short rotations ensure a good compromise between fast response and minimal heading overshoot.

```
ActualHeading = str2num(get(handles.heading_disp,'String'));
TargetHeading = str2num(get(handles.NavigationOrientation,'String'));

set(handles.targetheading_disp,'String',num2str(TargetHeading));
handles.activex2.CIOrdCourse = TargetHeading;

HeadingError = TargetHeading - ActualHeading;
HeadingError(HeadingError<-180) = HeadingError + 360;
HeadingError(HeadingError>180) = HeadingError - 360;
```

Figure 5.34 Heading error calculation for orientation control

By incorporating heading control with forward motion of the mechatron a set trajectory can be followed by keeping the robot pointing in the desired direction. A similar concept to stationary rotation is used to calculate the desired rotation direction and magnitude although it is the ratio of track velocities which is adjusted.

If the mechatron veers slightly off course to the right the proportional control algorithm decreases the left track velocity accordingly. For more extreme course variations it may be required to simultaneously adjust both track velocities (one faster, the other slower) to quickly correct the current heading.

5.8.3 Obstacle Avoidance

Obstacle avoidance is achieved using a reactive control algorithm based on the distance measurements supplied by the infrared sensors. The navigation system is halted in the event of an impending collision and the mechatron is manoeuvred away from the hazard before normal operation is resumed. Reactive obstacle avoidance works by initiating pre-programmed behaviours to move the mechatron in set direction based on the infrared sensor data. The task of interpreting obstacles and plotting an appropriate path around them is reserved for higher level navigation software in future projects.

Different distance thresholds initiate different behaviours based on their location around the robot periphery and conditional statements within the low level control loop are used to select the appropriate motion. Examples include forward motion when objects are detected at the rear, reversing for obstacles in the forward path and turning away from objects detected on the mechatron sides in addition to various combinations of these basic functions.

5.8.4 Navigation

This project is focused primarily on autonomous navigation to a target position or orientation as opposed to more complex path planning techniques. The three main steps involved are:

- Determine current state from sensors
- Acquire desired state from user
- Execute method to achieve target

The current robot state consists of a position and orientation obtained from the compass and GPS. A conversion between the WGS84 (World Geodetic System 1984) satellite data and meters provides positioning in Cartesian coordinates relative to the robot origin. The target heading is calculated using trigonometry and the robot is rotated before straight line driving towards the goal. Reactive avoidance is executed when obstacles are detected after which the above navigation steps are restarted.

5.9 MICROCONTROLER CODE

The embedded controller (section 3.8) is responsible for the control and monitoring of the motor driver modules. Code has been written to effectively receive control commands from both the PC and an external radio control interface. Failsafe mechanisms have been implemented to ensure undesirable robot motion does not occur in the event of a computer crash or software lock-up.

Communication with the digital potentiometer is through a SPI interface however, as hardware support for SPI is not directly available on the selected microcontroller the required control routines have been written entirely in software. This includes the individual control line manipulation that would normally be handled by the SPI controller. Consideration to the data setup and hold time was important to ensure a reliable communication interface and used assembler language "nop" commands to introduce delays. The function to send a data word to the digital potentiometer is shown in Figure 5.35 with other source code available on the CD.

```
/*** Send Data Word to Digital Pot ***/
void POTSendData(unsigned char *Data)
{
 unsigned char SDIcnt;

 CS = 0;              // chip select and clock signals
 CLK = 0;
 asm("nop");

 for(SDIcnt=0;SDIcnt<8;SDIcnt++)
 {
  SDI = Data[SDIcnt];
  asm("nop");      // minimum required data setup time tds=5ns (actual = 1.6us)
  CLK = 1;
  asm("nop");
  CLK = 0;
 }
 asm("nop");
 CS = 1;
 asm("nop");
 asm("nop");
}
```

Figure 5.35 SPI code to send data word to digital potentiometer

Signals from the radio control receiver consist of a pair of pulsed square waves with a 19 ms period. The steady state pulse width is approximately 1.5 ms which varies between 1 ms and 2 ms when the controls on the transmitter are manipulated. The microcontroller uses external capture interrupts and an onboard timer to measure the pulse width of the signals on each channel indicated by the rising and falling edges. The resulting pulse widths are then scaled to match the digital potentiometer range and form the velocity control signals for the RHINO controllers.

Calibration of the RC signals occurs at microcontroller start up where the user is required to move the transmitter controls through the full range of motion. The *RCCalibrate()* routine (Figure 5.36) compares the received pulse widths with reference limits and previous values to determine to actual pulse width range. A motor driver status line is toggled during calibration as an indication to the user and is displayed on graphical interface (section 5.10).

```
/*** Calibrate to RC Receiver Signals ***/
void RCCalibrate()
{
 RCConfigCount = 0;
 RCRangeOK = 0;

 while(RCConfigCount < 250)
 {
  P42 = 0; // Pulse Status 0 (P0.4 on DAQ card) during RC Calibration
  if(CapCVal>CapCValMAX && CapCVal>1000 && CapCVal <2800) CapCValMAX =
CapCVal;
  if(CapCVal<CapCValMIN && CapCVal>1000 && CapCVal <2800) CapCValMIN =
CapCVal;
  if(CapDVal>CapDValMAX && CapDVal>1000 && CapDVal <2800) CapDValMAX =
CapDVal;
  if(CapDVal<CapDValMIN && CapDVal>1000 && CapDVal <2800) CapDValMIN =
CapDVal;
  Delay(100);
  P42 = 1;
  Delay(100);
 }
   RCRangeOK = 1;
}
```

Figure 5.36 Radio control receiver calibration routine

Although independent control of each track is possible with each transmitter control, the signals have been combined to provide a more intuitive interface. The vertical lever controls velocity while the signal from the horizontal lever is used to modify track velocity and achieve turning according to the *RCUpdate()* function in Figure 5.37.

```
/*** Update Pots with RC Data ***/
void RCUpdate()
{
 PotVal[2] = 63;
 PotVal[3] = 63;

  if(CapCVal>1000 && CapCVal<2800 && CapDVal>1000 && CapDVal<2800)
  {
   RCPotVal0 = (char)(63*(CapCVal-CapCValMIN)/(CapCValMAX-CapCValMIN));
   RCPotVal1 = (char)(63*(CapDVal-CapDValMIN)/(CapDValMAX-CapDValMIN));

   PotVal[0] = RCPotVal0; // both motors same speed from channel 1 (RCPotVal0)
   PotVal[1] = RCPotVal0;

   // Modify values for turning using channel 2 (RCPotVal1)
   if(RCPotVal0>=40)       // going forwards
   {
    if(RCPotVal1>=33) PotVal[1] = PotVal[1] - (RCPotVal1-32); //turn right
    if(RCPotVal1<=31) PotVal[0] = PotVal[0] - (32-RCPotVal1); //turn left
   }

   else if(RCPotVal0<=26) // going backwards
   {
    if(RCPotVal1>=33) PotVal[1] = PotVal[1] - (RCPotVal1-32); //turn right
    if(RCPotVal1<=31) PotVal[0] = PotVal[0] - (32-RCPotVal1); //turn left
   }

 if(PotVal[0]<=8) PotVal[0]=0;                  // saturation limits
 if(PotVal[1]<=8) PotVal[1]=0;
 if(PotVal[0]>=55) PotVal[0]=63;
 if(PotVal[1]>=55) PotVal[1]=63;

 POTUpdate(PotVal);                             // update digital pot with new values
}
```

Figure 5.37 Update digital potentiometer with RC data if RC signals are valid

Analogue speed and digital direction values are read from the DAQ card using the microcontroller ADC. The 10 – bit ADC produces a signal range 0 – 1023 which is scaled to the digital potentiometer limits in a similar manner to the RC signals as shown by Figure 5.38. The control signal for motor driver power is also read from the DAQ card on P4.0 and converted to the required digital pot value.

```
void DAQUpdate()
{
 // Read Control values from DAQ Card
 DAQ_Speed0 = SampleADC(1);   // Speed 0 value from DAQ card
 DAQ_Speed1 = SampleADC(2);   // Speed 1 value from DAQ card
 DAQ_Direction0 = SampleADC(3);          // Direction 0 value from DAQ card
 DAQ_Direction1 = SampleADC(4);          // Direction 1 value from DAQ card
 DAQ_DriverPower = P40;                  // Motor Driver Power from DAQ card

 // Update Digital Pots as Necessary
 PotVal[2] = (char)(63*DAQ_DriverPower);
 PotVal[3] = (char)(63*DAQ_DriverPower);

 DAQ_Speed0 = DAQ_Speed0*31/1023;
 DAQ_Speed1 = DAQ_Speed1*31/1023;

 if(DAQ_Direction0<=200) PotVal[0] = 32 - (unsigned char)(DAQ_Speed0);
 else PotVal[0] = 32 + (unsigned char)(DAQ_Speed0);

 if(DAQ_Direction1<=200) PotVal[1] = 32 - (unsigned char)(DAQ_Speed1);
 else PotVal[1] = 32 + (unsigned char)(DAQ_Speed1);

 if(PotVal[0]>=60) PotVal[0]=63; if(PotVal[0]<=3) PotVal[0]=0;
 if(PotVal[1]>=60) PotVal[1]=63; if(PotVal[1]<=3) PotVal[1]=0;

 POTUpdate(PotVal);
}
```

Figure 5.38 Update digital potentiometer with DAQ card data if safety pulse is valid

A system of failsafe mechanisms are included to ensure undesired motor operation does not occur in the event of a PC or control software malfunction. The DAQ safety pulse is the primary protection measure when operating under PC control and is generated using the MATLAB based low level control loop. An external interrupt (IEN0) is used on the microcontroller to reset a counter variable each time the pulse is detected thus verifying valid control signals.

When the pulse is not present the counter cannot be reset and increments through the use of the overflow interrupt on the microcontroller timer, T2. Once the counter reaches a threshold value it is determined the pulse is not present and control of the motor drivers with the DAQ card is disabled. A similar method is used for the radio control signals using separate counter variables which are reset when the capture interrupt is detected and also incremented with the overflow timer.

These failsafe mechanisms used in combination with the mode select signal ensure the motor drivers are switched off when neither control signals are valid.

5.10 USER INTERFACE

A graphical user interface (GUI) has been developed to provide a front-end control panel for the robot control algorithms. The interface, shown in Figure 5.39 allows customization of robot parameters and control commands in addition to providing feedback information from the onboard sensors including robot heading, velocity and pose.

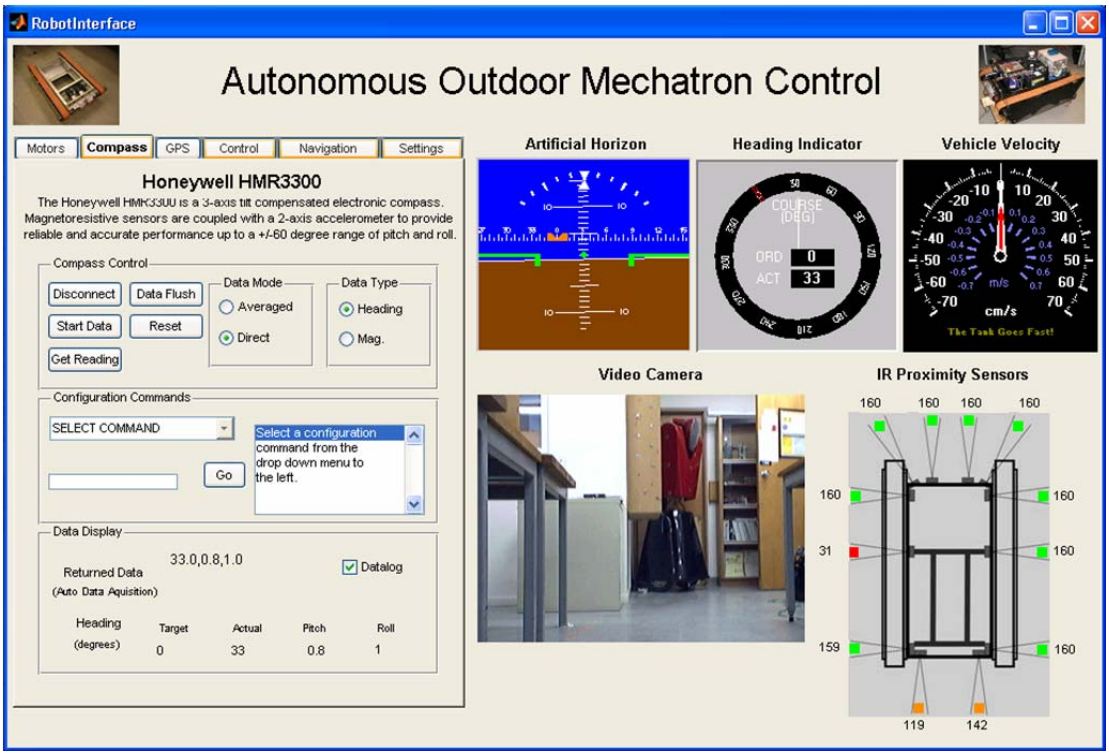

Figure 5.39 Graphical User Interface (GUI)

ActiveX controls have been integrated into the GUI to provide a visual representation of the robot state which is updated in real-time. The GMS (Global Majic Software) Angular Gauge ActiveX Control toolbox version 3.5 has been utilized to provide these functions.

An artificial horizon control displays the robot pitch and roll data extracted from the compass and accelerometer modules. The display is similar to those used in aircraft and gives an intuitive indication of robot pose relative to the horizontal sea-level plane.

A heading indicator displays the current robot orientation (ACT) relative to the Earth's North Pole and additionally shows the target heading (ORD) allowing an error comparison to be made. The ActiveX control automatically rotates the dial when the heading changes so the current heading is presented at the top of the indicator.

Robot velocity is displayed using a third ActiveX control with a customized scale and needle configuration with both cm/s and m/s to suit the outdoor mechatron. Current velocity (white arrow) is showed in addition to target velocity (red arrow) in both the forward and reverse directions as indicated by positive and negative values.

A push button control has been modified as a camera pane to display real-time image data from the onboard webcam. The size of the pane can be adjusted for different image resolutions and is capable of displaying a full colour picture. Additional options to capture the video stream or a screen shot are also available for logging to file for later image analysis.

Also shown on the GUI front panel is a graphical representation of the mechatron over-laid with infra-red sensor locations. This allows the users to immediate visualize potential obstacles and their relative positions around the robot perimeter. The currently detected object range is displayed in cm next to each sensor while coloured indicator boxes indicate the proximity in three ranges of severity, *Red – very close, Orange – medium, Green – out of danger zone or not detected.* The threshold values of each proximity range are easily modified depending on robot velocity and object position. For example, objects detected in the front of the mechatron while moving forward are of particular concern at the medium range level however less important if detected on the left or right sides because the robot may pass them by.

5.10.1 GUIDE

The graphical user interface development environment (GUIDE) within MATLAB has been used to design the current control panel. The program is initiated at the command window by typing *guide* and allows physical placement of the various GUI components on the design window. The user interface consists of two main files:

1) **RobotInterface.fig** contains the graphical components and is edited using GUIDE
2) **RobotInterface.m** consists of the MATLAB code and callback functions associated with the graphical components

Each component such as push buttons, sliders and text editing boxes require an unique identifier called the *Tag* and object settings are configured through the *Property Inspector* (an object configuration dialog box available from the toolbar). Callback functions are used to initiate segments of code when the objects are manipulated and are specified within the property inspector. A screen shot of the GUIDE development environment and the property inspector for the title text is shown in Figure 5.40. Each component of the GUI is located on the development area in the same way it appears on the final interface allowing easy customization of object placement.

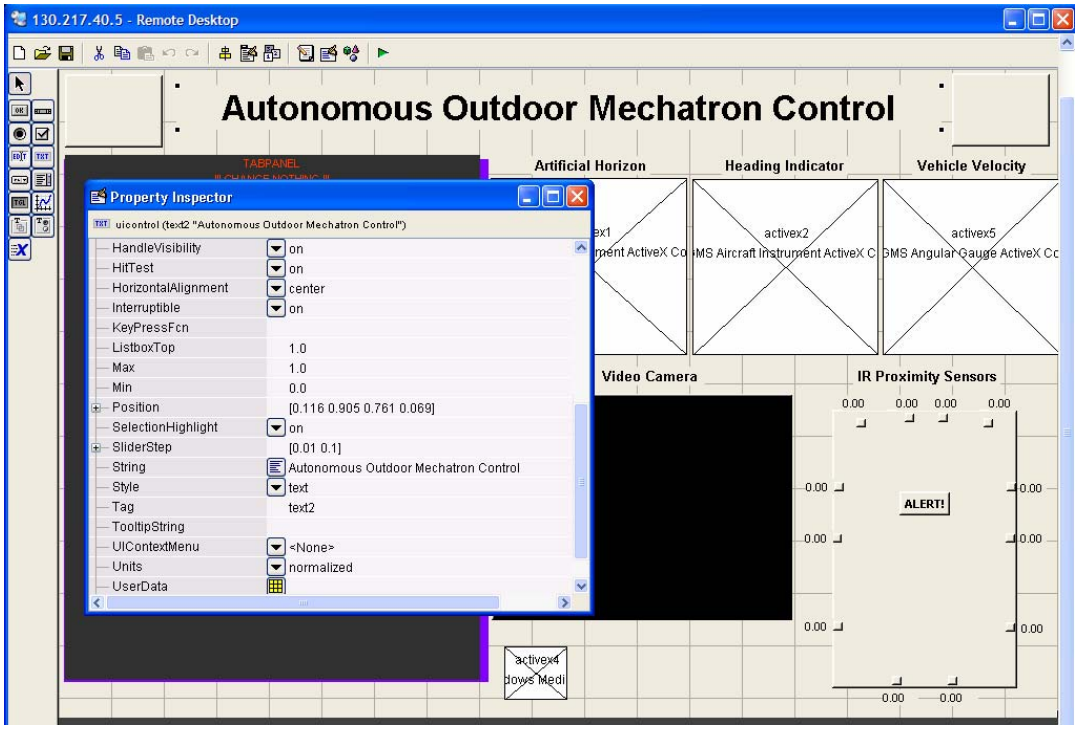

Figure 5.40 GUIDE interface development environment

5.10.2 TabPanels

A large number of interface components are required on the GUI to effectively control and display each component of the robot software. Due to the limited screen

size of the remote PC it is not possible to simultaneously display many elements to the user. For this reason, tab panels have been utilized to group similar functions into categories to provide a more intuitive and less cluttered interface.

The current version of MATLAB does not directly support the creation of tab panels however that ability to hide or show each component is available. This feature has been utilized by a third party MATLAB software developer to design a tab panel creation utility. The function **tabpanel** is available from the MATLAB support website (www.matlabcentral.com) and integrates with GUIDE to allow custom design of tab panels.

Tab panels are created by first reserving a space on the interface with a text box object in GUIDE. The tabpanel utility is then called with the figure file name, text box name and the names of the tab panels to be created as shown in Figure 5.41. An interface window is created which allows selection and then modification of each panel separately using the 'edit' button. During panel modification a temporary .fig file is created containing the graphics objects of that panel, for example Tabpanel_Motors.fig. The 'update' button must be pressed at completion to ensure the contents of the temporary .fig file are saved back to the main RobotInterface.fig file, otherwise the panel data is overwritten with the next 'edit' command.

```
Tabpanel('RobotInterface','TabPanel',
        {'Motors','Compass','GPS','Sensors','Control','Navigation','Settings' });
```

Figure 5.41 Initiate *tabpanel* configuration utility

The tab panels created are shown in Figure 5.42 and consist of the following:

- Motors
- Compass
- GPS
- Control
- Navigation
- Settings

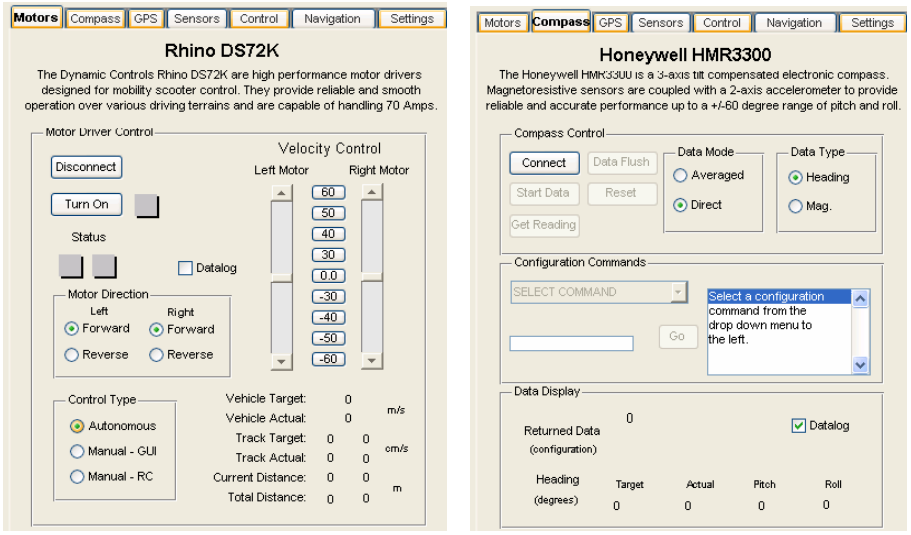

Figure 5.42 Sequence of tab panels (a) motor drivers panel (b) compass module panel

The motors panel initializes the DAQ card interface to the drivers and provides the user control and status feedback (green indicators). Sliders provide manual velocity control with the display panel showing vehicle and track velocities. The control type button group selects between the 3 modes of operation. The compass and GPS panels provide access to data extraction and preferences however, certain features such as the configuration menus are not available unless the modules are connected. The data display shows the returned information including heading, tilt, position and satellite data and dynamically adjusts the text headings for the different modes of operation. The hardware initialization and connection of other peripherals such as infrared sensors, video camera and accelerometer is available on the sensors panel.

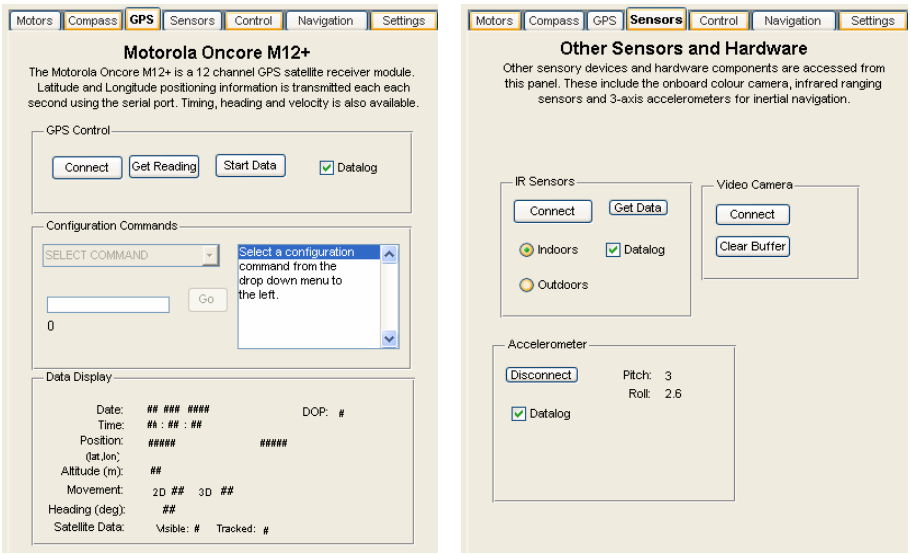

Figure 5.42 (c) Motorola GPS panel (d) other sensors panel

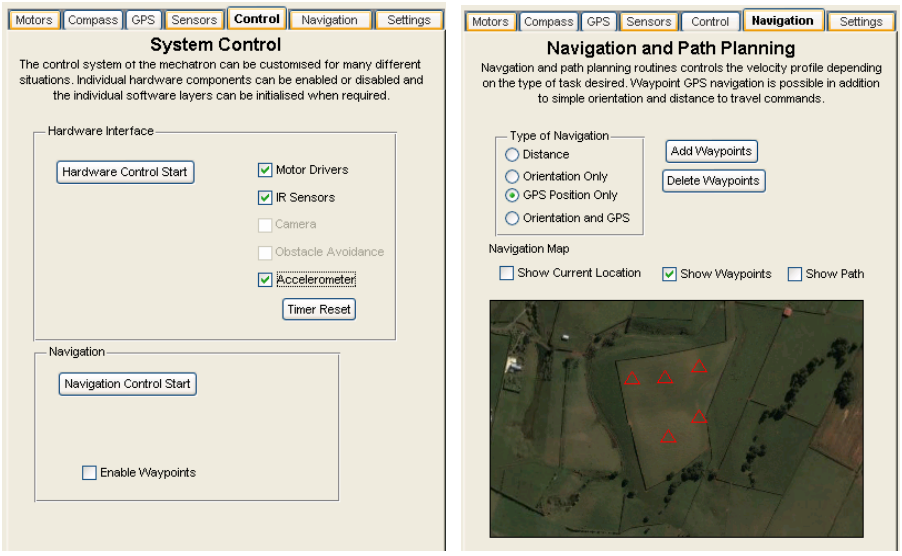

Figure 5.42 (e) system control panel (f) navigation panel

Access to the low level control and navigation loops are available on the control panel. Each component is individually enabled or disabled however functions are not available if their corresponding hardware interface is not initialized, therefore connection to devices should precede initialization of the control loops. The navigation panel provides a satellite image overlaid with current and desired GPS locations and the positions of specified waypoints. The robot configuration commands are available on the settings panel. This provides customization of control loop parameters and navigation objectives such as orientation. The task handles for the DAQ card are stored on this panel for extraction by the control loop and user verification of connection.

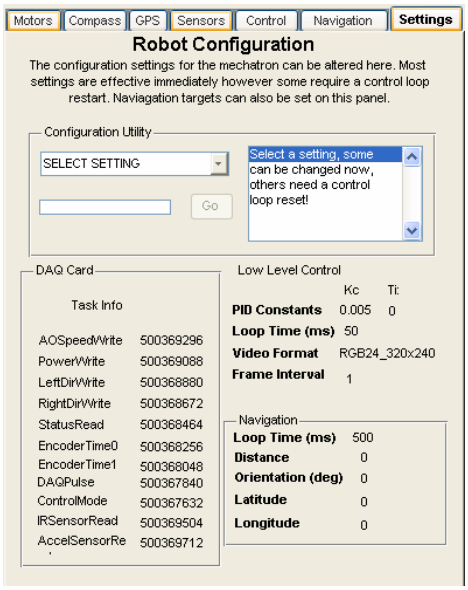

Figure 5.42 (g) settings and configuration panel

6. RESULTS & CONCLUSION

The mechatron is tested in an outdoor environment utilizing the various software routines created. Each of the installed sensory systems is assessed based on their functionality and suitability for satisfying the project requirements. The entire project is then summarized.

6.1 CURRENT CONSUMPTION

The power requirements of the mechatron are evaluated to determine suitable battery ratings (section 2.6.3). An LEM HT200 current transducer (Figure 6.1) was used for the electronic measurement of the DC current consumed by the mechatron. The device clamps around the primary current carrying wire providing galvanic isolation between the primary (high power) circuit and secondary (electronic) circuits. The transducer uses the Hall effect to measure the magnetic field generated around the current carrying wire.

Figure 6.1 LEM current transducer

This device provides good linearity and accuracy with a high immunity to external interference. Typical values taken from the datasheet indicate ±1% accuracy and ±0.5% linearity at 25°C. The unit is powered with a ±15 V supply and outputs an analogue ±5 V signal representing current. An electrical offset voltage dependant on ambient temperature is accounted for in the resulting equation giving current in terms

of measured voltage (Equation 6.1). The primary nominal DC current is 200 A which results in a 0.025 V/A slope with 5 V output range. Currents exceeding the 200 A limit do not provide accurate measurements.

$$I_p = \frac{V_{out} - V_{off}}{0.025} A \qquad \textbf{Equation 6.1}$$

I_p = primary current (A)
V_{out} = measured output voltage
V_{off} = output offset voltage (± 20 mV @ 25°C for I_p=0)

A number of different operating conditions were tested to determine current consumption on the mechatron under different loads. Tests range from operation of the PC or brakes only, up to operation on the floor under load including a human passenger as shown in Table 6.1.

Test #	Experiment Setup
1	Current draw of brakes only
2	Motors on full speed forwards, elevated from floor
3	Motors on full speed reverse, elevated from floor
4	PC on during boot up
5	PC on during steady state (no programs running)
6	Motors on full speed forwards, elevated from floor, PC on
7	Motors on full speed reverse, elevated from floor, PC on
8	Standing on robot, contact with floor, motors full speed forwards, PC on
9	Not standing on robot, contact with floor, motors full speed forwards, PC on
10	Standing on robot, contact with floor, motors full speed forwards, PC off
11	Not standing on robot, contact with floor, motors full speed forwards, PC off

Table 6.1 Mechatron power consumption test conditions

Seven measurement trials were carried out for each testing condition to ensure repeatable results were obtained (Figure 6.2), the data are then averaged and shown in Figure 6.3. The graphs show fairly consistent results over each trail with minor deviations possibly due to changing ambient temperatures (offset voltages) or changes in battery charge although each test was ideally conducted under the same conditions.

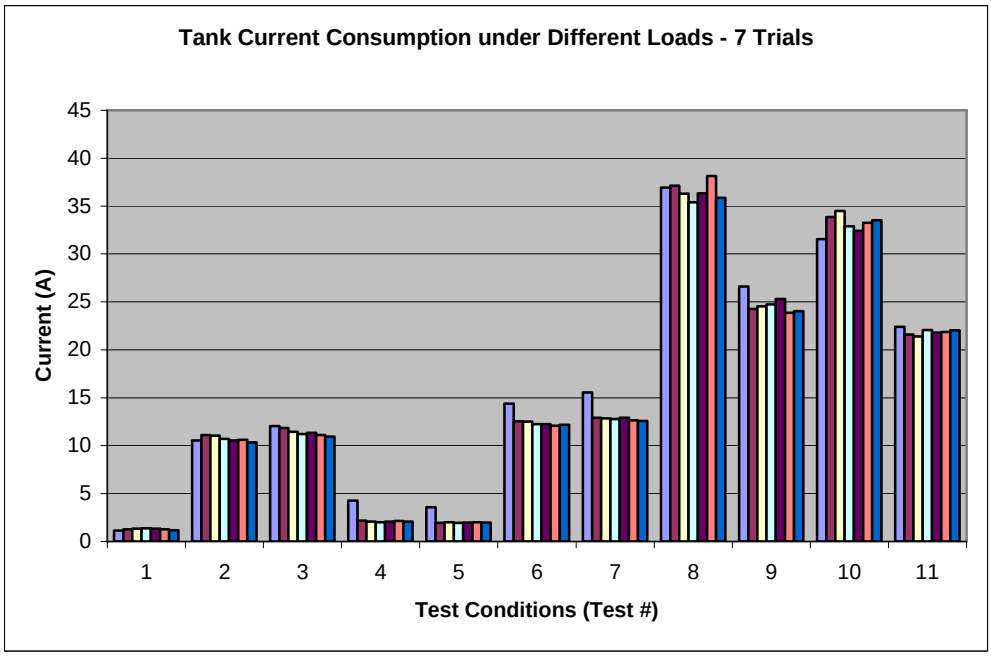

Figure 6.2 Current consumption for seven trials

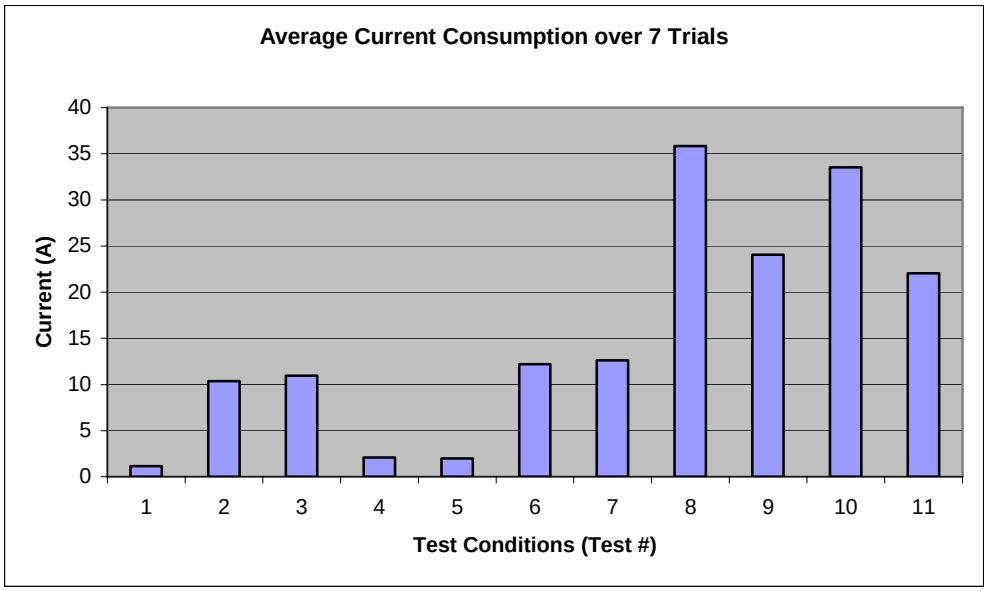

Figure 6.3 Average current consumption for each test condition

It is interesting to note the slightly higher current consumption during reverse operation compared to forwards movement as indicated by the trial pairs 2 & 3 and 6 & 7. This is due to the drive motors and gearing unit being designed primarily for forward motion and thus having a higher efficiency in this direction.

There is a significant difference between the loaded and unloaded mechatron current consumption as indicated by tests 8 – 11. The maximum current load was measured at

36.92 A, and occurred during forward motion with the PC switched on as indicated by trial 8. Although this case may represent fully loaded functioning in future conditions, this load will not occur during prototype development therefore the standard operating current is taken as 25 A. This significantly reduced the cost of the new deep cycle battery installation while still providing an adequate operating time of 1 – 1.5 hours (section 2.6.4).

The operating times of the newly installed deep-cycle batteries were compared to that of standard car starting batteries. It is important to note these car batteries were not new at the time of testing however a useful comparison can be made which reinforces the decision to implement deep-cycle batteries. The graphs of Figure 6.4 show the battery voltage over time for both the standard car batteries and the deep cycle units.

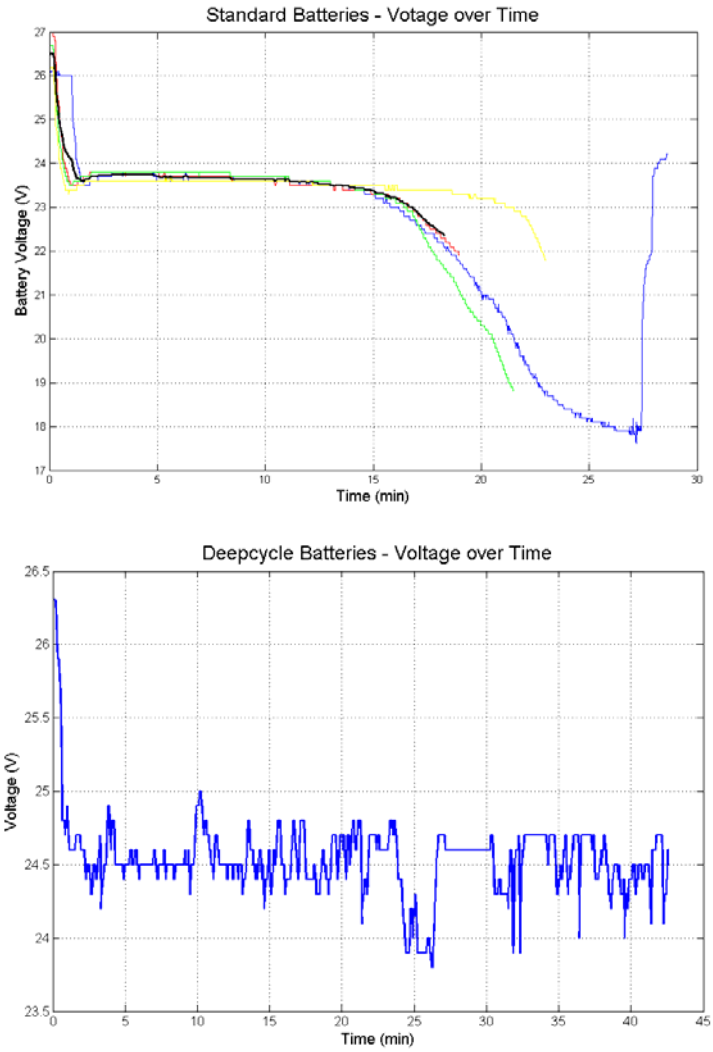

Figure 6.4 Operating time of starting vs deep cycle batteries

The car battery test was conducted with the mechatron operating off the ground (test 6 above) while the deep cycle based was conducted during non uniform movement in contact with the floor which accounts for the fluctuations of the voltage in the second figure. Despite the significantly lower load on the car batteries the operating time was significantly shorter which confirms the predicted battery life based on the RC rating.

It is important (under normal conditions) not to discharge a car battery too far as this causes permanent damage to the lead plates, so an operating time of only 15 minutes could be achieved. In contrast, the deep cycle batteries remained at a high charge for over 40 minutes. A communications error prevented subsequent data logging from the digital scope after this point however the mechatron continued to operate for over an hour without needing a recharge.

6.2 ACCELEROMETER

A number of tests were conducted on the accelerometer and interface board to determine measurement accuracy and suitability for use on a mobile robotic vehicle.

The integration with GPS to provide a standalone inertial navigation and absolute positioning system has not been fully realized however the initial foundations have been achieved to enable future development in this area.

6.2.1 Stationary Readings

Each of the three axes of the accelerometer are capable of both dynamic and stationary acceleration measurements where stationary values represent acceleration relative to Earth's gravity. Stationary readings are acquired on the mechatron using many possible orientations to analyze the resulting outputs and make a comparison with theoretical values given by the data sheet.

Under different orientations each axis will provide a different voltage representing the extent to which it is experiencing Earth’s gravity of 1 g. Theoretical values are based

on ideal power supply conditions and the precise alignment of the sensing cells within the accelerometer. Variations occur during attachment to the PCB and subsequent mounting in the enclosure making estimation of the accelerometer alignment relative to the mechatron difficult.

For this reason a number of readings were acquired while the module is attached to the robot thus generating the actual output voltages for each axis and orientation. Samples were acquired using NI VI Logger at a 0.001 s scan rate. The average of 20000 samples is taken and displayed in Table 6.2 with a comparison to theoretical values.

Pointing	**Theoretical (V)**			**Experimental (V)**		
Upwards	X	Y	Z	**X**	**Y**	**Z**
+Z	1.65	1.65	0.85	**1.69**	**1.58**	**0.81**
-Z	1.65	1.65	2.45	**1.71**	**1.61**	**2.39**
+Y	1.65	0.85	1.65	**1.68**	**0.79**	**1.59**
-Y	1.65	2.45	1.65	**1.72**	**2.39**	**1.57**
+X	0.85	1.65	1.65	**0.89**	**1.64**	**1.59**
-X	2.45	1.65	1.65	**2.50**	**1.58**	**1.54**

Table 6.2 Accelerometer stationary output voltages

Although some deviation exists between the theoretical and experimental values, this difference is small overall and therefore corresponds to a negligible difference in the resulting tilt calculations (section 6.2.3). These values will however, be required during position estimation calculations because a very accurate representation of acceleration is required on each axis and small offsets will cause position inaccuracies.

6.2.2 Collision Detection

The detection of a collision between the mechatron and an obstacle is important to enable effective navigation around the obstacle. Additionally, the continued acceleration of the motors during a collision can cause damage so a safety mechanism

to reduce power is necessary, preventing mechanical and electrical strain on the drive system. A common method is to install tactile switches ("whiskers") around the robot perimeter to provide a digital signal when contact with an obstacle occurs. Although effective as a collision detection system, a large number of devices are required to cover all possible contact points and the risk of damage to the switches is high. The accelerometer provides a single device, solid state solution enabling directional collision detection based on the initial shock of impact.

A number of tests were conducted to evaluate the collision detection performance from each of the four lateral direction planes, +X, -X, +Y and –Y (where +Y points forward). An example of the results obtained for front and rear impacts are shown in Figure 6.5.

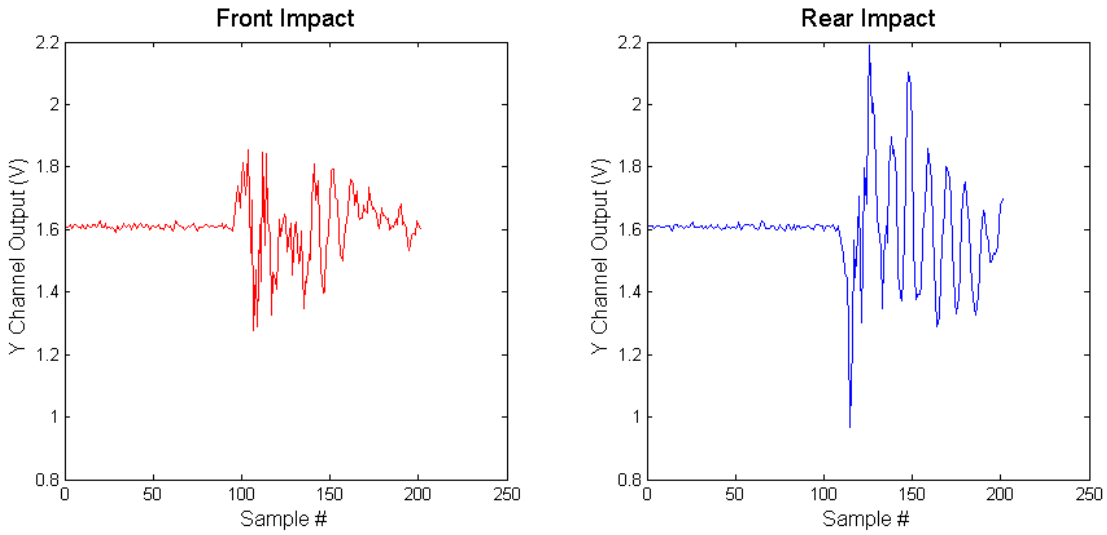

Figure 6.5 Comparison between frontal and rear impacts of different magnitude

The graphs show a clear distinction between the directions of impact by the initial sharp acceleration on the Y output channel. Front impact produces positive peaks while the rear impact was negative. These characteristics are projected onto other channels enabling left and right collision detection. Threshold voltages are used to alert the control system to different levels of shock as indicated by the peak magnitude. The subsequent oscillatory behaviour is due the continued movement of the g-cell sensing elements after the initial displacement and eventually decay by the laws of damped simple harmonic motion (SHM).

6.2.3 Tilt Measurements

The accelerometer and compass can both provide information on pitch and roll and therefore enable sensor redundancy. If one unit fails or cannot provide accurate data, the other is used. Sensor fusion algorithms can take advantage of this property by giving the data from the preferred sensor a higher weighting.

An important application of compass and accelerometer sensor redundancy for tilt applications is near magnetic disturbances such as power lines. The stray magnetic fields interfere with the electronic compass's Magnetoresistive sensors, producing erroneous results. The accelerometer however, works by measuring acceleration due to Earth's gravity and is therefore unaffected by magnetic fields and can be used as a replacement for the compass in this case.

A comparison between the pitch and roll outputs from the compass module are compared to those calculated (using Equation 5.5) from the accelerometer in Figures 6.6 and 6.7. Both modules are connected together and rotated through an angle range of ± 90° for both the pitch and roll axes.

The data show a close correlation between the tilt angles of both units throughout the different degrees of pitch and roll. A slight offset is consistently observed between the data from each sensor as indicated by region A in Figure 6.6. This shows an example of accelerometer data having a higher magnitude for pitch angles however, the compass data exhibits the higher magnitude for roll angles (Figure 6.7). Although the difference is negligible during normal operation, the slight variations (approx 1.9°) can be attributed to the non-exact mounting of the devices explained in section 6.2.1 and therefore may be eliminated by including the offset in the tilt equation.

The figures also show the tilt limitation of the compass compared to the accelerometer. Technical data for the HMR3300 suggest a maximum tilt range of ±60° in both pitch and roll and this is verified by the experimental data. In contrast the accelerometer is capable of the full ±90° range of tilt angles as shown in region B of Figure 6.7.

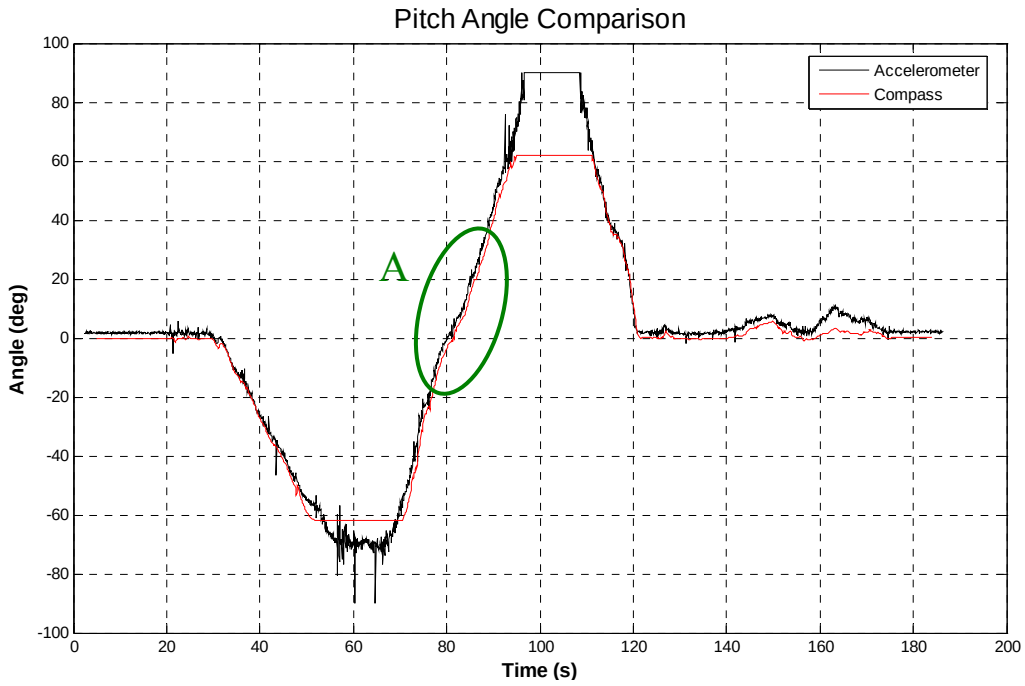

Figure 6.6 Compass and accelerometer pitch angle comparison

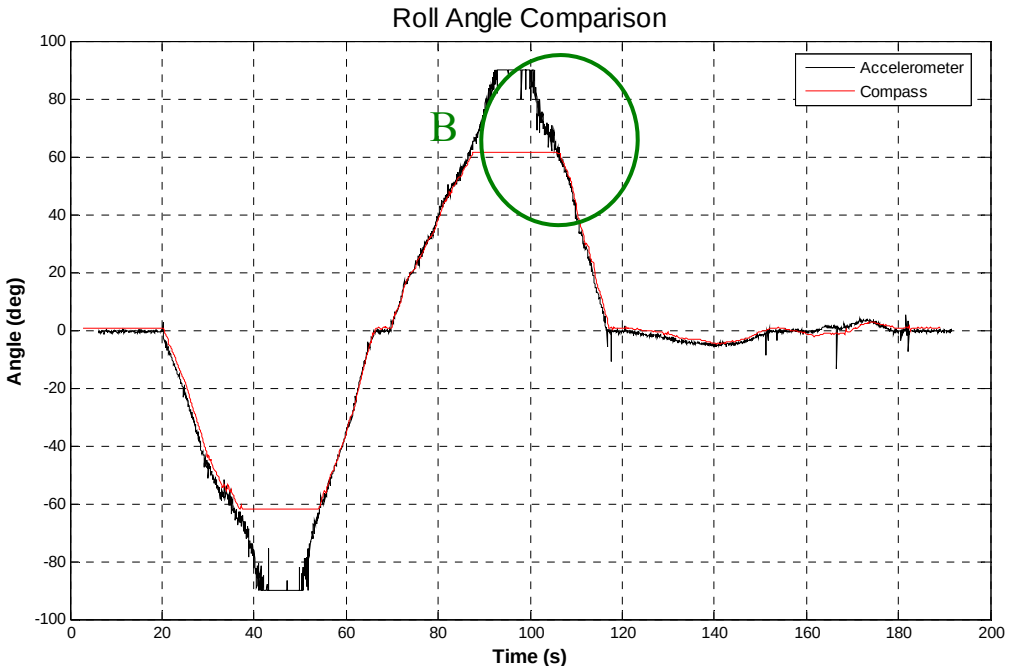

Figure 6.7 Compass and accelerometer roll angle comparison

Low pass filtering of the accelerometer data is used to remove much of the high frequency spikes illustrated in the above graphs. Onboard filtering of the compass acts to reduce noise however, the response time is reduced. As a result the accelerometer can produce a faster response time to change however the raw data can become noisy.

6.3 ELECTRONIC COMPASS

The electronic compass module is an important sensor for higher level robot control and outdoor navigation. For this reason a number of tests have been completed to evaluate its performance and suitability for implementation on robotic platforms.

Stationary repeatability is an important performance criterion because it gives an indication of the stability of the sensing elements. External interference and internal electrical noise due to switching components and temperature drift cause fluctuations in the output data. Theoretical values of accuracy from the datasheet suggest values of 1 – 4° RMS are obtainable depending on the level of tilt. It is important to note however, that these are RMS values and the actual accuracies gained experimentally can be as high as 8 – 10° for high tilt levels up to ±60°.

The onboard IIR (Infinite Impulse Response) filter also affects the accuracy and acts to remove electrical noise and other sources of interference thus smoothing the compass response. The filter setting can be adjusted through the user interface and practical values range from 0 (off) to approximately 20. Although higher values are selectable they do not produce favourable results. The effect of the system filter is evaluated and some of these results are illustrated in Figure 6.8.

The compass module is taken though straight line motion followed by turns, the section shown indicates a heading of roughly 260°, a clockwise turn of 250° and a resulting heading of 150°. Various filter settings were analyzed and this data set illustrates the effect of the values 0, 5, 10 and 20. The system filter affects the heading data in two distinct ways. Firstly, higher filter settings produce a smoother response. The high frequency noise components are low for the setting of 20 but are very prominent when the filter is disabled (setting 0) as shown by the standard deviation values. Secondly, by filtering out high frequency components, the response time is reduced such that the compass does not detect rapid changes in orientation as quickly. A compromise between noise immunity and response takes into account the slow movement of the mechatron therefore a higher filter value of approximately 10 – 20 is

chosen to provide the desired output stability. The resulting repeatability is approximately 0.7 – 1.5° standard deviation.

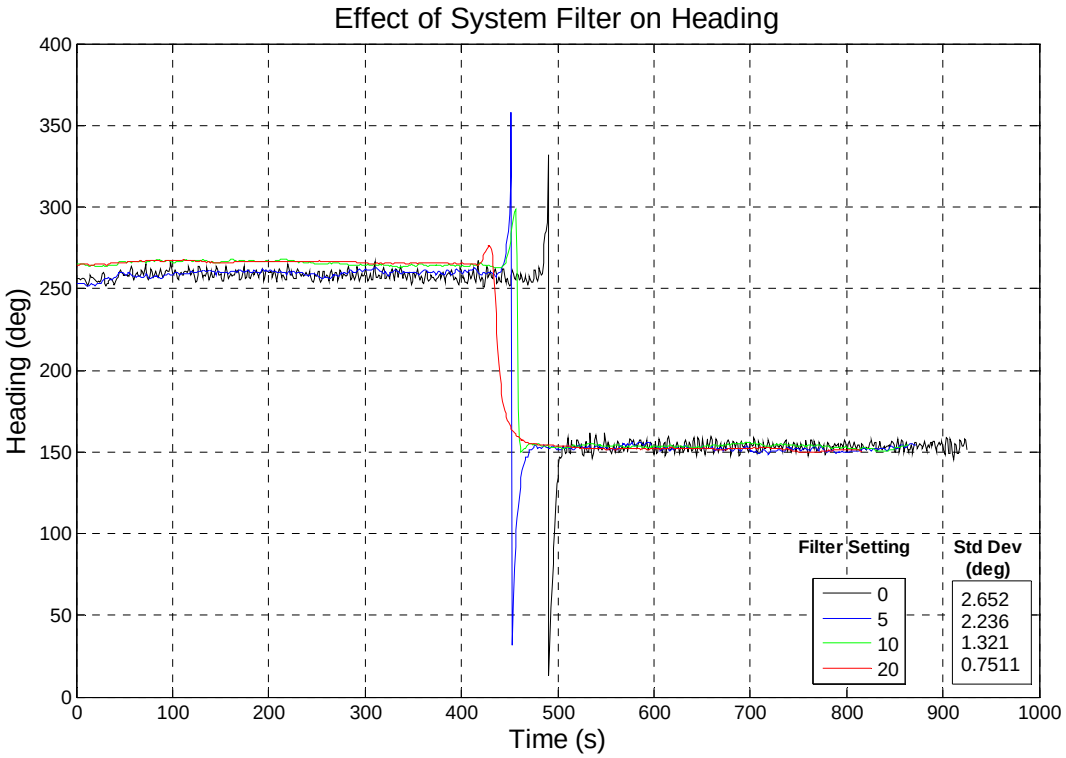

Figure 6.8 Effect of onboard IIR system filter on heading

Positioning of the compass module on the mechatron is an important consideration because the high frequency interference from the motors can affect performance. Tests have been carried out to determine effect of motor noise on response and thus the most suitable mounting location. Fortunately, the installed drive motors are shielded to prevent large amounts of EMI (Electromagnetic Interference) however the compass is still affected when mounted directly above the motors. As interference obeys the inverse square law[21] distance is the best protection and the compass is therefore mounted at the top-front of the mechatron, maximizing the radius to the motors.

Further tests with the compass examine the pitch and roll angles in comparison to the accelerometer data (section 6.2.3) and the heading with the heading obtained from the GPS module (section 6.4.2).

[21] The intensity of electromagnetic interference radiating through free space reduces as the inverse square of distance from the source.

6.4 GPS EVALUATION

The multi-terrain mechatron is designed for operation outdoors; therefore an absolute positioning system such as GPS is crucial for effective navigation and route planning relative to the local environment. Although advanced and expensive systems capable of very high precision (cm) positioning are available, the installed system cannot achieve these and so an evaluation of its capabilities and limitations is required.

6.4.1 Positioning

One of the applications of outdoor operation is waypoint navigation where the robot navigates to a series of locations in sequence. The projected application has been considered when evaluating the GPS thus properties such as stationary repeatability and the ability to close a loop are important. Some experimental results are shown in Figure 6.9 where the GPS module is taken around a 70 × 100 m path (black) and left stationary at the path vertices (coloured).

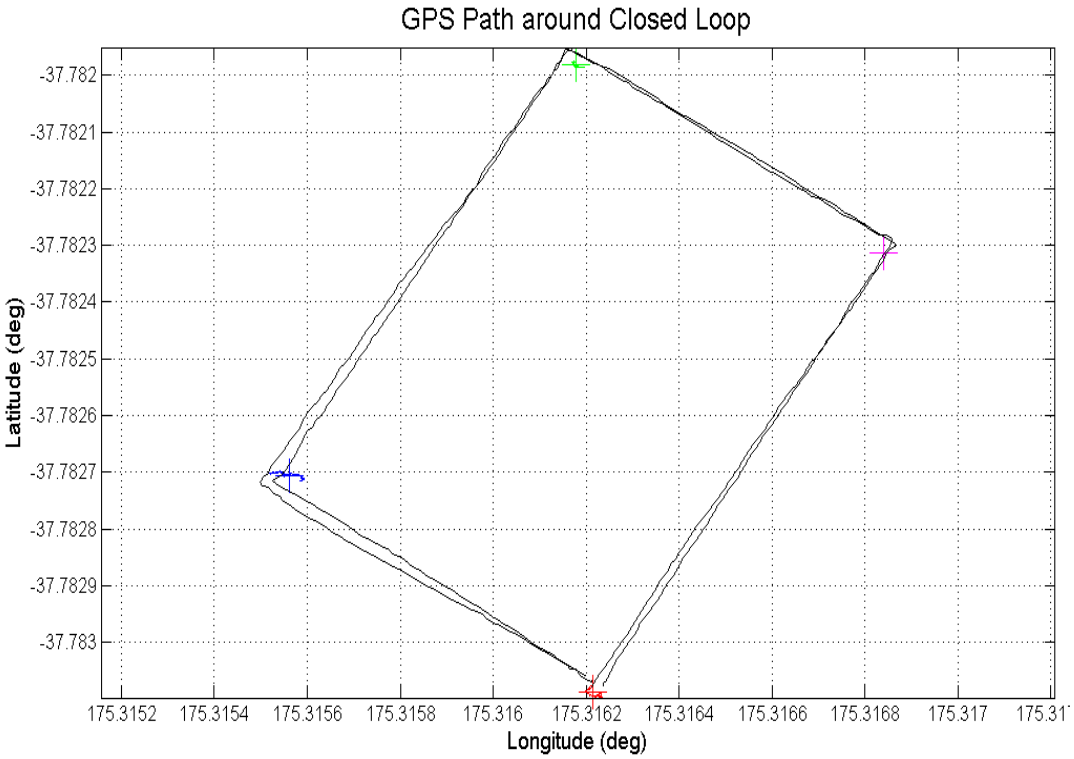

Figure 6.9 GPS Evaluation around 70 × 100 m path

Results show GPS provides an adequate approximation to position for large outdoor environments such as those the mechatron will operate in. Although differences occur between the different trials around the path, the loop is consistently closed and accuracy is sufficiently accurate for implementing waypoint navigation. This is reinforced by the stationary repeatability tests indicated by the coloured data points. The average latitude and longitude for each location is marked with a '+' sign and match closely with the tests in motion.

Results of these tests indicate longitude and latitude are accurate to a standard deviation of approximately 2 m and 4 m respectively. These values are suitable for location to large objects and landmarks however a different form of localization is required if multiple robots are operating in close proximity to reduce the risk of collision.

6.4.2 Heading

In addition to providing positioning, time and satellite information, the GPS modules are capable of indicating heading as does the electronic compass. Sensor fusion and therefore sensor redundancy can be utilized between the compass and GPS to better utilize the data and ensure operation can continue if one of the sensors malfunctions. Similar to the accelerometer, the GPS can still function within close proximity to magnetic fields however the compass cannot. The GPS can be used as a backup when the more accurate but noise sensitive compass cannot operate.

To evaluate the performance of the GPS in providing heading data the two units are taken through a rectangular course in both clockwise and anticlockwise directions. Example results are shown in Figure 9.10 which compares the response from both units. Discrepancies between the units for certain orientations initially indicated poor GPS response, however was later attributed to compass calibration which shows the importance of calibrating the compass while attached to the mechatron. Subsequent testing produced more favourable results with each device giving heading data within approximately 4°.

The GPS cannot produce reliable heading information while the unit is stationary as indicated by the initial 10 – 20 seconds of Figure 6.10. The reason is due to the heading calculation algorithm used by the GPS. Heading is computed from subsequent values of position so when the unit is stationary the only change in position is due to noise thus the heading is very inconsistent. Sensor fusion algorithms are therefore required to reduce or eliminate heading data from the GPS when the mechatron is stationary or moving slowly.

A positive result of the GPS heading algorithm is the rapid response to a direction change. The compass outputs the heading data continuously throughout the turn resulting in spikes. In contrast the GPS data produces a direct transition between the headings. This result is also an artefact of the longer time period between each GPS sample as compared to the compass.

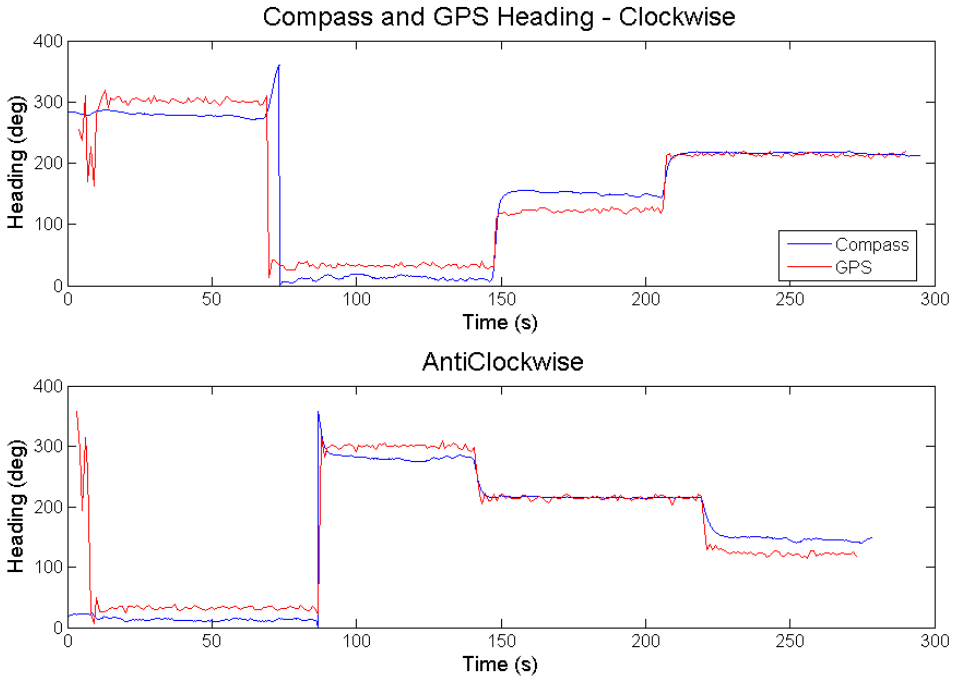

Figure 6.10 Heading comparisons between GPS and compass

6.4.3 Long Term GPS Response

The characteristics of GPS data over time is important for a mobile robotic platform that will operate for long periods. Changing accuracy and reliability of positioning

data could affect navigation algorithms that rely on the GPS data and therefore must be detectable and accounted for by the control system.

Positioning information that appears stable over the short term can change significantly due to many factors such as atmospheric conditions. Additionally satellites coming into and out of view of the receiver can change the position due to differences in the signals and ephemeris data.

To analyze the long term response, a number of stationary data logging sessions were completed over many hours. An example of GPS data logged from a residential area over approximately 11 hours is shown in Figure 6.11.

Both latitude and longitude data are collected and displayed in the upper two graphs. The variability of the position is clearly visible over time, particularly in the longitude where a low frequency cycle of 5 – 6 hours may be present. The gravitational effect of the moon may contribute to cycles of this length however further tests over longer time periods may be required to confirm this. Relative position from the initial datum point is shown in Figure 6.12 and scaled to meters using Equation 5.1. The standard deviation values are 2.89 m and 3.75 m for the X and Y directions respectively which also includes the large position jump out to 20 m. This is an error due to satellite tracking and can be easily detected and eliminated as false by using the accelerometer. Therefore positioning accuracy within ± 5 m is easily obtainable under normal conditions which are suitable for waypoint navigation outdoors.

The Dilution of Precision (DOP) is displayed and gives an indication of the quality of the triangulation calculation. Smaller values represent a higher accuracy of position data, and higher values indicate lower data quality. An example is the spike in longitude at 11 hours and an increase in DOP at this time. The DOP spike at 2 hours however, does not have a corresponding position jump indicating another factor.

Heading data that are displayed and described in section 6.4.2 provide a very poor and unusable value for robot orientation when stationary. Each position jump from a reference point produces a relative displacement and corresponding heading change. Even after short periods of time the heading changes through the full 360° range.

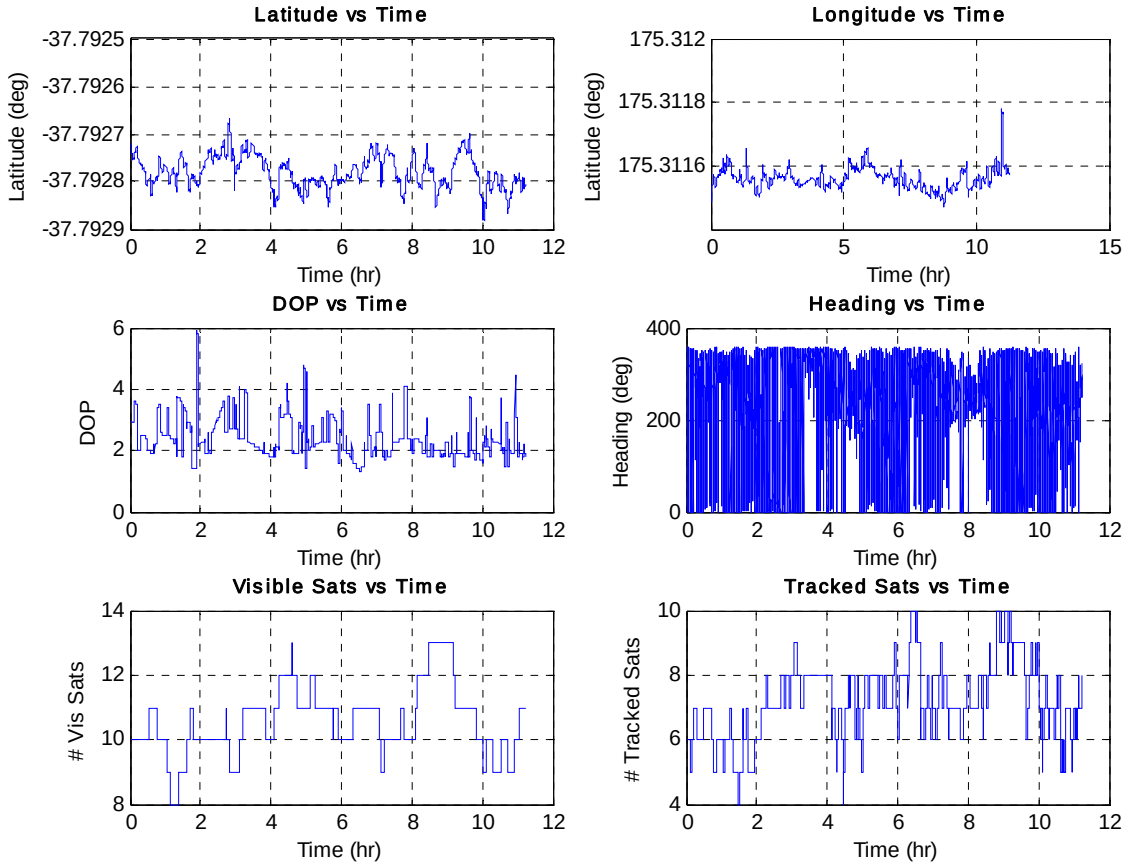

Figure 6.11 GPS data logged over approximately 11 hours

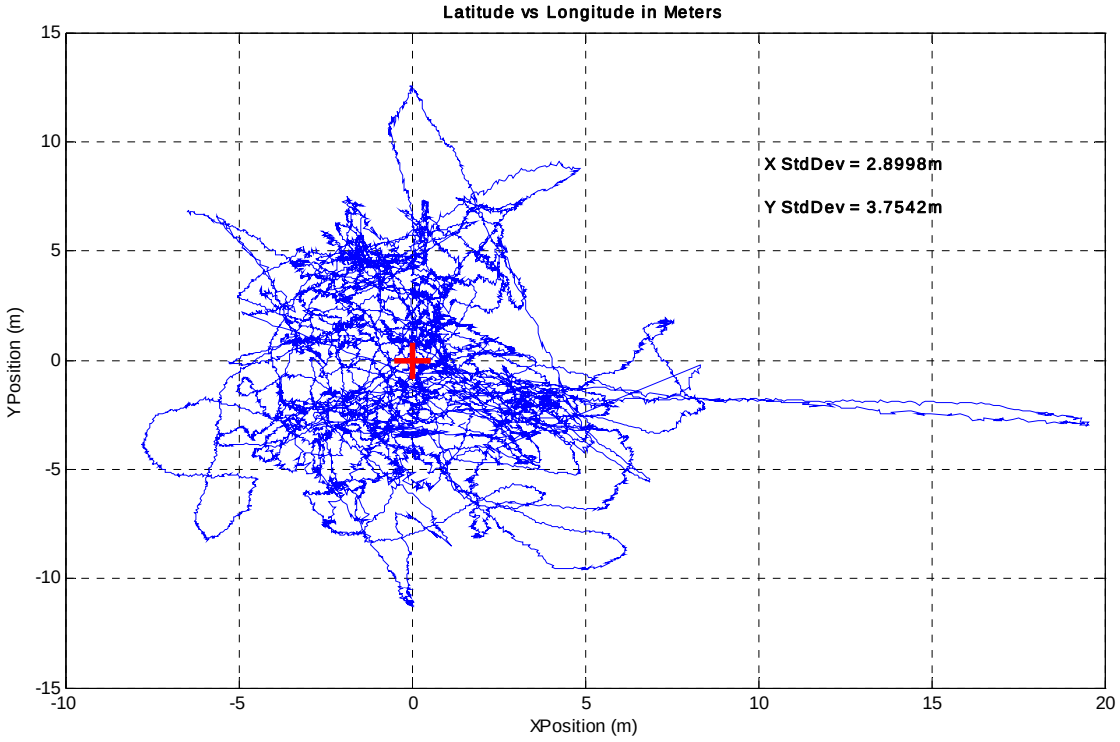

Figure 6.12 Relative position over time in meters

6.4.4 Improving GPS Positioning

Improving GPS position using DOP information has been investigated. DOP is not related to the number of tracked satellites as shown by Figure 6.13. It is related to satellite geometry where signals originating from satellites at broad angles give better data than those grouped close together.

Figure 6.14 shows the elimination of data points based on different DOP thresholds. Initial results are positive, showing decreasing standard deviations however, stray data points that are not caused by satellite geometry cause unpredictable operation. In addition, the effective operation time of the GPS is reduced if data are excluded thus requiring data from other sensors.

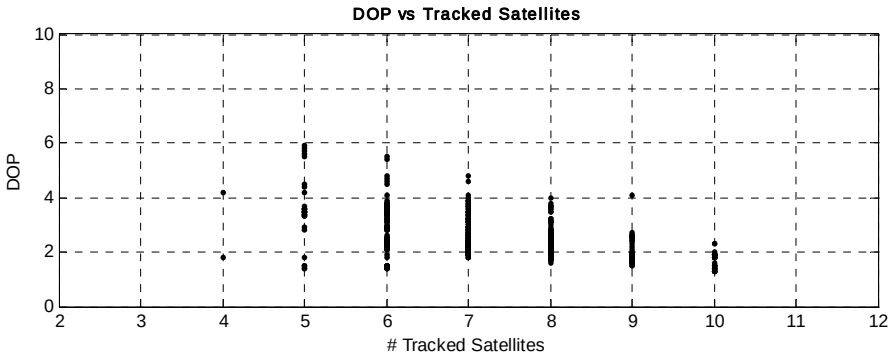

Figure 6.13 Dilution of Precision (DOP) vs Tracked satellites

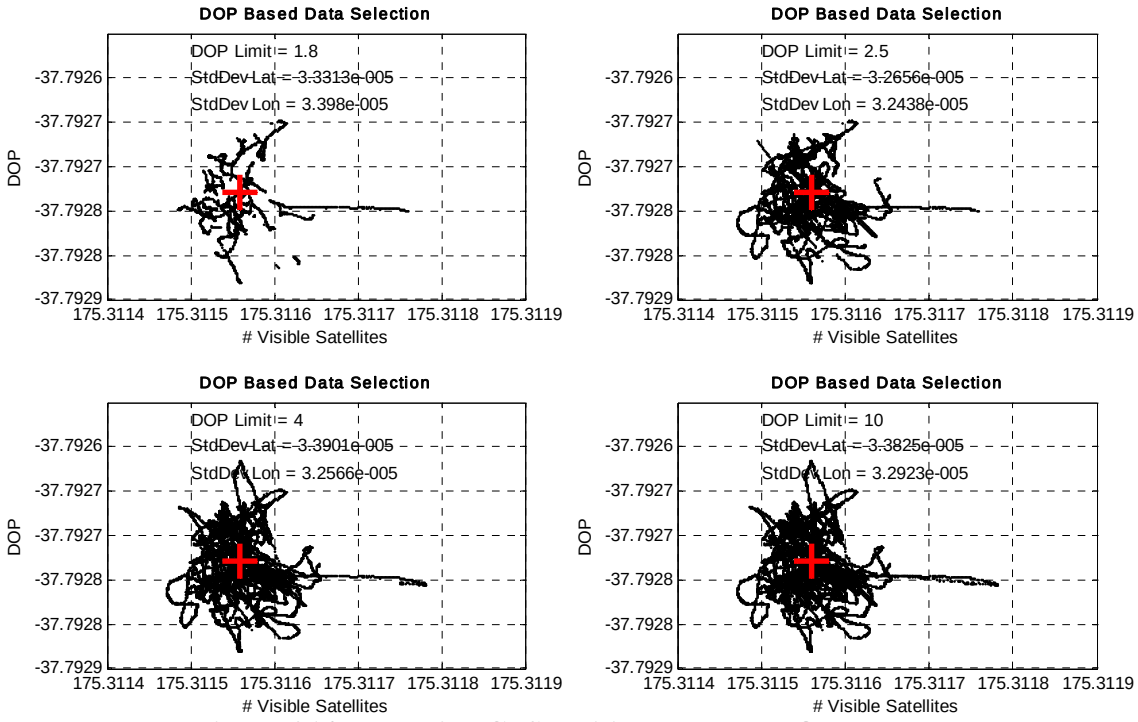

Figure 6.14 Improving GPS position based on DOP value

6.4.5 GPS Deficiencies

The testing and evaluation of positioning data from the GPS has revealed certain deficiencies related to the intended application of mobile robot localization. The errors in a non-corrected GPS signal typically arise in two main forms, high frequency noise and long term drift.

Although a formal definition of what constitutes noise in general has not been declared here, a general example is termed “single-epoch jumps”. An epoch is a single GPS cycle measured in the order of milli-seconds and the difficulty arises when the position can jump several meters before returning either on the next epoch or after a few seconds. The two main causes of this are satellites coming into and out of view and multi-path effects caused by the signal being reflected off nearby objects such as buildings.

The second class of error is drift, this is harder to examine because changes occur over hours as opposed to seconds in the case of noise. The exact cause is difficult to determine but usually attributed to atmospheric effects and satellite geometry. One of the useful pieces of data the GPS provides is the DOP or dilution of precision. This number gives a measure on the quality of the signal determined by the locations of the tracked satellites.

In conclusion, the GPS is a useful method of positioning for mobile robots and can provide sufficient accuracy for outdoor localization and way point navigation when combined with other sensors. Further investigation into different technologies in the future may be required for increased resolution and the ability to track multiple robots within close proximity.

6.5 ROBOT MOTION

The major objective of achieving motion of the multi-terrain mechatron has been realized. Manual control using both a radio transmitter/receiver and the user interface program has been achieved in addition to automatic operation.

6.5.1 Motor Operation

Motor control has been successfully implemented including direction and velocity control of both track units individually and in combination. A velocity curve, Figure 6.15 shows that the mechatron achieves forward accelerations of between 0.21 ms^{-2} and 0.32 ms^{-2} with a maximum velocity of approximately 60 cms^{-1}.

Deceleration rates are faster (Figure 6.16) to aid in obstacle evasion however, these parameters can be fully customized by programming the RHINO controllers as the application requires.

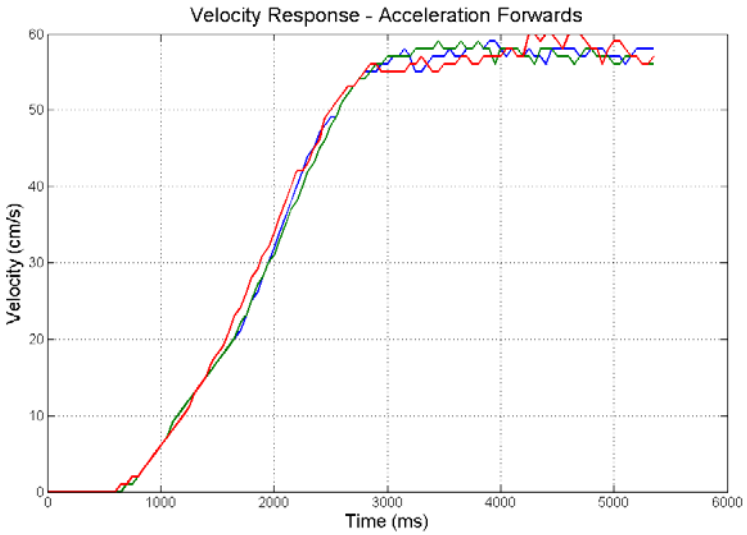

Figure 6.15 Mechatron velocity response forwards

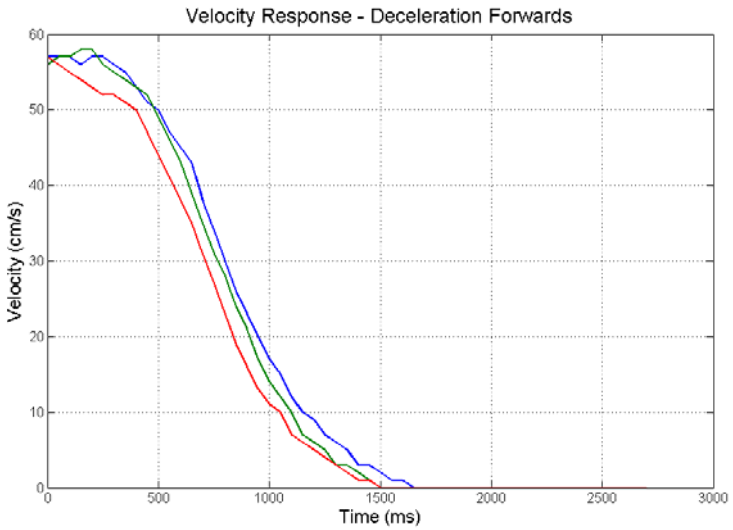

Figure 6.16 Mechatron velocity response reverse

6.5.2 Automatic Heading Control

Heading control is currently accomplished using a proportional algorithm to rotate on the spot, taking advantage of the robot's differential drive capabilities. Results of algorithm testing, Figure 6.17, are very good with final orientations within 3° of the target with minimal overshoot and oscillation.

It can be seen from the large transitions in the centre of the figure that the algorithm can automatically determine the most efficient direction to turn. Instead of rotating clockwise from 50° up to 340°, the robot is rotated anti-clockwise in the shorter path through the 360° point.

Heading control is also incorporated into forward movement to maintain a set trajectory. The orientation control routines were initially placed within the higher level *navigation control loop* but were later transferred to the *low level control loop* to achieve better response. The *navigation control loop* operates at a period of approximately 1 s therefore is slow to respond and causes oscillatory behaviour around the target heading. The *low level control loop* operates at 50 – 100 ms and therefore can respond to change and halt or activate the motors more efficiently.

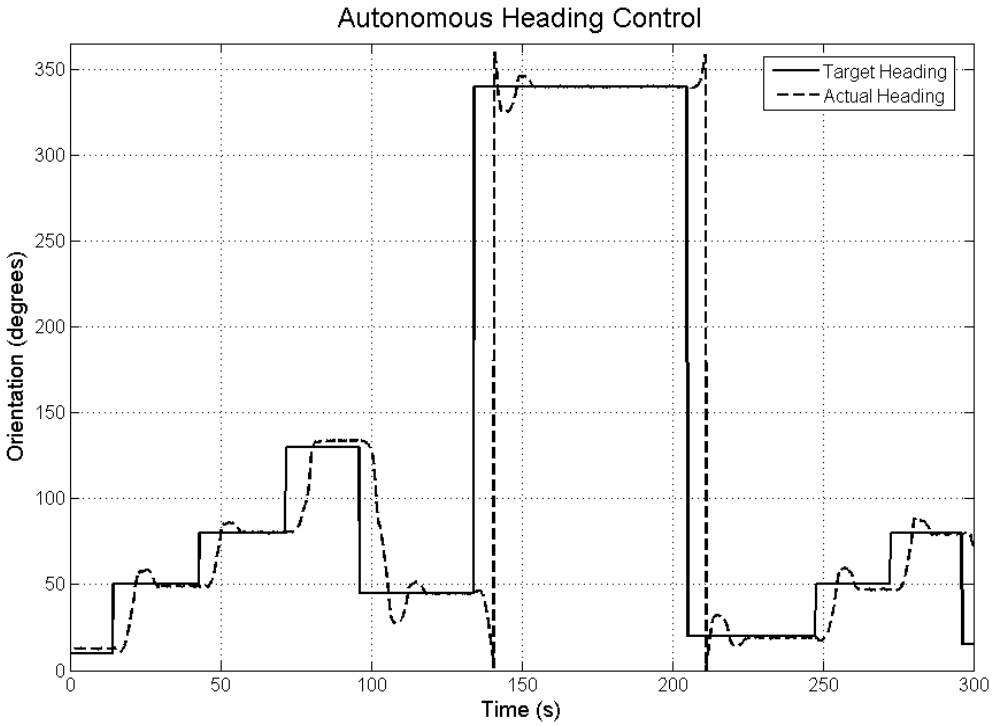

Figure 6.17 Example responses for autonomous heading control

6.5.3 Obstacle Avoidance

Reactive obstacle avoidance algorithms have been successfully implemented to steer the mechatron away from potential collisions. Reactive avoidance is defined as the immediate response to an obstacle as opposed to higher level software. Advanced software intended to plot a safe path and manoeuvre the robot around the obstacle is not implemented at this stage and could form the base of future projects.

Each of the 12 infra-red sensors produces a range value which is used in conditional statements to modify the motor velocity. Different magnitudes of range on the various sensors produce differing robot behaviours based on the obstacle position. As an example, detection of an obstacle by both front facing sensors produces immediate reverse motion whereas an obstacle on the front-left causes the mechatron to initiate a right turn.

The resulting obstacle detection and sequence of conditional statements has produced successful obstacle avoidance in both indoor and outdoor environments. Navigation through a corridor without collision is possible by ensuring a constant distance between the mechatron and walls. Pre-programmed routines are used outdoors to prevent collision with objects such as trees and fences however detection of hazards outside the lateral sensing axis (holes and valleys) is not currently possible due to the limited sensing elements.

6.6 INITIAL FIELD TRIAL

Initial tests of robot motion outdoors revealed certain limitations of the original mechanical design. The robot performed well on level surfaces and slopes if traversed directly up or down. The problem however was encountered when driving along a slope or turning while on a gradient.

The large weight of the mechatron produced significant lateral force vectors parallel to the ground gradient and focused on the track mechanisms. This effectively caused the mechatron to slide downhill and out of the rubber tracks causing the tracks to slide

over the guide pulleys and off the mechatron (Figure 6.18). The problem was caused by the small flange size of the original pulleys which could not retain the tracks effectively. The solution was to manufacturer new flange disks for the track pulleys that prevented track movement. The nylon pulleys were machined down using a lathe and custom made disks of aluminium are fitted with screws to each outside edge.

Consideration to the disk diameter was important to ensure the disks were large enough to support the tracks during large lateral forces while small enough not to contact the ground. Two sizes were therefore constructed, one for the upper pulleys and a smaller diameter for the lower pulleys as shown in Figure 6.19. The addition of rubber treads was also considered to increase traction and the clearance between ground and flanges. These were not implemented in this project due to cost but should be revisited in the future.

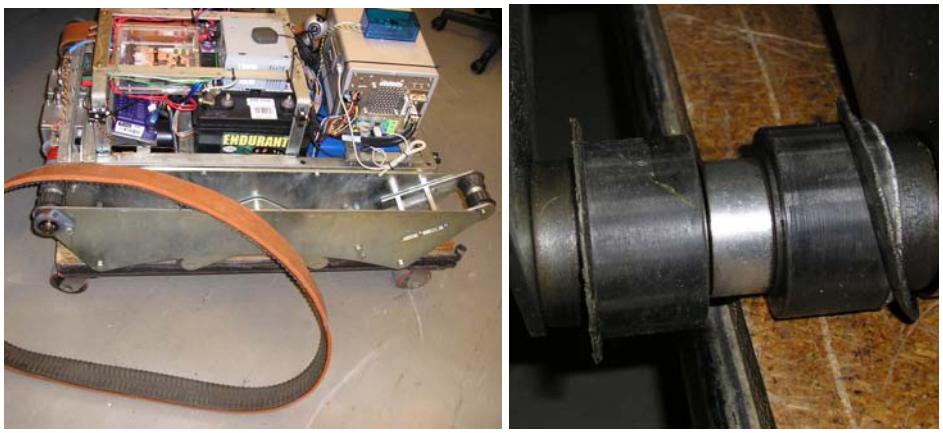

Figure 6.18 LEFT: Disengaged track RIGHT: Original pulleys with small flange

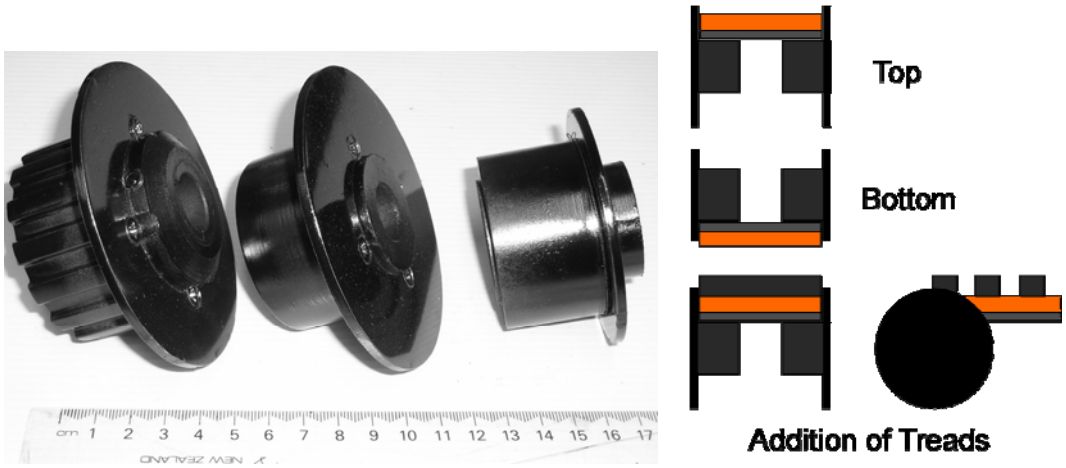

Figure 6.19 LEFT: New flange pulleys RIGHT: Track and flange positioning diagram

6.7 TESTING OUTDOORS

Further testing of the mechatron outdoors (Figure 6.20) after the flange modification produced positive results and outlines some of the capabilities of the multi-terrain robotic vehicle. The high manoeuvrability allows operation within close proximity to trees and scrub while motion in open fields is equally achievable. The high traction of the tread units allows successful negotiation of uneven and loose surfaces including bark, mud and other small obstacles. Stair climbing is a common ability amongst search and rescue robots therefore the task was successfully tested using the current platform. Concrete steps were easily traversed due to the mechatron weight and traction however caution is exercised to ensure the slope angle does not cause tipping.

Figure 6.20 Images of successful robot operation in outdoor conditions

6.8 FUTURE WORK

A number of extensions can be made to this project in the future to further enhance the functionality of the outdoor mechatron in an outdoor environment.

- **Artificial Intelligence software** can be designed to enable a range of tasks to be carried out by the mechatron such as terrain profiling or search and rescue. The higher level algorithms will utilize the low level control and hardware interface developed during this project to recognize obstacles and plot intelligent paths through the operating environment
- **Sensor fusion** algorithms can be designed to take full advantage of the wide range of sensors that have been installed. Examples include combining GPS positioning data with the accelerometer to increase localization accuracy.
- **Commercial applications** for a mobile autonomous multi-terrain mechatron are wide ranging and the full potential of these devices is yet to be utilized. Investigation into potential operation could focus the project and allow further development into the necessary onboard systems.
- **Robot manipulators** have many uses on a mobile robot from cargo transportation to landscaping and construction. A series of modular manipulator units could be designed giving the robot a wide range of uses. An example of a robotic appendage previously developed by the Mechatronics Group is shown mounted on the mechatron in Figure 6.21 and could potentially be interfaced to the newly designed control system and interface.

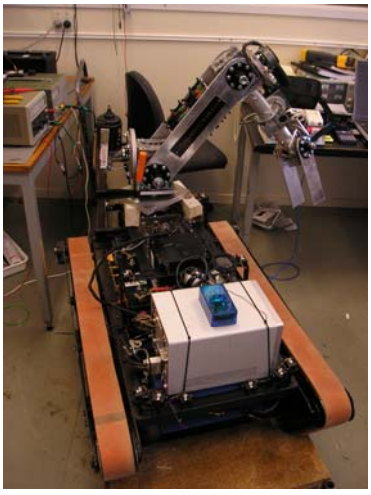

Figure 6.21 Robotic manipulator mounted on outdoor mechatron

6.9 SUMMARY

The modification of a multi-terrain robotic vehicle for autonomous outdoor applications has successfully been completed. All of the project objectives have been met and the software interface written has exceeded project requirements. The mechatron and installed components are designed to allow autonomous operation and includes onboard power supply and control electronics.

The previously designed mechanical shell of a self laying track mechatron formed the base of this project. The platform, constructed with a steel frame and differential drive system provides a durable and stable vehicle for the negotiation of difficult terrain in an outdoor environment. This project included a number of mechanical modifications and enhancements to the original platform to enable operation. These include the construction of new flanges for the guide pulleys and various mountings and brackets for the different components.

Working electronic components did not exist on the original platform therefore a complete design and installation of these systems was completed. An onboard power supply constituting two 12 V SLA Deep Cycle batteries connected in series and a ATX switch mode converter with 18 – 32 V input range is installed. The power system provides +12 V and +5 V rails to the various other systems through a modular designed connection system and power distribution board. The CPU is a ShuttleX desktop PC with a 2800+ processor and 512 MB of RAM. Motor control consists of a pair of RHINO scooter controllers with a custom designed interface board and microcontroller control. Communication with a remote base is provided using D-Link wireless network adapters, using a standard 802.11b protocol. Data input and output is achieved using a PCI-6229M data acquisition card manufactured by National Instruments.

A number of sensory systems have been researched and installed on the mechatron for robot localization and navigation outdoors. An evaluation of sensor response and suitability for the mechatron is completed before integration into robot control software. Sensors include GPS for positioning, electronic compass for heading and

tilt, accelerometer for relative positioning and tilt and infrared sensors for obstacle detection. Other onboard sensors include odometry encoders and a colour camera.

Mechatron control and hardware interfacing software is written in the MATLAB programming language. Hardware interfaces to the DAQ card and other peripherals have been developed including a DLL interface system to the DAQ card drivers. Low level control algorithms including velocity control and autonomous heading adjustment have been developed. Reactive obstacle avoidance software uses the onboard infrared sensors to move the mechatron away from nearby objects. A comprehensive graphical user interface provides the central control and sensor feedback from the mechatron during operation. Tab panels organize similar functions for easy access and provide the means for customization and control of each hardware component. The navigation panel also allows users to enter a set of waypoints superimposed on a satellite photo of the operating environment that the mechatron can navigate in sequence.

The comprehensive research and review of commercially available hardware components such as sensors, motor drivers and computer peripherals has provided a valuable resource to future robot developers. The Mechatronics Group will significantly reduce development time on new robotic vehicles by utilizing this resource which, in addition provides an important foundation into future work on the outdoor mechatron.

Figure 6.22 Completed mechatron in operation outdoors

GLOSSARY

802.11b	Wireless network communication protocol
ADC	Analogue to Digital Converter
DAC	Digital to Analogue Converter
DAQ	Data Acquisition
DC	Direct Current
DGPS	Differential GPS
DLL	Dynamic Linked Library
DMA	Direct Memory Addressing
DoD	United States Department of Defence
DOP	Dilution of Precision
EMI	Electromagnetic Interference
EOD	Explosive Ordnance Disposal
Ephemeris	Table of coordinates giving the location of a celestial body
GUI	Graphical User Interface
GPS	Global Positioning System
I/O	Input/Output
LAN	Local Area Network
MATLAB	Matrix Laboratory
MAX	Measurement and Automation Explorer
MOSFET	Metal Oxide Semiconductor Field Effect Transistor
NAVSTAR	Navigation satellite timing and ranging (US GPS system)
NI-DAQmx	Software drivers for National Instruments DAQ card
NI-PGIA	National Instruments Programmable Gain Instrumentation

	Amplifier
NI-STC2	National Instruments System Timing Controller 2
PCB	Printed Circuit Board
PCI	Peripheral Component Interconnect
PID	Proportional Integral Derivative
PWM	Pulse Width Modulation
RC	Radio Control
RF	Radio Frequency
TTFF	Time to First Fix
UPS	Uninterruptible Power Supply
USB	Universal Serial Bus
WGS84	World Geodetic System 1984

REFERENCES

Barr, M., "*Pulse Width Modulation*", Embedded Systems Programming, September 2001, pp.103-104 (www.netrino.com/Publications/Glossary/PWM.html).

Battery Town, 2005 *"Marine Batteries Made Simple"*, www.batterytown.co.nz.

Borenstein, J., Everett, H.R., and Feng, L., *Where am I? Sensors and Methods for Mobile Robot Positioning.*, The University of Michigan, 1996.

Braga, N.C., *Robotics, Mechatronics and Artificial Intelligence*., Butterworth-Heinemann, 2002.

Bruch, M.H., Gilbreath, G.A., Muelhauser, J.W., and Lum, J.Q., *Accurate waypoint navigation using non-differential GPS,* Space and Naval Warfare Systems Centre, San Diego, CA, www.spawar.navy.mil/robots/

Carnegie, D.A., Cree, M.J., Dorrington, A.A., "A high-resolution full field range imaging system," *Review of Scientific Instruments*, vol. 76.

Cawley, C.L., and Carnegie, D.A., *The Modification of a Multi-Terrain Robotic Vehicle for Autonomous Outdoor Applications,* Proceedings of the Twelfth Electronics New Zealand Conference, Manukau City, New Zealand, 14 – 15 Nov. 2005, pp. 123 – 128.

Cordes, J., *The Creation of an Autonomous Multi-Terrain Mechatron,* MSc Thesis, University of Waikato, 2002.

Dynamic, 2005 *"RHINO The New Force in Scooter Control Installation Manual"*, Dynamic Controls.

Franklin, G.F., Powell, J.D., and Emami-Naeini, A., *Feedback Control of Dynamic Systems*. 4rd edition, Prentice Hall, 2002.

Horenstein, Mark N., *Microelectronic circuits and devices*. 2nd edition, Prentice Hall Inc, 1996.

Ingle, V.K., and Proakis, J.G., *Digital Signal Processing using MATLAB.*, Brooks/Cole, 2000.

Jensen, C.H., *A Generic Motor Driver Design for Mobile Robotic Platforms,* MSc Thesis, University of Waikato, 2004.

Jungwirth, G., Mairhofer, M., Schmitzberger, T., Wagner, C., *Reworking of A Remote Underwater Vehicle Part II*, University of Waikato, 2004.

King, J., *The Development of an AUV,* MSc(Tech) Thesis, University of Waikato, 2002.

Kirkup, Les., *Experimental Methods – An introduction to the analysis and presentation of data.*, John Wiley and Sons, 1994.

Lee-Johnson, C., *Development of a Control System for an Autonomous Mobile Robot,* MSc Thesis, University of Waikato, 2004.

Matthies, L., Xiong, Y., Hogg, R., Zhu, D., Ramkin, A., Kennedy, B., Hebert, M., Maclachlan, R., Won, C., Frost, T., Sukhatme, G., McHenry, M., and Goldberg, S., "A portable, autonomous, urban reconnaissance robot," *Robotics and Autonomous Systems,* vol. 40, pp. 163 – 172, 2002.

Motorola, 2002 *"Motorola GPS Products – Oncore User's Guide",* Motorola Inc.

National Instruments, 2005 *"Data Acquisition – M Series Help"*, National Instruments Corporation.

National Instruments, 2005 *"Data Acquisition – NI-DAQ™mx Help"*, National Instruments Corporation.

Payne, A., *Design and Construction of a Pair of Cooperating Autonomous Robots,* MSc Thesis, University of Waikato, 2004.

Pratap, R., *Getting Started with MATLAB – A quick introduction for Scientists and Engineers*. 6th edition, Oxford University Press, 2002.

Rizos, C., *Introduction to GPS,* Satellite Navigation and Positioning Group University of New South Wales, 1999, www.gmat.unsw.edu.au/snap/gps/gps_notes1.pdf.

Thong, Y.K., Woolfson, J.A., Crowe, J.A., Hayes-Gill, B.R., and Challis, R.E., "Dependence of inertial measurements of distance on accelerometer noise," *Measurement Science and Technology*, vol. 13, pp. 1163 – 1172, 2002.

Thong, Y.K., Woolfson, M.S., Crowe, J.A., Hayes-Gill, B.R., and Jones, D.A., "Numerical double integration of acceleration measurements in noise," *Measurement*, vol. 36, pp. 73 – 92, 2004.

Zilog Application Note AN015002-1103, "*Digital to Analog Conversion Using PWM in the Z8 Encore!® MCU"* http://www.zilog.com

APPENDIX A: CIRCUIT DESIGN

A.1 MOTOR DRIVER INTERFACE BOARD

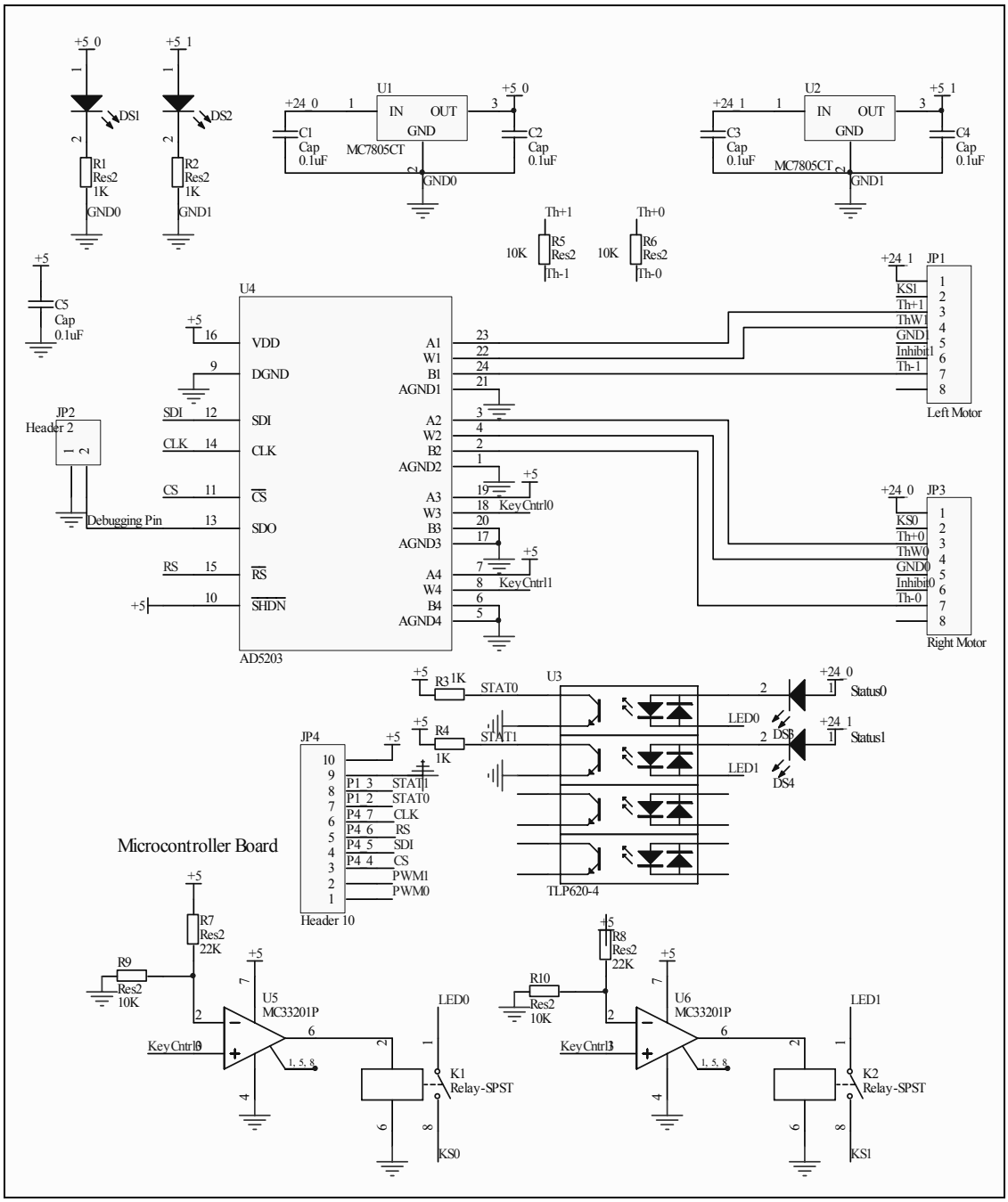

A.2 MICROCONTROLLER BOARD

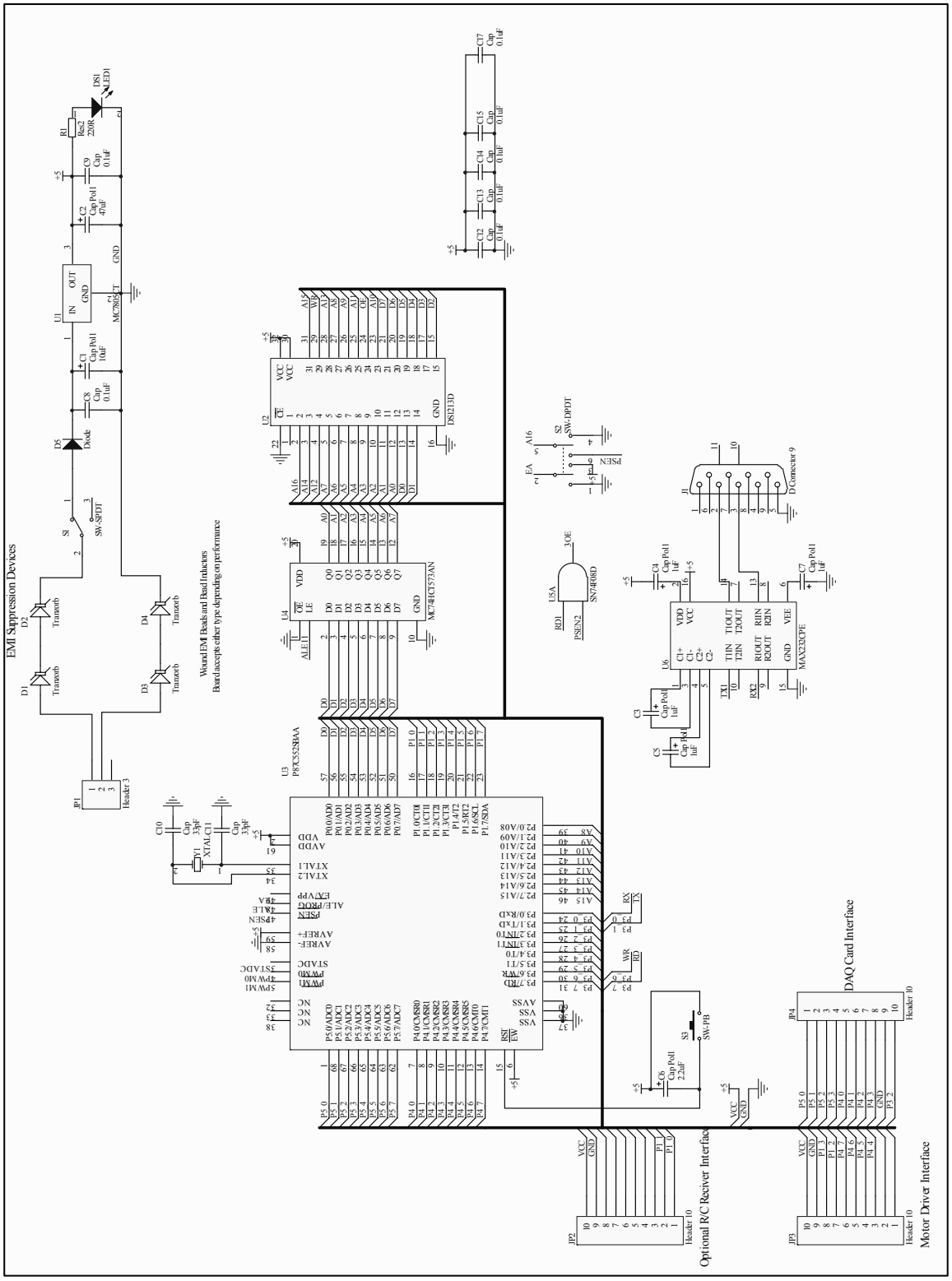

A.3 ELECTRONIC COMPASS INTERFACE

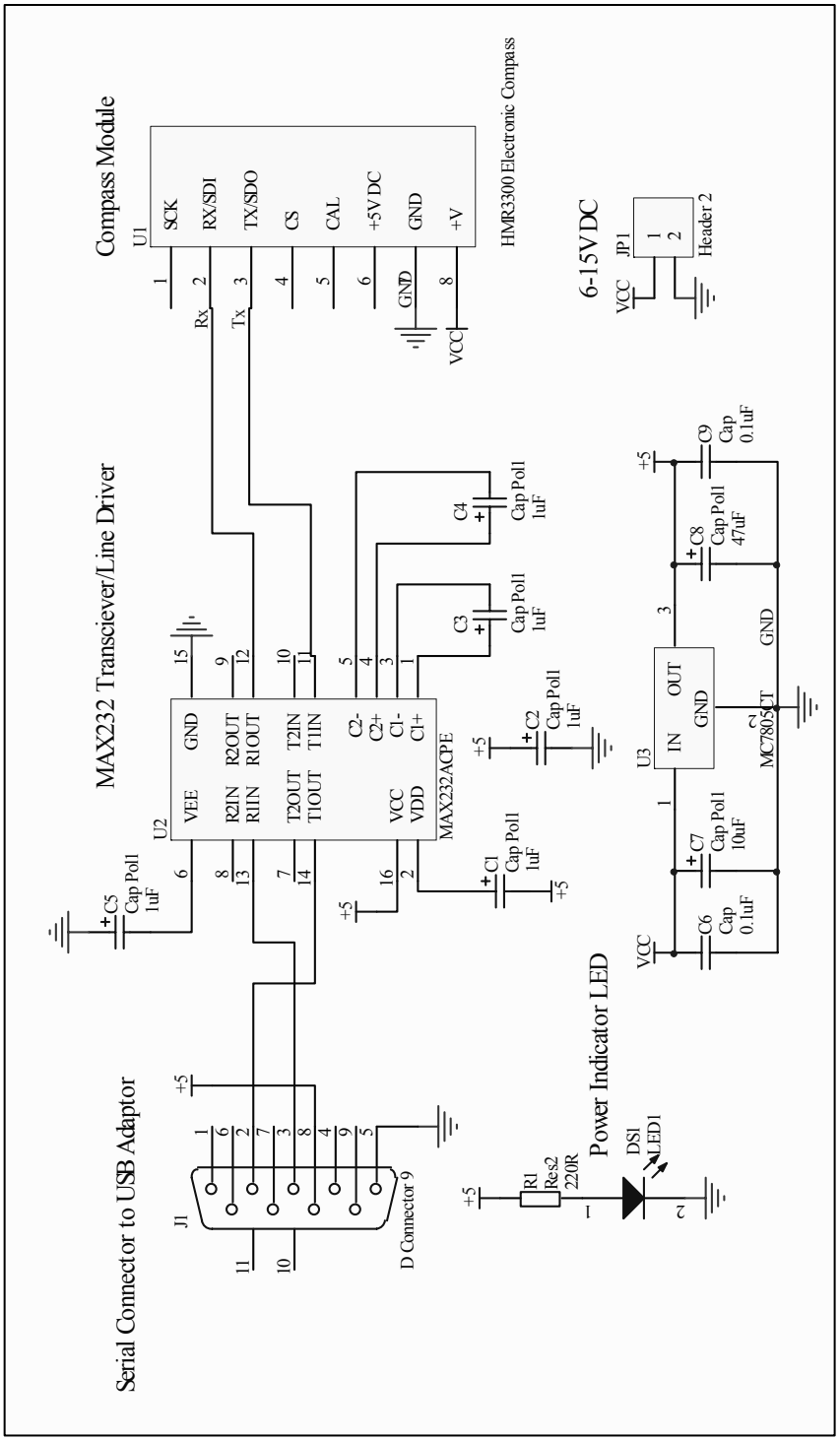

A.4 GPS INTERFACE

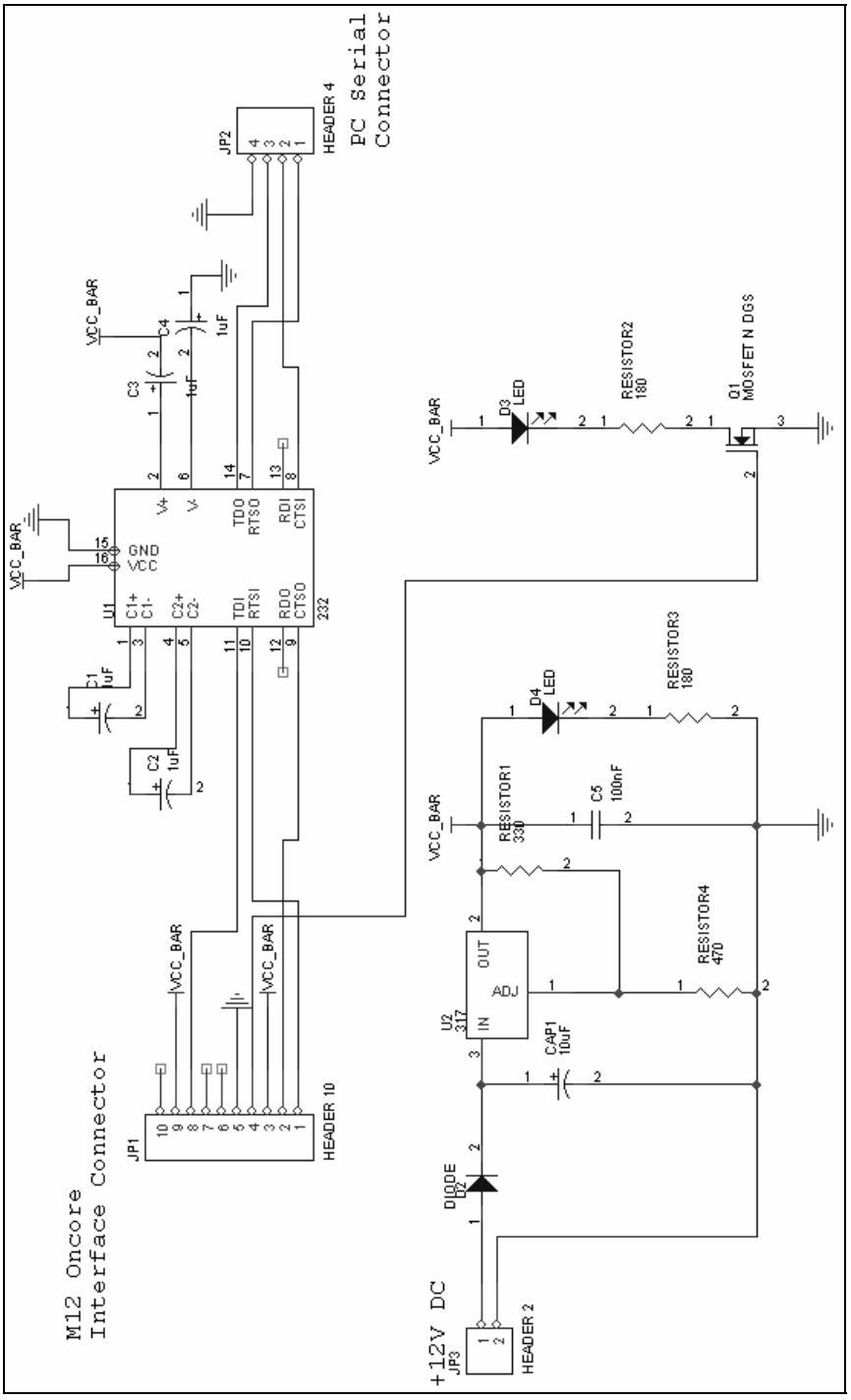

A.5 ACCELEROMETER BOARD

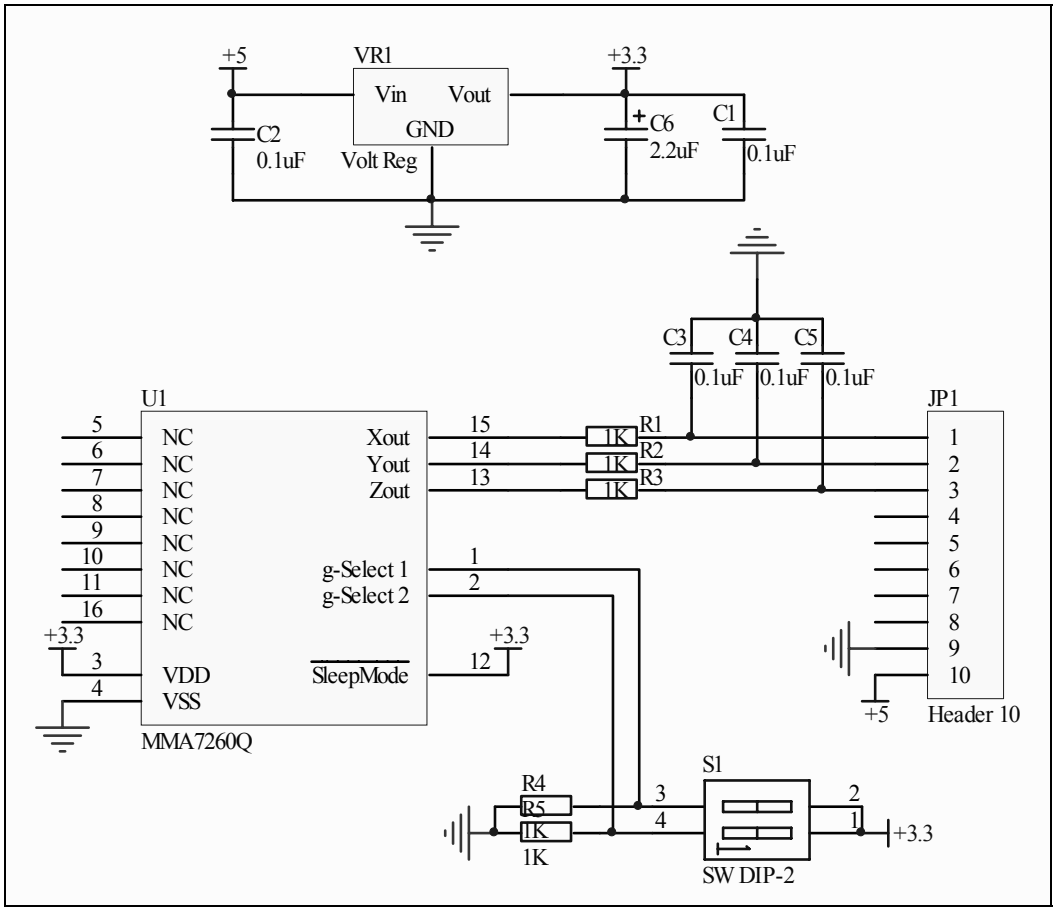

APPENDIX B: CD CONTENTS

The attached CD contains the following items:

- **Video clips of outdoor mechatron in operation**
  - Acceleration and deceleration on flat ground
  - Manoeuvrability of mechatron around obstacles
  - Negotiation of uneven terrain and low obstacles
  - High stability and ability to climb flights of stairs
- **Photo Gallery**
- **User Manual**
- **Software**
  - NI-DAQmx drivers and MAX Studio
  - HI-TECH IDE
  - HMR3300 compass demo program
  - USB to serial adapter drivers
  - Logitech webcam drivers
  - Other programs and utilities used for this project
- **Datasheets**
- **Protel DXP Schematics and PCB designs**
- **Electronic copies of this thesis**